Towards improving agricultural and environmental sustainability in the lower Apalachicola-Chattahoochee-Flint River Basin by understanding the agricultural and climate change impacts on the surface- and groundwater resources

by

Ritesh Karki

A dissertation submitted to the Graduate Faculty of
Auburn University
in partial fulfillment of the
requirements for the Degree of
Doctor of Philosophy

Auburn, Alabama
December 12, 2020

Keywords: SWAT, MODFLOW, SWAT-MODFLOW, Field-scale, Climate Change, Groundwater recharge

Approved by

Puneet Srivastava, Chair, Professor, Department of Biosystems Engineering
Latif Kalin, Co-Chair, Professor, School of Forestry and Wildlife Sciences
Di Tian, Assistant Professor, Department of Crop, Soil, and Environmental Sciences
Jasmeet Lamba, Assistant Professor, Department of Biosystems Engineering

Abstract

Surface- and groundwater resources in the lower Apalachicola-Chattahoochee-Flint (ACF) River Basin play an important role in the economic and ecological vitality of the region. Agriculture, which contributes more than $2 billion annually to the region's economy, is heavily dependent on the underlying Upper Floridan Aquifer (UFA) for irrigation. As the aquifer is close to the land surface and in direct connection with many surficial streams, it also plays a critical role in sustaining streamflow and maintaining the habitat of a wide range of flora and fauna including the endangered mussels species in the region. Intensive groundwater withdrawal from UFA for irrigation, which is further projected to increase in the future, has, however, led to decreases in streamflow and groundwater levels. This has led to detrimental impacts in the habitat of the aquatic species and also threatened the sustainability of agriculture in the region. The issue is further compounded by the emerging and potential impacts of climate change in the watershed hydrologic components in the region. As a result, the overarching goal of this dissertation was to help improve the agricultural and environmental sustainability of the region by evaluating the benefits of the change in agricultural management practices for the major row crops (cotton and peanut) along with understanding the regional impacts of the projected increase in irrigation and changing climate in the surface- and groundwater resources of the region.

A field-scale SWAT model can help evaluate the agricultural management practices in detail and also help to increase the confidence of the stakeholders in the evaluation results. As a result, a detailed literature review of the different methods SWAT can be set up as a field-scale model was first performed to identify the most suitable method for setting up the model for this study. The review study identified five different ways with which a SWAT model could be set up for field-

scale evaluation. Evaluating the range of agricultural management practices using a field-scale SWAT model for cotton and peanut production for irrigation water use, crop yield, and nitrate loss identified the management scenario with soil moisture sensor-based irrigation, cover crop, and strip tillage as having the highest potential for reducing irrigation water use and nitrate loss while maintaining high agricultural productivity. Although the management scenarios that are most adopted in the region, which included checkbook irrigation and no cover crops, had similar crop yields, irrigation water use and nutrient loss were considerably high.

Evaluating the regional impacts of the projected increase in irrigation using the MODular groundwater FLOW (MODFLOW) model showed that groundwater levels would decrease by as much as 2.38 m when compared to levels observed in a significant drought year of 2011. Reduction in groundwater levels was highest in the region of the lower ACF River Basin where the aquifer was comparatively thin. It was also observed that groundwater discharge from the UFA to the surficial streams would decrease by as much as 33% indicating that the projected increase in irrigation may not be sustainable, especially during prolonged drought conditions.

Assessing the impacts of streamflow and evapotranspiration (ET) calibration on groundwater recharge simulation by SWAT to determine if there is a calibration approach that results in improved groundwater recharge simulation showed that calibration of streamflow followed by ET provided the best estimates for groundwater recharge. The study also identified streamflow as the most important variable to be calibrated for groundwater recharge simulation while calibration of ET alone had a negligible impact in groundwater recharge simulation. A comparison of SWAT simulated groundwater recharge to estimates derived from RORA also showed that SWAT can accurately simulate groundwater recharge in the lower ACF River Basin. Information derived from

this study was critical in setting up and calibrating the SWAT-MODFLOW for evaluating the impacts of climate change.

Evaluation of the regional impacts of climate change in the surface- and groundwater resources of the lower ACF River Basin using the calibrated SWAT-MODFLOW model showed an increase in streamflow in most months throughout the region. There were, however, certain months, mostly at the beginning of the year, during which streamflow decreased in the Spring and Ichawaynochaway watersheds under future climate. Comparison of flow duration curves (FDCs) between the baseline and future climate identified a considerable increase in streamflow in extreme events indicating the possibility of flooding events in the future. Although the study indicated to an increase in surface- and groundwater (SW-GW) exchange (groundwater discharge to streams) in the main-stem of the Flint River, groundwater discharge to streams reduced in the ephemeral streams and the Spring and Ichawaynochaway watersheds signaling to the vulnerability of these watersheds to the change in the climate.

Overall, results from the field-scale evaluation of the agricultural management practices of the major crops can help reduce irrigation water while maintaining high agricultural productivity, which can be important, especially during prolonged drought conditions. Regional evaluation of the projected increase in irrigation as well as climate change helped us understand the challenges that lay ahead for the agricultural and ecological sustainability of the region, an understanding of which can help us plan and make better management decisions for the future.

Acknowledgments

I would like to express my sincere gratitude and appreciation to Dr. Puneet Srivastava for providing me with the opportunity to pursue my Ph.D. under his guidance and mentorship. I am also very thankful to him for the incredible support, encouragement, and patient guidance that he provided not only in my research but also in activities that were not directly related to my research which helped me grow as a researcher and an independent thinker. I am equally grateful to Dr. Latif Kalin for serving as my co-advisor and providing me with continued guidance, support, and time as I worked towards completing my Ph.D. I am also very appreciative of Dr. Jasmeet Lamba and Dr. Di Tian for serving in my committee and providing suggestions, and insightful feedback on my research.

I am very thankful for the time and support provided by Dr. Richard B. Winston (USGS) in helping me with my groundwater modeling work. I would also like to express my gratitude to Dr. Ryan Bailey, Dr. Seonggyu Park, Dr. Subhasis Mitra, Dr. Sarmistha Singh, Mr. Mark Masters, Mr. Lynn Torak, and Dr. Wesley Porter for their valuable help and feedback in this research. I would also like to thank my colleagues Hemendra Kumar, Henrique Haas, Bijoychandra Singh, Welber F. Alves, and Suman Budhathoki in the research group for their continuous words of encouragement and companionship.

I am forever indebted to my parents and my sister as they have been the greatest source of motivation and inspiration throughout my education journey. Lastly, I would like to express my deepest gratitude to the love of my life, my wife, Esha Bhattachan who has been a pillar of support through the highs and lows of my Ph.D. journey.

Table of Contents

List of Tables

List of Figures

Chapter 1

Introduction

1.1 Background and problem statement

Surface- and groundwater resources in the lower Apalachicola-Chattahoochee-Flint (ACF) River Basin of southeastern United States (U.S.) play a vital role in the economic and ecological vitality of the region. Agriculture, which is a critical component of the economy in the region generating more than $2 billion in farm-based revenue annually (CAES, 2018), is heavily dependent on the underling Upper Floridan Aquifer (UFA) for irrigation (Jones and Torak, 2006; Singh et al., 2016). It provided an estimated 1.7 million cubic meters of water for irrigation in 2015 but the withdrawals can exceed 3.6 million cubic meters in a drought year (Couch and McDowell, 2006). The aquifer also serves as the primary source of water for industrial and municipal water use. The river basin is also a habitat to a diverse range of flora and fauna having the highest density of reptiles and amphibians in North America (Couch et al., 1996). It is also home to multiple species of federally endangered mussel species as well as more than 58 species of the imperiled fish population (Couch and McDowell, 2006). The UFA, which consists primarily of karst limestone, is close to the land surface and is in direct connection with the surficial rivers and lakes throughout much of the lower ACF River Basin through sinkhole ponds, karst sinks, incised streambeds, and conduits that exposes the limestone to the surface (Torak and Painter, 2006). As a result, the UFA is an important contributor to streamflow in many of the surficial streams in the lower ACF River Basin contributing tens of million cubic meters of water every day (Torak and Painter, 2006).

A rapid increase in groundwater withdrawal for irrigation in the region since the expansion of the center pivot irrigation system in the 1970s, however, has led to detrimental impacts on the surface- and groundwater resources (GWC, 2017). Multiple studies have indicated to a reduction in

baseflow (Golladay et al., 2007; Singh et al., 2016, 2017) as well as short- and long-term declines in groundwater levels (Jones and Torak, 2006; Mitra et al., 2016; Singh et al., 2016). The situation is only exacerbated by the recurring drought conditions in the region. According to the National Drought Mitigation Center (NDMC), the region has experienced multiple severe drought years just in the last two decades including 2000-2002, 2007-2008, 2011-2012, and 2017. Pumpage induced groundwater level fluctuations of nearly 10 m were observed during the severe droughts of 2000 and 2001 while flows in the spring-fed streams of Spring and Ichawaynochaway watersheds decreased by 50 to 100% during drought conditions. Reduced streamflow compounded by prolonged drought conditions has also severely impacted the federally endangered mussel species (Gagnon et al., 2004; Golladay et al., 2004; Shea et al., 2013) and bass population (Couch and McDowell, 2006) in the region. The Georgia Water Planning and Policy Center (GWPCC) projects the agricultural irrigation demand to further increase by 16% from 2010 to 2050 during drought years (CH2M, 2017), which will further increase stress on the surface- and groundwater resources, agricultural industry, and ecology of the region. Along with intensive agriculture and climate variability, the threat of climate change is another growing concern for the economic and environmental sustainability in the region. The temperature in southeastern U.S. has increased by more than 1.1℃ since the 1970s (Karl et al., 2009) and an upward trend in precipitation has been identified in more than 70% of the precipitation recordings in the region (Reidmiller et al., 2017). The region has also witnessed an increase in frequency and intensity of extreme precipitation events along with more frequent drought conditions and extreme and prolonged heat waves (Reidmiller et al., 2017). Globally, the rise in temperature and subsequent change in climate has already altered the global hydrological cycle and led to change in precipitation patterns and intensity, changes in river discharge patterns, altered the water balance components, affected the

frequency and magnitude of fluvial floods, and increased heat waves and droughts (Ahiablame et al., 2017; Leta et al., 2016; Masson-Delmotte et al., 2018; Mohammed et al., 2017; Pachauri et al., 2014; Shrestha et al., 2017).

Understanding the impacts of agricultural management practices and improving them, especially as it relates to irrigation and nutrient management, for maintaining agricultural productivity but reducing the environmental impacts is of critical importance in the region for reducing irrigation demand. It is equally important to understand the impacts of the potential increase in irrigation in the region, as projected by GWPCC, to determine if the UFA can sustain the increased withdrawal and the resulting consequences in the surface- and groundwater interaction. Likewise, as climate change is an emerging threat, the impacts of which are already being felt in the region, it is very important to understand the potential impacts of climate change in the surface- and groundwater resources.

The Soil and Water Assessment Tool (SWAT) is a multi-process simulation tool that can simulate hydrology, sediments, nutrients, and pesticides, predominantly from agricultural watersheds (Neitsch et al., 2011). It has been widely used for evaluating a range of agricultural issues including water management, the impact of agricultural Best Management Practices (BMPs), land use change, climate change, water and nutrient transport, and water quality assessment at regional/watershed scale (Gassman et al., 2007; Krysanova and Arnold, 2008; Tuppad et al., 2011). Evaluation of the management practices including irrigation and fertilizer application for the major crops in detail requires the development of a field-scale SWAT model as it is the scale in which the BMPs are applied and the impacts of these BMPs can be better understood and evaluated at this scale. Recommendations to farmers and stakeholders by presenting SWAT outputs at this scale can also be critical in improving model confidence in stakeholders for implementing the BMPs. It

is, however, also important to make sure that SWAT can adequately simulate the complex hydrological and nutrient processes at field-scale for accurate evaluations of the BMPs. And, as a field-scale SWAT model can be set up in numerous ways, performing a detailed review of the methods used the for field-scale application of SWAT can provide an insight into the advantages and limitations of each method. This can help identify the most suitable method for setting up the field-scale SWAT model in this study. An added advantage of using SWAT as a field-scale model is the transferability of the calibrated crop database model parameters when performing regional-scale evaluations using SWAT.

Evaluation of the range of current management practices for the major crops in the region in detail for irrigation water use, fertilizer application rates, crop yield, and nutrient loss over a long-term climate can provide crucial information to farmers and stakeholders in making management decisions that can help reduce irrigation water and fertilizer application while maintaining high yields for productivity. This can help reduce competition for water resources for irrigation, especially during drought years, and also reduce nutrient loss from agricultural fields thereby enhancing the agricultural and environmental sustainability of the region.

It is also of paramount importance to evaluate the impacts of the projected increase in groundwater withdrawal from the Upper Florinda aquifer for agricultural irrigation use, especially in drought years, to determine if the aquifer can sustain this increased withdrawal to maintain agricultural productivity without adversely affecting the diverse ecological habitat of the region. Understanding the effects of the increased water withdrawal on the groundwater levels as well as the stream-aquifer interaction in the lower ACF River Basin is important for planning for the long-term sustainability of the aquifer. It will also help identify the critical regions within the lower ACF River Basin where the decrease in groundwater levels and reduction in stream-aquifer flux

can be expected to be the most for targeted conservation activities. Identifying the important geohydrologic zones in the region that contribute to the recharge of the UFA through the infiltration of precipitation is also important for the sustainability of the aquifer.

As infiltration from precipitation is an integral component for aquifer recharge in the lower ACF River Basin, it is important to accurately simulate groundwater recharge before any regional-scale hydrological evaluation study. However, it is also one of the least understood processes in hydrogeology (Rushton and Redshaw, 1979) that can only be estimated as it is impossible to measure directly (Healy, 2010). As a result, although SWAT has been used for multiple groundwater recharge evaluation studies, confidence in the model simulated groundwater recharge is often derived by evaluating the model performance in simulating other hydrological variables including streamflow and/or ET (Baker and Miller, 2013; Chinnasamy et al., 2018; Dakhlalla et al., 2016; Emam et al., 2015; Gemitzi et al., 2017; Lee et al., 2014). However, the impact of calibrating these hydrological variables in the simulation of groundwater recharge in SWAT has still not been evaluated. Understanding how SWAT groundwater recharge simulation is impacted by calibrating either streamflow or ET or when using a multi-variate approach and comparing it to recharge estimates obtained for the study region can provide important insight into accurately representing the surface hydrology as well as groundwater recharge simulation using SWAT. This information is vital in developing a SWAT-MODFLOW model that accurately represents the surface- and groundwater dynamics of the lower ACF River Basin before evaluating the impacts of climate change.

Evaluation of the potential impacts of climate change in the important hydrologic components of the surface- and groundwater resources of the region including streamflow, surface- and groundwater (SW-GW) exchange, evapotranspiration (ET), and groundwater recharge can provide

important insight into challenges that lay ahead in developing a long-term water management plan for the region. As there is an intricate connection between the surface- and groundwater resources in the study region, an integrated hydrologic modeling system that allows for a detailed simulation of both surface- and groundwater systems along with the interactions between the two components is vital. It is difficult to understand and quantify the spatio-temporal distribution of SW-GW exchange using only a surface- or groundwater model and the management decisions made based on the scenario results from such results could have little merit. SWAT-MODFLOW is an integrated hydrologic model that couples the SWAT model with the U.S. Geological Survey (USGS) finite-difference, three-dimensional groundwater flow model (MODFLOW-NWT) (Niswonger et al., 2011). SWAT is a robust model in simulating the land-surface hydrological and water quality processes and has been tested in a range of climate and geologic conditions (Francesconi et al., 2016; Gassman et al., 2007; Krysanova and Arnold, 2008) but is limited in simulating groundwater flow and storage (Gassman et al., 2007; Molina-Navarro et al., 2016; Nguyen and Dietrich, 2018). MODFLOW, on the other hand, has robust groundwater simulation capabilities but is limited in the simulation of surface hydrology, plant growth, and groundwater recharge. The coupling of SWAT and MODFLOW allows utilizing the strength of both models to develop an integrated model that is strong in both surface and sub-surface hydrological simulation and suitable for evaluating the impact of climate change in the lower ACF River Basin.

1.2 Dissertation Objectives

The overarching goal of this dissertation is to help improve the agricultural and environmental sustainability of the lower ACF River Basin by evaluating the benefits of change in agricultural management practices as well as understanding the impacts of an increase in irrigation and climate change in the surface- and groundwater hydrology of the region. Specific objectives include:

1. Performing a detailed literature review on the methods used for the field-scale SWAT modeling based on the modeling and research needs as well as its application to identify the appropriate method for setting up the field-scale SWAT model for the evaluation of the range of current management practices for the major row crops in south Georgia (GA).

2. Evaluating the importance of multi-variable calibration in improving runoff and nutrient simulation including crop yield at field-scale using the SWAT model and to quantify the effect of different agricultural management practices on crop yield, irrigation water use, and nutrient loss for cotton and peanut production in south GA.

3. Quantifying the impacts of the projected increase in groundwater withdrawals for irrigation in the groundwater levels of the UFA and surface- and groundwater interaction in the lower ACF River Basin along with the identification of critical zones for groundwater recharge and river sections sensitive to groundwater levels for flow.

4. Evaluating the ability of SWAT to estimate groundwater recharge in the karstic landscape of the lower ACF River Basin as well as analyzing the importance of multi-variable calibration of different hydrologic components in SWAT to accurately estimate groundwater recharge.

5. Simulating the regional impacts of climate change on the surface- and groundwater resources of the lower ACF River Basin using SWAT-MODFLOW.

1.3 Dissertation Organization

The dissertation is organized into seven chapters. Chapter 1 discussed the study area, problem statement, the rationale of the project, and dissertation objectives. Chapter 2 to 6 discusses the five

objectives of this dissertation. Each chapter further details the objective's rationale, the methods used, results, and major conclusions. Findings from the detailed literature review of methods used for field-scale modeling using SWAT is presented in chapter 2. The third chapter evaluates the range of agricultural management practices for the major row crops for irrigation water use, crop yield, and nutrient loss using a field-scale SWAT model. The chapter also discusses the importance of multi-variable calibration for field-scale SWAT modeling. Impacts of the projected increase in groundwater withdrawal for irrigation from the UFA in the aquifer system and the surficial streams in the lower ACF River Basin is discussed in chapter 4. Chapter 5 evaluates the importance of calibrating different hydrologic variables separately or using a multi-variate approach for accurately simulating groundwater recharge using SWAT. The chapter also evaluates the ability of SWAT to estimate groundwater recharge in the lower ACF River Basin. Chapter 6 discusses the impact of climate change in the surface- and groundwater resources of the lower ACF River Basin. Finally, chapter 7 summarizes the major findings from the five objectives along with practical implications of this research as well as recommendations for future research.

1.4 References

Ahiablame, L., Sinha, T., Paul, M., Ji, J.-H., Rajib, A. (2017). Streamflow response to potential land use and climate changes in the James River wa

tershed, Upper Midwest United States. *Journal of Hydrology: Regional Studies*, *14*, 150–166.

Baker, T. J., Miller, S. N. (2013). Using the Soil and Water Assessment Tool (SWAT) to assess land use impact on water resources in an East African watershed. *Journal of Hydrology*, *486*, 100–111.

CAES. (2018). *Georgia Farm Gate Value Report 2017*.

CH2M. (2017). *Coosa - North Georgia Water Planning Region Water and Wastewater Forecasting Technical Memorandum*.

Chinnasamy, P., Muthuwatta, L., Eriyagama, N., Pavelic, P., Lagudu, S. (2018). Modeling the potential for floodwater recharge to offset groundwater depletion: a case study from the Ramganga basin, India. *Sustainable Water Resources Management*, *4*(2), 331–344.

Couch, C. A., Hopkins, E. H., Hardy, P. S. (1996). *Influences of environmental settings on aquatic ecosystems in the Apalachicola-Chattahoochee-Flint River Basin* (Vol. 96). US Dept. of the Interior, US Geological Survey.

Couch, C. A., McDowell, R. D. (2006). Flint River Basin Regional Water Development and Conservation Plan.

Dakhlalla, A. O., Parajuli, P. B., Ouyang, Y., Schmitz, D. W. (2016). Evaluating the impacts of crop rotations on groundwater storage and recharge in an agricultural watershed. *Agricultural Water Management*, *163*, 332–343.

Emam, A. R., Kappas, M., Akhavan, S., Hosseini, S. Z., Abbaspour, K. C. (2015). Estimation of groundwater recharge and its relation to land degradation: case study of a semi-arid river basin in Iran. *Environmental Earth Sciences*, *74*(9), 6791–6803.

Francesconi, W., Srinivasan, R., Pérez-Miñana, E., Willcock, S. P., Quintero, M. (2016). Using the Soil and Water Assessment Tool (SWAT) to model ecosystem services: A systematic review. *Journal of Hydrology*, *535*, 625–636.

Gagnon, P. M., Golladay, S. W., Michener, W. K., Freeman, M. C. (2004). Drought responses of freshwater mussels (Unionidae) in coastal plain tributaries of the Flint River basin, Georgia. *Journal of Freshwater Ecology*, *19*(4), 667–679.

Gassman, P. W., Reyes, M. R., Green, C. H., Arnold, J. G. (2007). The soil and water assessment tool: historical development, applications, and future research directions. *Transactions of the ASABE, 50*(4), 1211–1250.

Gemitzi, A., Ajami, H., Richnow, H.-H. (2017). Developing empirical monthly groundwater recharge equations based on modeling and remote sensing data--Modeling future groundwater recharge to predict potential climate change impacts. *Journal of Hydrology, 546*, 1–13.

Golladay, S. W., Gagnon, P., Kearns, M., Battle, J. M., Hicks, D. W. (2004). Response of freshwater mussel assemblages (Bivalvia: Unionidae) to a record drought in the Gulf Coastal Plain of southwestern Georgia. *Journal of the North American Benthological Society*, *23*(3), 494–506.

Golladay, S. W., Hicks, D. W., Muenz, T. K. (2007). Stream flow changes associated with water use and climatic variation in the lower Flint River Basin, southwest Georgia.

GWC. (2017). *Watering Georgia: The State of Water and Agriculture in Georgia*. Athens, GA.

Healy, R. W. (2010). *Estimating groundwater recharge*. Cambridge University Press.

Jones, L. E., Torak, L. J. (2006). *Simulated effects of seasonal ground-water pumpage for irrigation on hydrologic conditions in the Lower Apalachicola-Chattahoochee-Flint River Basin, Southwestern Georgia and parts of Alabama and Florida, 1999-2002*.

Karl, T. R., Melillo, J. M., Peterson, T. C., Hassol, S. J. (2009). *Global climate change impacts in the United States*. Cambridge University Press.

Krysanova, V., Arnold, J. G. (2008). Advances in ecohydrological modelling with SWAT—a review. *Hydrological Sciences Journal*, *53*(5), 939–947.

Lee, J. M., Park, Y. S., Kum, D., Jung, Y., Kim, B., Hwang, S. J., … Lim, K. J. (2014). Assessing the effect of watershed slopes on recharge/baseflow and soil erosion. *Paddy and Water Environment*, *12*(1), 169–183.

Leta, O. T., El-Kadi, A. I., Dulai, H., Ghazal, K. A. (2016). Assessment of climate change impacts on water balance components of Heeia watershed in Hawaii. *Journal of Hydrology: Regional Studies, 8*, 182–197.

Masson-Delmotte, V., Zhai, P., Pörtner, H.-O., Roberts, D., Skea, J., Shukla, P. R., … others. (2018). *Global Warming of 1.5 OC: An IPCC Special Report on the Impacts of Global Warming of 1.5° C Above Pre-industrial Levels and Related Global Greenhouse Gas Emission Pathways, in the Context of Strengthening the Global Response to the Threat of Climate Chang*. World Meteorological Organization Geneva, Switzerland.

Mitra, S., Srivastava, P., Singh, S. (2016). Effect of irrigation pumpage during drought on karst aquifer systems in highly agricultural watersheds: example of the Apalachicola-Chattahoochee-Flint river basin, southeastern USA. *Hydrogeology Journal*, *24*(6), 1565–1582. https://doi.org/10.1007/s10040-016-1414-y

Mohammed, K., Saiful Islam, A. K. M., Tarekul Islam, G. M., Alfieri, L., Bala, S. K., Uddin Khan, M. J. (2017). Impact of high-end climate change on floods and low flows of the Brahmaputra River. *Journal of Hydrologic Engineering*, *22*(10), 4017041.

Molina-Navarro, E., Hallack-Alegr\'\ia, M., Mart\'\inez-Pérez, S., Ram\'\irez-Hernández, J., Mungaray-Moctezuma, A., Sastre-Merl\'\in, A. (2016). Hydrological modeling and climate change impacts in an agricultural semiarid region. Case study: Guadalupe River basin, Mexico. *Agricultural Water Management*, *175*, 29–42.

Neitsch, S. L., Arnold, J. G., Kiniry, J. R., Williams, J. R. (2011). *Soil and Water Assessment Tool Theoretical Documentation Version 2009*.

Nguyen, V. T., Dietrich, J. (2018). Modification of the SWAT model to simulate regional groundwater flow using a multicell aquifer. *Hydrological Processes*, *32*(7), 939–953.

Niswonger, R. G., Panday, S., Ibaraki, M. (2011). MODFLOW-NWT, a Newton formulation for MODFLOW-2005. *US Geological Survey Techniques and Methods*, *6*(A37), 44.

Pachauri, R. K., Allen, M. R., Barros, V. R., Broome, J., Cramer, W., Christ, R., … others. (2014). Climate change 2014: synthesis report. Contribution of Working Groups I. *II and III to the Fifth Assessment Report of the Intergovernmental Panel on Climate Change*, *151*.

Reidmiller, D. R., Avery, C. W., Easterling, D. R., Kunkel, K. E., Lewis, K. L. M., Maycock, T. K., Stewart, B. C. (2017). Impacts, risks, and adaptation in the United States: Fourth national climate assessment, volume II.

Rushton, K. R., Redshaw, S. C. (1979). *Seepage and groundwater flow: Numerical analysis by analog and digital methods*. John Wiley & Sons.

Shea, C. P., Peterson, J. T., Conroy, M. J., Wisniewski, J. M. (2013). Evaluating the influence of land use, drought and reach isolation on the occurrence of freshwater mussel species in the lower Flint River Basin, Georgia (USA). *Freshwater Biology*, *58*(2), 382–395.

Shrestha, N. K., Du, X., Wang, J. (2017). Assessing climate change impacts on fresh water resources of the Athabasca River Basin, Canada. *Science of the Total Environment*, *601*, 425–440.

Singh, S., Mitra, S., Srivastava, P., Abebe, A., Torak, L. (2017). Evaluation of Water-Use Policies for Baseflow Recovery during Droughts in an Agricultural Intensive Karst Watershed: Case study

of the Lower Apalachicola-Chattahoochee-Flint River Basin, Southeastern USA. *Hydrological Processes*.

Singh, S., Srivastava, P., Mitra, S., Abebe, A. (2016). Climate variability and irrigation impacts on streamflows in a Karst watershed—A systematic evaluation. *Journal of Hydrology: Regional Studies*, *8*, 274–286.

Torak, L. J., Painter, J. A. (2006). *Geohydrology of the lower Apalachicola-Chattahoochee-Flint River basin, southwestern Georgia, northwestern Florida, and southeastern Alabama*.

Tuppad, P., Douglas-Mankin, K. R., Lee, T., Srinivasan, R., Arnold, J. G. (2011). Soil and Water Assessment Tool (SWAT) hydrologic/water quality model: Extended capability and wider adoption. *Transactions of the ASABE*, *54*(5), 1677–1684.

Chapter 2

Application of the Soil and Water Assessment Tool (SWAT) at Field Scale: Categorizing Methods and Review of Applications

2.1 Abstract

Although the Soil and Water Assessment Tool (SWAT) has been widely used as a watershed/basin scale model, recently, there has been considerable interest in applying it at the field-scale, especially for the evaluation of best management practices, and for building stakeholder confidence. For this study, a thorough review of literature on the field-scale application of SWAT was conducted. It was determined that there is more than one way of setting up the field-scale SWAT model depending on the spatial scale of the research as well as the research question being answered. This paper provides a detailed literature review of the methods used for field-scale SWAT modeling along with the summary of applications. The paper also discusses the limitations and advantages of each method along with the future research needs. The overarching goal of this paper was to provide a valuable and time-conserving resource to future researchers interested in field-scale SWAT modeling.

2.2 Introduction

Agricultural intensification in the U.S. over the last 100 years has led to more than 120 million hectares currently under agriculture, with crop irrigation accounting for nearly two-thirds of the nation's total water use and with one-quarter of the nation's cropland now artificially drained (Capel et al., 2018). Additionally, pesticide and nitrogen fertilizer use have increased three- and fourfold, respectively, since 1960 (Capel et al., 2018). Nutrient, chemical, and sediment losses from agricultural fields can severely degrade the quality of streams, rivers, and shallow groundwater. Eleven billion kilograms of nitrogen are applied as fertilizer, of which 5% to 50% is

transported to surface and groundwater sources (Capel et al., 2018), and median total nitrogen (TN) and total phosphorus (TP) stream concentrations persist at about six times greater than background levels (Dubrovsky et al., 2010). As a result, agricultural producers are under ever-increasing pressure to reduce agricultural nonpoint-source (NPS) pollution while maintaining high levels of productivity for profitability. Thus, it is of critical importance to understand the underlying nutrient and water transport processes in agricultural fields and to assess the potential of alternate land uses and agricultural management practices to help maintain agricultural productivity while conserving surface and groundwater resources. Field-scale models including but not limited to CREAMS (Knisel, 1980), GLEAMS (Leonard et al., 1987), EPIC (Williams et al., 1989), APEX (Williams et al., 2006), AGNPS (Young et al., 1989), and WEPP (Flanagan et al., 2001) have been developed and widely used to simulate water, nutrient, pesticide, and plant processes in agricultural fields as well as to evaluate alternate irrigation and nutrient management, tillage operations, drainage, and manure application practices (Arnold et al., 2015). Hence, field-scale models are important for the evaluation of practices that can help increase agricultural productivity while reducing production cost and improving environmental sustainability.

The Soil and Water Assessment Tool (SWAT) is one of the most widely used multi-process simulation models for evaluating a range of agricultural issues, including water management, impacts of structural and non-structural best management practices (BMPs), climate change, land use change, water and nutrient transport processes, groundwater dynamics, and water quality assessment (Francesconi et al., 2016; Gassman et al., 2007; Krysanova and Arnold, 2008), most of which are done at the river basin or watershed scale. As BMPs (e.g., nutrient management, conservation tillage, cover cropping, and irrigation scheduling) that are critical to improving agricultural productivity and reducing NPS pollution by nutrients, sediments, pesticides, and

bacteria from agricultural fields are applied at the field scale, it is important to evaluate and make field-scale recommendations. Presenting SWAT outputs to stakeholders at the scale that is most relevant to them can also be helpful for increasing BMP adoption. This is especially important if the alternative practices have a direct impact on crop yield and production costs, which are primary concerns for the implementation of alternative practices by farmers. As a result, although SWAT has commonly been used for watershed-scale evaluations (Gassman et al., 2007), field-scale SWAT modeling has been conducted recently for a range of applications (Chen et al., 2017; Daggupati et al., 2011; Kalcic et al., 2015; Merriman et al., 2018; Sinnathamby et al., 2017; Uribe et al., 2018). Field-scale SWAT modeling has been done using different methods and for a range of spatial scales. As an example, it has been used to evaluate the outputs of a watershed-scale SWAT model for each field within a simulated watershed (Daggupati et al., 2011), which was not possible under the conventional SWAT setup. It has also been used to simulate and evaluate a single field (Maski et al., 2008).

Although many reviews of watershed-scale SWAT applications have been conducted (de Almeida Bressiani et al., 2015; Francesconi et al., 2016; Gassman et al., 2007; Krysanova and Arnold, 2008; Tuppad et al., 2011; van Griensven et al., 2012), none provide a detailed review of the methods used for field-scale application of SWAT. A detailed review of field-scale SWAT modeling can be a valuable and time-conserving resources for future research initiatives using SWAT at field scale. The main objective of this article is to summarize and categorize the current methods used for field-scale SWAT modeling based on the modeling and research needs. Examples for each category are provided to discuss the application of field-scale modeling. This article provides a brief description of the SWAT model and the subbasin and HRU delineation processes used in

field-scale SWAT modeling, along with the application of field-scale modeling, and discusses the limitations of each modeling method along with future research needs and directions.

2.3 SWAT Model

SWAT is a continuous time, physically based, computationally efficient, semi-distributed model with spatially distributed parameters that was developed by the USDA Agricultural Research Service (ARS) (Arnold et al., 1998; Neitsch et al., 2011). It is a direct outgrowth of the Simulator for Water Resources in Rural Basins (SWRRB) model (Arnold et al., 1990) and has been used to simulate watersheds of varying sizes, ranging from fields to large complex watersheds, to evaluate the impacts of land management practices, climate, and land use change on hydrology, sediments, nutrients, plant growth, and pesticides (Gassman et al., 2007; Neitsch et al., 2011). Primary inputs to the model include both spatial and tabular information: digital elevation model (DEM) data for topographical information, soil properties, land cover and management, weather, point sources, and reservoir characteristics. The SWAT-modeled components include hydrology, water and sediment movement, soil temperature, weather, nutrients, pesticides, bacteria, and land management (Neitsch et al., 2011).

The basic unit of all calculations in SWAT is the hydrologic response unit (HRU), which is a lumped land area composed of a unique combination of land cover, soil series, and optionally slope steepness within a subbasin (Neitsch et al., 2011). An important step in the SWAT model setup is the watershed delineation process, which divides a watershed into hydrologically connected subwatersheds or subbasins, and then divides each subbasin into HRUs (Winchell et al., 2013). Threshold area, which defines the minimum drainage area required to form the origin of a stream, can be defined during the watershed delineation and affects the number and size of subbasins when subdividing a watershed. Division of each subbasin into HRUs enables the model to evaluate the

differences in hydrology, plant growth, and contaminant transport processes for different combinations of land cover and soil (Winchell et al., 2013). A user-defined threshold percentage for the land use, soil, and slope class can be applied during the HRU definition process, which eliminates land use, soil, and slope classes that cover an area of the subbasin that is less than the threshold defined by the user. The area of the remaining land use, soil, and slope class is reapportioned after the elimination process so that all of the land area in the subbasin is simulated (Winchell et al., 2013). However, the use of thresholds can cause some fields that are critical for a watershed-level evaluation to be eliminated during the simulation process (Her et al., 2015). Lumping of land areas with similar attributes to form a single HRU within a subbasin can cause multiple fields to be simulated as a single HRU, or multiple HRUs can be within a single field, making field-level analysis and recommendation difficult. Additionally, there are no routing mechanisms between HRUs. Outputs from all HRUs within a subbasin are aggregated, and surface runoff and shallow subsurface flows and associated contaminants are routed to the stream network from one subbasin to another. This approach of using subbasins and HRUs helps SWAT maintain a balance between computational efficiency and preserving the spatial heterogeneity of the simulated watershed (Neitsch et al., 2011). However, this approach also limits evaluation and recommendation at field scale because each field does not correspond to unique HRU boundaries in a conventional SWAT setup.

2.4 Field-Scale SWAT Modeling

2.4.1 Methods and Applications

A thorough review of the literature on field-scale SWAT modeling identified five basic methods for evaluating model output at the field scale: (1) simulation of an individual field as a field-scale SWAT model; (2) modification of SWAT input files such that each field is represented by multiple

HRUs that reflect changes in the soil and slope classes within each simulated field; (3) modification of SWAT input files such that when SWAT runs the HRU definition process for a watershed with multiple fields, each HRU corresponds to a unique field located in the simulated watershed; (4) development of a post-processing tool that uses the SWAT output generated with conventional HRU delineation and converts this output to field scale using different techniques; and (5) defining a relationship between fields in the simulated watershed and HRUs from the SWAT model that was set up using conventional HRU delineation by comparing land use, soil, and slope attributes and evaluating the HRU-level outputs.

Field-scale SWAT modeling does not involve any modification to the algorithms that simulate hydrology, nutrient transport, or any other processes in SWAT. The HRUs are still disconnected from each other, and outputs for a subbasin are still generated by aggregating the outputs from the HRUs within the subbasin. Modification of SWAT input files or post-processing of SWAT outputs are the keys to field-scale SWAT modeling**.** Each of the following subsections summarizes published articles that describe field-scale modeling methods as well as applications of field-scale SWAT models.

2.4.1.1 Simulation of an individual field using SWAT

Marek et al. (2016) evaluated the ability of SWAT to simulate daily and monthly evapotranspiration (ET) for major irrigated summer crops including cotton, soybean, grain and silage sorghum, sunflower, and corn silage in the semi-arid Texas High Plains from a 4.7 ha irrigated field located at the USDA-ARS Conservation and Production Research Laboratory (CPRL) at Bushland, Texas, using lysimetric data. Because the irrigated field was square in shape and SWAT does not consider artificial boundaries that do not coincide with topographic features for watershed and subbasin delineation, a novel method was applied for simulating the irrigated

field. A polygon outlining the field was drawn using the "draw polygon" tool in the ArcSWAT 2012 interface with a satellite image overlay and a 30 m DEM. A single subbasin having the longest reach of the several subbasins and outlets generated for the field was selected to be representative of the slope and aspect of the entire field, which resulted in a watershed project with one subbasin, one HRU, and one reach. The area of the representative subbasin was then adjusted in the subbasin text file to match the field area of 4.7 ha, and a single management file was created for the HRU to reflect the agronomic practices used in the field during the study period. Model performance analysis for simulating ET for the manual calibration and validation period showed that SWAT adequately simulated ET with NSE of 0.67 and 0.78 for calibration and validation, respectively, for daily ET estimation and with NSE of 0.77 and 0.85 for calibration and validation, respectively, for monthly ET estimation.

Chen et al. (2017) evaluated the SWAT auto-irrigation function to simulate irrigation management strategies typical of the Texas High Plains while also evaluating the ability of SWAT, as a field-scale model, to simulate crop yield, leaf area index (LAI), and ET. The SWAT model was set up for a 4.7 ha irrigated lysimeter field located at the USDA-ARS CPRL at Bushland, Texas, using a single-HRU method. After calibration for LAI for the crops simulated, model performance evaluation for ET during calibration and validation showed good agreement (NSE $\geq$ 0.80). Simulation of crop yield after calibration also showed very good agreement (NSE = 0.99, PBIAS = 1.3%). Results from the scenario analysis using the SWAT auto-irrigation function demonstrated that the auto-irrigation function was not able to match field conditions and highlighted the shortcomings of the auto-irrigation function for users, modelers, and developers. Although the overall performance for ET simulation was satisfactory with the auto-irrigation function, there was a noticeable decrease in NSE. The study also emphasized the need to improve the SWAT auto-

irrigation function by including the management-allowed depletion (MAD), a framework for irrigation scheduling that can be useful to better simulate water balance and crop growth in irrigated regions.

Chen et al. (2018) modified the SWAT source code to incorporate MAD-based irrigation management and evaluated the MAD auto-irrigation algorithm for simulation of ET and crop ET by comparing results from the new algorithm with results from the default auto-irrigation function and observed data. The authors used the calibrated single-HRU SWAT model from Chen et al. (2017) for this study. A small watershed was delineated around the lysimeter field, and a single subbasin with the longest reach was selected as representative of the slope and aspect of the field. All other subbasins and associated outlets were removed, which resulted in a SWAT model consisting of a single subbasin, single reach, and single HRU. The modified SWAT code allowed simulation of a single constant MAD value throughout the growing season or for growth stage-specific MAD values (FAO-MAD). Results from the study indicated that although the SWAT default auto-irrigation algorithm simulated reasonable values for ET, the simulated irrigation was considerably higher than the actual irrigation. Use of the new constant MAD auto-irrigation algorithm greatly improved the simulation of seasonal irrigation, which improved further with the use of the FAO-MAD auto-irrigation algorithm.

Anand et al. (2007) calibrated and validated the runoff prediction of SWAT and Agricultural Drainage and Pesticide Transport (ADAPT) (Alexander, 1988) for individual field plots under no-till planting with surface-broadcast fertilizer/pesticide application (NT/SB), no-till with deep-banded fertilizer application (NT/DB), and tilled management practices. The study site was a 4.7 ha farm field in the Upper Marais des Cygnes basin in Kansas, which included two replicates of each BMP treatment. The models were calibrated for each BMP treatment using observed runoff

from one plot and validated using observed runoff from the replicate plots. The authors did not provide details on how the SWAT model was set up to simulate runoff from each plot under the different BMP treatments. Results from the study indicated that the best-fit curve number for antecedent soil moisture condition II (CN_{II}) for ADAPT was 66, 68, and 70 for the NT/SB, NT/DB, and tilled BMP treatments, respectively, while the best-fit CN_{II} for SWAT was 86 for all treatments. Although the calibration parameters were different for the two models, the best-fit model parameters had excellent correlation to monthly runoff totals and moderate correlation to individual events. Validation of the model using the calibrated parameters for the replicate plots showed improved or similar statistical results. It is possible that the differences in calibration parameters for the two models could be related to the differences in ET estimation in the two models.

Maski et al. (2008) evaluated the ability of SWAT set up for field scale to simulate runoff and sediments under different management practices and to verify optimal parameter sets for runoff and sediments simulation under different management practices. Because the experimental plots were the same as those used by Anand et al. (2007) for comparing SWAT and ADAPT, the three BMP treatments were the same, and the runoff calibration process for SWAT was adapted from that previous study. The model was calibrated for three field plots (0.39 to 1.46 ha) with different management practices and validated for three replicate plots (0.40 to 0.56 ha) with the same management practices. A field survey of the plots with a horizontal accuracy of 10 to 20 mm and vertical accuracy of 2 to 3 times the horizontal accuracy was used to derive slopes for individual plots. The field-scale model was set up such that each plot was simulated as a single subbasin with no routing between subbasins, and the outputs from the subbasin were evaluated against the plot outputs. Each subbasin had a single HRU, and management scenarios were specified for each plot,

scheduled by dates. Model performance was evaluated by comparing event-based flow and sediment yield values. The calibrated CN_{II} of 86 for the tilled treatment was slightly lower than the values for the no-till treatments of NT/SB (88), and NT/DB (89) for runoff simulation. Saturated hydraulic conductivity followed a similar trend, with lower values for tilled than no-tilled treatments, while the baseline soil available water capacity (AWC) was appropriate for all the treatments. Calibration of sediments showed that the baseline USLE cropping factor (C_{min}) was adequate for the tilled and deep-banding treatments with soil disturbance, while the best-fit C_{min} value for field conditions without soil treatment was 2.5 to 3 times greater than the baseline value. The authors cautioned that field- or watershed-scale models calibrated for tilled management practices may not function well for management scenarios with no-till.

Douglas-Mankin et al. (2010) built on the field-scale SWAT model calibrated and validated for runoff and sediment by Maski et al. (2008) and evaluated the ability of the SWAT model to simulate daily and monthly TN and TP yields in runoff at field scale under the different BMPs. The authors calibrated the model sequentially for TN and TP, followed by validation with paired treatment plots. Results showed that the calibrated parameter values used for TN and TP calibration were identical for all plots irrespective of tillage and fertilizer application method, indicating that runoff and sediment yield calibration alone can adequately simulate the differences in nutrient loss from different tillage and fertilizer placement practices. Evaluation of daily TN yield calibration for all treatments showed that SWAT had satisfactory robust modeling efficiency (E_f*) (0.54 to 0.64), good to very good PBIAS (31% to 7%), and satisfactory to good median RSR (RSR*) (0.72 to 0.62), while lower and more variable performance was observed for daily TP simulation (E_f* of 0.42 to 0.62, PBIAS of -48% to 2%, and RSR* of 0.76 to 0.62). The authors also noted that the model predicted greater TN loss from the no-till fields when compared to the

tilled fields, which was contrary to the observed values and a major concern, while also pointing out that the effects of tillage systems on nutrient loss are still very little understood.

Bosch et al. (2010) evaluated the SWAT landscape model (Arnold et al., 2010) for the simulation of surface runoff, lateral subsurface flow, and groundwater flow on a 1.77 ha hillslope with an upland field, grass buffer, and subdivided forested buffer in the Atlantic Coastal Plain near Tifton, Georgia. Flow simulation results from the SWAT landscape model that had been manually configured with four HRUs for the four-component hillslope were compared against a single-HRU model developed using SWAT 2005 with the dominant land use and soil type configuration of the upland field. The total area of the upland HRU in the single-HRU SWAT model was modified to 1.77 ha to match the total area of the simulated hillslope. The SWAT landscape model and observed results showed that surface runoff and groundwater flow dominated the upland field and grass buffer hydrology, respectively. Although the SWAT landscape model simulated the average annual surface runoff and groundwater flow satisfactorily and followed the general trends in the observed data, the difference between observed and simulated annual runoff at the edge of the grass and forested buffers was as great as 75%. The SWAT landscape model was also not able to simulate monthly observed surface runoff at the edge of the upland field, demonstrating a need for additional detail in the landscape model to better simulate the interactions between soil surface, vadose zone, and groundwater. The single-HRU SWAT model was not able to redistribute the water between surface and subsurface components, as done by the landscape model and observed in the field, resulting in considerably higher surface runoff and low groundwater flow.

2.4.1.2 Watershed-Scale SWAT Model with Each Field Represented as a Set of HRUs

Gitau et al. (2004) used SWAT, a genetic algorithm (GA), a BMP tool, and site-specific BMP costs to develop a method for determining the optimal selection and location of BMPs within a

farm to reduce phosphorus pollution in a cost-effective way. The farm was located in the Town Brook watershed (TBW) of Delaware County, New York. A SWAT model was set up for the TBW using a 10 m DEM for elevation data, a 10 m land use classification grid for base land use, and SSURGO for soil data with a 0% land use and soil definition threshold. Use of a 0% threshold prevented lumping of land use and soil, and the resulting HRU map was overlaid with the farm boundary to identify HRUs within the farm. The model was calibrated for monthly (R^2 = 0.76, NSE = 0.44) and annual (R^2 = 0.99, NSE = 0.84) streamflow, and the ten-year average annual loadings of phosphorus from each HRU within the farm were used as input for the GA. Cost-effective BMP implementation scenarios used the GA, the BMP tool, and the BMP costs. Results from the study showed that the most cost-effective scenario achieved an effectiveness of 0.6 kg dissolved P reduction per dollar spent per year.

Gitau et al. (2008) applied the SWAT model and a BMP characterization tool to a 163 ha farm that covered an entire subwatershed in Delaware County, New York. The authors compared pre- and post-BMP installation periods to determine the extent to which the model results matched the observed data at the watershed and field levels and to evaluate the impacts of the BMPs. Each field within the 163 ha watershed was simulated as a unique land use area to allow BMP evaluation at the field level and prevent masking of small but potentially high phosphorus (P) loss areas, which can happen when fields are lumped together during SWAT model setup. Georeferenced field boundary data were annotated as the base land use map for SWAT so that each field had a unique identifier to maintain each land use as a unique land use. The SWAT built-in crop database was then modified to accommodate the new land use identifiers by copying parameters from the appropriate corresponding general land use. A threshold of 0% was used for land use and soils to preclude lumping and preserving all fields and soils. This technique, also demonstrated by Veith

et al. (2005), allows each field to be represented by a unique set of multiple HRUs in the model and allows evaluation of SWAT field-level outputs against observed field experiments. Gitau et al. (2008) found that SWAT adequately simulated runoff, sediment, and phosphorus for the pre- and post-BMP periods, with annual NSE for the simulated components ranging between 0.56 and 0.8 and monthly values ranging between 0.45 and 0.78. Field-level simulations were also found to be adequate, with the simulated in-field P loads closely matching the observed data. BMP installation reduced dissolved phosphorus (DP), particulate phosphorus (PP), and TP by an average of 31%, 13%, and 21%, respectively, at the watershed scale. This finding was consistent with the findings from the observed data. The model was not able to evaluate the impacts of individual BMPs because the BMPs existed in various combinations within the fields. However, the model was able to evaluate the impacts of BMP combinations, such as nutrient management plans and rotations (31% DP, 25% TP reduction). The BMP characterization tool was also found to suitably complement the model, as it provided information on the impacts of individual BMPs as well as the efficiency of BMPs that were not simulated by SWAT.

Ghebremichael et al. (2008) built on the calibrated SWAT model for runoff, sediment, and phosphorus developed by Gitau et al. (2008) and assessed the benefits of three farm-level precision feed management (PFM) strategies at field and watershed level. The authors used the calibrated model results as the baseline scenario and evaluated the hydrologic, sediment, and nutrient responses to the PFM strategies of reduced manure P concentrations as a result of dietary P reduction (scenario 1), increased forage productivity + scenario 1 (scenario 2), and converting corn land to high-yielding grass + scenario 2 (scenario 3). Simulation of each field as a unique set of HRUs allowed assessment of the field-level impacts of PFM strategies for each field by evaluating

outputs from the HRUs that corresponded to each field. Results from the study showed that the PFM strategies reduced soil P buildup and P losses at both field and watershed level.

Ghebremichael et al. (2010) quantified and identified critical source area (CSAs) for P loss in the Rock River watershed in Vermont using SWAT. The watershed, which covers an area of about 71 km^2, is dominated by dairy agriculture and is considered a high-priority area for watershed management activities. Land use data for the SWAT model input were developed from a combination of the National Land Cover Database (NLCD) data layer, common land unit (CLU) maps, and digitized active farmsteads. Because the NLCD provides information only as either closely grown crops or row crops, without specific crop type identification, the NLCD data layer was updated wherever possible using CLU data and digitized farmsteads. HRUs in the study were defined using SSURGO soil data, the updated land use map, and four slope groups (0% to 3%, 3% to 8%, 8% to 15%, and >15%). The HRUs were defined by distinctly coding to specific fields using available field boundary data for crops to maintain the specific locations of the crop fields, which was critical for identifying CSAs for P loss. Assessment of daily and monthly streamflow (NSE of 0.60 and 0.74 during calibration and 0.60 and 0.70 during validation, respectively) showed that the streamflow predictions were acceptable for the project. The model also adequately simulated daily and monthly sediment loads (NSE of 0.4 and 0.7 during calibration and 0.4 and 0.6 during validation, respectively) and monthly total P loads (NSE of 0.7 during calibration and 0.6 during validation). Evaluation of CSAs for P loss showed that 80% of the total P loss in the watershed was contributed by 24% of the area, which can help managers and planners implement management strategies with limited resources.

2.4.1.3 Watershed-Scale SWAT Model with Fields Simulated as Unique HRUs

Kalcic et al. (2015) demonstrated a method for defining each SWAT HRU as a field boundary within a simulated watershed and compared the field boundary method to the standard method of HRU definition for streamflow, nitrogen, phosphorus, and sediment simulation in a 56 km^2 watershed in west-central Indiana. The authors used the CLU map layer provided by the USDA Farm Service Agency (FSA) for the field boundaries to first determine the major land use in each field boundary. A new soil map was created using the SSURGO and CLU maps such that each field boundary was assigned one soil type with the greatest number of cells assigned within the field, and a unique soil name was assigned for every field in the study area so that each field had one land use, a unique soil type, and one slope, which is required for simulating each field as a unique HRU and prevent lumping of HRUs. Each unique soil name required the addition of a new soil to the usersoil table in the SWAT database. A lookup table was also created to map each new soil name to the SSURGO soil map unit key (mukey), a unique identifier for each soil in the database. As a result, the model saw each field as having a unique soil type and defined each field as a unique HRU. Kalcic et al. (2015) provided a detailed step-by-step process for the field boundary method. The authors mentioned that each field could also be simulated as a unique HRU by creating a unique land use for each field, but an upper limit on the number of unique land use names can become an issue. Only one slope class (0% to 2%) and a 0% threshold for land use, soil, and slope characteristics were used for both the standard method and the field boundary method during the model setup. The authors noted that only 418 HRUs were produced by the field boundary method, as compared to 690 HRUs using the standard method. Model performance evaluation showed that the water balance and hydrology were quite similar for both methods, and the R^2 and NSE were >0.6 for daily and monthly flows for both methods, even though the models were not calibrated. Daily simulations of nitrogen, phosphorus, and sediment at the watershed

outlet were also similar for both methods, but the field boundary method masked extremely high soil erosion predicted for a few soils because only a majority soil type was chosen for each field.

Teshager et al. (2016) developed an ArcGIS preprocessing procedure using the USDA National Agriculture Statistics Service (NASS) Cropland Data Layer (CDL) land use/land cover (LULC) and soil data to spatially define a one-to-one match between farm fields and HRUs within a subbasin prior to SWAT simulations. The authors then used the preprocessing outputs to set up the SWAT model for evaluation of flow, sediment, nitrate, and mineral phosphorus for two midwestern watersheds, Raccoon River watershed (RRW) and Big Creek River watershed (BRW), at daily, monthly, and annual time scales. The preprocessing procedure is detailed step-by-step in the article. The general steps include converting LULC to polygons, splitting the polygons with road and river networks, intersecting the final polygons with predefined subbasin polygons from ArcSWAT, relabeling the LULC polygon codes by assigning different codes for the same LULC type and adding the new crop/LULC types to the SWAT crop database, and using the updated polygons to assign a dominant soil for each polygon. A threshold of 0% for land use, soil, and slope characteristics was used during the HRU definition process, and a single slope class was used to prevent HRU fragmentation. Evaluation of the model results for the two simulated watersheds showed that SWAT was able to replicate annual, monthly, and daily streamflow as well as sediment, nitrate, and mineral phosphorus within the accuracy recommended by Moriasi et al. (2007), although the model performed better in the RRW than in the BRW. The authors stated that older and limited observed data along with bias issues in estimating pollutant loads with LOADEST, especially for daily load estimates, could have led to the decreased model performance in the BRW.

Merriman et al. (2018) calibrated and validated the SWAT model for the 50 km^2 Alger Creek watershed in Michigan to identify CSAs with the highest runoff, erosion, and nutrient loss potential and to estimate the impact of BMPs on nutrient and sediment yields in the watershed. The authors also simulated additional scenarios of BMP implementation for evaluating reductions in nutrient and sediment yields. The SWAT model was configured to have HRUs approximately equal to one farm field in the watershed to allow accurate placement of BMPs with spatially correct land use and soil types modeled beneath the BMPs, and to identify CSAs. The National Conservation Planning (NCP) database, which is a repository of NRCS-funded BMPs, was used to identify the locations of BMPs in the watershed. The setup of each field as a unique HRU in the model was done by loosely following the methods used by Daggupati et al. (2011) and Kalcic et al. (2015). A CLU map was used to determine the farm outlines in the watershed. The land use map for the SWAT model was prepared by using the majority value for each outlined field through the CDL. A soil map was created using a similar approach with the dominant soil type in each field. A threshold of 0% was used for land use, soil, and slope characteristics, and the slope layer was created using the single slope option to keep the field boundaries as delineated. The BMPs installed in the watershed were mostly non-structural and were simulated by adjusting the management practices following an approach similar to Arabi et al. (2008). Monthly model calibration at the watershed outlet resulted in very good NSE values of 0.90, 0.79, 0.87, 0.88, and 0.77 for flow, sediment, TP, DP, and TN, respectively, and a satisfactory NSE of 0.51 for nitrate. Validation results were at least satisfactory, with NSE of 0.83, 0.54, 0.73, 0.53, and 0.60 for flow, sediment, TP, DP, and TN, respectively, and unsatisfactory for nitrate, with NSE of 0.28. Evaluation of the BMP effects at field scale showed that the most effective practice for reducing sediment, TP, and DP was no-till followed by cover crops, while nitrate loss was most reduced at the field scale by

cover crops. The BMPs were not as effective at reducing nutrient and sediment loss at the watershed scale.

2.4.1.4 Post-Processing Tool for Scaling HRU Outputs to Field Scale

Daggupati et al. (2011) created a SWAT HRU output post-processing tool that used CLU layer maps to convert SWAT HRU output from a watershed-scale model to field-level results for evaluating sediment yields at the field level and assessing the impact of topography, soil, land use, and land management source data on field-scale targeting. The authors set up the SWAT model for a 7,818 ha watershed in south Kansas using a 0% threshold for soil and land use so that all combinations of topography, soil, and land use were preserved. The model performance was evaluated for streamflow at the watershed outlet, and the model agreement with observed flow data was satisfactory, with monthly statistics of R^2 = 0.75, NSE = 0.66, and PBIAS = -18.8%. Model performance for sediment yield was evaluated against the published measurements for small cropland drainages because observed stream sediment data were not available. Post-processing the SWAT HRU output to field-level output was a two-step process in which the first step was to read in the SWAT HRU output table from the access database and export average annual yields for sediment, TN, and TP. The second step was to use the outputs from the first step, fullHRU shapefile, and boundary of interest (e.g., fields, counties) to produce maps of area-weighted average annual pollutant yields for the user-defined boundary using zonal statistics. An ArcGIS-based SWAT targeting toolbar was created using ArcGIS Visual Basic that automated the two processes. Results from the study showed that the post-processing tool can be useful for field-level targeting of critical areas of sediment loss. However, incorrect use of source data for model setup, such as misclassification of land use in NASS or missing land management datasets (e.g., terraces, contour farming, or no-till) in the NLCD datasets, along with low-resolution topographic

data (30 m DEM instead of 10 m) and soil data (STATSGO instead of SSURGO soil dataset) translate into incorrect field-level targeting.

Pai et al. (2012) developed a standalone tool called Field_SWAT, based on the MATLAB programming environment, for mapping SWAT HRU outputs to user-defined boundaries such as fields. The authors developed a spatial algorithm that aggregated HRU-level outputs to field boundaries using one of four different methods for spatial aggregation (mean, mode, geometric mean, and area-weighted mean) chosen by the user and incorporated the algorithm into user-friendly geospatial software that allows visualization and saving of SWAT output to user-defined field boundaries. Field_SWAT has three major components: input data, display, and status/output. The input data component requires the user to define a base folder, identify the SWAT project folder, and provide the field boundary layer in polygon vector format. The display component requires the user to choose between annual sediment or annual runoff options, which are the only outputs that can be mapped using this tool. The status/output component allows the user to save the output maps in the form of shapefiles. The tool was tested by the authors in the agriculturally dominated Second Creek watershed in northeast Arkansas by mapping outputs from 218 HRUs to 89 field boundaries. Using visual and statistical results, the authors determined that the area-weighted spatial aggregation method resulted in the most suitable mapping between HRU and field outputs. The study demonstrated that Field_SWAT can be a useful tool for field-scale targeting of conservation practices by identifying critical NPS pollution areas in a watershed and enhancing communication between SWAT modelers and watershed managers.

2.4.1.5 Evaluation of Field-Scale Results by Relating HRUs to Fields by Matching HRU and Field Properties

Sinnathamby et al. (2017) developed a new crop parameter dataset for sweet sorghum and evaluated the ability of SWAT to simulate corn and grain sorghum yields under a range of ecoclimatic regions using field-scale crop yield data from two research sites. The authors calibrated the model for corn and grain sorghum yields using ten years of field data in Kansas by developing a watershed-scale SWAT model for the 4,800 ha watershed that included the research sites. They calibrated the model by evaluating HRU-level outputs from two HRUs that had similar soil, slope, and land use characteristics, one each for corn and grain sorghum. Corn and grain sorghum yields were validated using five years of yield data from a research site in Oklahoma. Similar to the calibration method, a watershed-scale SWAT model for a 12,767 ha watershed was developed that included the research site with observed data, and two HRUs were selected that matched the research fields. Calibrated crop parameters from the Kansas site were used for model validation. Overall, SWAT was able to simulate corn, grain sorghum, and sweet sorghum yields reasonably over a range of climatic conditions. Results showed that calibration improved model performance for corn and grain sorghum yield simulation. Validation of the crop parameters showed improvement in corn yield but no improvement in sorghum yield, as the research site used for validation was influenced by drought and possibly had different management practices. The results also supported site-specific calibration for crop yields rather than using default or off-site calibrated parameters to minimize the effects of different soil, water, and nutrient management conditions.

Uribe et al. (2018) assessed the impact of intensive tillage (IT) and conservation tillage (CT) on runoff, sediment, TN, and TP yield at field and watershed scales in the 784 km^2 Fuquene Lake watershed in Colombia. The watershed was divided into 30 subbasins and five slope classes (0% to 5%, 5% to 15%, 15% to 25%, 25% to 45%, and >45%). Evaluation at the field scale was

performed by selecting HRUs that had similar slope, soil, and land use characteristics in a subbasin that corresponded spatially to where the observed plots were located in the watershed. Model calibration and validation were performed at two spatial levels. First, monthly streamflow was calibrated and validated using R^2, NSE, root mean square error (RMSE), and mean absolute error (MAE) (Moriasi et al., 2007) for four stream gauging stations located within the watershed. Next, the model was calibrated against plot-level data for surface runoff, sediment load, and NO_3 and soluble P concentrations using SWAT HRU outputs. Model results showed that the monthly streamflow predictions and calibration of nutrients and sediments were acceptable. At the plot level, assessment of the two tillage practices showed that CT reduced sediment and runoff by 46% and 27%, respectively, but increased TN and TP by 17% and 29%, respectively. Evaluation at the watershed scale showed that CT was able to reduce surface runoff and sediment by 11% and 26%, respectively. There was also a TP reduction of 18%, but TN increased by 2% at the watershed scale.

2.5 Benefits, Limitations, and Directions for Future Research

This literature review of field-scale SWAT modeling research identified multiple ways of setting up a field-scale SWAT model depending on the spatial scale of the research as well as the research questions to be addressed. Each method has its own advantages, limitations, and further research needs, which are detailed in the following paragraphs.

Simulation of an individual field using the single-HRU approach allows modelers to study complex hydrological and nutrient processes in more detail as well as evaluate the impacts of BMPs at the field scale. However, the single-HRU method allows only the single dominant or user-selected soil type in the field to be simulated and causes a loss in intra-field soil variability, which might otherwise be present. In addition, fields generally do not follow hydrological

boundaries, and calibration and validation of the hydrological and nutrient processes of an individual field using observed data should consider the uncertainty in the observed data pertaining to contributions from adjacent fields. Observed datasets used for field-scale calibration, including ET, soil moisture, or nutrients in runoff, that are measured at the field are also not readily available, and gathering these datasets can become expensive with the installation of instruments and sample analysis. Evaluation of soft data, such as satellite-based ET, LAI, soil moisture, and normalized difference vegetation index (NDVI), as potential datasets for field-scale calibration can be pivotal in simulating and evaluating fields for which observed datasets are not available.

The single-HRU method limits the number of crops grown in a field because a single HRU does not allow multiple crops to be grown simultaneously. The single-HRU method also does not allow hydrological or nutrient routing because SWAT allows routing only between subbasins, which could impact the evaluation of sediment and nutrient losses from a field, especially if the fields are large and flow routing could have an impact. Using SWAT to simulate a field as a small watershed rather than as a single HRU can be a potential method of field-scale SWAT simulation that preserves the intra-field soil and slope variability and allows multiple crops as well as flow and nutrient routing in the field. The importance of multi-objective calibration for hydrological and nutrient transport processes at the field scale for increasing model robustness has not been evaluated. However, field-scale simulation of a single field using SWAT provides an excellent opportunity to improve the trust of stakeholders, including farmers and landowners, in the model, as the model's outcome can be directly related to measurements that they see in their fields, and accurate field-scale simulation by SWAT can help increase stakeholder confidence in the model results. The method can also be an important tool for evaluating irrigation and nutrient

management BMP scenarios for water quantity and quality at the field scale, along with the effects on crop yield with detailed management practices.

Simulation of each field using a land use map with unique names for each field but preserving the intra-field soil heterogeneity and slope characteristics, if present, allows each field to be represented by a unique set of HRUs. This method of field-scale SWAT allows placing and evaluating multiple BMPs and growing multiple crops within a single field, if more than one HRU is created for a field, which is not possible with the single-HRU method at field or watershed scale. Identification and management scenario evaluation of CSAs for nutrient and sediment losses from a field can also be performed using this method. Field-level outputs can still be evaluated by combining the outputs from the HRUs that relate to any field in the simulated watershed. However, this method requires post-processing of model output for field-level evaluation, as the unique set of HRUs related to each field needs to be identified, and the outputs from each HRU need to be combined. The method can also potentially lead to the creation of a large number of HRUs if the simulated watershed is large with many fields and high soil and slope variability, leading to issues with model size and data post-processing.

Watershed-scale SWAT modeling with each field represented as a unique HRU is an important method for field-level targeting of BMPs as well as for implementing different management practices in separate fields with the same land use, soil, and slope characteristics within the same subbasin, which would have been lumped together in the conventional HRU definition process. Each field in this method is simulated as a single HRU by creating a unique land use and dominant soil type for each field in the simulated watershed. However, as in the single-HRU method for simulating a single field, use of a single soil type for each field to be simulated as an HRU can lead to loss of soil variability within a field and mask or eliminate small areas that have high

potential for soil erosion (Kalcic et al., 2015) and nutrient loss. The method is also limited to only one slope characteristics within a field, which can potentially lead to error in the simulation and representation of field conditions when a field has multiple slopes. Loss of important land cover sections within a field, such as grassland or forested buffers, to simulate the field as a single HRU can also lead to inaccurate simulation of surface and subsurface components, as shown by Bosch et al. (2010), which can lead to inaccuracies in simulating the field hydrological and nutrient transport processes.

Calibration and validation of watershed-scale SWAT models with each field simulated as an individual HRU or as a set of unique HRUs are often performed at the watershed outlet, while the outputs are evaluated at the HRU level, which can lead to uncertainty in the model output. Use of soft data in evaluating model-simulated outputs at the HRU level, at least in critical HRUs identified from the initial model analysis, can help improve the accuracy of model outputs at the field or HRU level. Missing spatial references for HRUs and routing water, nutrients, sediments, bacteria, and pesticides within a subbasin are still issues with SWAT and are not addressed by the use of either method.

The post-processing tools developed by Daggupati et al. (2011) and Pai et al. (2012) allow evaluation of field-level outputs using SWAT HRU outputs from a conventionally developed SWAT model, which can greatly reduce model setup time because manual development of land use or soil maps and tables is not required for delineating the HRUs required when simulating each field as a single HRU. However, the method does not allow simulating and evaluating field-specific BMP applications, as fields with the same land use and soil can still be lumped into one HRU within a subwatershed during model setup. This method was also evaluated for field-level outputs from SWAT HRU outputs, but the method was not evaluated for its accuracy by comparing

it to field observations, which can lead to uncertainty in model output. Use of soft data for the evaluation of post-processed output at field level can, again, be helpful in improving model simulation and post-processed model outputs. Daggupati et al. (2011) mentioned that the quality of input data can greatly influence critical areas for sediment loss and could easily lead to incorrect field-level targeting, thus making evaluation with field observations even more important. Both post-processing tools only prepare annual field-level outputs, and improvement to the tools might be required if intra-annual evaluations are desired.

Although field-scale evaluations can be done by relating HRUs defined using the conventional method to fields by using land use, soil, and slope characteristics, the method can be limited in its use. Field-specific BMP application and management practice data are critical for evaluating the impacts of BMPs and management practices on water quantity and quality, but field-specific BMP applications cannot be simulated using this method, as fields with the same land use, soil, and slope are lumped into one HRU, and there is no exclusive relationship between a field and an HRU. Lumping of fields also prevents simulation of field-specific management practices

2.6 References

Alexander, C. A. (1988). ADAPT-A model to simulate pesticide movement into drain tiles. MS thesis. Columbus, OH: Ohio State University, Department of Agricultural Engineering.

Anand, S., Mankin, K. R., McVay, K. A., Janssen, K. A., Barnes, P. L., & Pierzynski, G. M. (2007). Calibration and validation of ADAPT and SWAT for field-scale runoff prediction. *JAWRA, 43*(4), 899-910. https://doi.org/10.1111/j.1752-1688.2007.00061.x

Arabi, M., Frankenberger, J. R., Engel, B. A., & Arnold, J. G. (2008). Representation of agricultural conservation practices with SWAT. *Hydrol. Proc., 22*(16), 3042-3055. https://doi.org/10.1002/hyp.6890

Arnold, J. G., Allen, P. M., Volk, M., Williams, J. R., & Bosch, D. D. (2010). Assessment of different representations of spatial variability on SWAT model performance. *Trans. ASABE, 53*(5), 1433-1443. https://doi.org/10.13031/2013.34913

Arnold, J. G., Srinivasan, R., Muttiah, R. S., & Williams, J. R. (1998). Large area hydrologic modeling and assessment: Part I. Model development. *JAWRA, 34*(1), 73-89. https://doi.org/10.1111/j.1752-1688.1998.tb05961.x

Arnold, J. G., Williams, J. R., Nicks, A. D., & Sammons, N. B. (1990). *SWRRB: A basin-scale simulation model for soil and water resources management*. College Station, TX: Texas A&M University Press.

Arnold, J. G., Youssef, M. A., Yen, H., White, M. J., Sheshukov, A. Y., Sadeghi, A. M., ... Gowda, P. H. (2015). Hydrological processes and model representation: Impact of soft data on calibration. *Trans. ASABE, 58*(6), 1637-1660. https://doi.org/10.13031/trans.58.10726

Bosch, D. D., Arnold, J. G., Volk, M., & Allen, P. M. (2010). Simulation of a low-gradient coastal plain watershed using the SWAT landscape model. *Trans. ASABE, 53*(5), 1445-1456. https://doi.org/10.13031/2013.34899

Capel, P. D., McCarthy, K. A., Coupe, R. H., Grey, K. M., Amenumey, S. E., Baker, N. T., & Johnson, R. L. (2018). Agriculture: A river runs through it: The connections between agriculture and water quality. USGS Circular 1433. Reston, VA: U.S. Geological Survey. https://doi.org/10.3133/cir1433

Chen, Y., Marek, G. W., Marek, T. H., Brauer, D. K., & Srinivasan, R. (2017). Assessing the efficacy of the SWAT auto-irrigation function to simulate irrigation, evapotranspiration, and crop response to management strategies of the Texas High Plains. *Water, 9*(7), 509. https://doi.org/10.3390/w9070509

Chen, Y., Marek, G. W., Marek, T. H., Brauer, D. K., & Srinivasan, R. (2018). Improving SWAT auto-irrigation functions for simulating agricultural irrigation management using long-term lysimeter field data. *Environ. Model. Software, 99*, 25-38. https://doi.org/10.1016/j.envsoft.2017.09.013

Daggupati, P., R. Douglas-Mankin, K., Y. Sheshukov, A., L. Barnes, P., & L. Devlin, D. (2011). Field-level targeting using SWAT: Mapping output from HRUs to fields and assessing limitations of GIS input data. *Trans. ASABE, 54*(2), 501-514. https://doi.org/10.13031/2013.36453

de Almeida Bressiani, D., Gassman, P. W., Fernandes, J. G., Garbossa, L. H., Srinivasan, R., Bonumá, N. B., & Mendiondo, E. M. (2015). Review of Soil and Water Assessment Tool (SWAT) applications in Brazil: Challenges and prospects. *Intl. J. Agric. Biol. Eng., 8*(3), 9-35.

Douglas-Mankin, K. R., Maski, D., Janssen, K. A., Tuppad, P., & Pierzynski, G. M. (2010). Modeling nutrient runoff yields from combined in-field crop management practices using SWAT. *Trans. ASABE, 53*(5), 1557-1568. https://doi.org/10.13031/2013.34914

Dubrovsky, N. M., Burow, K. R., Clark, G. M., Gronberg, J. M., Hamilton P., A., Hitt, K. J., ... Wilber, W. G. (2010). The quality of our nation's waters: Nutrients in the nation's streams and groundwater, 1992-2004. USGS Circular 1350. Reston, VA: U.S. Geological Survey.

Flanagan, D. C., Ascough, J. C., Nearing, M. A., & Laflen, J. M. (2001). The Water Erosion Prediction Project (WEPP) model. In *Landscape erosion and evolution modeling* (pp. 145-199). Boston, MA: Springer. https://doi.org/10.1007/978-1-4615-0575-4_7

Francesconi, W., Srinivasan, R., Perez-Minana, E., Willcock, S. P., & Quintero, M. (2016). Using the Soil and Water Assessment Tool (SWAT) to model ecosystem services: A systematic review. *J. Hydrol., 535*, 625-636. https://doi.org/10.1016/j.jhydrol.2016.01.034

Gassman, P. W., Reyes, M. R., Green, C. H., & Arnold, J. G. (2007). The Soil and Water Assessment Tool: Historical development, applications, and future research directions. *Trans. ASABE, 50*(4), 1211-1250. https://doi.org/10.13031/2013.23637

Ghebremichael, L. T., Veith, T. L., & Watzin, M. C. (2010). Determination of critical source areas for phosphorus loss: Lake Champlain basin, Vermont. *Trans. ASABE, 53*(5), 1595-1604. https://doi.org/10.13031/2013.34898

Ghebremichael, L. T., Veith, T. L., Hamlett, J. M., & Gburek, W. J. (2008). Precision feeding and forage management effects on phosphorus loss modeled at a watershed scale. *J. Soil Water Cons., 63*(5), 280-291. https://doi.org/10.2489/jswc.63.5.280

Gitau, M. W., J. Gburek, W. J., & Bishop, P. L. (2008). Use of the SWAT model to quantify water quality effects of agricultural BMPs at the farm-scale level. *Trans. ASABE, 51*(6), 1925-1936. https://doi.org/10.13031/2013.25398

Gitau, M. W., Veith, T. L., & Gburek, W. J. (2004). Farm-level optimization of BMP placement for cost-effective pollution reduction. *Trans. ASAE, 47*(6), 1923-1931. https://doi.org/10.13031/2013.17805

Her, Y., Frankenberger, J., Chaubey, I., & Srinivasan, R. (2015). Threshold effects in HRU definition of the Soil and Water Assessment Tool. *Trans. ASABE, 58*(2), 367-378. https://doi.org/10.13031/trans.58.10805

Kalcic, M. M., Chaubey, I., & Frankenberger, J. (2015). Defining Soil and Water Assessment Tool (SWAT) hydrologic response units (HRUs) by field boundaries. *Intl. J. Agric. Biol. Eng., 8*(3), 69-80.

Knisel, W. G. (1980). CREAMS: A field-scale model for chemicals, runoff, and erosion from agricultural management systems (No. 26). Washington, DC: USDA Science and Education Administration.

Krysanova, V., & Arnold, J. G. (2008). Advances in ecohydrological modeling with SWAT: A review. *Hydrol. Sci. J., 53*(5), 939-947. https://doi.org/10.1623/hysj.53.5.939

Leonard, R. A., Knisel, W. G., & Still, D. A. (1987). GLEAMS: Groundwater loading effects of agricultural management systems. *Trans. ASAE, 30*(5), 1403-1418. https://doi.org/10.13031/2013.30578

Marek, G. W., Gowda, P. H., Evett, S. R., Louis Baumhardt, R., Brauer, D. K., Howell, T. A., ... Srinivasan, R. (2016). Calibration and validation of the SWAT model for predicting daily ET over irrigated crops in the Texas High Plains using lysimetric data. *Trans. ASABE, 59*(2), 611-622. https://doi.org/10.13031/trans.59.10926

Maski, D., Mankin, K. R., Janssen, K. A., Tuppad, P., & Pierzynski, G. M. (2008). Modeling runoff and sediment yields from combined in-field crop practices using the Soil and Water Assessment Tool. *J. Soil Water Cons., 63*(4), 193-203. https://doi.org/10.2489/jswc.63.4.193

Merriman, K. R., Russell, A. M., Rachol, C. M., Daggupati, P., Srinivasan, R., Hayhurst, B. A., & Stuntebeck, T. D. (2018). Calibration of a field-scale Soil and Water Assessment Tool (SWAT) model with field placement of best management practices in Alger Creek, Michigan. *Sustainability, 10*(3), 851. https://doi.org/10.3390/su10030851

Moriasi, D. N., Arnold, J. G., Van Liew, M. W., Bingner, R. L., Harmel, R. D., & Veith, T. L. (2007). Model evaluation guidelines for systematic quantification of accuracy in watershed simulations. *Trans. ASABE, 50*(3), 885-900. https://doi.org/10.13031/2013.23153

Neitsch, S. L., Arnold, J. G., Kiniry, J. R., & Williams, J. R. (2011). Soil and Water Assessment Tool theoretical documentation Ver. 2009. College Station, TX: Texas Water Resource Institute.

Pai, N., Saraswat, D., & Srinivasan, R. (2012). Field_SWAT: A tool for mapping SWAT output to field boundaries. *Comput. Geosci., 40*, 175-184. https://doi.org/10.1016/j.cageo.2011.07.006

Sinnathamby, S., Douglas-Mankin, K. R., & Craige, C. (2017). Field-scale calibration of crop-yield parameters in the Soil and Water Assessment Tool (SWAT). *Agric. Water Mgmt., 180*, 61-69. https://doi.org/10.1016/j.agwat.2016.10.024

Teshager, A. D., Gassman, P. W., Secchi, S., Schoof, J. T., & Misgna, G. (2016). Modeling agricultural watersheds with the Soil and Water Assessment Tool (SWAT): Calibration and validation with a novel procedure for spatially explicit HRUs. *Environ. Mgmt., 57*(4), 894-911. https://doi.org/10.1007/s00267-015-0636-4

Tuppad, P., R. Douglas-Mankin, K., Lee, T., Srinivasan, R., & G. Arnold, J. (2011). Soil and Water Assessment Tool (SWAT) hydrologic/water quality model: Extended capability and wider adoption. *Trans. ASABE, 54*(5), 1677-1684. https://doi.org/10.13031/2013.39856

Uribe, N., Corzo, G., Quintero, M., van Griensven, A., & Solomatine, D. (2018). Impact of conservation tillage on nitrogen and phosphorus runoff losses in a potato crop system in Fuquene watershed, Colombia. *Agric. Water Mgmt., 209*, 62-72. https://doi.org/10.1016/j.agwat.2018.07.006

van Griensven, A., Ndomba, P., Yalew, S., & Kilonzo, F. (2012). Critical review of SWAT applications in the upper Nile basin countries. *Hydrol. Earth Syst. Sci., 16*(9), 3371-3381. https://doi.org/10.5194/hess-16-3371-2012

Veith, T. L., Sharpley, A. N., Weld, J. L., & Gburek, W. J. (2005). Comparison of measured and simulated phosphorus losses with indexed site vulnerability. *Trans. ASAE, 48*(2), 557-565. https://doi.org/10.13031/2013.18330

Williams, J. R., Izaurralde, R. C., Singh, V. P., & Frevert, D. K. (2006). The APEX model. *Watershed Models*, 437-482.

Williams, J. R., Jones, C., Kiniry, J. R., & Spanel, D. A. (1989). The EPIC crop growth model. *Trans. ASAE, 32*(2), 497-511. https://doi.org/10.13031/2013.31032

Winchell, M., Srinivasan, R., Diluzio, M., & Arnold, J. G. (2013). ArcSwat interface for SWAT 2012: User's guide. Temple, TX: Texas AgriLife Research, Blackland Research Center.

Young, R. A., Onstad, C. A., Bosch, D. D., & Anderson, W. P. (1989). AGNPS: A nonpoint-source pollution model for evaluating agricultural watersheds. *J. Soil Water Cons., 44*(2), 168-173.

Chapter 3

Multi-Variable Sensitivity Analysis, Calibration, and Validation of a Field-Scale SWAT Model: Building Stakeholder Trust in Hydrologic and Water Quality Modeling

3.1 Abstract

Multi-variable calibration of a field-scale Soil and Water Assessment (SWAT) model is critical for understanding the true impacts of irrigation and nutrient best management practices on hydrology, water quality, and agricultural productivity, and for building stakeholder trust for its eventual implementation at the watershed scale. This study evaluated the ability of the SWAT model to simulate runoff, soil moisture, cotton and peanut yield, and nitrate in conventionally- and strip-tilled plots while also evaluating the differences in hydrological and nutrient simulation parameters in the two tillage practices. Modeling results showed that SWAT can adequately simulate runoff, soil moisture, cotton and peanut yield, and nitrate at the field scale and that calibrated values for the Curve Number Of Operation (CNOP) were different for the conventionally- and strip-tilled plots and critical to runoff calibration. We found that it was also important to change the routing method from Variable Storage to Muskingum and adjust DIS_STREAM for runoff simulation if the fields were to be simulated as a watershed rather than as an HRU. Sequential calibration of surface runoff, soil moisture, crop yield, and nitrate showed that crop yield can be an important consideration for improving SWAT model robustness in nutrient transport simulations. Soil moisture calibration did not have a significant effect on runoff simulations. Evaluation of the impacts of different management scenarios showed that soil moisture sensor-based irrigation, cover crop, and strip tillage had the highest potential for reducing nutrient loss and conserving water while maintaining agricultural productivity in South GA. The

study also demonstrated to stakeholders that the SWAT model can successfully quantify the impacts of different management scenarios on their farm fields.

3.2 Introduction

Elevated levels of nitrogen and phosphorus in the rivers, streams, and shallow groundwater of the United States, especially in agricultural watersheds, is an important concern for aquatic life and human health. Concentrations exceeding 2 to 10 times regional limits set by the U.S. Environmental Protection Agency (USEPA) indicate that substantial changes in land use management and agricultural practices are needed to reduce nutrient loadings to surface and groundwater systems (Dubrovsky et al., 2010). Along with nutrient loss reduction, irrigation water management is crucial for agriculture sustainability and conservation of surface and subsurface water resources. Agricultural Best Management Practices (BMPs), which include nutrient management, cover crops, conservation tillage, and buffers, among others, are important tools for reducing water quality and quantity impacts in agricultural watersheds (Prokopy et al., 2008). Many field and watershed scale models have been utilized for evaluating the impacts of BMPs including Dynamic Watershed Simulation Model (DWSM), Water Erosion Prediction Project (WEPP), Annualized Agricultural NonPoint Source model (AnnAGNPS), Revised Universal Soil Loss Equation Version 2 (RUSLE2), Environmental Policy Integrated Climate (EPIC), Agricultural Policy/Environmental eXtender (APEX) and Soil and Water Assessment Tool (SWAT) (Arnold et al., 1998; Bingner et al., 2015; D K Borah et al., 2002; Flanagan et al., 2001; Foster et al., 2002; Williams et al., 1989, 2006). Among these, SWAT is arguably the most widely used model, especially at the watershed scale.

SWAT is a physically-based, watershed-scale, continuous-time, semi-distributed, quasi process-based model designed for the simulation of flow, sediment, nutrient, and pesticide transport from

predominantly agricultural watersheds (Neitsch et al., 2011). The model has been evaluated and applied extensively for simulation of a wide range of watershed problems (Gassman et al., 2007) including evaluation of BMPs at the field scale (Y Chen et al., 2017; Gitau et al., 2008; Maski et al., 2008) and watershed scales (Her et al., 2016; Ni and Parajuli, 2018; Uribe et al., 2018).

Although field and watershed models have been used for decades to address a variety of water quality and quantity problems, stakeholder trust in models is still low and scientific findings are often rejected when demonstrating a need of unpopular decisions (Voinov and Gaddis, 2008). This can also be said to be true for the SWAT model. Demonstrating that SWAT can simulate the farm/field scale processes well under different BMPs can be critical to increase stakeholder trust in a model and for the eventual evaluation of BMP application at watershed scale for water quantity and quality protection. In the SWAT model, the basic unit for all calculations is the hydrologic response unit (HRU), which are lumped land areas with a unique combination of land cover, soil, and/or slope class within a sub-watershed delineated based on thresholds defined by the modeler. As a result, HRUs do not have spatial orientation, and multiple fields within a sub-watershed can be represented by a single HRU. This can make it difficult to apply as well as evaluate the impacts of conservation practices at the field level as fields similar in land use, soil, and slope within a sub-watershed can have different management practices. As BMPs are implemented at the field/farm scale, it is important to evaluate the ability of SWAT to simulate the hydrological and nutrient processes at the field scale and present the model outputs to farmers, land-owners, and other stakeholders at this scale in order to build stakeholder trust in models. As a consequence, there have been recent studies evaluating the hydrological, sediment, and nutrient processes of SWAT using a field/plot scale SWAT model as well as the evaluation of watershed-scale SWAT model outputs at field-scale (Anand et al., 2007; Daggupati et al., 2011; Kalcic et al., 2015; Pai et al.,

2012). Merriman et al. (2018) identified critical sources areas for highest runoff, erosion, and nutrient losses as well as evaluated the impacts of BMPs at the field and watershed scales by setting up the SWAT model such that each field was represented by an individual HRU. Kalcic et al. (2015), Gitau et al. (2008), Teshager et al. (2016), and Ghebremichael et al. (2010) conducted similar studies where they set up the SWAT model such that each HRU represented a unique field in the watershed. Maski et al. (2008) evaluated the effects of conventional tillage and no-tillage management practices on a sorghum-soybean rotation for runoff and sediment yield from three plots with each plot simulated as an individual HRU, while Chen et al. (2017) investigated the auto-irrigation function of the SWAT model by simulating the experimental field as a single HRU. Daggupati et al. (2011) and Pai et al. (2012) developed post-processing tools that utilized SWAT outputs from a watershed-scale model to evaluate individual fields.

Most field-scale SWAT studies for BMP evaluation have used only a single hydrologic (surface runoff) and/or nutrient (nutrient concentrations in surface runoff) variable for model calibration. This approach can often provide good model performance results by compensating for errors in model simulation with erroneous simulation of other hydrological and nutrient variables that are not calibrated. Calibration and validation strategy using multiple variables can help reduce parameter uncertainty as well as the problem of equifinality as fewer sets of calibration parameters can satisfy the calibration criterion due to interaction among other parameters (Daggupati et al., 2015) and thereby increase model robustness. It is also important to note that many BMP evaluation studies using SWAT at the field-scale have not considered crop yield (Douglas-Mankin et al., 2010; Maski et al., 2008; Merriman et al., 2018), which is an important consideration for farmers looking to implement management practices, especially when the BMPs involve nutrient and irrigation management. Availability of long-term runoff, soil moisture, crop yield, and

nutrients in surface runoff data along with detailed management practice data for two experimental plots in a cotton-peanut rotation at the University of Georgia farms in Tift County, Georgia (GA) presented a unique opportunity for evaluating the importance of multi-variable calibration in the simulation of hydrological (using surface runoff and soil moisture) and nutrient (using crop yield, and nutrient in surface runoff) processes at the field scale using SWAT for BMP evaluation. This can be critical in evaluating the environmental and/or economic trade-offs of implementing agricultural BMPs that focuses on nutrient and irrigation management for reducing nutrient loss from agricultural fields and water conservation as these BMPs can impact crop yield and thereby provide critical information to stakeholders. As the two experimental plots are in conventional and strip tillage, the study also provided the opportunity to evaluate the differences in parameterization in simulating runoff and nutrients in fields under the two tillage practices at field scale.

Cotton and peanut are the 2nd and 4th ranked agricultural commodities in the state of GA accounting for about 12.5% of the total agricultural economy (University of Georgia CAES, 2018). Since a wide range/level of irrigation, nutrient, and tillage management operations are being practiced by farmers for cotton and peanut production in GA, understanding their effects on irrigation water use, crop yield, and nutrient losses is critical for farmers and stakeholders for protecting water quality and reducing water use while optimizing crop yield. Three different nutrient, irrigation, and tillage management practices that represent a wide range of cotton and peanut production practices in GA were also evaluated to determine the ability of the SWAT model to simulate crop yield, irrigation water use, and nutrient loss at the field-scale under different management practices.

There were two main objectives of this study. The first objective was to quantify model accuracy, evaluating the importance of multi-variable calibration in improving runoff and nutrient simulation

including crop yield. The second objective was to quantify the effect of different levels of management practices on crop yield, irrigation water use, and nutrient loss at the field scale for cotton and peanut production.

3.3 Methods

3.3.1 Study Area

The two experimental plots that were simulated in this study are located in the University of Georgia research farm in Tift County (31^{o} 26’ 13”N, 83^{o} 35’ 17”W) in south-central GA, USA (Fig. 3.1). The two plots have been utilized for multiple long-term studies including studying the effects of tillage and slope position on field-scale hydrologic processes (Bosch et al., 2012), effects of conservation tillage on hydrology and water quality in the coastal plains (Bosch et al., 2005, 2015), APEX calibration and validation for water and herbicide transport (Plotkin et al., 2013), and sediment loss and runoff in a coastal plain landscape (Endale et al., 2014). Plots 1 and 2 (Fig. 3.1) were selected from a set of six experimental plots due to the availability of soil moisture data for these plots. The average annual precipitation of this area is 1209 mm and the average daily maximum and minimum temperatures are 25^{o}C and 15^{o}C, respectively. Of the two plots, one was under conventional tillage (referred to herein as Plot1), and the second one was under strip tillage (referred to herein as Plot2) (. 1). The total drainage area was approximately 0.18 ha and the total planted area was approximately 0.14 ha for both plots 1 and 2. Interceptor drains were installed upslope of the two plots and between the plots, and earthen berm of 0.6 m were installed around each plot to keep the plots hydrologically isolated. H flumes and autosamplers were installed at each plot to measure flow and to collect flow-weighted composite samples for water quality analyses (Fig. 3.1). Plot2 consisted of Tifton sandy loam soil while Plot1 consisted of Tifton loamy

sand and Carnegie sandy loam soils. Both soils are deep and well drained and have moderate available water capacity (AWC) (USDA-NRCS, 1983).

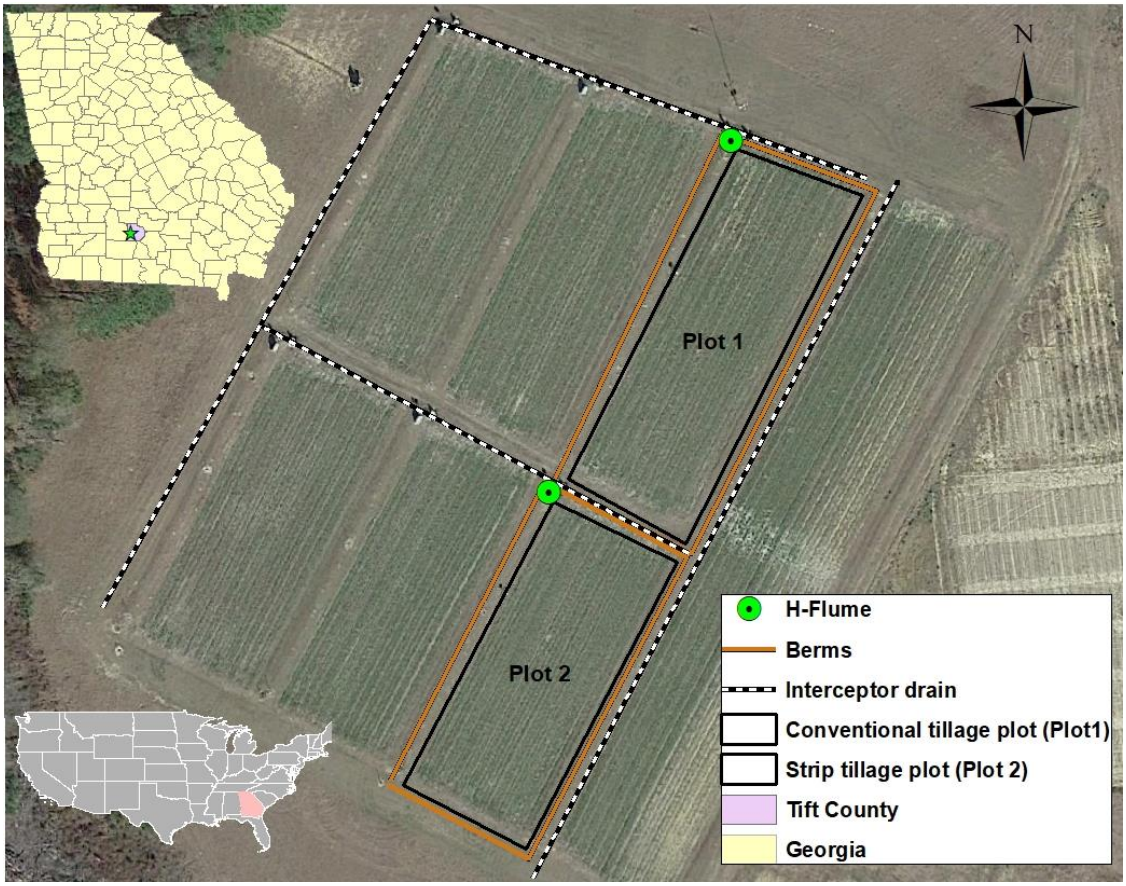

Figure 3.1 Experimental plots 1 and 2 at the University of Georgia research farm used for this study. Also shown are the location of the experimental farm in Georgia, surface flow and water quality data collection points (i.e., H-flume), and berms and interceptor drains that isolate each plot horizontally and vertically.

Both fields were under a cotton and peanut rotation and had the same management practices except for tillage operations. Table 3.1 summarizes the crop rotation, cover crop, planting and harvest dates, total irrigation and fertilizer application for both the plots from 1999 to 2006.

Table 3.1 Crop rotation, fertilizer application, cover crop, and planting and harvesting dates in the conventional tillage (Plot1) and strip tillage plots (Plot2) over the simulation period.

Year	Crop	Winter Cover Crop	Planting Date	Harvest Date	Irrigation (mm)	Precipitation (mm)	Fertilizer
1999	Cotton	Rye	5/6/1999	9/16/1999	67.05	915.67	Poultry litter - 4483 kg/ha N - 87 kg/ha
2000	Cotton	Rye	5/1/2000	9/14/2000	105.66	1041.9	Poultry litter - 4483 kg/ha N - 41.6 kg/ha
2001	Cotton	Rye	5/7/2001	10/5/2001	228.6	886.2	Poultry litter - 4483 kg/ha N - 97.65 kg/ha
2002	Peanut	Rye	5/9/2002	9/10/2002	177.8	1145.02	Poultry litter - 4483 kg/ha
2003	Cotton	Rye	5/12/2003	10/22/2003	25.4	1249.93	N - 104.8 kg/ha
2004	Peanut	Rye	5/10/2004	9/21/2004	127	1131.06	----------
2005	Cotton	Rye	5/23/2005	10/13/2005	50.74	1486.66	Poultry litter - 4483 kg/ha N - 107.9 kg/ha
2006	Peanut	Rye	5/15/2006	10/2/2006	50.8	1120.65	----------

3.3.2 SWAT model inputs

SWAT is a river basin or watershed scale, process-based, semi-distributed, continuous simulation model that predicts the effect of land management practices, land-use change, and climate on water, sediment, nutrient, crop yield, pesticide, and bacteria in complex watersheds (Neitsch et al., 2011). As discussed above, although SWAT is a watershed scale model, to increase stakeholder trust in SWAT and for its eventual application at the watershed scale for BMP evaluation and water quality protection, it is important to demonstrate that the model is simulating farm/field-scale processes well. As the major calculations in the SWAT at the HRU level incorporates processes from the CREAMS, GLEAMS, and EPIC models (Neitsch et al., 2011), which are applicable at the field/farm scale, SWAT can also be used to simulate small fields. Major inputs to the SWAT, irrespective of the model scale, includes topographic, climate, land-use, soils, and management practices.

As fine-scale topographic elevation dataset that represented the manual changes to experimental plots due to the construction of berms were not available for use in the model setup, 10 m digital elevation model (DEM) dataset was acquired from the United States Geological Survey (USGS) (Gesch et al., 2002) and modified so that the topographic changes could be represented and each field could be simulated as an independent sub-basin. The average slope steepness for the HRU was also provided to the model (.hru) based on field calculation. The field-scale SWAT model was set up using conventional SWAT model watershed delineation steps (Winchell et al., 2013), unlike the single HRU delineation method employed by Maski et al. (2008) and Chen et al. (2017) that represented each field using only a single HRU. This allowed for the surface runoff routing and soil heterogeneity to be preserved. Daily precipitation and temperature data were recorded on-site while the other weather variables required for the model including wind speed, relative humidity, and solar radiation were acquired from a station located 8.3 km from the site and maintained by the Georgia Automated Environmental Monitoring Network in Tifton, GA. Detailed management practices of the two plots including fertilizer and irrigation application, planting and harvest dates, tillage operations, cover crop planting and kill operations were available to set up the management file (.mgt) for the two plots in the model. Base soil data for the two experimental plots were obtained from the Soil Survey Geographic (SSURGO) database (USDA-NRCS, 2019).

Soil moisture data in the experimental plots were collected using Stevens Water Monitoring Systems Inc., (Portland, OR) installed at depths of 51, 127, and 305 mm beneath the soil surface. The probes collected soil moisture data every 30 minutes which were averaged to produce daily averages for depth intervals of 0-85 mm, 85-216 mm, and 216-305 mm. Hence, the base soil data downloaded from SSURGO was modified such that each soil moisture observed depth was represented as a layer in the SWAT soil input (.sol) file, which allowed for SWAT to simulate soil

moisture at depths consistent with field observation for evaluation. Figure 3.2A shows the DEM and resulting basin, subbasin, and reach (stream network) delineation for Plot1 and Plot2. Figures 3.2B and 3.2C, respectively, show the land-use and soil map for model setup.

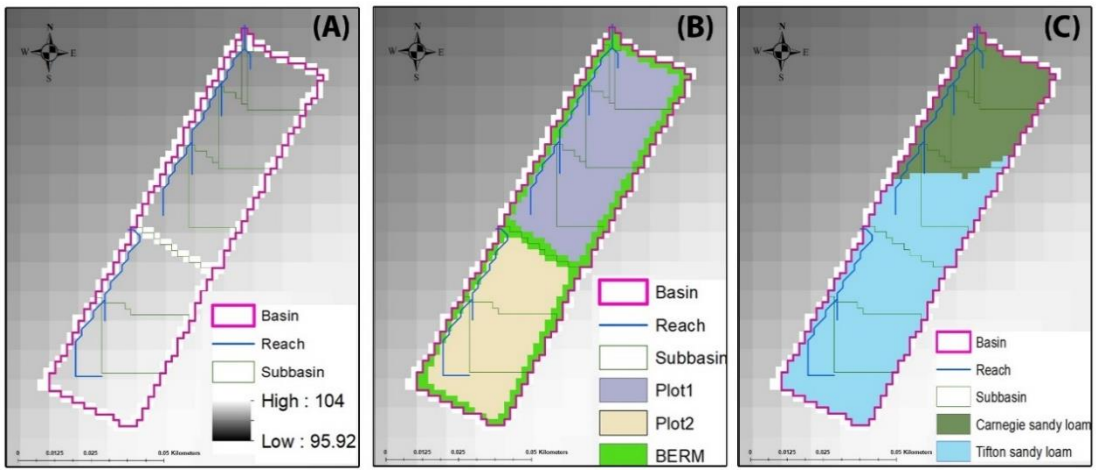

Figure 3.2 Subbasin and HRU delineation and stream network derived from DEM (A); land-use map of planting area for Plot1 and Plot2, and contributing area (B); and, soil map over the simulated watershed (C).

3.3.3 Model calibration and validation

The SWAT model was set up from 1999-2006 as climate, management, and runoff data were available for that period. A warm-up period of 3 years was set up by replicating the climate and management data from 1999-2001 to minimize loss of observed data for calibration and validation to warm-up. The model was calibrated and validated for surface runoff, soil moisture, crop yield, and nitrate in surface runoff. Plot1 and Plot2 were calibrated and validated separately as the observed hydrology was different for the two plots. The model was, however, calibrated and validated for crop yield by calibrating the model to the crop yield of Plot1 and validating to the crop yield of Plot2 as the same crop varieties were planted on both plots and only crop parameters were adjusted during crop yield calibration. This allowed for using a longer crop yield dataset for

model calibration. The model was calibrated using automated and manual techniques. Model parameters sensitivity analysis and automated calibration were conducted using the Sequential Uncertainty Fitting Algorithm – Version 2 (SUFI-2), an optimization and uncertainty analysis program that uses Latin hypercube sampling (Abbaspour et al., 2004), located within SWAT-CUP, an automated calibration and uncertainty program developed for SWAT (Abbaspour, 2013). Initial parameters selected for the automated calibration were based on literature (Arnold et al., 2012) and prior knowledge of the study area (Plotkin et al., 2013). The model was calibrated for sensitive model parameters in the sequential order of surface runoff, soil moisture, crop yield, and nitrate in surface runoff to first calibrate the hydrological processes followed by nutrient processes loosely following the sequence adopted by Nair et al. (2011) and Parajuli et al. (2013).

The model was calibrated for surface runoff from 1999-2002 and validated from 2003-2006 at a daily time step. Curve Number Of Operation (CNOP), which allows for adjusting the curve number according to planting or management operations, was used for calibrating surface runoff instead of CN2 which represents a general curve number for an HRU, irrespective of the management operation. CNOP was adjusted for each planting operation. This also allowed for optimizing CNOP values for cotton and peanut grown in conventional tillage and strip tillage separately, which was important for simulating management scenarios under conventional and strip tillage.

Soil moisture data were available only from 2001to 2006. Hence, the model was calibrated for soil moisture from 2001-2003 and validated from 2004-2006 at a daily time step. The model was calibrated for total soil moisture for the top 305 mm (combined soil moisture for the top 3 soil layers). The default configuration of SWAT allows for soil moisture simulation output to be printed only for the whole soil column in the output.hru file, which is utilized by SWAT-CUP for

the auto-calibration process. Hence, the SWAT source code was modified in the hruday.f90 subroutine and a new SWAT executable was compiled such that the total simulated soil moisture for the top 305 mm was exported as an additional variable in the hru output file, which was then utilized for automated soil moisture calibration through SWAT-CUP.

The crop growth module of SWAT simulates biomass accumulation and nutrient content in plant at various stages of crop growth along with crop yield at harvest at the end of the growing season (Neitsch et al., 2011). The model was calibrated for annual crop yield by calibrating for cotton and peanut yield separately. Cotton yield was calibrated using 5 years of yield data (1999, 2000, 2001, 2003, 2005) and peanut was calibrated using 3 years of yield data (2002, 2004, 2006) for Plot1. The model was validated against the observed crop yield of Plot2.

As the nitrate loading data in surface runoff were available from 2004-2006, the model was calibrated for nitrate from 2004-2005 and validated for 2006. Unlike surface runoff and soil moisture, nitrate was calibrated and validated at a monthly time scale.

Coefficient of determination (R^2), Nash-Sutcliffe efficiency (NSE), and percent bias (PBIAS) were the three objective functions used to optimize the model simulation and were also the statistical parameters utilized for model performance evaluation. R^2 describes the degree of collinearity between simulated and measured data. Value of R^2 ranges from 0 to 1 with values close to 1 indicating less error variance, and values greater than 0.5 are typically considered acceptable (Moriasi et al., 2015). NSE demonstrates how well the measured vs simulated plot fits the 1:1 line and determines the relative magnitude of the residual variance vs the measured data variance. Its value ranges from $-\infty$ to 1 with 1 indicating a perfect fit between simulated and measured data and values smaller than 0 indicating that the mean observed value is a better predictor than the

simulated value (Moriasi et al., 2015). PBIAS indicates the average tendency of the simulated data to be larger or smaller than the observed data. Optimal value of PBIAS is 0.0 and positive or negative values of PBIAS indicate bias, underestimation or overestimation, respectively (Moriasi et al., 2015).

3.3.4 Scenario Analysis

Three levels of management operations with varying levels of fertilizer and irrigation applications and tillage operations that represent the wide range of management practices observed in south GA were developed for a cotton-cotton-peanut rotation with suggestions and input from the University of Georgia (UGA) Extension. Management levels were developed for a cotton-cotton-peanut rotation as it is the most common rotation being practiced in GA for cotton and peanut.

Management level 1 (Mgt1) represents the most environmentally friendly practice with optimized fertilizer and irrigation water application with soil moisture sensor (SMS) based irrigation and UGA recommended fertilizer application, strip tillage, and cover crop. Management level 2 (Mgt2) represents the most common agricultural practices being practiced by farmers in south GA which includes UGA recommended fertilizer and irrigation application for both crops with conventional tillage and no cover crop, and Management level 3 (Mgt3) represents the operations with high fertilizer and irrigation application, conventional tillage and no cover crop. Details of the three management levels for cotton and peanut are presented in Table's 3.2 and 3.3, respectively.

Table 3.2 Description of the three management level scenarios for Cotton in South GA.

Cotton	Management level 1	Management level 2	Management level 3
Tillage	Strip tillage	Conventional tillage	Conventional tillage
Irrigation	Soil moisture sensor based	UGA checkbook based	Minimum 25.4 mm per week
Fertilizer	33.6 kg/ha N – starter	4483 kg/ha poultry litter before planting	4483 kg/ha poultry litter before planting
	78.6 kg/ha N- sidedress	78.6 kg/ha N- sidedress	33.6 kg/ha N - starter
			78.6 kg/ha N - sidedress
Cover crop	Rye	No cover crop	No cover crop

Table 3.3 Description of the three management level scenarios for Peanut in South GA.

Peanut	Management level 1	Management level 2	Management level 3
Tillage	Strip tillage	Conventional tillage	Conventional tillage
Irrigation	Soil moisture sensor based	UGA checkbook based	Minimum 25.4 mm per week
Fertilizer	----------	----------	4483 kg/ha poultry litter before planting
Cover crop	Rye	No cover crop	No cover crop

The three management level scenarios were simulated using the calibrated model over a 30-year historical climate data for the study area which was derived from the North American Land Data Assimilation System (NLDAS-2) climate forcing dataset. NLDAS-2 has a spatial resolution of $1/8^{th}$ degree covering the continental United States (CONUS) and is available at 1-hour temporal resolution (Xia et al., 2012).

The SMS based irrigation in Mgt1 scenario was simulated using the auto-irrigation feature available in SWAT. Auto-irrigation in SWAT can be triggered based on two water stress threshold: 1) plant water demand and 2) soil water content (Neitsch et al., 2011). Plant water demand threshold triggers irrigation when the plant experiences a user-defined reduction in plant growth and was used as the trigger for auto-irrigation in this study. Multiple simulation trials and comparison to typical irrigation amounts observed over the growing season using SMS in the region for cotton and peanut showed that a threshold of 0.6 for cotton and 0.7 for peanut provided the most reasonable irrigation values and was used in the scenario analysis. SWAT applies a

default value of 25.4 mm each time auto-irrigation is triggered which was also adjusted to 19.05 mm based on the recommendation from the UGA Extension office. To make sure that the auto-irrigation function triggered only during the growing season and not when the cover crop is growing, a new threshold of 0.1 was used after harvest. Evaluation of SWAT output showed no auto-irrigation application in the non-growing season with the adjusted threshold. The UGA checkbook irrigation method for Mgt2 estimates irrigation requirement for each week by calculating the difference in precipitation and plant water requirement for that week. Table 3.4 shows the plant water required for cotton and peanut based on UGA Extension recommendation (University of Georgia Extension, 2018; Whitaker et al., 2018). Irrigation scenario in Mgt3 was simulated such that a minimum of 25.4 mm of water was applied by a combination of precipitation and irrigation, except for weeks which had the crop water demand higher than 25.4 mm, and the corresponding values were matched. Strip tillage and conventional tillage were simulated by using the calibrated CNOP values of cotton, peanut, or rye.

Results from the long term simulation of the three management levels for the crop rotation allowed us to understand the differences in irrigation water use, nutrient loss, and crop yield at the farm/field-scale level which can provide critical information to farmers, decision-makers, and stakeholders regarding BMPs and cost-share programs that can be introduced to reduce the water quality and quantity impacts from agricultural fields.

Table 3.4 UGA recommended crop water demand for cotton and peanut.

Weeks after planting	Cotton water demand (mm/week)	Peanut water demand (mm/week)
1	1.1	2.1
2	4.5	6.5
3	7.3	10.0
4	10.3	13.9
5	14.3	19.3
6	18.0	24.0
7	21.7	27.6
8	27.4	32.8
9	32.6	37.8
10	37.3	40.4
11	38.5	40.2
12	36.3	38.0
13	36.1	37.4
14	33.8	32.9
15	29.4	29.4
16	22.4	24.6
17	17.6	21.2
18	12.9	17.0
19	9.0	12.4
20	5.5	7.5
21	3.0	3.5
22	1.3	0.4
23	0.5	0.0

3.4 Results and Discussion

The initial parameter and parameter ranges used for model sensitivity analysis to identify important parameters for calibration using SWAT-CUP are presented in Table 3.5. During automated and manual calibration, the calibrated model parameters (identified through sensitivity analysis) were made sure to be within a realistic uncertainty range typical of the management practices and land use.

Table 3.5 SWAT parameters and parameter ranges for initial sensitivity analysis for surface runoff, soil moisture, crop yield, and nitrate in surface runoff calibration.

Variable	Parameter	Description	SWAT input file	Adjustment [a]	Initial Range
Surface runoff	CNOP	Curve number Of operation, moisture condition II	HRU	r	-0.3,0.3
	ALPHA_BF	Baseflow alpha factor	GW	v	0.01,1
	GW_DELAY	Groundwater delay, days	GW	v	0, 500
	OV_N	Manning's "n for overland flow"	HRU	r	-0.3,0.3
	SURLAG	Surface runoff lag coefficient	BSN	v	1-20
	GWQMN	Threshold depth of water in shallow aquifer for required for return flow to occur	GW	v	0.01 – 5000
Soil moisture	SOL_K	Saturated hydraulic conductivity	SOL	r	-0.3,0.3
	SOL_BD	Moist bulk density	SOL	r	-0.3,0.3
	ESCO	Soil evaporation compensation factor	HRU	v	0.01,1
	SOL_AWC	Available water capacity of the soil layer	SOL	r	-0.3,0.3
Crop yield	BIO_E	Radiation use efficiency	Plant	r	-0.3,0.3
	HVSTI	Harvest index for optimal growing conditions	Plant	r	-0.3,0.3
	BLAI	Maximum potential leaf area index	Plant	r	-0.3,0.3
	WSYF	Lower limit of harvest index	Plant	r	-0.3,0.3
Nitrate	SOL_CBN	Amount of organic carbon in the soil layer	SOL	r	-0.3,0.3
	CMN	Rate coefficient of mineralization of active organic nutrients	BSN	r	-0.3,0.3
	RSDCO	Residue decomposition coefficient	BSN	r	-0.3,0.3
	NPERCO	Nitrate percolation coefficient	BSN	v	0.01,1
	SDNCO	Denitrification threshold water content	BSN	v	0.9,1.10
	CDN	Denitrification exponential rate coefficient	BSN	v	0,3

[a] Indicates the type of model parameter adjustment. 'r' represents the model parameter adjustment by multiplying the original parameter with the adjustment factor (1 + r). 'v' represents replacement of the original parameter value by a value within the initial range.

3.4.1 Surface runoff calibration and validation

Preliminary evaluation of simulated surface runoff before calibration showed small volumes of simulated runoff (@10^{-7} m^3/s) at the outlet of both plots for multiple days following precipitation when there was no flow observed in the plots. These volumes were below the level of detection of the instrumentation. Changing the default Variable Storage channel routing method, which is based on continuity equation, to Muskingum which uses a combination of wedge and prism storage

(Neitsch et al., 2011) simulated no flow conditions better and was used in the model. Along with adjusting the channel routing method, DIS_STREAM (average distance to the stream in .hru file), which has a default value of 35 m, was another important parameter that was adjusted to reduce simulated flow in days with no flow. Adjusting DIS_STREAM, however, did not have much effect on model performance as the simulated flows were very close to 0 in days with no observed flow. DIS_STREAM was adjusted to 15 m in Plot1 HRUs and 25 m in Plot2 HRUs after multiple iterations of manual adjustment. It is important to note that the adjustment of routing method and DIS_STREAM were influential in the flow routing simulation from within the field to the outlet.

Global sensitivity analysis results from SWAT-CUP showed CNOP (P-value < 0.0001) and GWQMN (P-value = 0.001) as the two sensitive parameters to surface runoff calibration in Plot1 and CNOP (P-value < 0.0001) and GW_DELAY (P-value = 0.0005) as the two parameters sensitive to surface runoff calibration in Plot2 from the initial parameters used in surface runoff calibration. It is important to note that surface runoff was not sensitive to baseflow alpha factor (ALPHA_BF) for either plot. Also, the calibrated GWQMN value for Plot1 was 3753 mm and GW_DELAY value for Plot2 was 42.4 days, which, although unrealistic, constrained the model to have no groundwater return flow contribution to streamflow. As a result, the total simulated streamflow consisted of contributions only from overland flow and lateral sub-surface flow, accurately representing the overland and lateral sub-surface flow dominated surface hydrology in the field plots. This also implied that surface and lateral flows are the important flow mechanisms that need to be considered for field-scale SWAT simulation.

Model performance evaluation after calibration showed that SWAT does a satisfactory job of simulating daily surface runoff in the conventionally tilled Plot1, with daily values of R^2 of 0.68, NSE of 0.64, and PBIAS of 4.90%, as well as in the strip-tilled Plot2 with a R^2 of 0.50, NSE of

0.49, and PBIAS of 1.50% (Table 3.7) based on the model performance metrics of Moriasi et al. (2015). Plot2 during the calibration period from 1999-2002 had very little runoff from 1999-2001 and exceptionally high runoff in 2002. This led to the model under-simulating runoff events in 2002 and over-simulating other years, producing a poor model performance for surface runoff simulation for Plot2 when compared to Plot1 (Fig. 3.3). It is significant to note that there were a number of particularly large events which occurred in 2002, beginning with 196 mm of rainfall occurring in July of that year followed by high precipitation in October and November of the same year (Endale et al., 2014). The model appeared to have difficulty representing these high surface runoff producing conditions following extended dry periods. Similar to Plot2, the model was not able to simulate the runoff events of July-Nov 2002 in Plot1 which was also not observed in the preceding July-Nov months of calibration although the precipitation and management operations for that time periods were similar (Fig. 3.3). This shows the importance of calibrating the model over a long climate period for the model to be able to simulate surface runoff under various weather conditions.

Simulated flow evaluation for the conventionally-tilled and strip-tilled plot shows that SWAT can adequately simulate surface hydrology in fields under both tillage operations. The calibrated CNOP values (Table 3.6), which was the most sensitive parameter for surface runoff calibration in both plots, were different for the two plots. This shows that selecting the right CNOP or CN2 values is critical for simulating the effects of strip tillage and conventional tillage on surface hydrology at the field scale.

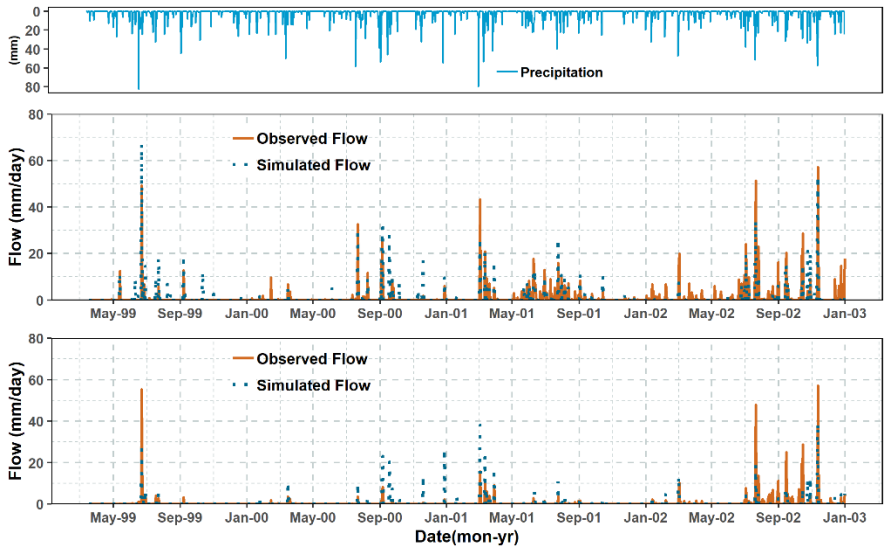

Figure 3.3 Precipitation (top), and Simulated vs Observed daily runoff for Plot1 (middle) and Plot2 (bottom) for the calibration period (1999-2002).

Table 3.6 Average CNOP values for Plot1 and Plot2 for different crops after calibration.

Adjusted CNOP	Default		Calibration	
	Plot1	Plot2	Plot1	Plot2
CNOP (Cotton)	83	83	86	75
CNOP (Peanut)	83	83	86	75
CNOP (Rye)	81	81	71	71

Model performance for surface runoff simulation during validation was similar to calibration for Plot1 with R^2 of 0.72, NSE of 0.59, and PBIAS of 4.00%. However, the model evaluation statistics were much improved for Plot2 with R^2 and NSE both equals to 0.83. PBIAS of -17.20% showed that the model over simulated runoff in the validation period while slightly under-simulated in the calibration period (Table 3.7). This also shows that the model was adequately parameterized for simulation of surface runoff in both fields. Larger precipitation events during validation having higher total rainfall than during calibration could have contributed to the model overestimating runoff in large precipitation events during validation in both fields (Fig. 3.4). This indicates that the model parameterization could be further improved with a longer calibration period with bigger

rainfall events. Successful calibration and validation of runoff simulation for the two fields also demonstrated that SWAT can adequately simulate flow routing even at the field scale although the flow routing methods and mechanisms in SWAT were ideally designed for large watersheds.

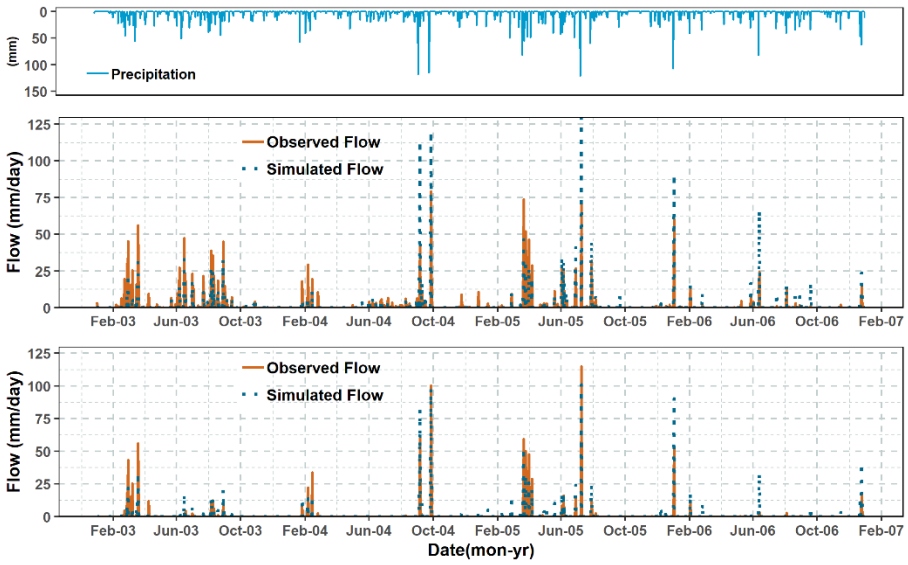

Figure 3.4 Precipitation (top), and Simulated vs Observed daily runoff for Plot1 (middle) and Plot2 (bottom) for the validation period (2003-2006).

Table 3.7 Model performance evaluation of surface runoff simulation for Plot1 and Plot2 during calibration (1999-2002) and validation (2003-2006).

Goodness of Fit Measure	Plot1		Plot2	
	Calibration	Validation	Calibration	Validation
R^2	0.68	0.72	0.50	0.83
NSE	0.64	0.59	0.49	0.83
PBIAS	4.9%	4.0%	1.5%	-17.2%

3.4.2 Soil moisture calibration and validation

Soil moisture is an important hydrologic variable driven by saturated and unsaturated flow conditions that can affect surface runoff, infiltration, crop growth, and other important processes. SWAT has a simplified module for soil moisture simulation that only simulates saturated soil water

flow between the multiple soil layers and uniformly distributes soil water within a given layer using a cascading approach. Soil water is allowed to percolate or move between soil layers only when the water quantity exceeds the field capacity for the layer (Neitsch et al., 2011). Global sensitivity analysis showed that soil moisture was sensitive to SOL_AWC, SOL_BD, SOL_K, and ESCO for both fields (P-value < 0.05). Unlike surface runoff, there is no recommended statistical performance measure for soil moisture evaluation. Evaluation of SWAT soil moisture simulation using remotely sensed data had R^2 ranging from 0.18 to 0.3 (Rajib et al., 2016). Cao et al. (2006) showed similar difficulty with simulating soil moisture when compared to observed soil moisture data.

Soil moisture simulation evaluation after the calibration of sensitive parameters (Table 3.8) at the field scale for Plot1 and Plot2 showed that SWAT was able to simulate soil moisture adequately for both plots capturing the daily trend well (Fig. 3.5 and 3.6; Table 3.9) demonstrating that SWAT can simulate soil moisture at the field level. The model was, however, not able to match the peak soil moisture conditions in both plots, especially during the non-growing season. The measured peak conditions represented rather short periods where the soil moisture exceeded field capacity, a condition the model is unable to represent. It is also important to note that the soil moisture was slightly under-simulated during validation in 2004 in Plot2 (Fig. 3.6), although it captured the trend well. As the observed soil moisture for Plot2 was lower than that observed in Plot1 even though Plot2 was in strip tillage which tends to enhance infiltration and increase the soil water holding capacity (Truman et al., 2003), calibration to observed soil moisture resulted in Plot2 having lower SOL_AWC values than Plot1 (Table 3.8). Lower observed soil moisture in Plot2 could have possibly resulted from the easy transfer of water to increased depths due to the absence of tillage pan as a result of reduced tillage operations in the strip tilled Plot2 along with the fact that enough

water must infiltrate to allow sorption into the highly aggregated soil that results from strip tillage. A sequential calibration approach was followed in which soil moisture was calibrated after surface runoff, and it was observed that although soil moisture calibration improved simulation of soil moisture, it did not have a considerable effect on the simulation of surface runoff, which was also noted by several other studies (Nilawar et al., 2017; Patil and Ramsankaran, 2017; Rajib et al., 2016). This tends to indicate the importance of the CNOP parameter relative to the soil moisture related parameters for runoff calibration.

Table 3.8 Adjusted .sol and .hru parameters for soil moisture calibration in Plot1 and Plot2.

Parameters	SWAT input file	Adjustment [a]	Plot 1		Plot 2	
			Initial	Calibrated	Initial	Calibrated
SOL_AWC	SOL	r	-0.3,0.3	0.26	-0.3,0.3	0.05
SOL_BD	SOL	r	-0.3,0.3	-0.12	-0.3,0.3	-0.02
SOL_K	SOL	r	-0.3,0.3	0.3	-0.3,0.3	0.21
ESCO	HRU	v	0.01,1	0.84	0.01,1	0.80

[a] Indicates the type of model parameter adjustment. 'r' represents the model parameter adjustment by multiplying the original parameter with the adjustment factor (1 + r). 'v' represents replacement of the original parameter value by a value within the initial range.

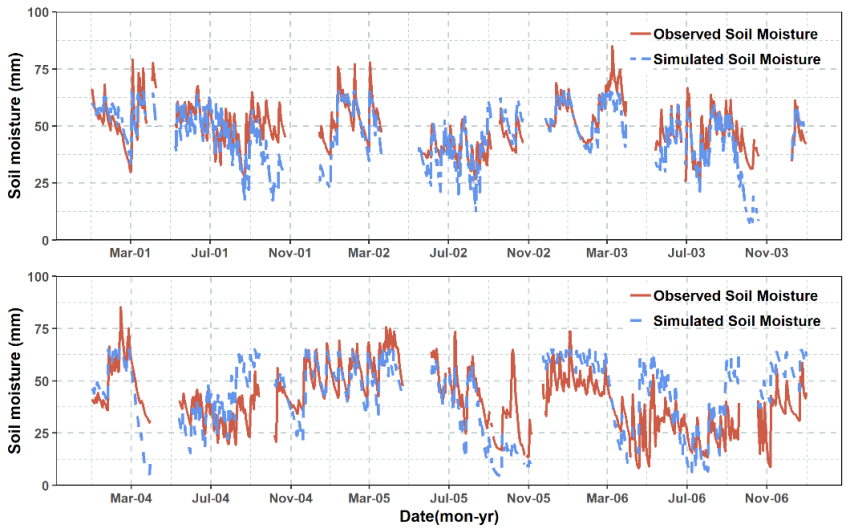

Figure 3.5 Comparison of daily simulated and observed soil moisture for Plot1 during calibration (top) and validation (bottom).

Table 3.9 Model performance evaluation of daily soil moisture simulation for Plot1 and Plot2 during calibration (2001-2003) and validation (2004-2006).

Goodness of Fit Measure	Plot1		Plot2	
	Calibration	Validation	Calibration	Validation
R^2	0.58	0.44	0.39	0.45
NSE	0.20	0.14	0.14	0.29
PBIAS	7.20%	-5.00%	1.70%	15.50%

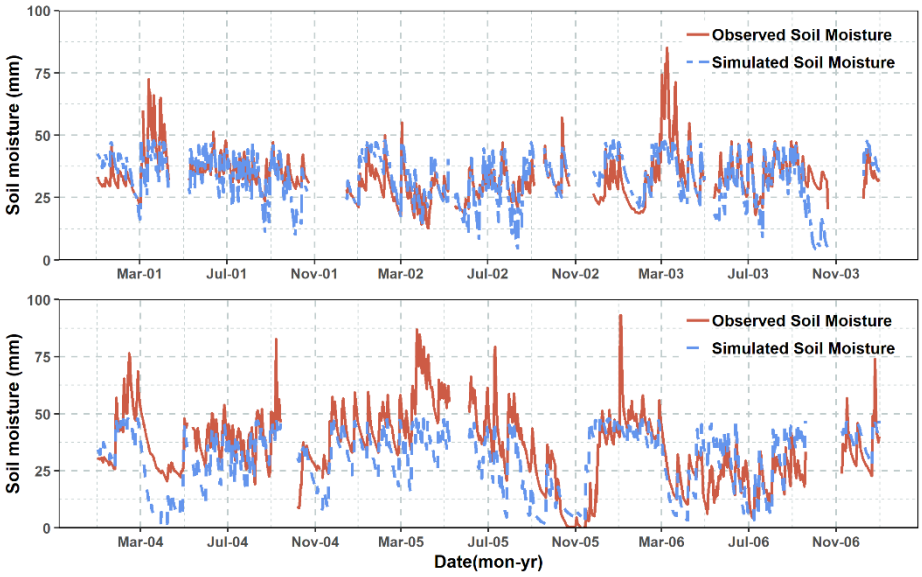

Figure 3.6 Comparison between simulated and observed soil moisture for Plot2 during calibration (top) and validation (bottom).

3.4.3 Crop yield calibration and validation

Global sensitivity analysis on the selected initial crop yield parameters showed that BIO_E, HVSTI, BLAI, and EPCO were the sensitive parameters for both cotton and peanut (P-value < 0.05), while WSYF was not sensitive for either crop (P-value = 0.47 (cotton); P-value = 0.33 (peanut)). Cotton and peanut yields were calibrated using observed yield data from Plot1, the calibrated parameter values for which are presented in Table 3.10. Statistical results showed satisfactory model performance in the simulation of cotton and peanut with R^2 of 0.41, NSE of 0.35 and PBIAS of -0.30%. Year-by-year analysis of crop yield during calibration (Fig. 3.7) shows that the model was able to simulate peanut much better than cotton as the annual percent discrepancy of peanut yield was less than 18% but was as high as 41% for cotton. Chen et al. (2016) and Mittelstet et al. (2015) reported similar difficulty in simulating irrigated cotton yields using SWAT. Cotton yield in 2000 is the only year when the percent discrepancy between simulated and observed yield was greater than 30% during calibration (Fig. 3.7). Assessment of

the field management practices showed that a much lower amount of nitrogen fertilizer (41.6 kg/ha) was applied when compared to other years (> 87 kg/ha) with cotton which could have resulted in the lower observed cotton yield. It seems SWAT was not able to replicate that N deficiency observed in the field which could have resulted in higher simulated yield for that year. Incomplete and variable boll opening of cotton in the plot leading to reduced observed cotton yield could also have contributed to the increased difference between the simulated and observed cotton yield.

Table 3.10 Adjusted plant and .hru parameter values for cotton and peanut yield calibration.

Parameters	SWAT input file	Cotton		Peanut	
		Initial	Calibrated	Initial	Calibrated
BIO_E	Plant	15	20.56	20	18.6
HVSTI	Plant	0.4	0.56	0.4	0.45
BLAI	Plant	4	4.59	4	5.25
EPCO	HRU	0.6	0.5	0.6	0.5

Figure 3.7 Comparison of simulated vs observed annual crop yields during calibration in Plot1 (top) and validation in Plot2 (bottom). Percentage indicates the difference between simulated and observed crop yield for each year.

Validation of the crop yield by using the calibrated parameters to simulate crop yield in Plot2 showed slightly better performance with R^2 of 0.48, NSE of 0.48, and PBIAS of 0.60%. Similar to the crop yield during calibration, peanut was simulated better than cotton and 2000 cotton yield had the highest discrepancy between simulated and observed yield. The percent discrepancy was less than 31% in all the other years. Evaluation of the difference between observed yields and simulated yields for Plot1 and Plot2 for each year shows that SWAT is able to simulate yield variability for cotton for the two plots much better than peanut (Table 3.11). The observed yield difference for peanut between the two plots was as high as 922.7 kg ha^{-1} in 2004 but the highest simulated yield difference was only 17.8 kg/ha. Hence, although SWAT could simulate the temporal variability of peanut, the model was not able to simulate the tillage impacts on peanut yield.

Table 3.11 Observed and simulated crop yield difference between Plot1 and Plot2 for each year.

Crop	Year	Observed crop yield difference between plots (kg/ha)	Simulated crop yield difference between plots (kg/ha)
Cotton	1999	209.5	-201.1
Cotton	2000	249.8	64.9
Cotton	2001	-218.0	26.4
Peanut	2002	-42.5	3.3
Cotton	2003	-124.3	267.3
Peanut	2004	-922.7	-17.8
Cotton	2005	256.8	85.4
Peanut	2006	315.1	-7.4

3.4.4 Nitrate calibration and validation

A review of multiple studies by Borah and Bera (2004) has shown that SWAT is more suitable for simulating nutrients at a monthly time scale and many of the studies with daily nutrient simulation had poor results. As a result, SWAT was calibrated and validated for nitrate loading in surface runoff at a monthly time scale. Automated calibration for nitrate loading with SWAT-CUP resulted

in drastically reduced model performance for crop yield simulation even after running a multi-objective calibration scheme using both crop yield and nitrate loading data. Hence, the model was manually calibrated for nitrate loading and the automated calibration run was only utilized for global sensitivity analysis to determine the sensitive parameters for nitrate calibration in surface runoff. Global sensitivity analysis showed that nitrate loads were sensitive to SDNCO, NPERCO, CMN, and CDN (P-value < 0.05). The automated calibration trial, however, showed that calibration of crop yield can be an important constraint for calibrating nutrient simulation and can help reduce the uncertainty in nutrient simulation in SWAT. The calibration process also gives a higher confidence in the other nutrient processes in SWAT that were not directly calibrated.

Model performance statistics for nitrate loading simulation in surface runoff after calibration (Table 3.12) for both Plot1 and Plot2 are presented in Table 3.13. Overall, the model did a satisfactory job of simulating monthly nitrate loadings in surface runoff. However, the model performed better in simulating nitrate loadings in the strip-tilled Plot2 than the conventionally-tilled Plot1 during calibration and validation, likely due to the better predictions of surface runoff for the strip-till (Table 3.7). Bosch et al. (2015) had noted that nitrate loads were highly influenced by water volumes in the experimental plots as nitrate concentrations were fairly stable. It is important to note that the calibration parameters for surface runoff and soil moisture were controlled at the hru level (Table 3.5); thus, calibration of surface runoff was performed individually for Plot1 and Plot2. Nitrate calibration was, however, performed concurrently for both plots as the parameters adjusted for nitrate loading calibration were adjusted in the .bsn file which applies to both Plot1 and Plot2 during simulation.

Table 3.12 Adjusted .bsn parameter values for nitrate loading calibration.

Parameters	SWAT input file	Initial	Calibrated
SDNSCO	BSN	1.1	0.99
NPERCO	BSN	0.2	0.15
CMN	BSN	0.0003	0.0015
CDN	BSN	1.4	3

Table 3.13 Model performance evaluation of monthly nitrate loading simulation for Plot1 and Plot2 during calibration (2004-2005) and validation (2006).

Goodness of Fit Measure	Plot1		Plot2	
	Calibration	Validation	Calibration	Validation
R^2	0.46	0.46	0.70	0.58
NSE	0.29	0.41	0.65	0.51
PBIAS	-10.30%	21.00%	21.80%	-26.40%

PBIAS values for Plot1 and Plot2 show that the total nitrate loading simulated during calibration and validation was within 26.4% of the observed nitrate loading, which shows that SWAT can estimate nitrate loss from agricultural fields reasonably well at the field scale. This also shows that SWAT is capable of simulating the impacts of BMPs on nitrate loss at the field scale. Although nitrate loading was evaluated over only a 3-year period, the evaluated period included years with both cotton and peanuts. This gives us confidence that the model is capable of simulating nitrate loss in years with either cotton or peanut. Graphical comparison of the simulated vs observed nitrate loading also shows that the model is able to capture the temporal variation in nitrate loss in both Plot1 (Fig. 3.8) and Plot2 (Fig. 3.9).

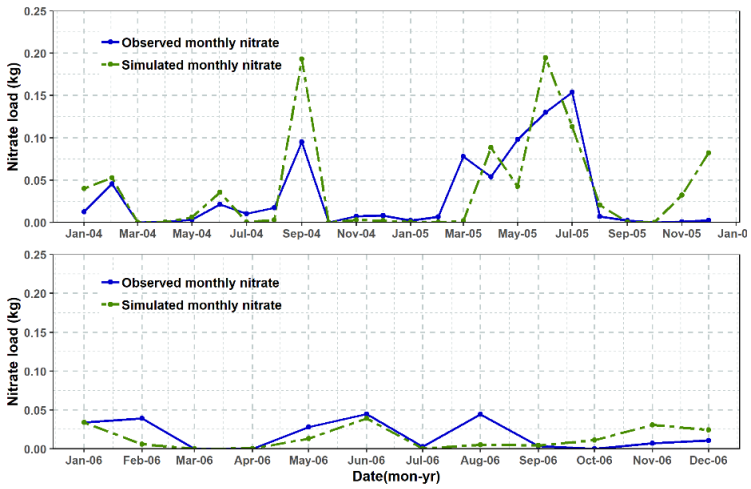

Figure 3.8 Comparison of simulated vs observed monthly nitrate loading for Plot1 during calibration (top) and validation (bottom).

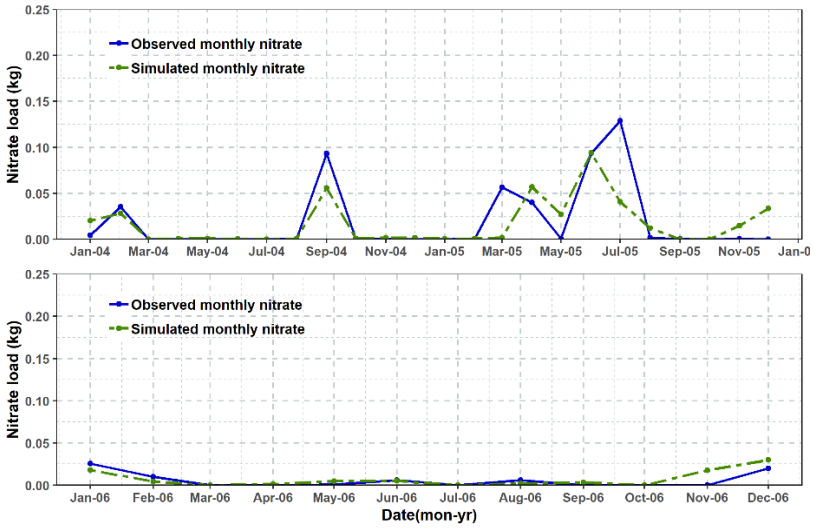

Figure 3.9 Comparison of simulated vs observed monthly nitrate loading for Plot2 during calibration (top) and validation (bottom).

3.4.5 Management scenario analysis

The calibrated model was run for 27 years of historical data (1990-2016) with a 3-year warmup period (1987-1989) for the three management level scenarios (Tables 3.2 and 3.3). Mean

differences in yield, irrigation water use, and nutrient loss between the three levels were evaluated using One-way ANOVA with post-hoc Tukey test at 95% confidence interval (CI).

Cotton yield evaluation for the three management levels showed that Mgt1 had a slightly lower yield averaging close to 4500 kg/ha. Mgt2 and Mgt3 averaged close to 5000 kg/ha (Fig. 3.10). Cotton yield for Mgt2 and Mgt3 were not significantly different. Mgt1 also showed a higher variability in cotton yield than Mgt2 and Mgt3 as demonstrated by the larger interquartile range for Mgt1 (Fig. 3.10). Evaluation of the nitrogen and water stress for the three management levels in the SWAT output showed that cotton suffered from higher nitrogen stress in Mgt1, which could have resulted from the lack of poultry litter application before planting as applied in Mgt2 and Mgt3, thereby resulting in lower and more variable yield. Peanut yield, on the other hand, had statistically similar yield for all three levels (Fig. 3.10). Peanuts are legumes and SWAT does not allow legumes to experience nitrogen stress, which led to no nitrogen stress in all three levels and the yield variability observed is a result of water stress. Yield variability in peanuts was slightly higher in Mgt2 than in Mgt1 and Mgt3 but was much lower when compared to the variability in cotton yield for the three managements.

Irrigation water use for cotton were not statistically different for Mgt1 and Mgt2 but lower than irrigation water use for Mgt3 by an average of 100 mm per year (Fig. 3.11). Evaluation for peanut showed that Mgt1 with SMS irrigation had the lowest application averaging close to 100 mm per year, while Mgt3 had the highest irrigation water use averaging close to 300 mm per year. Mgt2 averaged slightly less than 250 mm per year (Fig. 3.11). For both crops, Mgt1 with SMS irrigation had the lowest average water use and Mgt3 had the highest average water use even though average yield for Mgt1 was similar to Mgt3 for peanut and only slightly lower than Mgt3 for cotton which resulted due to higher nitrogen stress.

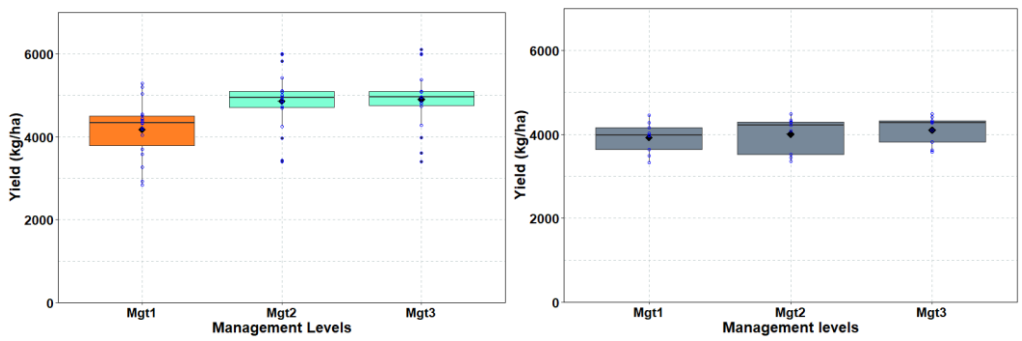

Figure 3.10 Simulated annual cotton yield (left) and peanut yield (right) for the three management scenarios. Same colors indicate that the means are not significantly different for each other. Blue circles in the box-plots represent the simulated data for each year of the scenario simulation.

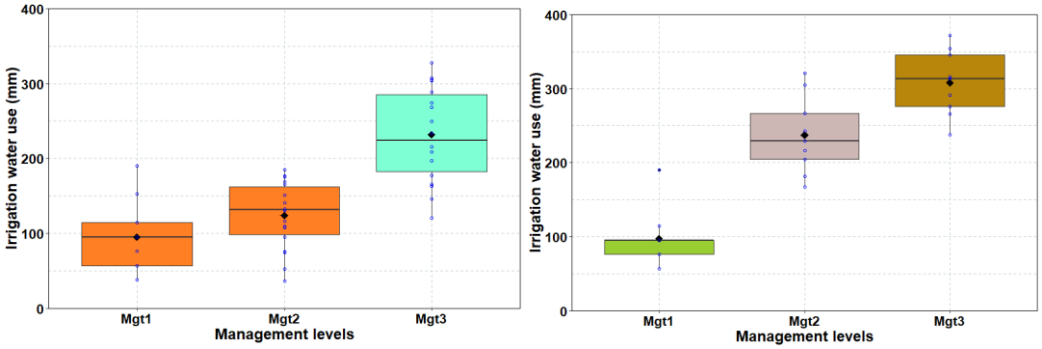

Figure 3.11 Simulated annual water use for cotton (left) and peanut (right) for the three management scenarios. Same colors indicate that the means are not significantly different for each other. Blue circles in the box-plots represent the simulated data for each year of the scenario simulation.

Although the model was only calibrated for nitrate loading in surface runoff, nitrate loss for the three scenarios were evaluated in both surface runoff and leaching from below the root zone. Calibration and validation of the model for multiple variables in the hydrological and nutrient processes gives confidence in nutrient leaching evaluation and assessing the relative differences in nutrient leaching between the three scenarios.

Mgt3 had the highest nitrate loss in both surface runoff and leaching while Mgt1 had the lowest loss (Fig. 3.12). This result was expected as Mgt3 had the highest nitrogen fertilizer application, was under conventional tillage, and had no cover crop while Mgt1 had no poultry litter application, had cover crop, and was under strip tillage practice. Other studies have also shown that poultry litter application can be a considerable source of nutrient loss from agricultural fields (Karki et al., 2018). As nitrate is highly soluble and mobile, and does not absorb in soils (Jury and Nielsen, 1989), it is easy to lose nitrate in leaching with excess irrigation and precipitation. Comparison between nitrate loss in surface runoff and leaching showed that nitrate loss from leaching below the soil zone was many times higher and a critical information for water quality management of sub-surface sources if the groundwater table is near the surface.

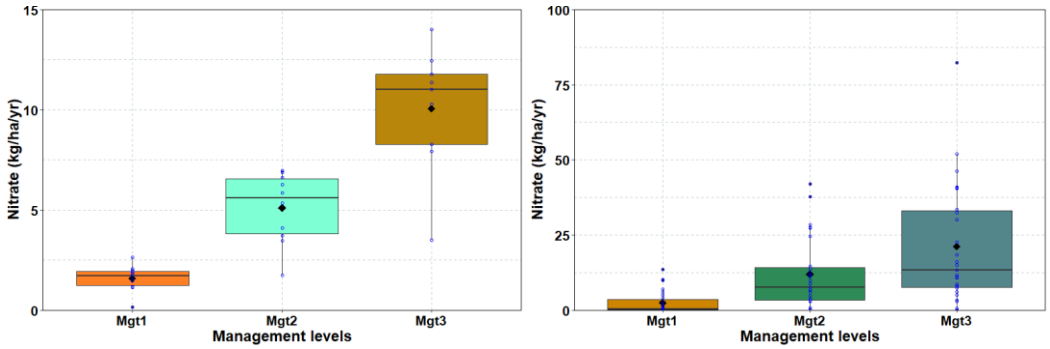

Figure 3.12 Simulated annual nitrate loss in surface runoff (left) and leaching below soil root zone (right) for the three management scenarios. Same colors indicate that the means are not significantly different from each other. Blue circles in the box-plots represent the simulated data for each year of the scenario simulation.

Time series evaluation of nitrate leaching for the 3 scenarios (Fig. 3.13) showed that nitrate leaching was higher in Mgt2 and Mgt3 for majority of the simulation years which could be expected because of higher fertilizer application as well as the absence of rye cover crop in Mgt2 and Mgt3. It was also observed that nutrient leaching from Mgt2 and Mgt3 was higher in years

with higher precipitation (Fig. 3.13). The highest nitrate leaching was observed in 2013 which was preceded by three years of low precipitation and indicates storage of excess nutrient over the low precipitation years. Nitrate loss was also higher in most years with cotton than with peanut which resulted from the additional nitrogen application in cotton.

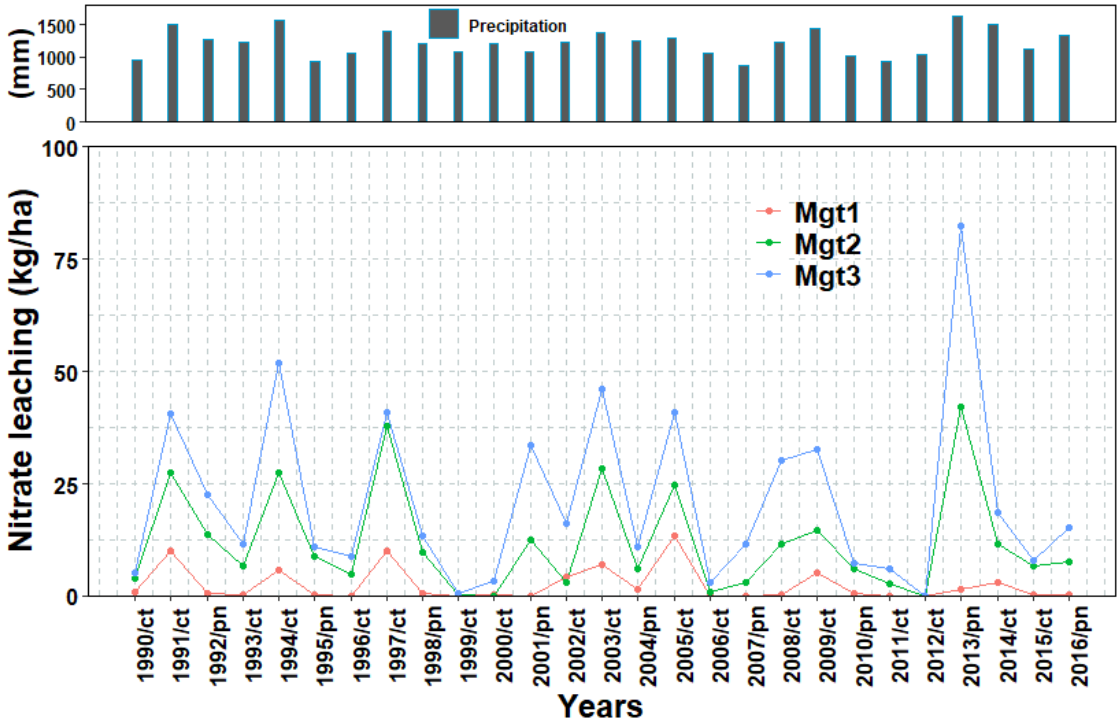

Figure 3.13 Time series of nitrate leaching from the three management levels (bottom) and annual precipitation (top). "ct" and "pn" indicates year with cotton and peanut plantation, respectively.

Evaluation across the three management levels showed that Mgt1 has the highest potential for reducing nitrate loss in surface runoff and leaching, efficiently using water for irrigation, and maintaining high yield as it used the least amount of water for irrigation and had the lowest nitrate loss with comparable yields. The study shows that changing farming practices from Mgt2, which is being practiced by the majority of farmers for cotton and peanut production in south GA, to Mgt1 can potentially help reduce nitrate pollution and conserve water resources without any yield

loss for peanuts and only slight loss for cotton. Additional costs associated with installing SMS systems and winter cover crops could be a big deterrent in persuading farmers and stakeholders to shift from Mgt2 to Mgt1 which is where cost-share and incentive programs by federal and state agencies can play a pivotal role. Although the scenario analysis from the calibrated model provides a good understanding of the differences in irrigation water use, nitrate loss, and cotton yield for the three management systems, exact numbers provided by the model for irrigation water use, crop yield, and nitrate loss should be used with caution.

3.5 Summary and Conclusions

This study showed that SWAT can adequately simulate surface runoff, soil moisture, cotton and peanut yield, and nitrate transport at the field scale. Adjusting the routing methods from Variable Storage to Muskingum and adjustment of DIS_STREAM was critical for flow routing and simulating surface runoff at the plot scale, a scale that can have multiple no-flow days. Surface runoff calibration for the conventionally- and strip-tilled plots 1 and 2 separately showed that adjusting CNOP values accordingly for conventional tillage and strip for tillage is very important. Although SWAT was able to simulate soil moisture, it did not have a large influence on the model performance for surface runoff simulation at the field scale. Furthermore, although the model was able to simulate both cotton and peanut yields reasonably well, the model was able to simulate temporal variation in peanut yield better than cotton yield. However, the simulated peanut yield differences between Plot1 and Plot2 was much lower than observed in the two plots, indicating that SWAT was not able to simulate the tillage impact on peanut yield. Inability of the model to simulate low observed cotton yields in 2000 which had low fertilizer application as compared to other years possibly indicates to the inability of the model to simulate N deficiency. Sequential calibration of crop yield and nitrate showed that crop yield calibration can be an important

consideration for simulating nitrate transport while reducing model uncertainty and increasing model robustness, as calibration of nitrate had an effect on model performance for crop yield calibration.

Simulation of the three management scenarios showed that SWAT can be used as a tool to evaluate BMPs for crop yield, nutrient transport, and irrigation water use at the field scale. Evaluation of the three management scenario results showed that Mgt1 with soil moisture sensor-based irrigation, cover crop, and strip tillage had the highest potential for reducing nutrient loss and conserving water while maintaining agricultural productivity in south GA. The results also showed that poultry litter can be an important source of nitrate loss from agricultural fields and that nitrate loss occurred predominantly through leaching from below the root zone. Application of the SWAT model at the field scale as done in this study can increase stakeholder trust in the model, for its eventual application at the watershed scale for best management practice evaluation and water quality protection.

3.6 References

Abbaspour, K. C. (2013). SWAT-CUP 2012. *SWAT Calibration and Uncertainty Program—A User Manual*.

Abbaspour, K. C., Johnson, C. A., Van Genuchten, M. T. (2004). Estimating uncertain flow and transport parameters using a sequential uncertainty fitting procedure. *Vadose Zone Journal*, *3*(4), 1340–1352.

Anand, S., Mankin, K. R., McVay, K. A., Janssen, K. A., Barnes, P. L., Pierzynski, G. M. (2007). Calibration and Validation of ADAPT and SWAT for Field-Scale Runoff Prediction 1. *JAWRA Journal of the American Water Resources Association*, *43*(4), 899–910.

Arnold, J. G., Moriasi, D. N., Gassman, P. W., Abbaspour, K. C., White, M. J., Srinivasan, R., … Van Liew, M. W. (2012). SWAT: Model use, calibration, and validation. *Transactions of the ASABE*, *55*(4), 1491–1508.

Arnold, J. G., Srinivasan, R., Muttiah, R. S., Williams, J. R. (1998). Large area hydrologic modeling and assessment part I: model development 1. *JAWRA Journal of the American Water Resources Association*, *34*(1), 73–89.

Bingner, R. L., Theurer, F. D., Yuan, Y. (2015). AnnAGNPS Technical Processess, Version 5.4. USDA.

Borah, D K, Xia, R. J., Bera, M., Singh, V. P., Frevert, D. (2002). DWSM-a Dynamic Watershed Simulation Model. *Mathematical Models of Small Watershed Hydrology and Applications*, 113–166.

Borah, Deva K, Bera, M. (2004). Watershed-scale hydrologic and nonpoint-source pollution models: Review of applications. *Transactions of the ASAE*, *47*(3), 789.

Bosch, D. D., Potter, T. L., Strickland, T. C., Hubbard, R. K. (2015). Dissolved nitrogen, chloride, and potassium loss from fields in conventional and conservation tillage. *Transactions of the ASABE*, *58*(6), 1559–1571.

Bosch, D. D., Potter, T. L., Truman, C. C., Bednarz, C. W., Strickland, T. C. (2005). Surface runoff and lateral subsurface flow as a response to conservation tillage and soil-water conditions. *Transactions of the ASAE*, *48*(6), 2137–2144.

Bosch, D. D., Truman, C. C., Potter, T. L., West, L. T., Strickland, T. C., Hubbard, R. K. (2012). Tillage and slope position impact on field-scale hydrologic processes in the South Atlantic Coastal Plain. *Agricultural Water Management*, *111*, 40–52.

Cao, W., Bowden, W. B., Davie, T., Fenemor, A. (2006). Multi-variable and multi-site calibration and validation of SWAT in a large mountainous catchment with high spatial variability. *Hydrological Processes: An International Journal*, *20*(5), 1057–1073.

Chen, Y, Marek, G., Marek, T., Brauer, D., Srinivasan, R. (2017). Assessing the efficacy of the SWAT auto-irrigation function to simulate irrigation, evapotranspiration, and crop response to management strategies of the Texas High Plains. *Water*, *9*(7), 509.

Chen, Yong, Ale, S., Rajan, N., Morgan, C. L. S., Park, J. (2016). Hydrological responses of land use change from cotton (Gossypium hirsutum L.) to cellulosic bioenergy crops in the Southern High Plains of Texas, USA. *Gcb Bioenergy*, *8*(5), 981–999.

Daggupati, P., Douglas-Mankin, K. R., Sheshukov, A. Y., Barnes, P. L., Devlin, D. L. (2011). Field-level targeting using SWAT: Mapping output from HRUs to fields and assessing limitations of GIS input data. *Transactions of the ASABE*, *54*(2), 501–514.

Daggupati, P., Pai, N., Ale, S., Douglas-Mankin, K. R., Zeckoski, R. W., Jeong, J., … Youssef, M. A. (2015). A recommended calibration and validation strategy for hydrologic and water quality models. *Transactions of the ASABE*, *58*(6), 1705–1719.

Douglas-Mankin, K. R., Maski, D., Janssen, K. A., Tuppad, P., Pierzynski, G. M. (2010). Modeling nutrient runoff yields from combined in-field crop management practices using SWAT. *Transactions of the ASABE*, *53*(5), 1557–1568.

Dubrovsky, N. M., Burow, K. R., Clark, G. M., Gronberg, J. M., Hamilton, P. A., Hitt, K. J., … others. (2010). The quality of our Nation's waters—Nutrients in the Nation's streams and groundwater, 1992--2004. *US Geological Survey Circular*, *1350*(2).

Endale, D. M., Bosch, D. D., Potter, T. L., Strickland, T. C. (2014). Sediment loss and runoff from cropland in a Southeast Atlantic Coastal Plain landscape. *Transactions of the ASABE*, *57*(6), 1611–1626.

Flanagan, D. C., Ascough, J. C., Nearing, M. A., Laflen, J. M. (2001). The water erosion prediction project (WEPP) model. In *Landscape erosion and evolution modeling* (pp. 145–199). Springer.

Foster, G. R., Yoder, D. C., Weesies, G. A., McCool, D. K., McGregor, K. C., Bingner, R. L. (2002). User's Guide—revised universal soil loss equation version 2 (RUSLE 2). *USDA--Agricultural Research Service, Washington, DC*.

Gassman, P. W., Reyes, M. R., Green, C. H., Arnold, J. G. (2007). The soil and water assessment tool: historical development, applications, and future research directions. *Transactions of the ASABE*, *50*(4), 1211–1250.

Gesch, D., Oimoen, M., Greenlee, S., Nelson, C., Steuck, M., Tyler, D. (2002). The national elevation dataset. *Photogrammetric Engineering and Remote Sensing*, *68*(1), 5–32.

Ghebremichael, L. T., Veith, T. L., Watzin, M. C. (2010). Determination of critical source areas for phosphorus loss: Lake Champlain basin, Vermont. *Transactions of the ASABE*, *53*(5), 1595–1604.

Gitau, M. W., Gburek, W. J., Bishop, P. L. (2008). Use of the SWAT model to quantify water quality effects of agricultural BMPs at the farm-scale level. *Transactions of the ASABE*, *51*(6), 1925–1936.

Her, Y., Chaubey, I., Frankenberger, J., Smith, D. (2016). Effect of conservation practices implemented by USDA programs at field and watershed scales. *Journal of Soil and Water Conservation*, *71*(3), 249–266.

JURY, W. A., NIELSEN, D. R. (1989). Nitrate transport and leaching mechanisms. In *Developments in Agricultural and Managed Forest Ecology* (Vol. 21, pp. 139–157). Elsevier.

Kalcic, M. M., Chaubey, I., Frankenberger, J. (2015). Defining Soil and Water Assessment Tool (SWAT) hydrologic response units (HRUs) by field boundaries. *International Journal of Agricultural and Biological Engineering*, *8*(3), 69–80.

Karki, R., Tagert, M. L. M., Paz, J. O. (2018). Evaluating the nutrient reduction and water supply benefits of an on-farm water storage (OFWS) system in East Mississippi. *Agriculture, Ecosystems & Environment*, *265*, 476–487.

Maski, D., Mankin, K. R., Janssen, K. A., Tuppad, P., Pierzynski, G. M. (2008). Modeling runoff and sediment yields from combined in-field crop practices using the Soil and Water Assessment Tool. *Journal of Soil and Water Conservation*, *63*(4), 193–203.

Merriman, K., Russell, A., Rachol, C., Daggupati, P., Srinivasan, R., Hayhurst, B., Stuntebeck, T. (2018). Calibration of a field-scale Soil and Water Assessment Tool (SWAT) model with field placement of best management practices in Alger Creek, Michigan. *Sustainability*, *10*(3), 851.

Mittelstet, A. R., Storm, D. E., Stoecker, A. L. (2015). Using SWAT to simulate crop yields and salinity levels in the North Fork River Basin, USA. *International Journal of Agricultural and Biological Engineering*, *8*(3), 110–124.

Moriasi, D. N., Gitau, M. W., Pai, N., Daggupati, P. (2015). Hydrologic and water quality models: Performance measures and evaluation criteria. *Transactions of the ASABE*, *58*(6), 1763–1785.

Nair, S. S., King, K. W., Witter, J. D., Sohngen, B. L., Fausey, N. R. (2011). Importance of Crop Yield in Calibrating Watershed Water Quality Simulation Tools 1. *JAWRA Journal of the American Water Resources Association*, *47*(6), 1285–1297.

Neitsch, S. L., Arnold, J. G., Kiniry, J. R., Williams, J. R. (2011). *Soil and water assessment tool theoretical documentation version 2009*.

Ni, X., Parajuli, P. B. (2018). Evaluation of the impacts of BMPs and tailwater recovery system on surface and groundwater using satellite imagery and SWAT reservoir function. *Agricultural Water Management*, *210*, 78–87.

Nilawar, A., Calderella, C., Lakhankar, T., Waikar, M., Munoz, J. (2017). Satellite Soil Moisture Validation Using Hydrological SWAT Model: A Case Study of Puerto Rico, USA. *Hydrology*, *4*(4), 45.

Pai, N., Saraswat, D., Srinivasan, R. (2012). Field_SWAT: A tool for mapping SWAT output to field boundaries. *Computers & Geosciences*, *40*, 175–184.

Parajuli, P. B., Jayakody, P., Sassenrath, G. F., Ouyang, Y., Pote, J. W. (2013). Assessing the impacts of crop-rotation and tillage on crop yields and sediment yield using a modeling approach. *Agricultural Water Management*, *119*, 32–42.

Patil, A., Ramsankaran, R. (2017). Improving streamflow simulations and forecasting performance of SWAT model by assimilating remotely sensed soil moisture observations. *Journal of Hydrology*, *555*, 683–696.

Plotkin, S., Wang, X., Potter, T. L., Bosch, D. D., Williams, J. R., Hesketh, E. S., Bagdon, J. K. (2013). APEX calibration and validation of water and herbicide transport under US Southern Atlantic Coastal Plain conditions. *Transactions of the ASABE*, *56*(1), 43–60.

Prokopy, L. S., Floress, K., Klotthor-Weinkauf, D., Baumgart-Getz, A. (2008). Determinants of agricultural best management practice adoption: Evidence from the literature. *Journal of Soil and Water Conservation*, *63*(5), 300–311.

Rajib, M. A., Merwade, V., Yu, Z. (2016). Multi-objective calibration of a hydrologic model using spatially distributed remotely sensed/in-situ soil moisture. *Journal of Hydrology*, *536*, 192–207.

Teshager, A. D., Gassman, P. W., Secchi, S., Schoof, J. T., Misgna, G. (2016). Modeling agricultural watersheds with the soil and water assessment tool (swat): Calibration and validation with a novel procedure for spatially explicit hrus. *Environmental Management*, *57*(4), 894–911.

Truman, C. C., Reeves, D. W., Shaw, J. N., Motta, A. C., Burmester, C. H., Raper, R. L., Schwab, E. B. (2003). Tillage impacts on soil property, runoff, and soil loss variations from a Rhodic Paleudult under simulated rainfall. *Journal of Soil and Water Conservation*, *58*(5), 258–267.

University of Georgia CAES. (2018). *Georgia Farm Gate Value Report 2017*.

University of Georgia Extension. (2018). *UGA Peanut Production Quick Reference Guide*.

Uribe, N., Corzo, G., Quintero, M., van Griensven, A., Solomatine, D. (2018). Impact of conservation tillage on nitrogen and phosphorus runoff losses in a potato crop system in Fuquene watershed, Colombia. *Agricultural Water Management*, *209*, 62–72.

USDA-NRCS. (1983). *Soil Survery of Tift County, Georgia*.

USDA-NRCS. (2019). *Soil Survey Geographic (SSURGO) Database*.

Voinov, A., Gaddis, E. J. B. (2008). Lessons for successful participatory watershed modeling: a perspective from modeling practitioners. *Ecological Modelling*, *216*(2), 197–207.

Whitaker, J., Culpepper, S., Freeman, M., Harris, G., Kemerait, B., Perry, C., … Smith, A. (2018). *2018 Georgia Cotton Production Guide*.

Williams, J. R., Izaurralde, R. C., Singh, V. P., Frevert, D. K. (2006). The APEX model. *Watershed Models*, 437–482.

Williams, J. R., Jones, C. A., Kiniry, J. R., Spanel, D. A. (1989). The EPIC crop growth model. *Transactions of the ASAE*, *32*(2), 497–511.

Winchell, M., Srinivasan, R., Diluzio, M., Arnold, J. (2013). ArcSwat Interface for SWAT 2012: User's Guide. *Blackland Research Center, Texas AgriLife Research*.

Xia, Y., Mitchell, K., Ek, M., Sheffield, J., Cosgrove, B., Wood, E., … others. (2012). Continental-scale water and energy flux analysis and validation for the North American Land Data Assimilation System project phase 2 (NLDAS-2): 1. Intercomparison and application of model products. *Journal of Geophysical Research: Atmospheres*, *117*(D3).

Chapter 4

Assessing the Impacts of Increased Groundwater Withdrawal in the lower Apalachicola-Chattahoochee-Flint River Basin using MODFLOW

4.1 Abstract

Groundwater withdrawal for irrigation is an important issue in the lower Apalachicola-Chattahoochee-Flint (ACF) River Basin of southeastern United States (U.S.) as it has led to a decline in groundwater levels as well as a reduction in baseflow. As the withdrawal is further projected to increase in the future, understanding the potential impacts of this increase is critical for developing long-term management plans, especially during prolonged drought conditions. This study developed a two-layered three-dimensional groundwater model for the Upper Floridan Aquifer (UFA) in the lower ACF River Basin using MODFLOW-NWT to evaluate the impacts of the projected increase in irrigation in the groundwater levels as well as the stream-aquifer flux in the region. A transient model was developed from 2007-2013 that was calibrated for 2,360 daily groundwater level observations and stream-aquifer flux at six reach sections. Simulation of the projected irrigation scenario showed a reduction in groundwater levels by as much as 2.38 m while a general reduction was observed in much of the model domain. Large groundwater level reductions were mostly observed in the regions where the aquifer is comparatively thinner. Evaluation of the changes in stream-aquifer flux showed that flux reduced by as much as 33% with high reductions observed in the Lower Flint and Kinchafoonee watersheds within the model domain. This study also helped identify regions within the lower ACF River Basin that were important for groundwater recharge and most susceptible to the impacts of an increase in irrigation which can be critical for the sustainability of the aquifer and the surficial streams.

4.2 Introduction

Agriculture is critical to the economy of the lower Apalachicola-Chattahoochee-Flint (ACF) river basin in South Georgia, United States (U.S.), with more than $2 billion generated in farm-based revenue annually (University of Georgia CAES, 2014). The region is the leading producer of peanuts and pecan in the U.S. and is also a major producer of cotton and corn. A major underlying factor for the intense agricultural production in the region is the presence of the Upper Floridan Aquifer (UFA), which supplies about 80% of the total irrigation demand for irrigating more than 200,000 hectares of agricultural land through more than 4,000 irrigation wells (GA EPD, 2016). The UFA, which is made up of karst limestone, is the primary source of water for agricultural, industrial, and municipal use in the region and is amongst the most productive aquifer systems in the world. It supplied an estimated 1.7 million cubic meters (MCM) of water for irrigation in 2015, but withdrawals from the UFA can be as high as 3.6 MCM during a drought year (GA EPD, 2016). The UFA is in direct hydraulic connection with the surficial rivers and lake systems throughout much of the lower ACF river basin through sinkhole ponds, karst sinks, incised streambeds, and conduits that exposes the limestone to the surface (Torak and Painter, 2006). As a result, the UFA is an important contributor to streamflow in many of the surficial streams in the lower ACF river basin contributing tens of million cubic meters of water every day as baseflow (Torak and Painter, 2006). However, intense groundwater withdrawal for irrigation has led to a decline in groundwater levels and has also resulted in the baseflow reduction to the streams in the lower ACF river basin (Jones and Torak, 2006; Singh et al., 2016; Singh et al., 2017). Groundwater withdrawal during the growing season has led to an increase in no-flow and low-flow periods in many perineal streams (Singh et al., 2016). The situation is only exacerbated by the recurring drought conditions including 1985-1989, 1999-2002, 2010-2012, and 2016 drought periods. Pumpage induced

groundwater level fluctuations of nearly 10 m were observed during the severe droughts of 2000 and 2001 with a record or near-record low groundwater levels in most wells (Torak and Painter, 2006). Flow in the spring-fed streams in the region has decreased by 50 to 100% during drought periods (GWC, 2017). The recurring drought conditions along with agriculture intensification in the lower ACF has threatened the already limited groundwater resources as well as the future of the agricultural economy in the region. Along with agriculture, the low flow and no-flow stream conditions have severely affected the endangered and threatened species of freshwater mussels in the lower ACF river basin (Gagnon et al., 2004; Golladay et al., 2004; Shea et al., 2013). Declining downstream flow as a result of reduced baseflow conditions in the lower ACF river basin, especially during drought periods, has also led to the tri-state water wars since the 1980s between the neighboring states of Alabama, Georgia, and Florida (Center, 2015; Gilbert and Turner-Nesmith, 2019).

The adverse impact of groundwater over-exploitation in the region has led to numerous studies to evaluate the spatio-temporal impacts of groundwater use on the groundwater levels and surface- and groundwater interaction. Lynn and Torak (2006) developed a finite-element groundwater model and evaluated the impacts of seasonal groundwater pumpage for irrigation in drought conditions including a comprehensive water budget for the UFA in the lower ACF river basin. Mitra et al. (2016) utilized the model developed by Lynn and Torak (2006) and simulated the transient drought conditions from 2010-2012 to evaluate its impact on the groundwater levels and the groundwater budget of the region. They also assessed the impacts of irrigation during drought conditions. The MODular Finite-Element Model (MODFE) used by Lynn and Torak (2006) was calibrated under steady-state conditions, while Mitra et al. (2016) validated the model utilizing data from a single day. Singh et al. (2017) identified critical streams and tributaries that were

adversely affected by irrigation pumping using principal component and K-means clustering analysis and evaluated the effectiveness of water restriction scenarios on the stream-aquifer flux. Jones et al. (2017) developed a USGS Modular Finite-Difference Groundwater Flow Model (MODFLOW) (Harbaugh, 2005) that was calibrated for transient conditions for groundwater levels and baseflow for the UFA and the overlying semi-confining unit to evaluate the hydrologic budget for the 2008-2012 drought. Baseflow calibration for the model was performed for only a limited area in the model domain.

The Georgia Water Planning and Policy Center (GWPCC) prepared the agricultural water demand forecast for the whole of Georgia for 2020, 2030, 2040, and 2050 at the county and/or drainage area level for a range of weather conditions, which projects the agricultural irrigation groundwater demand in the lower ACF river basin to further increase from 2010 to 2050 during dry years (CH2M, 2017). It is of paramount importance to understand the spatial and temporal impacts of this increased groundwater withdrawal from the UFA on groundwater levels and surface-aquifer interactions, especially in drought years, to determine if the UFA can sustain this increased withdrawal to maintain agricultural productivity without adversely affecting the diverse aquatic species. Although Mitra et al. (2019) also evaluated the impacts of increase in irrigation in the region, the simulated increase in irrigation was a constant % increase of the 2011 groundwater pumpage values over the entire model domain. This might not accurately reflect the change in spatial variability as well as increase in irrigation with increasing agricultural lands that is captured by the GWPCC agricultural demand forecast and can potentially help get a more accurate understanding of the potential impacts of increase in irrigation. Understanding quantitative interactions between the UFA and the surface streams in the study region under projected water withdrawals scenario is critical for protecting endangered and threatened species residing in this

region. Failure to protect aquatic habitat due to low flow conditions in surface streams of this region, because of unsustainable withdrawals from UFA, can potentially lead to water use restrictions, which can negatively affect agricultural productivity and rural communities of the region. Understanding of the change in stream-aquifer flux due to the projected withdrawals in drought years can also help water managers to avoid potential conflict amongst the water users of this region.

This paper adds to the previous modeling efforts in the region by developing a two-layered three-dimensional MODFLOW model for the UFA in the lower ACF river basin that is calibrated for transient conditions for groundwater level and stream-aquifer flux (baseflow discharge from aquifer) for both wet and dry years and throughout the model domain. The study also identifies sensitive recharge zones within the model domain that has not been performed in any of the previous studies. A comprehensive analysis of the impacts of the projected increase in groundwater withdrawal for irrigation is also presented. This study is part of a larger project that aims to improve the agricultural sustainability in the Lower Flint River basin of the lower ACF while also protecting the UFA and the ecological habitat it sustains. The three main objectives of this paper are to i) develop a three-dimensional calibrated groundwater flow model for the UFA in the lower ACF using the USGS Modular Three-Dimensional Finite-Difference Groundwater Flow Model (MODFLOW) – NWT, ii) identify critical zones for groundwater recharge sensitive to groundwater levels and flow, and iii) simulate projected irrigation scenario and quantify the effects of the projected withdrawals on the UFA.

4.3 Materials and methods

The focus area for this research is the UFA in the agriculturally intensive region of the lower ACF river basin. Hence, the modeled region includes parts of South Georgia (GA), southeastern

Alabama (AL), and northwestern Florida (FL) and is about 12,003 km^2 in area (Fig. 4.1). Forests and agricultural land are the dominant land cover and land use types in the study area covering about 46% and 39% respectively, while urban area accounts for only about 6% of the total area (Homer et al., 2020). The climate of the region is humid subtropical with long, hot, and humid summers and mild winters. The average temperature ranges from about 17℃ in the winter to about 33.7℃ in the summer (Arguez et al., 2012), but temperatures above 37.7℃ are common in the summer. Precipitation is evenly distributed throughout the year and averages annually about 1365 mm in the south to about 1161 mm in the north of the study area (Arguez et al., 2012). Precipitation in the winter, however, accounts for almost all of the areal recharge to the UFA as the frontal, low-intensity, and long-duration nature of the rainfall along with low evapotranspiration demand in winter is conducive for recharge. Summer precipitation events are convective with high intensity and short duration resulting in more surface runoff. Land-elevation of the study region ranges from about 76 m in the northwestern boundary of the study area to about 46 m in the southwestern boundary (Fig. 4.1). Agriculture accounts for the highest water use in the area of which more than 80% is supplied by the UFA (Rugel et al., 2012). Groundwater withdrawals for irrigation have steadily increased in the lower ACF river basin since the 1970s with the expansion of center pivot irrigation systems (GWC, 2017). Groundwater irrigation increased by 59% from 2005 to 2010 while surface-water irrigation decreased during the same time period (Lawrence, 2016).

The modeled area lies in the Coastal Plain physiographic province and consists mostly of a low-lying karstic region called the Dougherty Plain physiographic district. The Dougherty plain is characterized by relatively flat, inner lowland containing sub-surface and internal drainage, and heterogeneous stream development typical to a karst topography (Torak and Painter, 2006). The modeling domain and the geohydrologic setting for the domain are based on the area described by

Torak and Painter (2006), which describes in detail the groundwater flow and geohydrology of the UFA and the overlying and underlying units in the study region and are referred to for further detail. The UFA in most of the modeling domain consists of the Ocala Limestone of the Eocene period. Overlying the UFA is the discontinuous, undifferentiated overburden, weathered residuum, and undifferentiated surficial deposits that may contain water-bearing zones and are together referred to as the Upper Semi-Confining Unit (USCU). Regions where the USCU is absent or thin or where the UFA outcrops to the surface are sources for direct recharge to the aquifer while the aquifer also receives recharge through the USCU as vertical leakage of water (Torak and Painter, 2006). Major rivers and streams have cut shallow channels through the USUC to the underlying UFA that is close to the land surface resulting in a direct connection between the UFA and the rivers and streams that flow through the area. The UFA outcrops in the northwestern boundary of the study domain and dips towards the southeast with the thickness of the aquifer ranging from about 9 m in the outcrop area to more than 130 m in the southern end of the modeling domain (Torak and Painter, 2006; Williams and Kuniansky, 2016).

4.3.1 Study area and geohydrology of the UFA

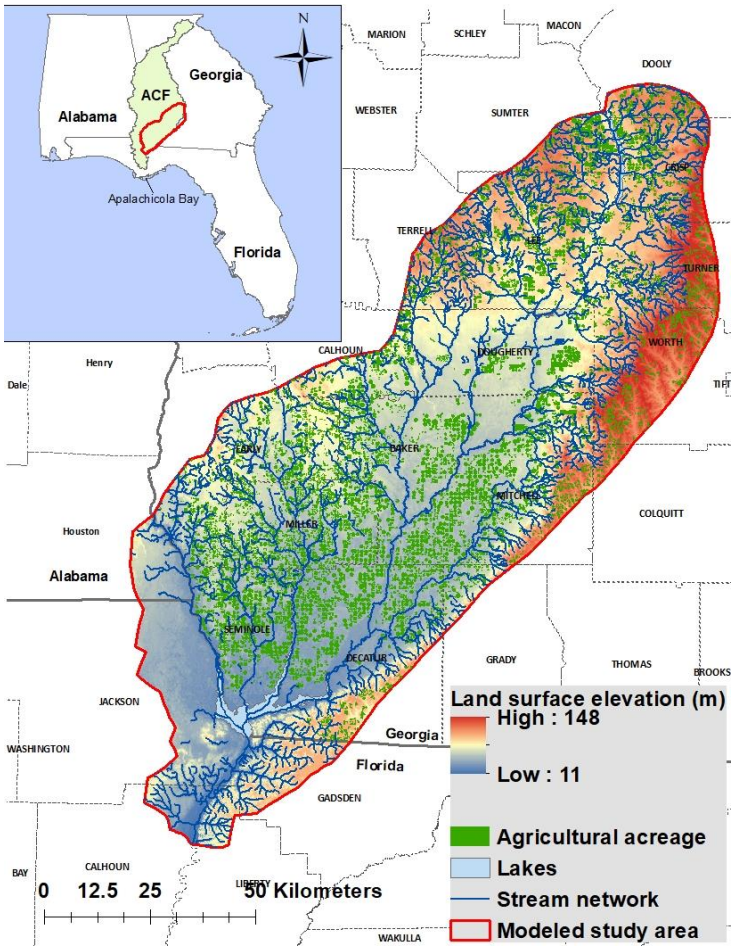

Figure 4.1 Groundwater model domain and study area including the major lakes, rivers, and agricultural acreage in the study area.

4.3.2 MODFLOW-NWT

MODFLOW is a block-centered finite difference groundwater model developed by USGS that can be utilized for two- or three-dimensional applications in solving groundwater flow problems. MODFLOW uses a modular structure that allows for each option to be independent of each other and allows for adding or removing of options (Harbaugh, 2005). The groundwater flow model for this study was developed using MODFLOW-NWT, a Newton formulation of MODFLOW-2005 (Niswonger et al., 2011). MODFLOW-NWT is a standalone version that must be used with the

Upstream-Weighting Package (UPW). It expands on the capacity of MODFLOW-2005 to solve the problem of constant drying and rewetting non-linearities when simulating unconfined systems that can lead to the issue of model instability and convergence issue when using other versions of MODFLOW (Hunt and Feinstein, 2012; Niswonger et al., 2011). Although the karstic system of the UFA could have the presence of conduit and fractured flow and the use of an equivalent porous media model could probably not represent the system very accurately, Kuniansky (2016) showed than an equivalent porous media model without representation of local conduit flows can adequately simulate the groundwater levels of a karstic system and hence was used in this research.

The governing equation for each cell in MODFLOW for groundwater flow is based on the continuity equation and is expressed as (Harbaugh, 2005):

$$\sum Q_i = SS \frac{\Delta h}{\Delta t} \Delta V \quad (1)$$

where, Q_i is the flow rate into the cell [L^3T^{-1}], SS is the specific storage [L^{-1}], ΔV is the volume of the cell [L^3], Δh is the change in the head [L], and Δt is the time interval [T].

4.3.3 Conceptual model development

The conceptual flow model for the UFA in the lower ACF river basin is based on the geohydrologic study of Torak and Painter (2006) of the region and similar to the model developed by Jones and Torak (2006) and Jones et al. (2017). The groundwater recharge from precipitation as vertical leakage from the overlying semi-confining unit where present and as direct recharge where it is thin or absent is the biggest source of groundwater flow into the system. The northwestern boundary, where the UFA outcrops, is considered the saturated updip limit of the aquifer, and the regional groundwater flow occurs from the northwest to southeast as the UFA downdips in that

direction. Groundwater level in the updip area of the UFA fluctuates very little throughout the year. The regional outflow of groundwater occurs from the south and southeastern boundary based on the potentiometric maps of the UFA (Gordon and Peck, 2010; Kinnaman and Dixon, 2011). The biggest outflow from the UFA is to the rivers and streams in the region as the aquifer and the surficial streams are in direct connection throughout the region. Groundwater pumpage is another important source of outflow from the aquifer, which peaks during the June/July of the growing season when the irrigation is at the highest level. Lake Seminole and Lake Blackshear, which are within the model domain, are maintained at or near-constant levels throughout the year and impact the local groundwater levels. Underlying the UFA is an impermeable layer known as the Lisbon formation that acts as the lower confining unit to the aquifer.

4.3.4 Numerical model development

A three-dimensional groundwater flow model was developed using MODFLOW-NWT based on the conceptualization of the flow system for the modeled region which is defined by the following partial differential equation (Harbaugh, 2005):

$$\frac{\partial}{\partial x}\left(K_{xx}\frac{\partial h}{dx}\right) + \frac{\partial}{\partial y}\left(K_{yy}\frac{\partial h}{dy}\right) + \frac{\partial}{\partial x}\left(K_{zz}\frac{\partial h}{dz}\right) + W = S_s\frac{\partial h}{\partial t} \qquad (2)$$

where, $K_{xx}, K_{yy}, and\ K_{zz}$ are values of hydraulic conductivity along the x, y, and z coordinate axes parallel to the major axes of hydraulic conductivity [LT^{-1}]; h is the potentiometric head [L]; W is the volumetric flux per unit volume representing sources and sinks [T^{-1}]; S_s is the specific storage of the porous material [L^{-1}]; and t is time [T].

Data pre-processing and post-processing for preparing the model inputs for the MODFLOW-NWT was performed using ModelMuse, a graphical user interface developed by USGS (Winston, 2009).

4.3.4.1 Model discretization

A two-layered groundwater model with a uniform grid size of 750 m x 750 m was constructed that represents the USCU and the UFA (Fig. 4.2). The model has 282 rows and 102 columns resulting in a total of 28,764 grid cells of which 21,394 are active. The bottom elevation of the UFA was combined with the thickness of the UFA, both acquired from Williams and Dixon (2015), to determine the top of the UFA. A digital elevation model (DEM) of the land-surface was then acquired from USGS (Gesch et al., 2002) to determine the thickness and the top of the USCU. Manual adjustments had to be made for grid cells that resulted in having the top of the UFA higher than the top of the USCU using the two datasets. A transient model was built from 2007 to 2013 with monthly stress periods and daily time steps. This allowed for comparison between model-simulated groundwater level and flux with observed daily groundwater levels rather than comparing with monthly averages, thus giving better confidence in model performance. Initial hydraulic conductivity for the UFA and USCU as well as the specific yield and specific storage information for model setup were derived from the previous studies in the region which were then adjusted during model calibration (Jones et al., 2017; Jones and Torak, 2006).

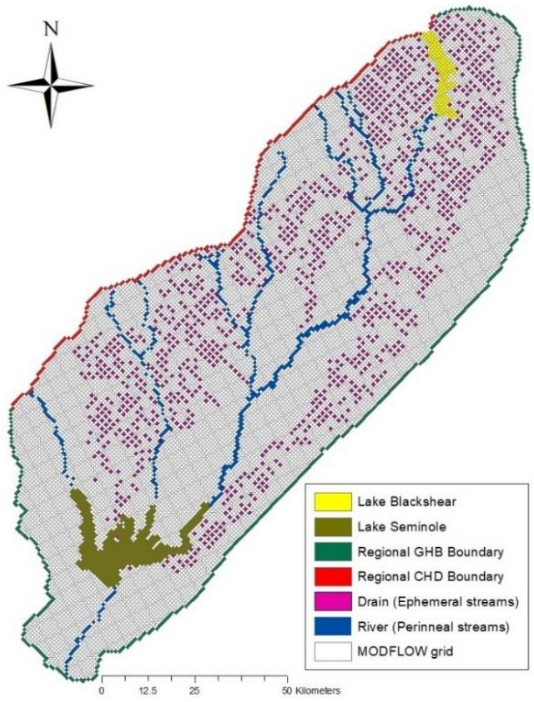

Figure 4.2 Groundwater model discretization and the regional and internal boundary conditions.

4.3.4.2 Boundary conditions

The base of the UFA was simulated as a no-flow boundary as the lower confining unit below the UFA acts as an impermeable layer. The updip limit of the UFA in the northwestern boundary of the model was simulated as a specified head boundary condition (Anderson et al., 2015) (Fig. 4.2) using the time-variant specified head package (CHD) as there was a minimal fluctuation in the groundwater head throughout the year. The remaining of the regional boundary of the model was simulated as a general head-dependent boundary (GHB) condition (Anderson et al., 2015) using the GHB package (Fig. 4.2). Two lakes in the model domain were also simulated using the GHB package and lake level elevation was provided for each stress period (Fig. 4.2). Groundwater head for the regional CHD and GHB boundaries were provided by averaging the potentiometric heads from Gordon and Peck (2010) and Kinnaman and Dixon (2011) and kept constant throughout the simulation for model simplicity.

Groundwater pumpage was an important boundary condition that needed to be estimated accurately for input in the model. Monthly groundwater withdrawal estimates from the UFA were acquired from the Georgia Environmental Protection Division (EPD) at Hydrologic unit code (HUC)-12 level, which was then divided equally to each well within the HUC-12 watershed (Fig. 4.3). Groundwater pumpage was simulated as a specified flux package (Anderson et al., 2015) using the well package (WEL).

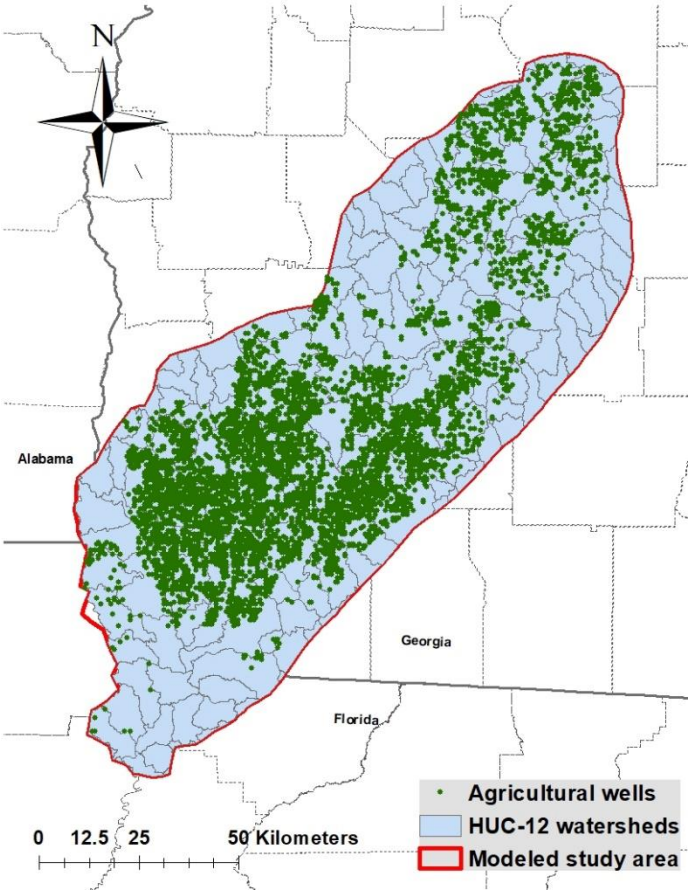

Figure 4.3 Groundwater wells pumping from the UFA and the HUC-12 watersheds in the model domain.

Ephemeral streams that had the possibility of going dry were simulated using the Drain package (DRN) while the perennial streams were simulated using the River package (RIV) (Fig. 4.2).

Streambed depth for the DRN and RIV packages were acquired from previous studies performed in the region (Jones et al., 2017; Jones and Torak, 2006). Initial values for streambed conductance were also acquired from the previous studies which were then calibrated during the model calibration period. Stream elevation for the RIV package was estimated by interpolating stream-stages from USGS stations with continuous observed data for the simulation period and the lake levels from the two lakes.

Areal recharge from precipitation is a very important boundary condition in the model as it has the greatest influence in the groundwater budget but is also the most difficult to estimate (Healy, 2010). Groundwater recharge can vary greatly spatially and temporally as it is influenced by the variation in land use, vegetation, geohydrologic conditions, climate, and land management practices among others (Healy, 2010; Sophocleous, 2005). Groundwater recharge for this study was estimated using a physically-based, semi-distributed, watershed-scale, continuous simulation, water-balance based model called the Soil and Water Assessment Tool (SWAT) (Neitsch et al., 2011). SWAT accounts for the spatial and temporal variability in recharge as it maintains the spatial heterogeneity of a watershed by dividing it into sub-watersheds and each sub-watershed is further divided into hydrologic response units (HRUs), which are the basic units for calculation. Many studies have successfully used SWAT to estimate groundwater recharge (Arnold et al., 2000; Raposo et al., 2013; Sun and Cornish, 2005). A SWAT model was developed for the study region (Fig. 4.4) that incorporated the major land-types and agricultural crop rotations. The model was then calibrated and validated for streamflow for 5 USGS streamflow stations within the watershed (Table 4.1; Fig. 4.4) after which groundwater recharge estimates were acquired for each sub-watershed and incorporated into the MODFLOW as a specified flux (Anderson et al., 2015) using the recharge package (RCH) (Fig. 4.5). The developed SWAT model had a total of 160 sub-

watersheds of which 89 were partially or completely located within the groundwater model domain (Fig. 4.4) and used for estimating groundwater recharge.

Table 4.1 Monthly streamflow statistics for the simulation period (2007 – 2013).

USGS Station	R^2	NSE
2349605	0.83	0.85
2352500	0.86	0.89
2353000	0.83	0.87
2356000	0.80	0.85
2358000	0.92	0.94

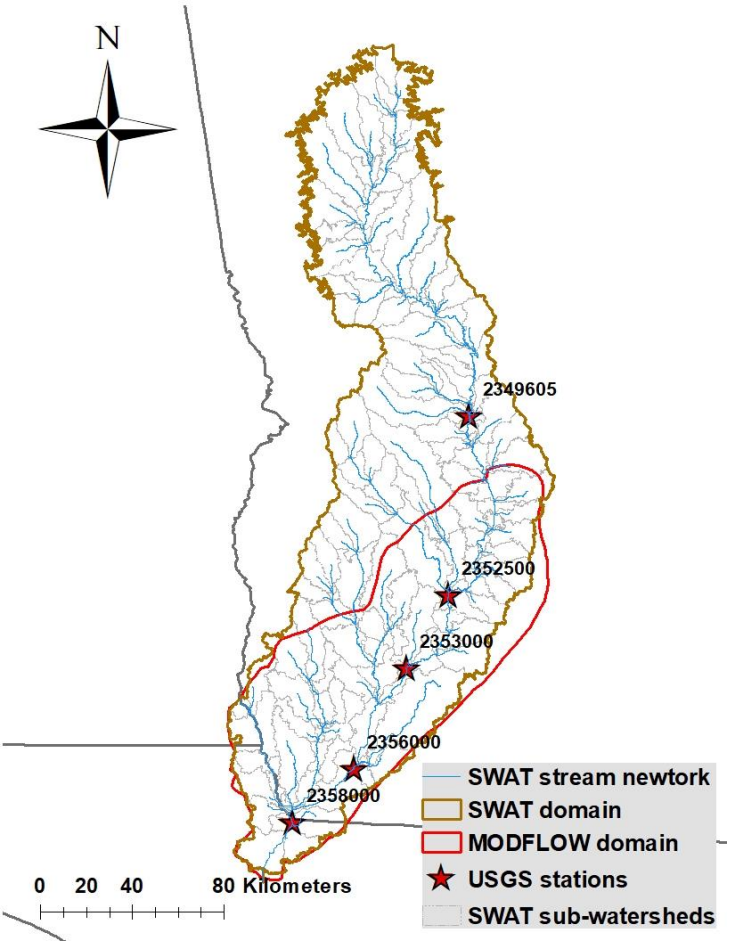

Figure 4.4 SWAT model domain used for estimating groundwater recharge.

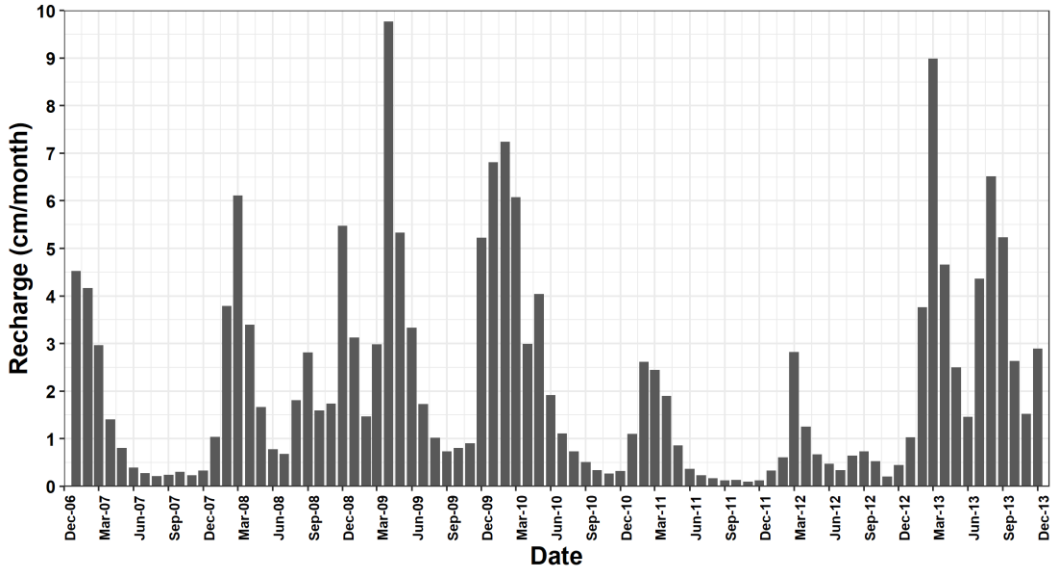

Figure 4.5 SWAT estimated monthly groundwater recharge for the groundwater model domain.

4.3.5 Model calibration

Model calibration was a two-step process and involved matching simulated groundwater levels to observed levels followed by matching model predicted stream-aquifer flux to its counterpart for the 2007-2013 period. Observed groundwater levels and streamflow data used for model calibration were acquired from the USGS National Water Information System (NWIS) (USGS, 2019). 2,360 daily groundwater observation data of the UFA were acquired from 359 wells in the model domain. Lack of observed groundwater observation data in the overlying USCU limited us to calibrating the groundwater head only for the UFA. Model performance for evaluation for simulating groundwater head was performed by calculating the root mean square (RMS) of the groundwater head residual, which can be calculated as:

$$RMS = \left[\frac{1}{N}\sum_{i=1}^{N}(h_{i\,sim} - h_{i\,obs})^2\right]^{\frac{1}{2}} \quad (3)$$

where, N is the number of residuals, $h_{i\ sim}$ is the simulated head [L], and $h_{i\ obs}$ [L] is the observed head

Along with RMS, a value of less than 0.1 for the ratio of the standard deviation of residuals (STD) divided by the range (R) of observed groundwater levels also indicates a good model fit (Kuniansky et al., 2004) and was also used for evaluation. Along with the statistical measures, graphical measures including the plot of the frequency histogram of residuals and spatial distribution of residuals were also used for evaluating model performance.

Calibration of stream-aquifer flux was performed by comparing the simulated flux to monthly averaged estimated flux for a reach section, which was estimated by subtracting the baseflow at the downstream from the upstream end of a reach. A positive flux indicates a gaining stream and that the aquifer contributed water to streamflow in the reach section while a negative flux indicates a losing stream and that the stream lost water in that section. As there are uncertainties associated with streamflow, the estimation of baseflow, and the resulting estimated/observed flux for a reach section, a target range of flux was calculated for each reach section to aid in calibration following the procedure mentioned in Jones and Torak (2006). The error factors (EF) of 10% (0.10) and 5% (0.05) were applied to reach sections having average streamflow less than and greater than 7.07 m^3/s, respectively (Jones and Torak, 2006), and the target range was calculated as follows:

$$Flow_{min} = (Q_d - EF * Q_d) - (Q_u + EF * Q_u) \quad (4)$$

$$Flow_{max} = (Q_d + EF * Q_d) - (Q_u - EF * Q_u) \quad (5)$$

where, $Flow_{min}$ is the minimum target flow, $Flow_{max}$ is the maximum target flow, Q_d is the downstream flow, Q_u is the upstream flow, and EF is the error factor.

Daily baseflow estimates for calculating the target range fluxes were acquired using the USGS groundwater toolbox (Barlow et al., 2015). The model was calibrated for stream-aquifer flux for 6 reach sections – reach 2, 3, 4, 5, 6, and 8 (Fig. 4.6). As the Lower Flint River basin region was the major focus of the study, stream reaches in and contributing to the Lower Flint were calibrated for stream-aquifer flux in this study. Fig. 4.6 also shows the upstream and downstream USGS stations that were used to estimate the target flux range for each reach section.

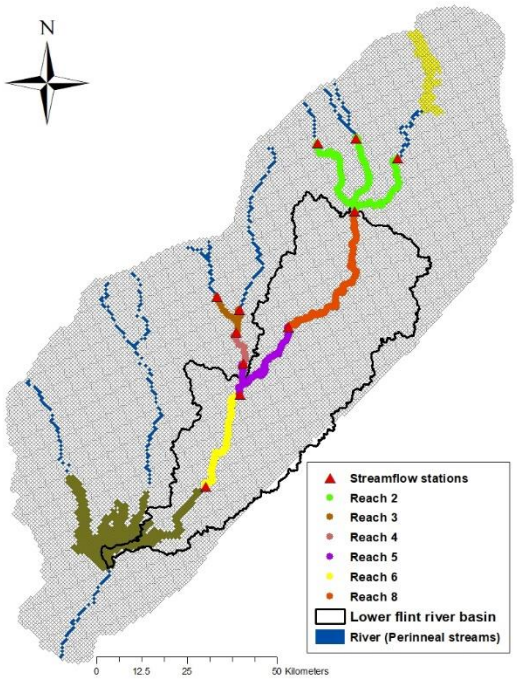

Figure 4.6 Reach sections that were calibrated for stream-aquifer flux.

Model calibration was performed by adjusting the hydraulic conductivity of the UFA, streambed conductance for the RIV and DRN packages, and specific storage values using automated and trial-by-error methods. The model domain was divided into 14 hydraulic conductivity zones for the UFA, 10 DRN zones, and 15 RIV zones for calibration purposes. UCODE, an inverse modeling tool for model calibration (Poeter and Hill, 1998, 1999) was used to identify the sensitive hydraulic conductivity zones and river sections and perform initial automated calibration runs after which

the model was calibrated manually for further refinement. A sensitivity analysis was also performed by dividing the SWAT estimated RCH into zones to identify critical groundwater recharge areas within the model domain that were sensitive and critical for groundwater level and flow. This can potentially help decision-makers identify target zones for land management for potentially improving groundwater recharge.

4.3.6 Irrigation scenario

Evaluating the spatio-temporal impacts in groundwater levels and stream-aquifer flux of a fine resolution projected irrigation scenario – at HUC-12 level – can provide important information that can be critical for developing management plans for the long-term sustainability of the aquifer, the agricultural productivity, and the ecological habitat of the UFA and the lower ACF river basin. GWPCC estimated agricultural water demand for the years 2020, 2030, 2040, and 2050 for five different climate scenarios to include the potential climate extremes and included the 10^{th}, 25^{th}, 50^{th}, 75^{th}, and 90^{th} percentile scenarios. Of the five scenarios, the 75^{th} percentile represented dry conditions with higher irrigation demands and is used by GWPCC for planning purposes (CH2M, 2017). Hence, the irrigation scenario in this study was also evaluated for the 75^{th} percentile. Evaluation of the 75^{th} percentile irrigation scenario from 2020 to 2050 for each month showed a similar increasing trend in irrigation demand from 2020-2050 (Fig. 4.7a). Hence, only the 2040 75^{th} percentile irrigation scenario was selected for evaluation in this study. Scenario analysis was performed by replacing the irrigation demand of the year 2011, which was a dry year, with the 2040 75^{th} percentile irrigation demand and comparing the changes in groundwater levels and stream-flux to estimate the impacts of the projected increase in agricultural irrigation demand in a dry year (Fig. 4.7b). This also allowed us to evaluate the aquifer rebound potential and long-term impact by comparing the calibrated and scenario model results for 2012 and 2013.

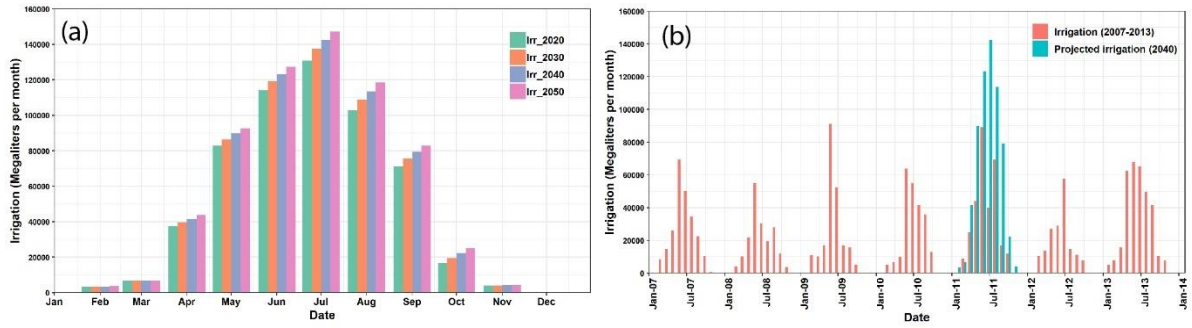

Figure 4.7 (a) GWPCC projected 75th percentile irrigation from 2020-2040, and (b) current and projected 2040 75th percentile irrigation.

4.4 Results and discussion

4.4.1 Groundwater level calibration

As the model was calibrated only for transient conditions, a model warm-up period was performed by replicating the stress periods of the first year of simulation for four years. Replication of the stress period for four years allowed for adequate model warm-up without the loss of observed data that can be used for model calibration.

The scatter plot between simulated and observed groundwater levels for the total simulation period of 2007-2013 (Fig. 4.8a) shows that simulated groundwater levels from the calibrated model closely matched the observed groundwater levels in the UFA for much of the simulation period. RMS of groundwater head residual for the whole simulation period was 2.68 m which was close to the RMS values in the previous modeling studies in the area (Jones et al., 2017; Jones and Torak, 2006; Mitra et al., 2016). Jones and Torak (2006) had also stated that a simulation error of less than 2.8 m can be considered acceptable accounting for the uncertainties and potential error in the aquifer geometry and groundwater level measurement. The calculated ratio of STD/R was 0.03 which is less than 0.1 and indicated a good model fit. Frequency histogram (Fig. 4.8b) and cumulative distribution plot (Fig. 4.8c) of the residuals showed that more than 80% of the residuals

were less than 3m and more than 92% of the residuals were less than 4.5m. The histogram also shows no skewness in the simulation of the groundwater level.

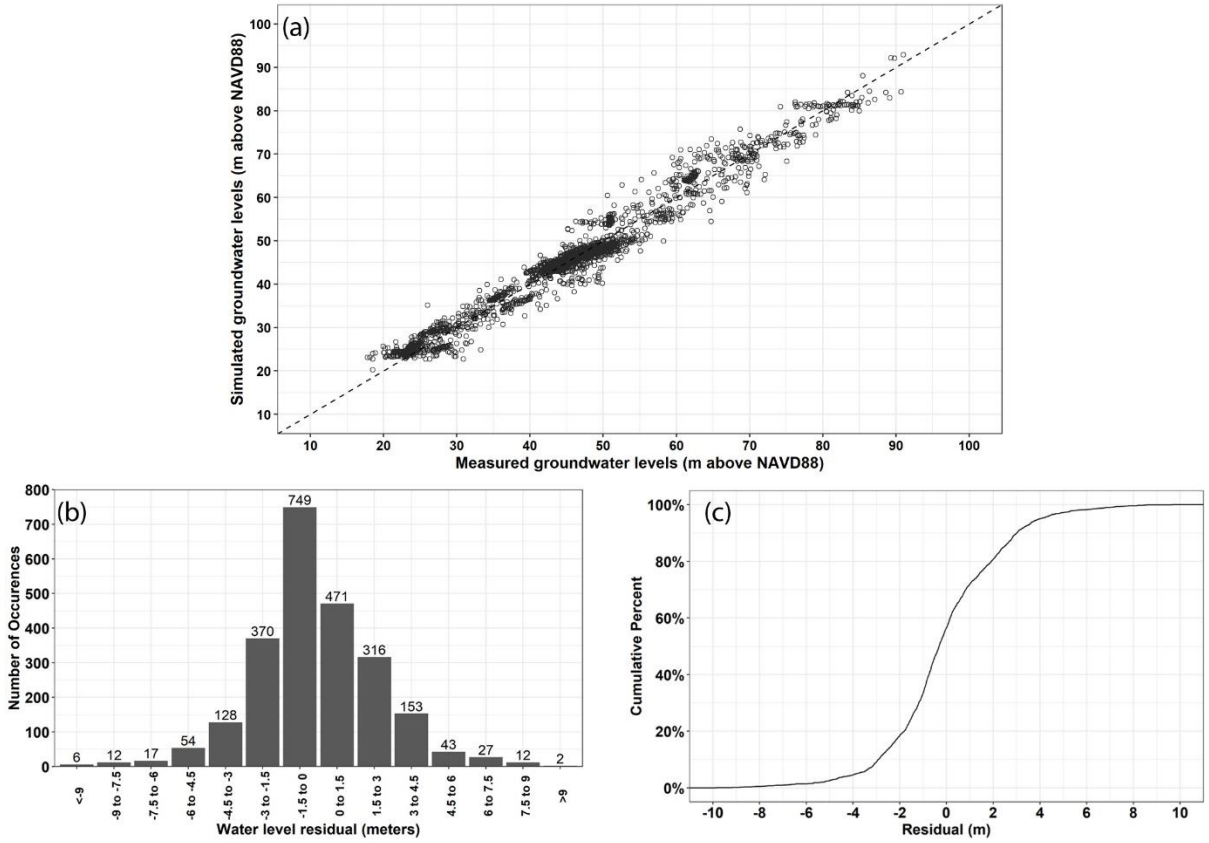

Figure 4.8 (a) Comparison between simulated and observed groundwater levels for the total simulation period, (b) frequency histogram of groundwater residual for the whole simulation period, and (c) cumulative distribution plot of groundwater residuals.

Evaluation and plotting of the mean groundwater head residual for each groundwater well showed that the model was also able to simulate adequately the spatial variability of groundwater levels in the model domain as shown by the random distribution of residuals (Fig. 4.9). RMS of the groundwater residual was also calculated for each month in the simulation period to evaluate the groundwater model for simulating the temporal variation of the groundwater head. RMS of less than 2.86 m in 65 of the 83 months and less than 4 m in 79 of the 83 months (Fig. 4.10)

demonstrated that the model was also able to adequately simulate the temporal variability in groundwater level for the UFA in the model domain.

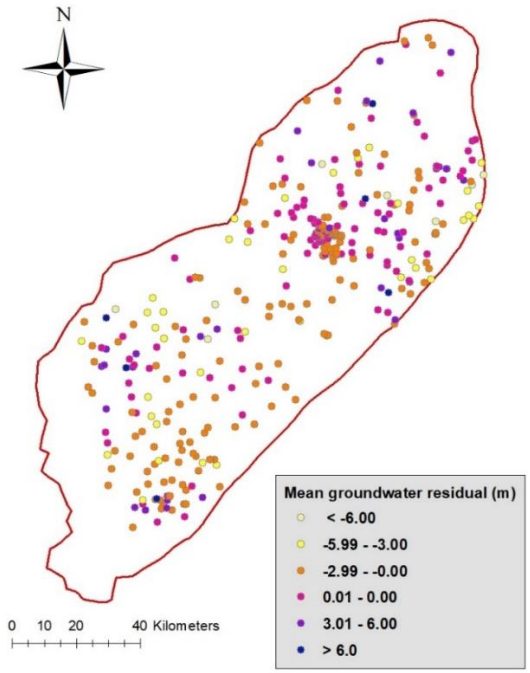

Figure 4.9 Mean groundwater head residual for each observation well used for model calibration.

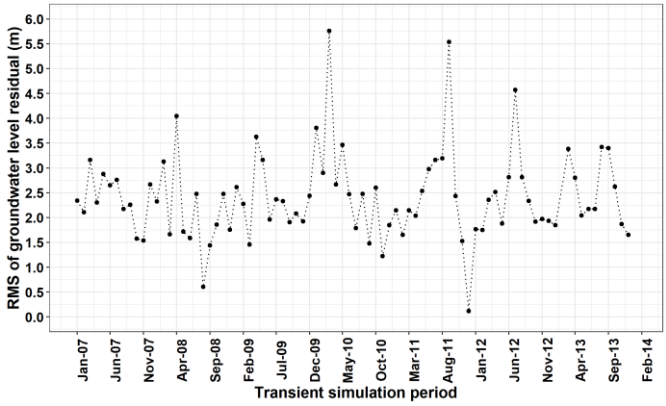

Figure 4.10 Monthly RMS of residual for groundwater level simulation.

Overall, groundwater calibration results have shown that the model can adequately simulate groundwater levels for the UFA both temporally and spatially. The model also performed adequately for dry as well as wet climate conditions as the calibration period included both dry (2011-2012) and wet periods (2008-2010).

4.4.2 Groundwater flux calibration

Calibration of stream-aquifer flux along with groundwater levels in the model is critical for increasing model robustness and confidence in the simulation results as calibration of multiple variables helps constrain the model parameters better. Simulated stream-aquifer flux and the target flux range for each reach section estimated based on the flow difference between the upstream and downstream end of the reach and the EF are presented in Fig. 4.11. Stream-aquifer flux for each section was calibrated by adjusting the streambed conductance. Estimated baseflow for reach 2, 3, and 4, and as a result target flux, were much smaller as compared to the other reach sections as the three reach sections are located in the region where the UFA is thin and have a smaller baseflow contribution.

Comparison between the simulated flux and target flux for all reach sections demonstrates that the model does an adequate job of simulating the stream-aquifer flux as most of the simulated flux is within or close to the target range for much of the simulation. The model is, however, not able to capture the high flux estimates for Oct 2010 – April 2011 in reach 2 (Fig. 4.11a) and 3 (Fig. 4.11b), where the estimated target flux is much higher than the rest of the simulation period and could potentially indicate the inability of the baseflow filter program to estimate accurate baseflow because of increased surface runoff and potentially sub-surface later runoff during that period. The model was also able to capture the temporal variability in stream-aquifer flux for all reach sections except for reach 2. The smallest reach section calibrated in the model was reach 4 and also the

only section that had negative flux for most of the time period indicating that the reach was behaving as a losing reach for much of the simulation period, and consistently during the drought periods of 2011-2012. Simulation of stream-aquifer flux was much better for reach 5, 6, and 8 (Fig. 4.11d, 4.11e, and 4.11f) which were along the main-stem of the Flint River in the Lower Flint River basin and had a direct connection to the aquifer section that was much deeper. Overall, the flux calibration result shows that the calibrated model can adequately simulate and capture the temporal and spatial variability of stream-aquifer flux for the stream reaches in the Lower Flint and adjoining reaches. The model was, however, able to estimate stream-aquifer flux better at reach sections that were in the region where the aquifer was thicker and had less variability in groundwater levels.

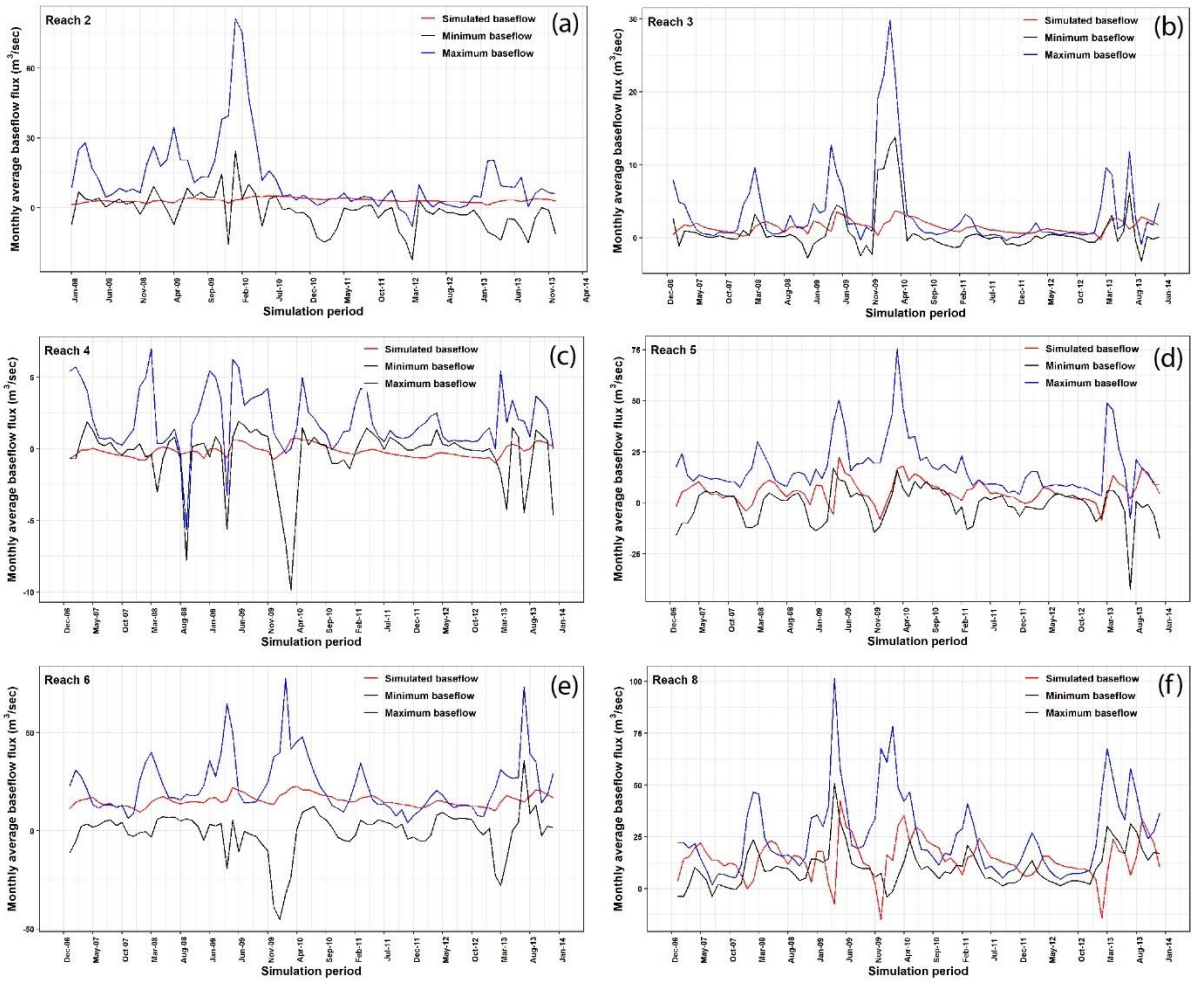

Figure 4.11 Simulated stream-aquifer flux and estimated target flux range for (a) reach 2, (b) reach 3, (c) reach 4, (d) reach 5, (e) reach 6, and (f) reach 8.

4.4.3 Groundwater budget

Groundwater budget evaluation provides critical information about the important groundwater components of the region and the impact on different components with a change in boundary conditions such as recharge and groundwater pumpage. Evaluation of net flux (inflow-outflow) for each boundary condition for the whole simulation period showed that recharge (RCH) was the biggest source of groundwater inflow and averaged about 8,500 Megaliters per day (MLD) with a minimal contribution also from the outcrop area (CHD) averaging about 1,100 MLD (Fig. 4.12).

Perennial rivers (RIV) accounted for the biggest outflow from the model domain (about 6,300 MLD) (Fig. 4.12) showing evidence to the fact that the UFA is an important contributor to streamflow in the region. Groundwater wells (WEL) and ephemeral streams (DRN) averaged less than 1,000 MGD of outflow while there was also a net outflow from the remaining regional boundary and lakes (GBH) at slightly higher than 1,000 MLD (Fig. 4.12).

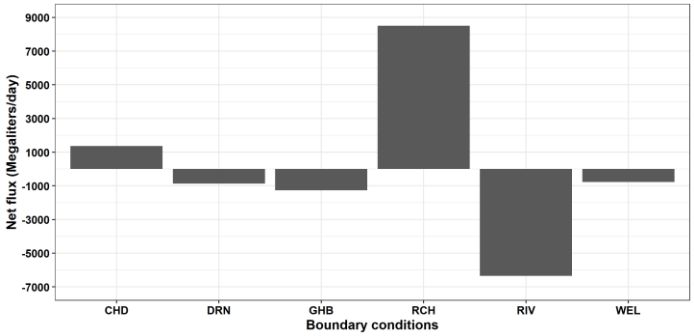

Figure 4.12 Total net groundwater budget for the major boundary conditions.

As the groundwater levels in the UFA follow a distinct pattern of seasonality, monthly groundwater budget evaluation for the model was also performed (Fig. 4.13) to evaluate its impact on the groundwater components. As most groundwater recharge occurs in the winter months (December-March), the groundwater level of the aquifer system is normally highest in the spring (April – May). Groundwater outflow to perennial rivers and ephemeral streams, as a result, is biggest during this time of the year which gradually decreases with summer and fall as there is a gradual decrease in groundwater level due to minimal recharge and increased groundwater pumpage for irrigation (Fig. 4.13). The year 2011 and 2012 were drought years and the monthly groundwater budget of the two years clearly show the impact on the stream-aquifer flux with reduced outflow to rivers due to drought conditions. February 2013, which was preceded by prolonged drought, was the only month during the whole simulation period that had a net positive flux for the river outflow (RIV) indicating a net inflow of water from the rivers to the aquifer and

demonstrates the negative impact drought can have in the region (Fig. 4.13). The river flux returns to normality with higher than normal recharge in 2013. This exhibits the potential of the aquifer system in the region and the river flux to rebound quickly to normal levels after drought conditions but also demonstrates the vulnerability of the stream-aquifer flux and streamflow in the region to prolonged drought that can be exacerbated by increased groundwater pumpage demand and withdrawal for irrigation during such periods.

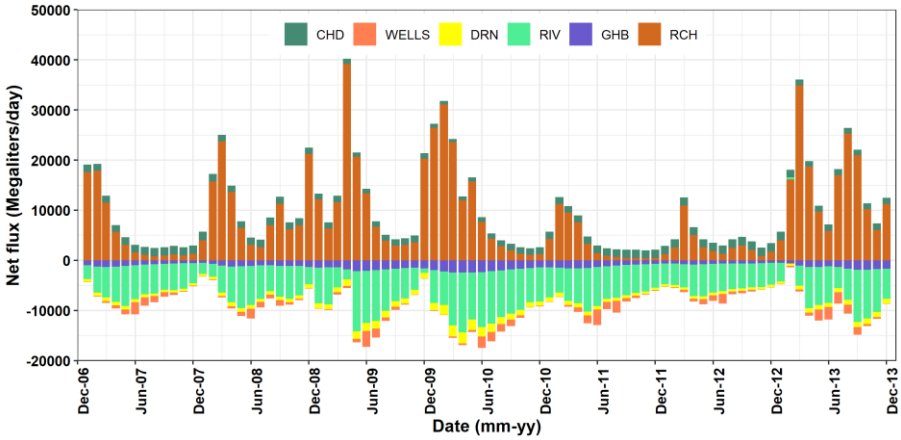

Figure 4.13 Monthly groundwater budget for the simulation period for the major boundary conditions including the specified head boundary (CHD), groundwater pumpage (wells), ephemeral streams (DRN), perennial rivers (RIV), general head boundary (GHB), and recharge (RCH).

4.4.4 Groundwater recharge critical zones

The USCU was divided into 15 geohydrologic zones by Torak and Painter (2006) based on the hydrologic and geologic setting and the potential for recharge to the UFA (Fig. 4.14a). Scarcity of groundwater wells in the USCU make it difficult for evaluating the recharge potential and sensitivity of the geohydrologic zones for recharge into the UFA. Hence, monthly recharge estimates obtained from the SWAT model were divided into 15 recharge zones based on the geohydrologic zones and sensitivity analysis was performed using UCODE to determine the

sensitivity of each zone to simulating groundwater levels and stream-aquifer flux. Fig. 4.14b presents the composite scaled sensitivity (CSS) for the 15 zones. CSS in UCODE indicates the sensitivity of the parameter to the observed values for estimating the parameter value accurately with higher values indicating higher sensitivity. Results showed that zone 11, upland interstream karst, was the most sensitive recharge zone, followed by zones 10, 4, 3, 6, 12, and 7 (upland instream, instream karst swamp, instream karst, upland outcrop, and solution escarpment) (Torak and Painter, 2006). Recharge zones were mostly sensitive in the region where the UFA is thin and close to the land surface where groundwater recharge can reach to the UFA quickly and can create substantial variations in the groundwater level. Identification of the sensitive recharge zones can provide potential information in identifying the critical recharge zones that are most sensitive to groundwater levels and stream-aquifer flux. It should be, however, noted that sensitivity analysis results are dependent on the observations provided and although a concerted effort was made to include observations that were distributed temporally and spatially, lack of observations in some zones (e.g. zone 5, and zone 9), could have biased the sensitivity analysis results.

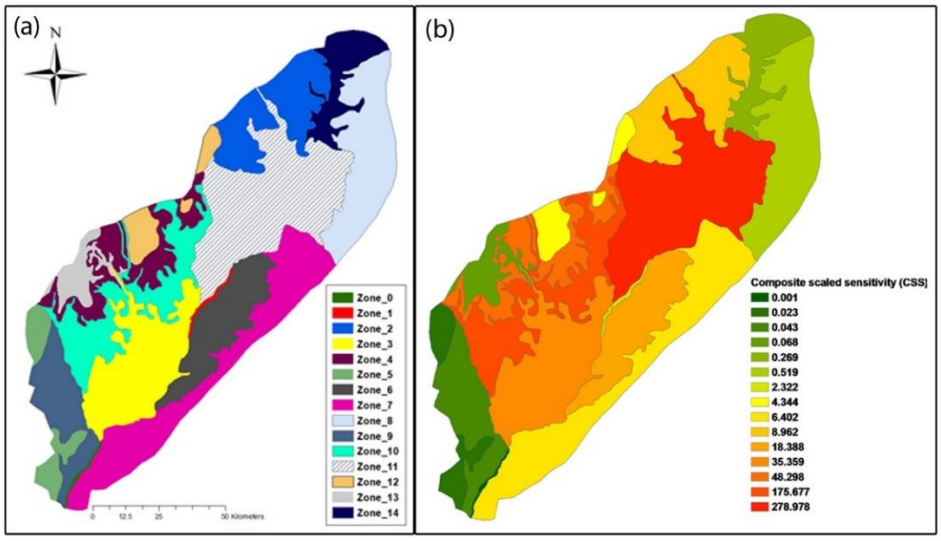

Figure 4.14 (a) Geohydrologic zones of the USCU (Torak and Painter, 2006) and, (b) Composite scaled sensitivity (CSS) results for the recharge zones. Higher CSS values indicates to higher sensitivity of the recharge zones to simulating groundwater levels and fluxes.

4.4.5 Impact of projected increase in irrigation demand

Groundwater levels from the scenario model run that replaced the January to December 2011 irrigation data with the 2040 projected scenario were compared against the calibrated model run for four specific time periods to study the short- (first day of September 2011, December 2011) and long-term (first day of March 2012, and December 2013) impacts of the projected increase in irrigation (Fig. 4.15). Evaluation of change in groundwater levels towards the end of the growing season (Fig. 4.15a) showed that the groundwater levels would have further decreased by more than 1 m in many parts of the UFA and by as much as 2.38 m in the Lower Flint River basin as compared to the groundwater levels of 2011 for that time period. Large groundwater level decrease was mostly observed in regions where the aquifer is comparatively thinner in the Lower Flint and the adjoining Kinchafoonee, Ichawaynochaway, and spring HUC-8 watersheds, but there was some groundwater level decrease throughout most of the aquifer. Assessment of the groundwater level in December 2011 (Fig. 4.15b) and March 2012 (Fig. 4.15c) showed gradual rebounding of the aquifer levels although groundwater levels were still lower by half a meter in many places. The aquifer was not able to fully recover to the groundwater levels of December 2013 (Fig. 15d) even after the higher than normal recharge (Fig. 4.5) in 2013.

Decrease in stream-aquifer flux (river outflow from the aquifer) was also observed in all the evaluated reach sections because of the increase in irrigation and the subsequent reduction in groundwater levels (Fig. 4.16). Reach 2 and 8, that are in the Kinchafoonee and Lower Flint watersheds, respectively, saw the biggest relative reduction in aquifer outflow as the two reach

sections were in the region that observed the high reduction in groundwater levels (Fig. 4.16). Flux decreased by as much as 33% in reach 8 and 14% in reach 2. It was also observed that reach 2 was not able to recover to the calibrated model flux levels even in December of 2013 while all the other reaches did not recover till at least December 2012 (Fig. 4.16).

Simulation of the projected irrigation scenario helped identify the critical regions in the model domain and reach sections that are most susceptible to increase in groundwater irrigation. Substantial reduction in groundwater levels and stream-aquifer flux, especially at the end of the growing season, also indicates the UFA might not be able to provide a sustainable supply of groundwater for irrigation in the future, especially under drought conditions. Impact on the UFA and the streams that are connected to it could be worse if the drought persists for a longer time-period and the aquifer has to sustain the projected irrigation for multiple years. Increased loss of stream-aquifer flux can lead to more streams going dry and severely impact the local ecological habitat.

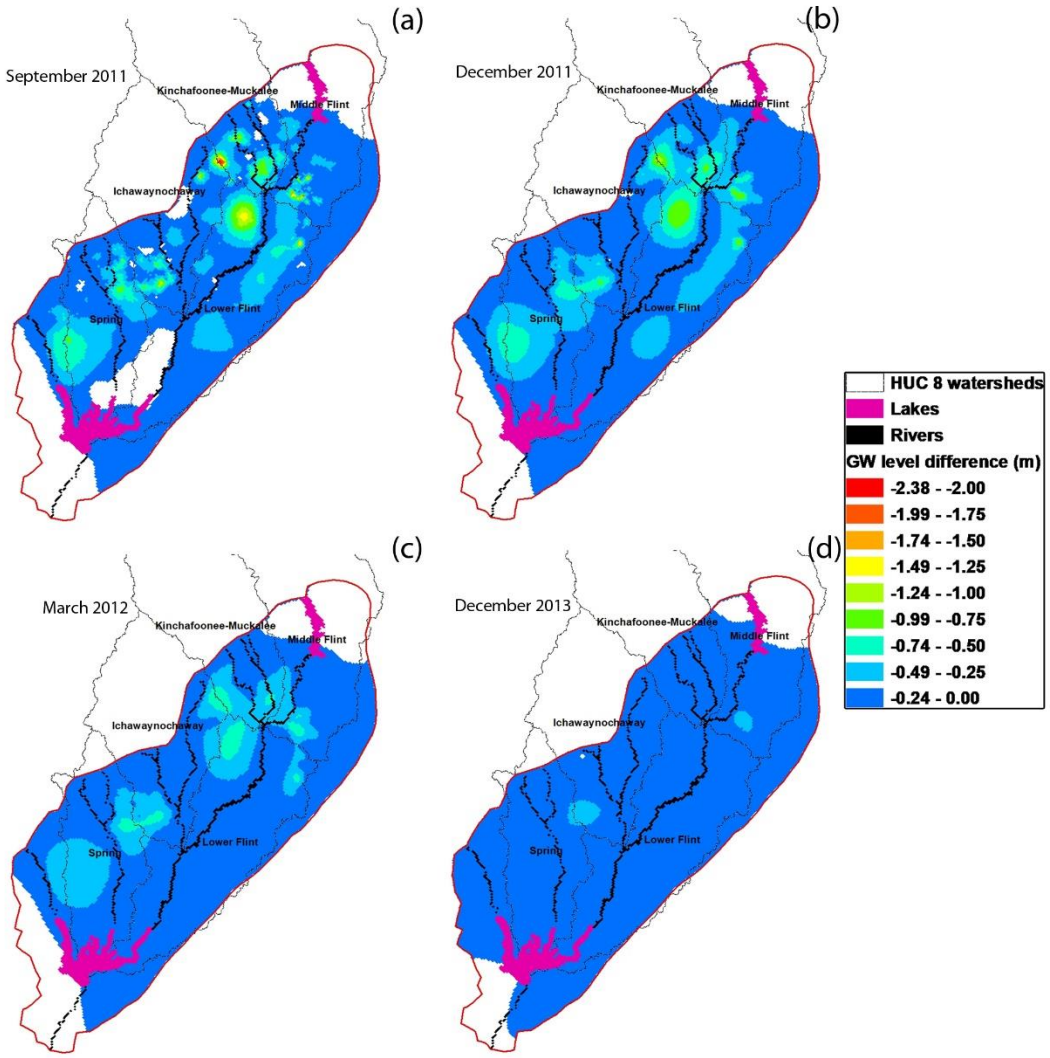

Figure 4.15 Difference in groundwater levels between the calibrated model and projected scenario for (a) September 2011, (b) December 2011, (c) March 2012, and (d) December 2013.

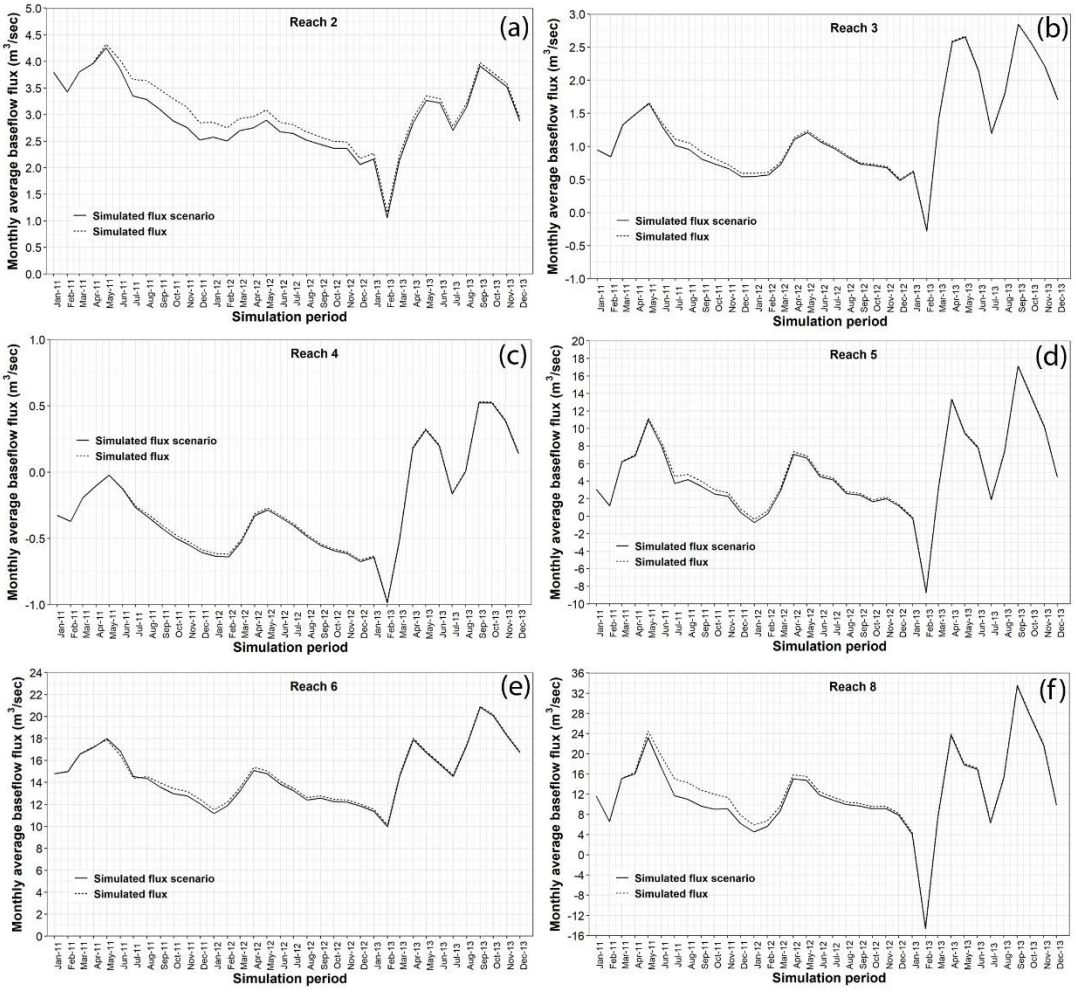

Figure 4.16 Simulated flux between calibrated and scenario model run from 2011 to 2013 for (a) reach 2, (b) reach 3, (c) reach 4, (d) reach 5, (e) reach 6, and (f) reach 8.

4.5 Summary and Conclusions

This study developed a groundwater model for the UFA in the lower ACF river basin that can adequately simulate for groundwater levels and stream-aquifer flux in the region. Spatio-temporal calibration and evaluation of both groundwater levels and stream-aquifer flux was performed to make sure that the model can accurately simulate groundwater levels and stream-aquifer flux throughout the model domain and for both wet and dry climatic periods. Evaluation of the groundwater budget showed that recharge was the most important groundwater inflow into the

system while river outflow was the most important source of groundwater outflow. This also indicated the importance of the UFA in maintaining streamflow in the region, especially under drought conditions. Monthly evaluation of groundwater budget showed that decrease in groundwater recharge due to prolonged drought conditions can severely reduce flow from the aquifers to the rivers in the region. The rebound of the stream-aquifer flux with the return of normal precipitation indicated to the rebound potential of the aquifer but also to the vulnerability of the region to prolonged drought conditions. Sensitivity analysis of recharge zones helped identify upland instream karst as the most sensitive geohydrologic zone for recharge into the aquifer. Simulation and comparison of the projected irrigation scenario to the calibrated model showed that groundwater levels decreased by as much as 2.38 m in the UFA in the Lower Flint and, as a result, decrease in stream-aquifer flux was also observed. Reach sections in the Lower Flint and the adjoining Kinchafoonee watershed saw the greatest % reduction in stream-aquifer flux. The scenario run helped identify the aquifer regions that are most susceptible to the increase in groundwater pumpage for irrigation and also indicated that the aquifer might not be able to sustain the projected increase in groundwater pumpage for irrigation, especially under prolonged drought conditions.

4.6 References

Anderson, M. P., Woessner, W. W., Hunt, R. J. (2015). *Applied groundwater modeling: simulation of flow and advective transport*. Academic press.

Arguez, A., Durre, I., Applequist, S., Vose, R. S., Squires, M. F., Yin, X., … Owen, T. W. (2012). NOAA's 1981--2010 US climate normals: An overview. *Bulletin of the American Meteorological Society*, *93*(11), 1687–1697.

Arnold, J. G., Muttiah, R. S., Srinivasan, R., Allen, P. M. (2000). Regional estimation of base flow and groundwater recharge in the Upper Mississippi river basin. *Journal of Hydrology*, *227*(1–4), 21–40. https://doi.org/10.1016/S0022-1694(99)00139-0

Barlow, P. M., Cunningham, W. L., Zhai, T., Gray, M. (2015). *US Geological Survey groundwater toolbox, a graphical and mapping interface for analysis of hydrologic data (version 1.0): user guide for estimation of base flow, runoff, and groundwater recharge from streamflow data*. US Department of the Interior, US Geological Survey.

Center, S. E. L. (2015). Tri-state water wars (AL, GA, FL).

CH2M. (2017). *Coosa - North Georgia Water Planning Region Water and Wastewater Forecasting Technical Memorandum*.

GA EPD. (2016). *Flint River Basin Regional Water Development and Conservation Plan*.

Gagnon, P. M., Golladay, S. W., Michener, W. K., Freeman, M. C. (2004). Drought responses of freshwater mussels (Unionidae) in coastal plain tributaries of the Flint River basin, Georgia. *Journal of Freshwater Ecology*, *19*(4), 667–679.

Gesch, D., Oimoen, M., Greenlee, S., Nelson, C., Steuck, M., Tyler, D. (2002). The national elevation dataset. *Photogrammetric Engineering and Remote Sensing*, *68*(1), 5–32.

Gilbert, A., Turner-Nesmith, A. (2019). The War Over Water Continues. *Science Scope*, *43*(3), 53–63.

Golladay, S. W., Gagnon, P., Kearns, M., Battle, J. M., Hicks, D. W. (2004). Response of freshwater mussel assemblages (Bivalvia: Unionidae) to a record drought in the Gulf Coastal Plain of southwestern Georgia. *Journal of the North American Benthological Society*, *23*(3), 494–506.

Gordon, D. W., Peck, M. F. (2010). *Stream base flow and potentiometric surface of the Upper Floridan aquifer in south-Central and southwestern Georgia, November 2008*.

GWC. (2017). *Watering Georgia: The State of Water and Agriculture in Georgia*. Athens, GA.

Harbaugh, A. W. (2005). *MODFLOW-2005, the US Geological Survey modular ground-water model: the ground-water flow process*. US Department of the Interior, US Geological Survey Reston.

Healy, R. W. (2010). *Estimating groundwater recharge*. Cambridge University Press.

Homer, C., Dewitz, J., Jin, S., Xian, G., Costello, C., Danielson, P., … others. (2020). Conterminous United States land cover change patterns 2001--2016 from the 2016 National Land Cover Database. *ISPRS Journal of Photogrammetry and Remote Sensing*, *162*, 184–199.

Hunt, R. J., Feinstein, D. T. (2012). MODFLOW-NWT: Robust handling of dry cells using a Newton formulation of MODFLOW-2005. *Groundwater*, *50*(5), 659–663.

Jones, L. E., Painter, J. A., LaFontaine, J. H., Sepúlveda, N., Sifuentes, D. F. (2017). *Groundwater-flow budget for the lower Apalachicola-Chattahoochee-Flint River Basin in southwestern Georgia and parts of Florida and Alabama, 2008--12*.

Jones, L. E., Torak, L. J. (2006). *Simulated effects of seasonal ground-water pumpage for irrigation on hydrologic conditions in the Lower Apalachicola-Chattahoochee-Flint River Basin, Southwestern Georgia and parts of Alabama and Florida, 1999-2002*.

Kinnaman, S. L., Dixon, J. F. (2011). *Potentiometric Surface of the Upper Floridan Aquifer in Florida and Parts of Georgia, South Carolina, and Alabama, May-June 2010*. US Department of the Interior, US Geological Survey.

Kuniansky, E. L. (2016). *Simulating groundwater flow in karst aquifers with distributed parameter models—comparison of porous-equivalent media and hybrid flow approaches*.

Kuniansky, E. L., Gomez-Gomez, F., Torres-Gonzalez, S. (2004). Effects of Aquifer Development and Changes in Irrigation Practices on Ground-Water Availability in the Practices on Ground-Water Availability in the Santa Isabel Area, Puerto Rico.

Lawrence, S. J. (2016). *Water use in the Apalachicola-Chattahoochee-Flint River Basin, Alabama, Florida, and Georgia, 2010, and water-use trends, 1985-2010*.

Mitra, S., Srivastava, P., Singh, S. (2016). Effect of irrigation pumpage during drought on karst aquifer systems in highly agricultural watersheds: example of the Apalachicola-Chattahoochee-Flint river basin, southeastern USA. *Hydrogeology Journal*, *24*(6), 1565–1582. https://doi.org/10.1007/s10040-016-1414-y

Neitsch, S. L., Arnold, J. G., Kiniry, J. R., Williams, J. R. (2011). *Soil and Water Assessment Tool Theoretical Documentation Version 2009*.

Niswonger, R. G., Panday, S., Ibaraki, M. (2011). MODFLOW-NWT, a Newton formulation for MODFLOW-2005. *US Geological Survey Techniques and Methods*, *6*(A37), 44.

Poeter, E. P., Hill, M. C. (1998). *Documentation of UCODE, a computer code for universal inverse modeling*. DIANE Publishing.

Poeter, E. P., Hill, M. C. (1999). UCODE, a computer code for universal inverse modeling. *Computers & Geosciences*, *25*(4), 457–462.

Raposo, J. R., Dafonte, J., Molinero, J. (2013). Assessing the impact of future climate change on groundwater recharge in Galicia-Costa, Spain. *Hydrogeology Journal*, *21*(2), 459–479.

Rugel, K., Jackson, C. R., Romeis, J. J., Golladay, S. W., Hicks, D. W., Dowd, J. F. (2012). Effects of irrigation withdrawals on streamflows in a karst environment: lower Flint River Basin, Georgia, USA. *Hydrological Processes*, *26*(4), 523–534.

Shea, C. P., Peterson, J. T., Conroy, M. J., Wisniewski, J. M. (2013). Evaluating the influence of land use, drought and reach isolation on the occurrence of freshwater mussel species in the lower Flint River Basin, Georgia (USA). *Freshwater Biology*, *58*(2), 382–395.

Singh, S., Mitra, S., Srivastava, P., Abebe, A., Torak, L. (2017). Evaluation of Water-Use Policies for Baseflow Recovery during Droughts in an Agricultural Intensive Karst Watershed: Case study of the Lower Apalachicola-Chattahoochee-Flint River Basin, Southeastern USA. *Hydrological Processes*.

Singh, S., Srivastava, P., Mitra, S., Abebe, A. (2016). Climate variability and irrigation impacts on streamflows in a Karst watershed—A systematic evaluation. *Journal of Hydrology: Regional Studies*, *8*, 274–286.

Singh, S., Srivastava, P., Mitra, S., Abebe, A., Srivastava, P., Abebe, A., Torak, L. (2017). Evaluation of water-use policies for baseflow recovery during droughts in an agricultural intensive karst watershed: Case study of the lower Apalachicola--Chattahoochee--Flint River Basin, southeastern United States. *Hydrological Processes*, *31*(21), 3628–3644.

Sophocleous, M. (2005). Groundwater recharge and sustainability in the High Plains aquifer in Kansas, USA. *Hydrogeology Journal*, *13*(2), 351–365.

Sun, H., Cornish, P. S. (2005). Estimating shallow groundwater recharge in the headwaters of the Liverpool Plains using SWAT. *Hydrological Processes: An International Journal*, *19*(3), 795–807.

Torak, L. J., Painter, J. A. (2006). *Geohydrology of the lower Apalachicola-Chattahoochee-Flint River basin, southwestern Georgia, northwestern Florida, and southeastern Alabama*.

University of Georgia CAES. (2014). *Georgia Farm Gate Value Report*. Retrieved from http://caes2.caes.uga.edu/center/caed/pubs/documents/2014UGACAEDFGVR_FINAL.pdf.

USGS. (2019). USGS water data for the Nation: US Geological Survey National Water Information System database.

Williams, L. J., Dixon, J. F. (2015). Digital surfaces and thicknesses of selected hydrogeologic units of the Floridan aquifer system in Florida and parts of Georgia, Alabama, and South Carolina. *US Geological Survey Data Series*, *926*, 24.

Williams, L. J., Kuniansky, E. L. (2016). *Revised hydrogeologic framework of the Floridan aquifer system in Florida and parts of Georgia, Alabama, and South Carolina*. United States Department of the Interior, United States Geological Survey.

Winston, R. B. (2009). *ModelMuse: a graphical user interface for MODFLOW-2005 and PHAST*. US Geological Survey Reston, VA.

Chapter 5

Impact of hydrological calibration in SWAT groundwater recharge simulation: A case study in the Flint River Basin, USA

5.1 Abstract

Accurate estimation of groundwater recharge is essential for the sustainable management of groundwater resources. Although quantifying groundwater recharge is critical, it is one of the least understood processes in hydrogeology and can only be estimated at a regional scale as it is almost impossible to measure directly. The Soil and Water Assessment Tool (SWAT) has often been used as a tool for performing groundwater recharge studies. And, as calibration of groundwater recharge simulation is not possible due to the lack of direct measurements, confidence in the SWAT simulated groundwater recharge is often derived by evaluating the model performance in simulating other hydrological variables including streamflow and/or evapotranspiration (ET). However, the impact and sensitivity of calibrating these variables in the simulation of groundwater recharge in SWAT are yet to be evaluated to develop a better calibration approach for accurately simulating groundwater recharge. This study evaluated the sensitivity of calibrating either streamflow or ET or using a multi-variate approach in the SWAT simulation of groundwater recharge by doing a case study in the Flint River Basin of southeastern United States (U.S.). The study showed that streamflow is the most important and influential variable to be calibrated in SWAT for simulating groundwater recharge accurately while the calibration of ET alone had a negligible impact in the simulation of groundwater recharge. Evaluation of the multi-variate calibration approach showed that streamflow calibration followed by ET calibration provided the most accurate estimates for groundwater recharge. A flipped calibration sequence, however, did not result in simulated groundwater recharge that was representative of the region's hydrogeology.

The study also demonstrated the importance of calibrating the different sub-sections of the watershed that differ in geology separately for better estimation of groundwater recharge as the parameters that are critical for groundwater recharge simulation can be fine-tuned for the region.

5.2 Introduction

Groundwater is an integral component of the hydrologic system accounting for more than 97% of the available freshwater in the world (Lall et al., 2020; Shiklomanov and Rodda, 2003). It is an indispensable water resource supplying over half of the world's water for drinking and irrigation, along with a third of the industrial demand (Lall et al., 2020; Siebert et al., 2010). Groundwater plays a critical role in mitigating impacts of prolonged drought conditions, especially in agriculture, serving as a source when the surficial sources are depleted (Famiglietti, 2014; Lall et al., 2020). However, groundwater around the world is being pumped at a rate higher than it can be naturally replenished, and this has resulted in short- and long-term declines in groundwater levels. Wada et al. (2010) determined that the global groundwater depletion increased from 126 (± 32) $km^3\ yr^{-1}$ to 283 (± 40) $km^3\ yr^{-1}$ from 1960 to 2000. The United States, during the same time period, increased the groundwater depletion by 32 (± 7) $km^3\ yr^{-1}$. This has led many aquifers to the brink of extinction or being seasonally exhausted, and the aquifers will only be further stressed with the continuous increase in population, irrigated agriculture, urbanization, and climate change (Famiglietti, 2014; Gleeson et al., 2012; Konikow and Kendy, 2005; Lall et al., 2020). Along with the reduction in freshwater availability, groundwater level reduction also results in severe ecological impacts, including a reduction in streamflow, loss of springs, wetlands, and the ecological habitat associated with it, seawater intrusion, and land subsidence (Famiglietti, 2014). Hence, sustainable management of groundwater resources is a priority topic for many stakeholders, policymakers, and researchers around the world and in the United States for which

an accurate estimation of groundwater recharge is a critical component (De Vries and Simmers, 2002).

Groundwater recharge can be described as the amount of water that percolates past the unsaturated zone of the land surface and adds to the groundwater storage through diffused and focused mechanisms (Healy, 2010). Although quantifying groundwater recharge is critical for assessing aquifer sustainability, it is one of the least understood processes in hydrogeology (Rushton and Redshaw, 1979) and can only be estimated as it is almost impossible to measure directly (Healy, 2010; Kinzelbach and others, 2002). Groundwater recharge can vary significantly in time and space as it is influenced by multiple factors, including temporal and spatial variability in climate, land use, vegetation, and hydrogeology. Multiple methods at the point- and watershed-scale have been used to estimate groundwater recharge. Examples include water budget method, lysimeters, seepage meters, tracers (heat, isotopic, and environmental), numerical modeling, and baseflow discharge (Scanlon et al., 2002). Point scale methods provide a detailed estimate of groundwater recharge for a location but can have high uncertainty when extrapolated to a large region while recharge estimates based on streamflow/baseflow only provide an average value for the whole contributing watershed. Hence, catchment-scale hydrological models that simulate spatially variable groundwater recharge by accounting for the spatial and temporal distribution of the factors impacting groundwater recharge can be valuable and cost-effective tools for indirectly estimating groundwater recharge (Jayakody et al., 2014; Sun and Cornish, 2005) and provide critical information for sustainable management of groundwater resources.

The Soil and Water Assessment Tool (SWAT), developed by United States Department of Agriculture (USDA) – Agricultural Research Service (ARS), is a watershed scale, continuous-time, physically-based, semi-distributed model that has spatially distributed parameters and uses

water balance as the driving force for all calculations in the model (Arnold et al., 1998; Neitsch et al., 2011). The SWAT model performs spatial disaggregation of a watershed by dividing it into sub-basins, which is further divided into hydrologic response units (HRU's). HRU's are lumped land areas with a unique combination of land use, soil, and/or slope class within a sub-basin (Neitsch et al., 2011). This allows SWAT to differentiate the different areas of the watershed spatially and simulate spatially variable groundwater recharge by accounting for different land use and soil within a sub-basin. Hydrological components simulated by SWAT includes overland flow, sub-surface lateral flow, soil moisture storage, evapotranspiration, transmission losses, and groundwater recharge (Neitsch et al., 2011). As the model divides a watershed with spatially distributed parameters and can simulate groundwater recharge, SWAT has been widely used for performing groundwater recharges studies including simulating the impacts of land use change (Emam et al., 2015; Eshtawi et al., 2016; Fallatah et al., 2019; Kalin and Hantush, 2009), climate (Awan and Ismaeel, 2014; Mechal et al., 2015; Raposo et al., 2013), and agricultural management practices (Dakhlalla et al., 2016).

As with any physically based hydrological model including SWAT, it is necessary to calibrate the model parameters after the initial model setup to make sure that the model is simulating the critical hydrological processes of the target watershed with accuracy to have confidence in the model output. As direct calibration of groundwater recharge is not possible due to the lack of direct measurements, confidence in the model simulated groundwater recharge in SWAT is often derived by evaluating the model performance in simulating other hydrological variables. Many groundwater recharge studies using SWAT have utilized only streamflow to calibrate the hydrological component of the SWAT model (Baker and Miller, 2013; Chinnasamy et al., 2018; Eshtawi et al., 2016; Ghaffari et al., 2010; Gyamfi et al., 2017; Lee et al., 2014; Lin et al., 2013;

Mechal et al., 2015; Sun and Cornish, 2005). Others have, in addition to streamflow calibration, evaluated SWAT simulated evapotranspiration (ET) against observed ET (Gemitzi et al., 2017), calibrated crop yield as an estimate for ET simulation (Emam et al., 2015; Izady et al., 2015), or calibrated water table fluctuation of the shallow groundwater level (Dakhlalla et al., 2016; Raposo et al., 2013). Studies have also been performed where the SWAT model was simultaneously calibrated for streamflow and ET (Githui et al., 2012) or just ET (Awan and Ismaeel, 2014) to develop confidence in the model for groundwater recharge simulation.

Even though calibration of SWAT for streamflow and ET, which are critical components of the hydrologic water balance, can help increase confidence in SWAT groundwater recharge simulation as a residual variable of the water balance, impact of calibrating these hydrological variables in the simulation of groundwater recharge in SWAT, to the authors knowledge, has not been evaluated. It is essential to evaluate the sensitivity of groundwater recharge simulation in SWAT to calibrating either streamflow or ET or when using a multi-variate approach. Understanding the changes in magnitude and trend of SWAT groundwater recharge simulation due to streamflow and ET calibration as well as comparing to the basin- and point-scale estimated recharge through other methods under different land use and soil types can provide valuable insight into groundwater recharge simulation in SWAT. This information can be pivotal to researchers for efficiently and accurately calibrating the SWAT model for groundwater recharge estimation. Hence, the main objective of this study was to understand in detail how the SWAT calibration approach of streamflow and ET independently as well as using a multi-variate approach through sequential calibration affected the groundwater recharge simulation in SWAT by performing a case-study in the Flint River basin of Southeastern United States. The study also compared the SWAT simulated recharge at the basin- and point-scale against groundwater recharge estimated

through the RORA program (Rutledge, 2007) and groundwater levels in the surficial aquifer system, respectively, to determine if any calibration approach shows better model performance. As the Flint River basin consists of independent sub-basins that are vastly different in soil and land use types, the evaluation was also performed for different land uses and soil. The overarching goal of this project was to identify a SWAT calibration approach that can provide a reliable estimate of groundwater recharge.

5.3 Methods

5.3.1 Study area

The study area, located in the Southeastern United States (Fig. 5.1a), covers about 24,000 km^2 and includes six Hydrologic Unit Code (HUC)-8 watersheds (Seaber et al., 1987) of the Flint River basin (Fig. 5.1b). As the study area spans over 3 degrees in latitude, temperature and precipitation vary spatially and temporally across the area. The mean daily temperature in the winter ranges from about 9.8℃ in the south to about 5.5℃ in the north, while the summer temperature averages about 28℃ across the study area (Arguez et al., 2012). Temperature above 37.7℃ in the summer, however, is not uncommon in the region. Annual precipitation averages about 1348 mm in the south and about 1244 mm in the north (Arguez et al., 2012). Forest, most of which is loblolly pine (*Pinus taeda*) in the region (Ruefenacht et al., 2008), is the dominant land use/land cover (LULC) and occupies about 55% of the study area (Fig. 5.1c). Parts of the study area that is underlain by the Upper Floridan Aquifer (UFA), which is very close to the land surface and serves as the primary source of water for irrigation, has intensive agriculture (Torak and Painter, 2006; Fig. 5.1b and 5.1c). Row crop agriculture covers about 17% of the watershed. Cotton and peanut are the two major crops produced in the region. Urban area accounts for only about 7% of the watershed (University of Georgia CAES, 2018; Fig. 5.1c). Accurate estimation and understanding of

groundwater recharge in the study area, especially in the lower Flint region, is critical for agricultural sustainability in the region. Agriculture generates annual revenue of about $2 billion (University of Georgia CAES, 2014) and is heavily dependent on the underlying aquifer for irrigation water. The aquifer also plays a critical role in maintaining streamflow, spring flow, and the ecological habitat of endangered and threatened species that depend on the river system.

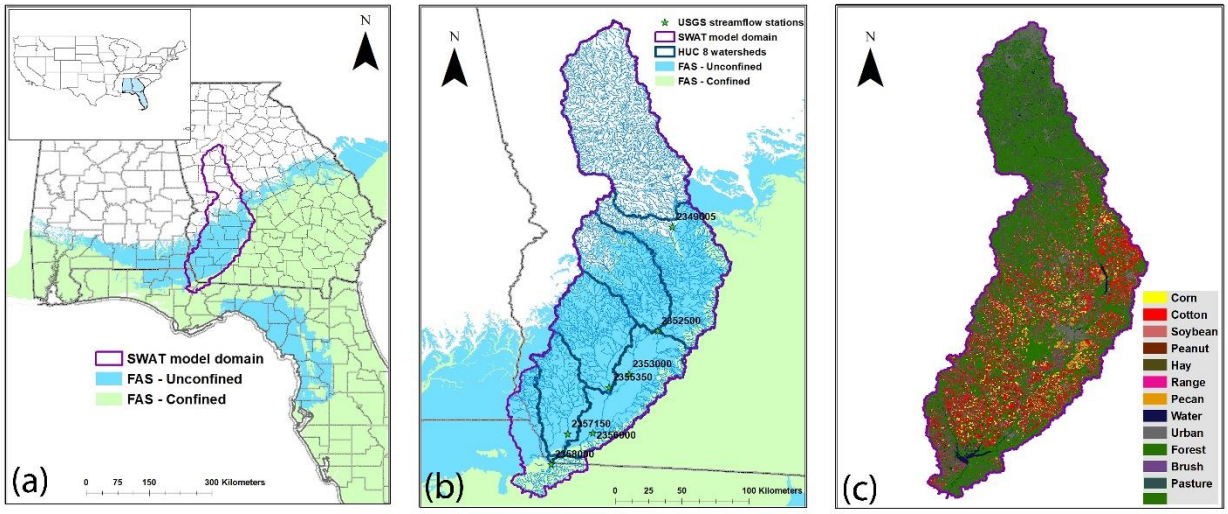

Figure 5.1 SWAT model domain and location of the study area in the southeastern United States (a), the six HUC-8 watersheds located within the model domain (b), and major land use/land cover (LULC) types in the study region (c).

5.3.2 Groundwater recharge simulation in SWAT

This section provides a summary of the theory behind groundwater recharge simulation in SWAT; the readers are referred to Neitsch et al. (2011) for further detail. The water balance equation that is the basis of all land phase hydrologic calculations in SWAT, which is computed at the HRU level, is:

$$SW_i = SW_{i-1} + \sum_{i=1}^{i=t}(R_i - Q_{surf,i} - E_{a,i} - w_{seep,i} - Q_{gw,i}) \quad (6)$$

where, SW_i is the final soil water content for the day, SW_{i-1} is the final soil moisture content for day $i-1$ and initial soil water content for day i, $R_{day,i}$ is the amount of precipitation on day i, $Q_{surf,i}$ is the amount of surface runoff on day i, $E_{a,i}$ is the amount of evapotranspiration on day i, $w_{seep,i}$ is the amount of percolation and bypass flow exiting the soil profile bottom on day i, and $Q_{gw,i}$ is the amount of return flow on day i.

Vertical movement of water through the soil layers in SWAT after entering the soil profile is simulated using a simplified soil module that only simulates saturated flow using a cascading approach. Water is allowed to move from a layer to the layer below only if the field capacity is exceeded for that layer and the layer below is unsaturated, after accounting for losses to other pathways such as evapotranspiration and lateral flow. Water that moves past the bottom layer of the soil through percolation or bypass flow becomes groundwater recharge after accounting for the time delay it takes for the water to move from the bottom of the soil profile to the top of the water table. Groundwater recharge in SWAT, after water moves past the soil profile, is calculated using an exponential decay weighing function:

$$W_{rchrg,i} = \left(1 - \exp\left[\frac{-1}{\delta_{gw}}\right]\right) W_{seep} + \exp\left[\frac{-1}{\delta_{gw}}\right] W_{rchrg,i-1} \quad (7)$$

where, $W_{rchrg,i}$ is the amount of recharge entering the aquifer on day i, δ_{gw} is the delay time for the water to travel through the vadose zone, W_{seep} is the water exiting the bottom of the soil profile on day i, and $W_{rchrg,i-1}$ is the amount of recharge entering the aquifer on day $i-1$

The groundwater delay function (δ_{gw}; GW_Delay in *.gw* file), which estimates the time for water to pass through the vadose zone, cannot be measured and is often used as a calibration variable when calibrating SWAT for streamflow and/or baseflow (Karki et al., 2020; Risal and Parajuli, 2019). The estimated groundwater recharge is then distributed into the two aquifers that are simulated in SWAT, the shallow aquifer and the deep aquifer, using a percolation coefficient (RCHGRG_DP, *.gw* file) and is calculated as:

$$W_{deep} = \beta_{deep} * W_{rchrg} \quad (8)$$

where, W_{deep} is the amount of water moving to the deep aquifer, β_{deep} is the aquifer percolation coefficient, and W_{rchrg} is the amount of recharge

Shallow aquifer recharge is then calculated as the difference between the total recharge and the deep aquifer recharge. SWAT simulated total groundwater recharge (W_{rchrg}) value represents the total water contribution to the groundwater system. Hence, the value was used as a simulated groundwater recharge for evaluating the different calibration approaches as well as comparing to estimated groundwater recharge from other studies.

5.3.3 SWAT model setup

Major inputs into SWAT for the initial model set up include elevation, climate, LULC, and soil dataset (Neitsch et al., 2011). A 30m x 30m Digital Elevation Model (DEM) provided by the United States Geological Survey (USGS) (Gesch et al., 2002) was used as the elevation dataset for the model (Fig. 5.2a) while initial soil parameters for the region was acquired from the State Soil Geographic (STATSGO) dataset (Schwarz and Alexander, 1995). Cropland Data Layer (CDL) developed by the USDA – National Agricultural Statistics Service (NASS) for the year 2015 was

used as the base LULC map for the model (Han et al., 2012). As LULC is mostly dynamic and changes year by year, especially in the row crop agricultural region, major crop rotations in the study area were identified by downloading the 2010-2015 CDL and performing an overlay analysis using ArcGIS which was then added to the model. It is also equally important to accurately represent the agricultural management practices for the major crops as it can help simulate the crop growth and yield accurately, which can impact ET simulation in the model and thereby affect the simulation of groundwater recharge. Hence, detailed management practices including fertilizer application rates and timing, tillage, plant and harvest dates, and irrigation were developed with help from the University of Georgia Extension Service and incorporated into the model. As loblolly pine made up almost all of the forest in the modeled area, all forest classes in the CDL were changed to a single class – FRSE for ease of calibration. Similarly, the default forest management file created by ArcSWAT 'plants and kills' forest every year of the simulation. The forest management file was modified, following steps implemented by Haas (2020), such that the forest was growing in the initial model set up and was not killed every year. Climate data was acquired from the North American Land Data Assimilation Phase-2 (NLDAS-2) climate forcing dataset, which has a spatial resolution of $1/8^{th}$ degree and temporal resolution of 1 h covering the continental United States (Xia et al., 2012). A SWAT model with 118 sub-basins (Fig. 5.2b) and 7,068 HRUs was developed in the end.

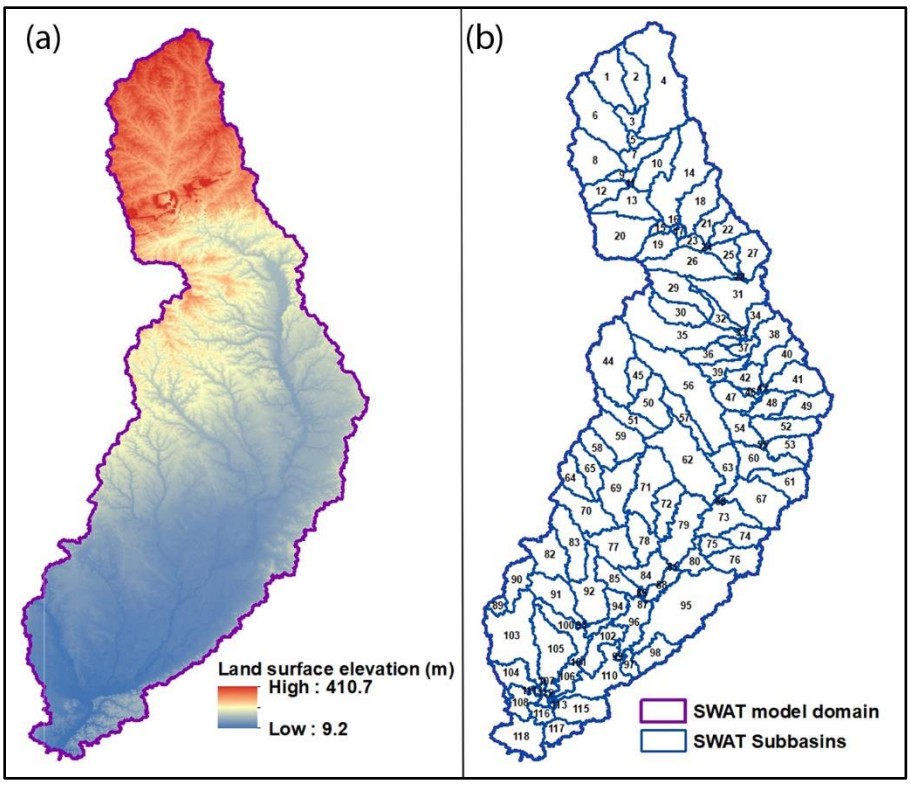

Figure 5.2 Topography (a), and SWAT delineated 118 sub-basins (b) for the study area.

5.3.4 SWAT calibration scenarios

As the main objective of this study was to evaluate the impact of streamflow and ET calibration on groundwater recharge simulation individually as well as using a multi-variate approach and also to determine if there is a calibration sequence that provides better groundwater recharge estimation, two calibration approaches were tested in this study. Streamflow and ET were chosen as the hydrologic variables for calibration as these two variables are major components of the land phase hydrologic water balance. Observed streamflow as well as remotely sensed ET data set for the calibration of these two variables are readily available and have been widely used for hydrologic calibration of SWAT.

The first calibration approach, from herein referred to as approach-1, resembled the calibration strategy that has been used by many researchers for groundwater recharge estimation in SWAT.

Streamflow was the first variable calibrated after the initial model set up to constrain the model, which was followed by ET calibration. Simulated groundwater recharge after each calibration step was evaluated against default SWAT simulated groundwater recharge as well as the recharge estimated using the RORA program. This allowed for evaluating the impact of just streamflow calibration on groundwater recharge as well as the impact of multivariable calibration using a sequential approach in which streamflow calibration was followed by ET calibration. RORA, which is based on the recession-curve displacement method for estimating groundwater recharge from observed streamflow data, has been used in multiple studies for estimating groundwater recharge (Chen and Lee, 2003; Delin et al., 2007; Rutledge, 2007) as well as evaluating the performance of hydrological models in simulating groundwater recharge (Arnold et al., 2000; Zhu et al., 2020).

The second approach, from herein referred to as approach-2, was the exact opposite of approach-1 with ET calibration being performed after the initial model setup followed by streamflow evaluation. This, again, allowed to evaluate how groundwater recharge simulation is impacted if only ET is calibrated. ET calibration was then be followed by streamflow calibration, and model performance was again evaluated. This allowed us to evaluate if there is any difference in model performance for hydrological simulation between the two calibration sequences of ET and streamflow.

5.3.5 SWAT model calibration and evaluation

The SWAT model was set up for the period 2000-2015 with a 3-year warm-up. As the focus of this research was to evaluate how the calibration approaches impacted groundwater recharge simulation, model performance evaluation after calibration was performed for the total simulation period. The model was, however, calibrated for the period 2003-2010 to make sure that the model

was not over-parameterized during calibration and the simulation included time period independent of model calibration. This also allowed to keep the study focused on the impact of calibration on groundwater recharge simulation without having to differentiate results between calibration and validation periods. Streamflow calibration was performed using daily observed data, while ET calibration was performed at a monthly scale. Although the two calibration scenarios were evaluated in this study that differed in the sequence of streamflow and ET calibration, the calibration approach used for each variable in both scenarios were the same. Calibration for both streamflow and ET was performed using SWAT-CUP, an optimization program specifically developed for SWAT that uses the Sequential Uncertainty Fitting Algorithm-Version 2 (SUFI-2) (Abbaspour, 2013).

Streamflow calibration was performed by utilizing observed streamflow data from seven USGS monitored streamflow stations (USGS, 2019) that were within the study area (Fig. 5.1). A sequential approach to streamflow calibration was applied in which flows to streamflow stations that received water from independent sub-sections of the watershed, as well as the most upstream streamflow station, were calibrated separately. This was followed by calibrating streamflow at the downstream stations without modifying the calibrated parameter values for the upstream and independent sub-sections of the watershed. A sequential approach to streamflow calibration was necessary as this allowed to evaluate groundwater recharge as well as the calibrated model parameter values, especially pertaining to groundwater recharge, on how it differed for different parts of the watershed that varied in LULC, soil, and proximity to the underlying aquifer. Initial parameters for streamflow calibration were selected based on literature as well as the SWAT theoretical documentation and are presented in Table 5.1 (Arnold et al., 2012; Neitsch et al., 2011; White and Chaubey, 2005).

MODerate Resolution Imaging Spectroradiometer (MODIS) 8-day global terrestrial ecosystem ET data product (MOD16A2) was used as the observed ET data for calibration of model-simulated ET (Running et al., 2017). The data product is based on the logic of the Penman-Monteith equation and uses daily meteorological reanalysis data as well as MODIS remotely sensed data products to calculate ET and is available at 500 m grid resolution. The 8-day ET data product was aggregated to monthly values for each grid and the observed monthly ET value was calculated for each sub-basin by averaging the monthly gridded values of all grids that were within a sub-basin. Field-scale SWAT studies performed by Haas (2020) and Tadych (2020) identified forest parameters for loblolly pine and crop parameters for cotton and peanut, respectively, by calibrating the model for yield, leaf area index (LAI), and biomass. To make use of this valuable forest and crop dataset, an ET calibration scheme was developed in which the calibrated plant database parameters for loblolly pine from Haas (2020), which was represented as FRSE, was first incorporated into the model. This was followed by identifying a sub-basin in the model that had the highest percentage of forested land and further calibrating ET for that sub-basin by only adjusting the parameters important for ET calibration (Table 5.1). The forest ET calibrated parameters were then extrapolated to all HRUs with FRSE as the LULC. Calibration of parameters for forest ET simulation was followed by incorporating the calibrated crop parameters of cotton and peanut from the study of Tadych (2020) followed by further calibration of cotton and peanut ET parameters. RNGE was the only other LULC type that covered more than 5% of the study area. Evaluation of ET simulation in a sub-basin with the highest RNGE percentage after forest and crop ET calibration showed a good correlation between simulated and observed ET and hence ET for RNGE was not further calibrated.

Model performance evaluation for streamflow and ET simulation was performed using the coefficient of determination (R^2), Nash-Sutcliffe Efficiency (NSE), and percent bias (PBIAS). The three statistics have been widely used for performance evaluation of hydrological models and describe the collinearity between simulated and observed variables, indicate how well the simulated and observed data fit the 1:1 line, and describe the average tendency of the simulated value to be over or under the observed value, respectively (Arnold et al., 2015). NSE was also the objective function used for optimization in SWAT-CUP.

Table 5.1 SWAT calibration parameters for streamflow and ET

Variable	Parameter	Description	SWAT input file	Adjustment [a]	Initial Range
Streamflow	CN2	Curve number of operation, moisture condition II	MGT	r	-0.3,0.3
	ALPHA_BF	Baseflow alpha factor	GW	v	0.01,1
	GW_DELAY	Groundwater delay, days	GW	v	0, 500
	GWQMN	Threshold depth of water in the shallow aquifer required for return flow (mmH_2O)	GW	v	0,5000
	REVAPMN	Threshold depth of water in the shallow aquifer for "revap" or percolation to the deep aquifer to occur (mmH_2O)	GW	v	0,1000
	GW_REVAP	Groundwater "revap" coefficient	GW	v	0.02,0.2
	SOL_K	Saturated hydraulic conductivity	SOL	r	-0.3,0.3
	SOL_BD	Moist bulk density	SOL	r	-0.3,0.3
	SOL_AWC	Available water capacity of the soil layer	SOL	r	-0.3,0.3
	OV_N	Manning's "n for overland flow"	HRU	r	-0.3,0.3
	SURLAG	Surface runoff lag coefficient	HRU	v	0.5-20
	SLSUBBSN	Average slope length (m)	HRU	r	-0.3,0.3
	HRU_SLP	Average slope steepness (m/m)	HRU	r	-0.3,0.3
	LAT_TIME	Lateral flow travel time (days)	HRU	v	0,180
Streamflow/ET	EPCO	Plant uptake compensation factor	HRU	v	0.01,1
	ESCO	Soil evaporation compensation factor	HRU	v	0.01,1
ET	CANMX	Maximum canopy storage (mmH_2O)	HRU	v	0.1,20
	CHTMX	Maximum canopy height (m)	DAT	v	0.5,30
	GSI	Maximum stomatal conductance at high solar radiation and low vapor pressure deficit (ms^{-1})	DAT	v	0.001,0.01

"a" Indicates the type of model parameter adjustment. 'r' represents the model parameter adjustment by multiplying the original

parameter with the adjustment factor (1 + r). 'v' represents the replacement of the original parameter value by a value within the initial range.

5.3.6 Groundwater recharge estimation and groundwater well observation

As RORA utilizes streamflow data for estimating groundwater recharge, the estimated recharge is the averaged value for the entire surficial drainage area contributing to the streamflow station. Estimated groundwater recharge using the RORA program for comparison against the SWAT simulated groundwater recharge were derived for three streamflow stations (Fig. 5.3a, 5.3b, and 5.3c). The three streamflow stations were selected such that SWAT groundwater recharge simulation could be evaluated in a forested region where the underlying aquifer is not connected to the surficial streams (Fig. 5.3a; USGS station 2349605), an agriculture dominated region where the aquifer is close to the land surface (Fig. 5.3b; USGS station 2357150), and recharge simulation evaluation for most of the model domain (Fig. 5.3c; USGS station 2356000). The most downstream USGS station (USGS station 2358000; Fig 5.1) was not selected for estimating groundwater recharge for the whole model through RORA as the station was downstream of Lake Seminole, which could impact groundwater recharge estimation through the RORA program. It is important to note that the RORA program, which estimates groundwater recharge based on streamflow peaks, does not explicitly account for gradual recharge to the water table and can cause errors in the recharge estimates (Rutledge, 2007). Hence, only a graphical comparison was performed between the SWAT simulated, and RORA estimated groundwater recharge to perform a general comparison between the two methods. And, although it is suggested to use RORA for seasonal or quarterly estimation of groundwater recharge (Rutledge, 2007), RORA provides monthly estimates of groundwater recharge and was used in this study for comparison against simulated recharge to evaluate SWAT simulated groundwater recharge in more detail.

A comparison of the temporal trend in SWAT estimated groundwater recharge was also performed against groundwater level observation in two shallow wells (Fig. 5.3d) that were completed close to the land surface to compare the daily trend in groundwater recharge simulation and groundwater level. Temporal changes in groundwater levels in the two wells can be used as an indicator to evaluate the trend of groundwater recharge in the region and be compared against SWAT simulated groundwater recharge. Groundwater well data for the two wells were acquired from the USGS National Water Information System (NWIS) (USGS, 2019). The two wells were selected such that one was in a forest dominated sub-basin with deep soils (well 11AA01; Fig. 5.3d) while the second one was in an agricultural dominated sub-basin and the underlying aquifer was close to the land surface (well 08G001; Fig. 5.3d).

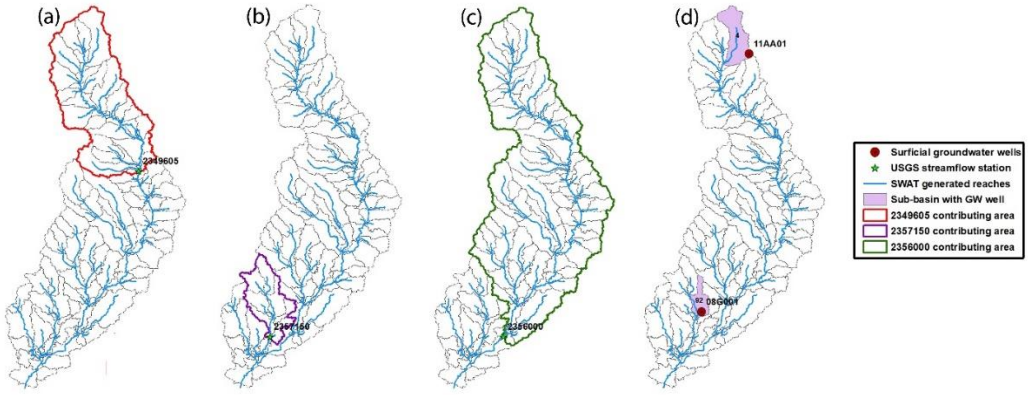

Figure 5.3 Sub-watersheds contributing to streamflow and RORA estimated groundwater recharge for station (a) 2349605, (b) 2357150 and (c) 2356000. Figure (d) shows the location of the two groundwater wells and the sub-watershed associated with it for comparing the temporal trend in groundwater recharge and groundwater levels.

5.4 Results and discussion

5.4.1 Default model

The first step in understanding the sensitivity of streamflow and ET calibration, as well as the impact/change on groundwater recharge simulation is to evaluate SWAT simulation of streamflow, ET, and groundwater recharge under default parameters.

5.4.1.1 Default streamflow simulation

Model performance evaluation for streamflow simulation showed that the model performed poorly for all seven USGS stations with default parameters (Table 5.2). SWAT simulation of daily streamflow is considered satisfactory when the R^2 and NSE values are higher than 0.5, and PBIAS is less than ±15% (Moriasi et al., 2015), and it was observed that R^2 was less than 0.5 and NSE values were negative for all stations. Evaluation of PBIAS showed that the default model significantly over simulated streamflow for all stations.

Table 5.2 Model performance for streamflow simulation with default parameters for the total simulation period for all stations

USGS streamflow station	R^2	NSE	PBIAS (%)
2349605	0.14	-2.38	62
2352500	0.16	-3.32	74.9
2353000	0.14	-4.56	70.2
2355350	0.09	-19.96	123.2
2356000	0.13	-6.18	71.9
2357150	0.04	-29.31	83.9
2358000	0.42	-0.49	27.3

5.4.1.2 Default ET simulation

Evaluation of ET simulation for each sub-basin with default parameters shows that the model does a much better job of simulating ET with the default parameters (Fig. 5.4 and Fig. 5.5) when compared to streamflow simulation. R^2 values were all greater than 0.2, and the average was about

0.5. Mean NSE for all sub-basins was close to 0.4, while more than 50% of the sub-basins have NSE close to 0.5 or higher (Fig. 5.5). Evaluation of PBIAS shows that the default model under simulates ET with mean and median values both close to -20% (Fig. 5.5). Spatial evaluation of R^2, NSE, and PBIAS shows that the model does a much better job of simulating ET on the non-forest dominated sub-basins (Fig. 5.2a and Fig 5.4) than the forest dominated sub-basins (upper part of the study area) with default plant database parameters. It should, however, be noted that although default plant database parameters were used for row crops, detailed management practices, including fertilizer application and irrigation, were provided, which could have led to better simulation of row crops and hence, better ET estimates.

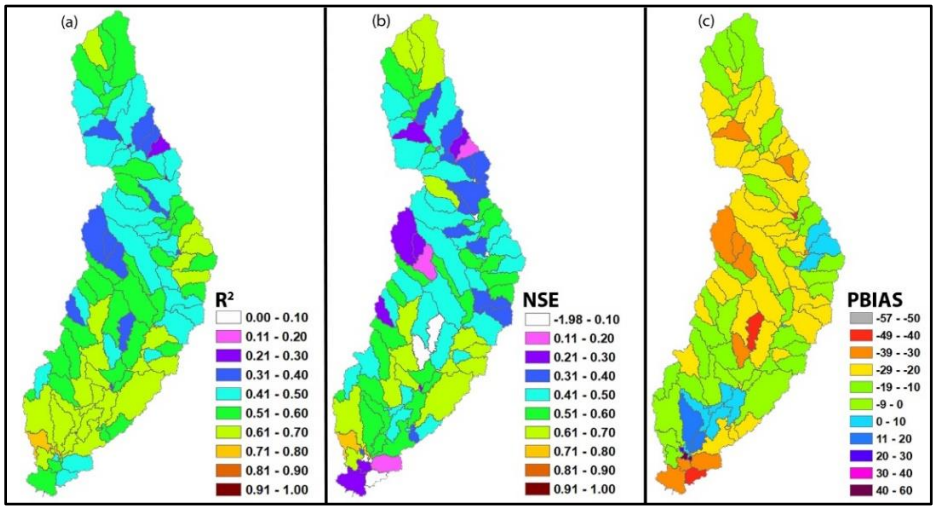

Figure 5.4 (a) R^2, (b) NSE, and (c) PBIAS for ET simulation with default parameters for each sub-watershed in the model.

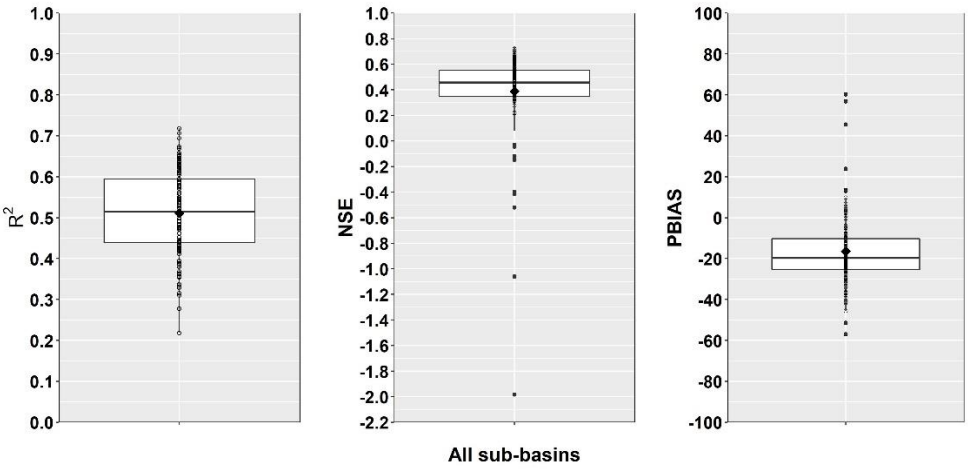

Figure 5.5 Box plots showing the distribution of (a) R^2, (b) NSE, and (c) PBIAS for all sub-basins for ET simulation with default parameters.

5.4.1.3 Default groundwater recharge

As the RORA estimated groundwater recharge using USGS streamflow station is an average value for the whole area that drains to that station, simulated groundwater recharge for comparison was calculated by averaging the simulated recharge of all HRUs that were in the contributing sub-watersheds associated with the respective streamflow station and aggregating to monthly values (Fig. 5.3a, 5.3b, and 5.3c). Comparison between simulated monthly recharge from the SWAT model with default parameters and the RORA estimated monthly recharge for all three sub-watersheds show a good match (Fig. 5.6). The model seems to catch the temporal trend, especially peak recharges, well for all three regions. Comparison for the periods with low RORA estimated recharge showed that the model does a better job of estimating recharge for USGS station 2349605 than for stations 2357150 and 2356000 (Fig. 5.6). It is important to note that station 2357150 and 2356000 have contributing sections of the watershed in which the aquifer is close to the land surface and can have gradual discharge to the streamflow. This can potentially lead to error in

groundwater recharge estimation with RORA and hence the months with no RORA estimated recharge for stations 2357150 and 2356000.

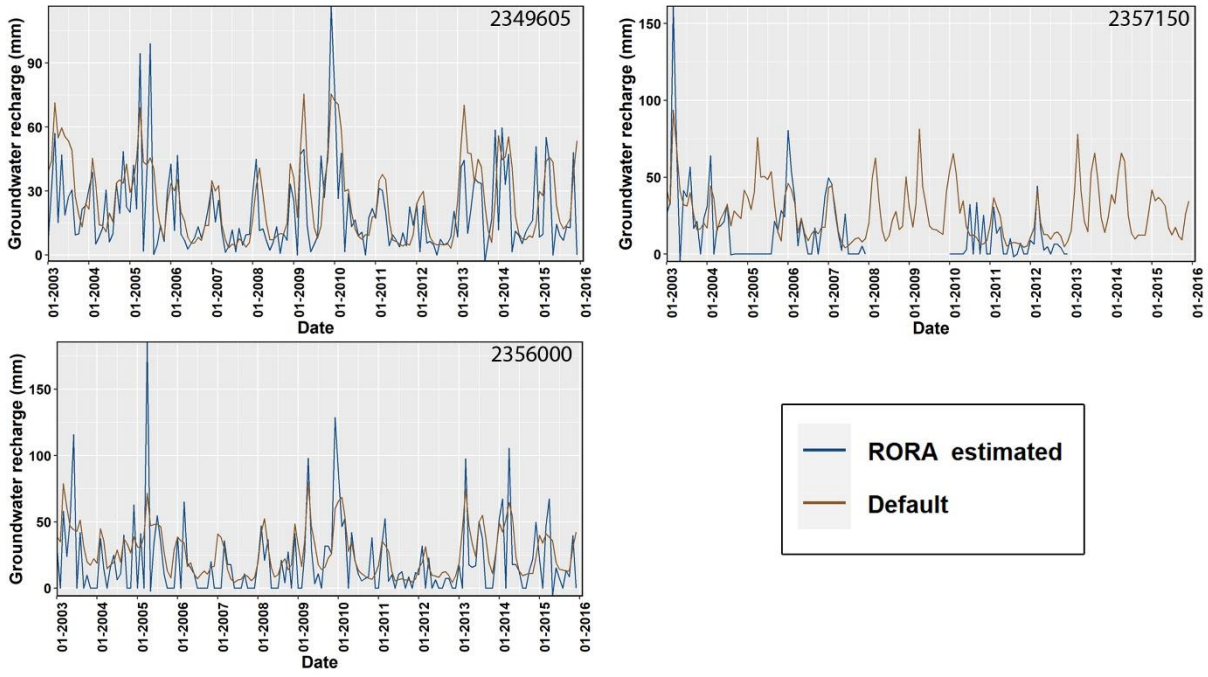

Figure 5.6 Comparison between RORA estimated and SWAT simulated groundwater recharge with default SWAT parameters.

Temporal trend comparison between the daily groundwater levels observed in two groundwater wells and SWAT simulated daily groundwater recharge for the sub-watershed in which the groundwater well is located showed that SWAT simulated groundwater recharge with default parameters is more episodic with sharp rise and fall in groundwater recharge when compared to the change in observed groundwater levels (Fig. 5.7). The change in groundwater level in the well was gradual, indicating a more delayed recharge phenomenon than simulated by SWAT with default parameters for both wells. Well 11AA01 (Fig. 5.3d), which was located in the region with deep soils, had a gradual change in groundwater level than compared to well 08G001 (Fig. 5.3d), which was in a region where the aquifer was close to the land surface**.**

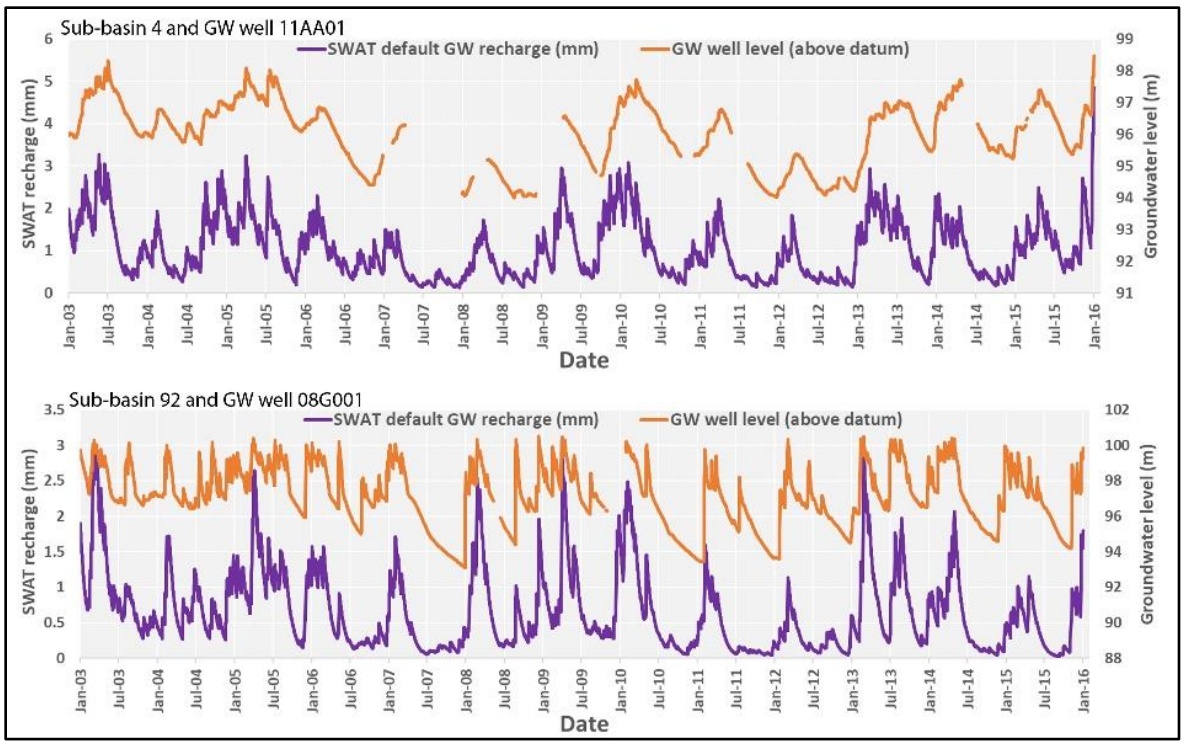

Figure 5.7 Temporal trend comparison between SWAT simulated groundwater recharge with default parameters and groundwater well 11AA01 (top) and 08G001 (bottom).

5.4.2 Calibration approach-1

Flow at each station was calibrated using multiple iterations of 500 simulations until there was no noticeable improvement in the objective function between two successive iterations. SWAT-CUP recommended parameter ranges were used after each iteration to keep the calibration process objective. The calibrated parameters were, however, kept within the parameter ranges specified in Table 5.1 to make sure that values were within a realistic range. As the sub-watersheds were calibrated separately, the calibrated parameter values for streamflow simulation varied spatially. The spatial distribution of calibrated parameter values important to groundwater recharge is discussed in section 3.4.

Calibration of streamflow was followed by ET calibration. The SWAT plant database parameters for loblolly pine developed by Haas (2020) were first imported into the model. This was followed by identifying a sub-basin which had the highest percentage of FRSE (sub-basin 24 – 92%) and calibrating the selected parameters (Table 5.1) for ET. The plant database parameters, GSI and CHTMX (Table 5.1), were further calibrated in this study, as Haas (2020) identified these parameters to be sensitive for ET simulation. EPCO and ESCO, although calibrated for streamflow, were also calibrated again as these parameters play an important role in ET simulation in SWAT (Neitsch et al., 2011). The calibrated *.hru* file parameters were replaced only in HRUs with FRSE as the LULC. ET calibration was also performed for multiple iterations using SWAT-CUP until no noticeable improvement was observed between successive iterations. After completion of forest ET calibration, crop database parameters for cotton and peanut from the study of Tadych (2020) were imported into the model, and an approach similar to FRSE calibration was performed for further calibration of ET for cotton and peanut.

5.4.2.1 Streamflow simulation after calibration approach-1

Streamflow evaluation at all seven streamflow stations showed that the model was satisfactorily able to simulate streamflow in the study watershed after streamflow calibration (Table 5.3; Fig. 5.8). R^2 and NSE values greater than 0.6 were observed for all stations except for stations 2355350 and 2357150, which had NSE values of 0.55 and 0.52, respectively. The area that contributes streamflow to the two stations is near the outcrop of the underlying aquifer, where the aquifer is thin and close to the land surface. The complex hydrogeology of the region as well as missing observed data for the two stations during high flows (Fig. 5.8) that limited streamflow calibration could have led to the comparatively poor model performance for the two stations.

Evaluation of streamflow simulation after the calibration of ET (Table 5.3; Fig. 5.8) showed that the model performance for streamflow simulation slightly weakened, especially for simulating the runoff volume. The simulated streamflow was lower than observed for six of the seven stations, with three stations having a negative PBIAS of over 20% (Table 5.3; Fig. 5.8). R^2 and NSE values, as a result, were also lower for the six stations when compared to values after only streamflow calibration (Table 5.3).

Table 5.3 Model performance for streamflow simulation after sequential calibration of streamflow and ET in calibration approach-1.

	After streamflow calibration			**After ET calibration**		
USGS streamflow station	**R^2**	**NSE**	**PBIAS (%)**	**R^2**	**NSE**	**PBIAS (%)**
2349605	0.68	0.67	0.7	0.64	0.6	-10.3
2352500	0.73	0.72	-7.9	0.7	0.62	-24.2
2353000	0.69	0.67	-11.6	0.67	0.58	-28.2
2355350	0.66	0.55	11.2	0.6	0.49	-10.1
2356000	0.69	0.65	-9.3	0.68	0.61	-25.3
2357150	0.67	0.52	7.2	0.69	0.55	12.8
2358000	0.86	0.85	-7.7	0.85	0.83	-14.2

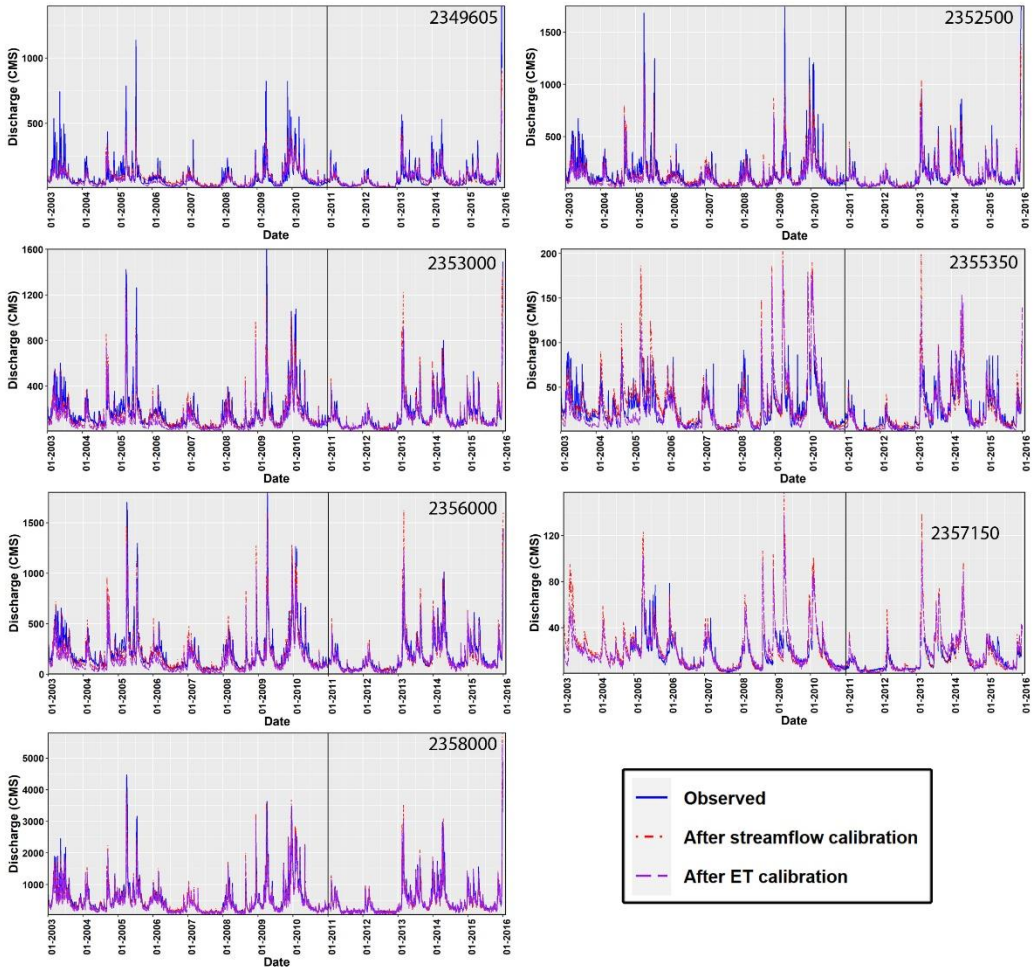

Figure 5.8 Graphical comparison between observed streamflow and simulated streamflow after streamflow calibration and subsequent ET calibration for all seven stations (approach -1). The vertical black line indicates the time frame of the observed dataset that was used for streamflow calibration.

5.4.2.2 ET simulation after calibration approach-1

The spatial distribution and box-plot summary of R^2, NSE, and PBIAS for ET simulation in each SWAT sub-watershed after each calibration step of approach-1 is presented in Fig. 5.9. It can be seen from the figure that ET simulation in SWAT shows general improvement even after the calibration of only streamflow (Fig. 5.9) with better results for R^2, NSE, and PBIAS. The most significant improvement is seen in PBIAS value as the mean PBIAS improves from about -17.5%

in the default model to about -5% after streamflow calibration. Improvement in R^2 and NSE after only streamflow calibration was more profound in the lower sub-basins of the study area that had more agricultural crops while the improvement in the upper sub-basins that is more forest dominated was marginal. There was, however, a general increase in ET throughout the study area after streamflow calibration, as indicated by the upward shift of the PBIAS box plot.

Calibration of ET after streamflow simulation further improved the ET simulation. Mean R^2 improved from about 0.55 to about 0.65 and mean NSE improved to about 0.55 from about 0.4. There was a marked improvement in ET simulation in the forest dominated upper sub-basins. However, when evaluating the overall watershed, ET simulation in the lower sub-basins, which had more agriculture, was better. There was also an improvement in the PBIAS values with the mean and median values, both close to 0. The spatial distribution of PBIAS (Fig. 5.9 – bottom figure) showed that the forest dominated landscapes slightly under-simulated ET even after calibration while the agriculture dominated lower sub-basins slightly over-estimated ET. The under-estimation of ET by the default model and the increase in ET after calibration also explains the reduction in streamflow performance and the under-estimation of streamflow after ET calibration. The outlier sub-basins with negative NSE and high PBIAS even after ET calibration were the ones that had a high percentage of water in the sub-basin and could have led to the model having difficulty in simulating ET accurately.

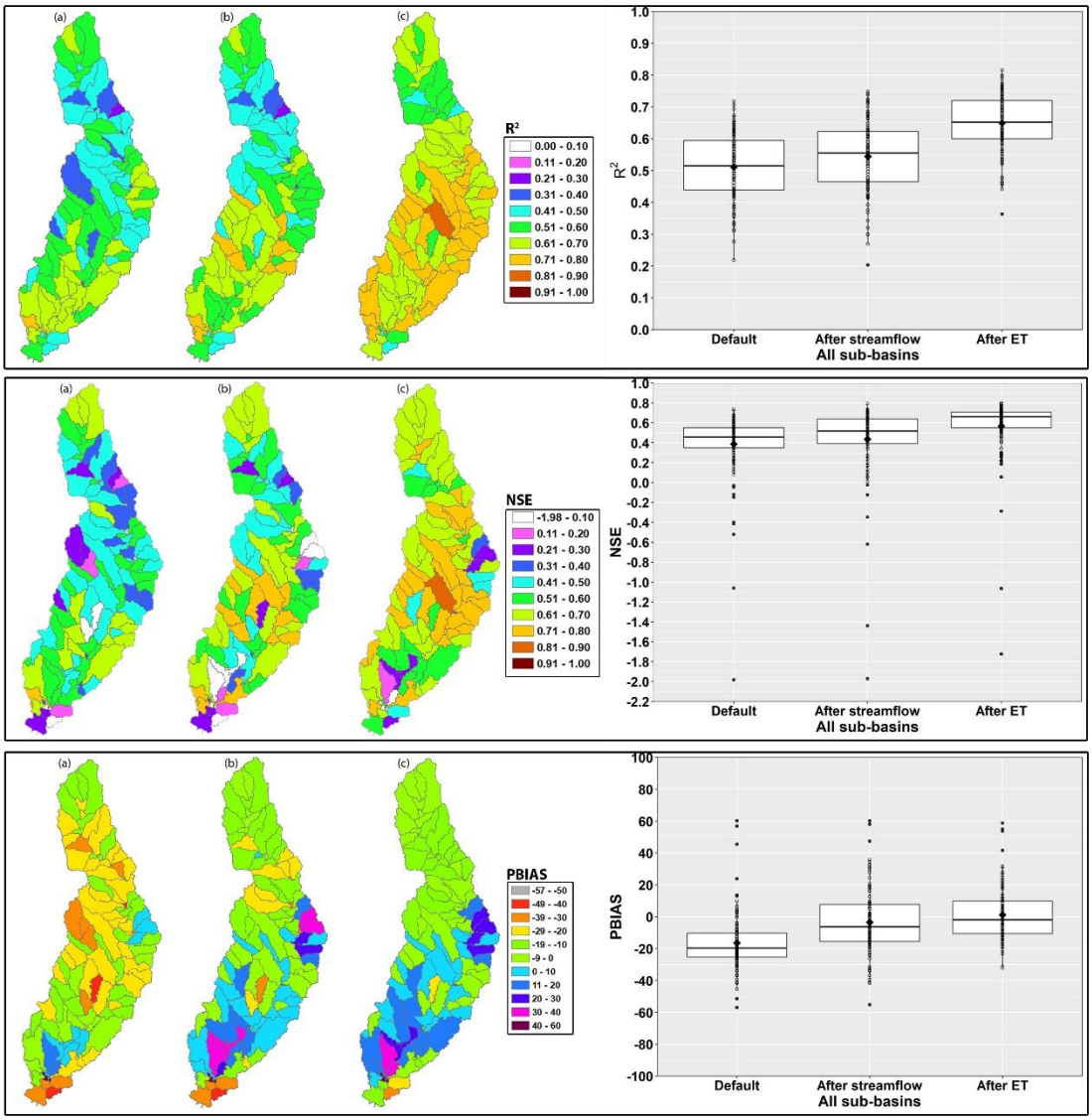

Figure 5.9 Spatial distribution and box plot of R^2 (top), NSE (middle), and PBIAS (bottom) for the (a) default model, (b) streamflow calibration, and (c) subsequent ET calibration (approach-1).

5.4.2.3 Groundwater recharge simulation after calibration approach-1

Groundwater recharge evaluation for all three sub-watersheds after streamflow calibration showed that the SWAT simulated groundwater recharge was smoother with less temporal variation as compared to the default model as well as the RORA estimated recharge (Fig. 5.10). The streamflow calibrated recharge still followed the temporal trend of the RORA estimated groundwater recharge,

but the fluctuations in the recharge magnitude were much smaller when compared to the RORA estimated and default SWAT groundwater recharge. Peak groundwater recharge for the upper sub-watershed with deep soils (Fig. 5.10 – station: 2349605) after streamflow calibration was much lower than compared to the default and RORA estimated recharge and the temporal change in recharge were also not very drastic as expected in the geology with deep clayey soils. Temporal change in groundwater recharge in the lower sub-watershed where the aquifer is close to the land surface (Fig. 5.10 – station:2357150) was more drastic, indicating a much faster recharge. This is not surprising knowing the geology of the area where the aquifer is close to the land surface.

Calibration of ET, however, did not seem to make a big difference in the simulation of groundwater recharge in SWAT as the groundwater recharge after streamflow and thereafter ET calibration were similar (Fig. 5.10). It is, however, important to note that groundwater recharge slightly decreased after ET calibration in the upper forest dominated sub-watershed, especially between 2003 and 2010, which had under-estimated ET in the default model and improved after ET calibration (Fig. 5.10 – station: 2349605). Evaluation at the whole basin scale, however, did not show any difference in groundwater recharge estimations after the calibration of ET (Fig. 5.10 – station: 2356000).

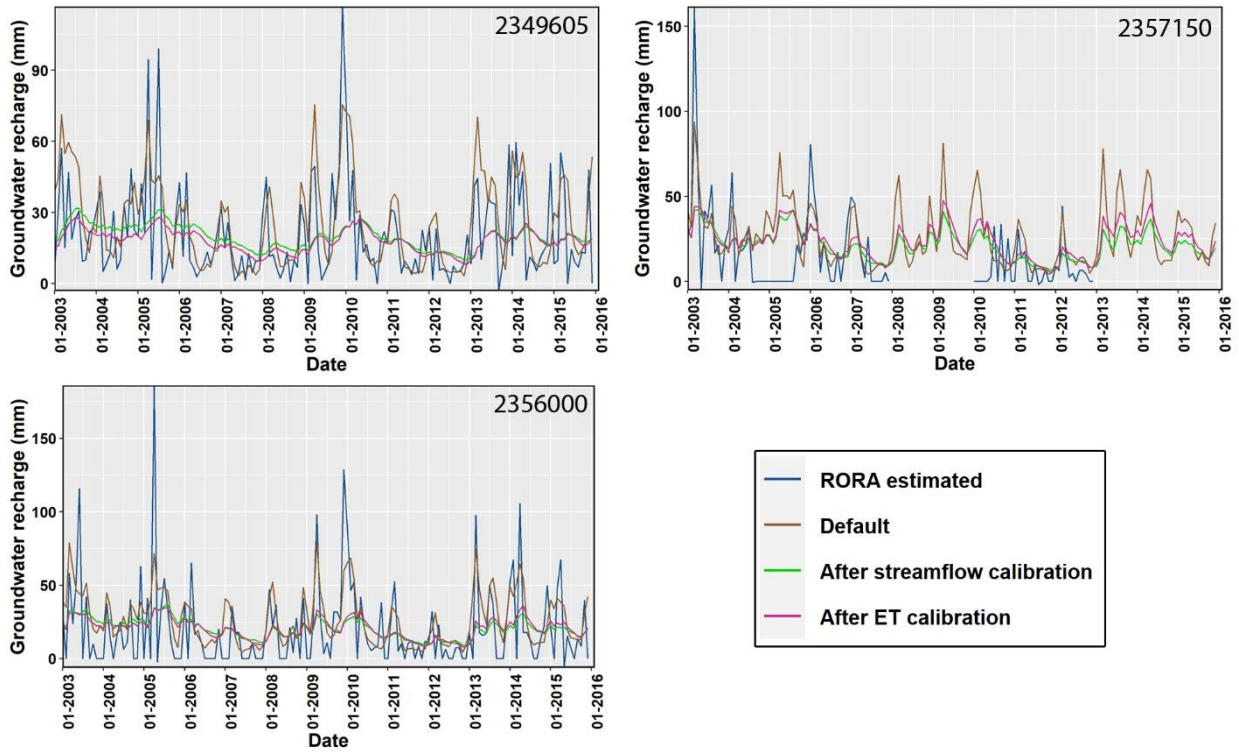

Figure 5.10 Comparison between RORA estimated groundwater recharge and SWAT simulated groundwater recharge for the three sub-watersheds after streamflow and subsequent ET calibration (approach-1).

Comparing the SWAT simulated groundwater recharge for the sub-basins after calibration approach-1 to the groundwater level observed in wells located in the sub-basin showed that the temporal change in groundwater recharge simulation as a result of streamflow calibration closely matched the temporal change in the groundwater levels in the wells (Fig. 5.11). SWAT closely matched the temporal as well as the change in the magnitude of groundwater recharge to the groundwater well in the forested watershed with deep soils (well 11AA01; Fig 5.11). Although the temporal trend of groundwater recharge matched well even in well 08G001, where the groundwater is close to the land surface, and the geology is karstic, resulting in significant water movement also in lateral directions, SWAT was not able to match the change in the magnitude of groundwater recharge to that observed in the groundwater well. This could potentially indicate the

limitation of SWAT in that HRU's in the SWAT are isolated, and there is no lateral flow between HRU's in SWAT. This potentially is not an issue in the region with clay soils where the lateral flow is very minimal (sub-basin 4 – well 11AA01) but can cause errors in the region where the soil is more sandy, and lateral flow can be prominent (sub-basin 92 – well 08G001). This could have led to SWAT not match the change in the magnitude of groundwater recharge to the groundwater level observed in the well in sub-basin 92 as it could not account for groundwater recharge due to lateral flows.

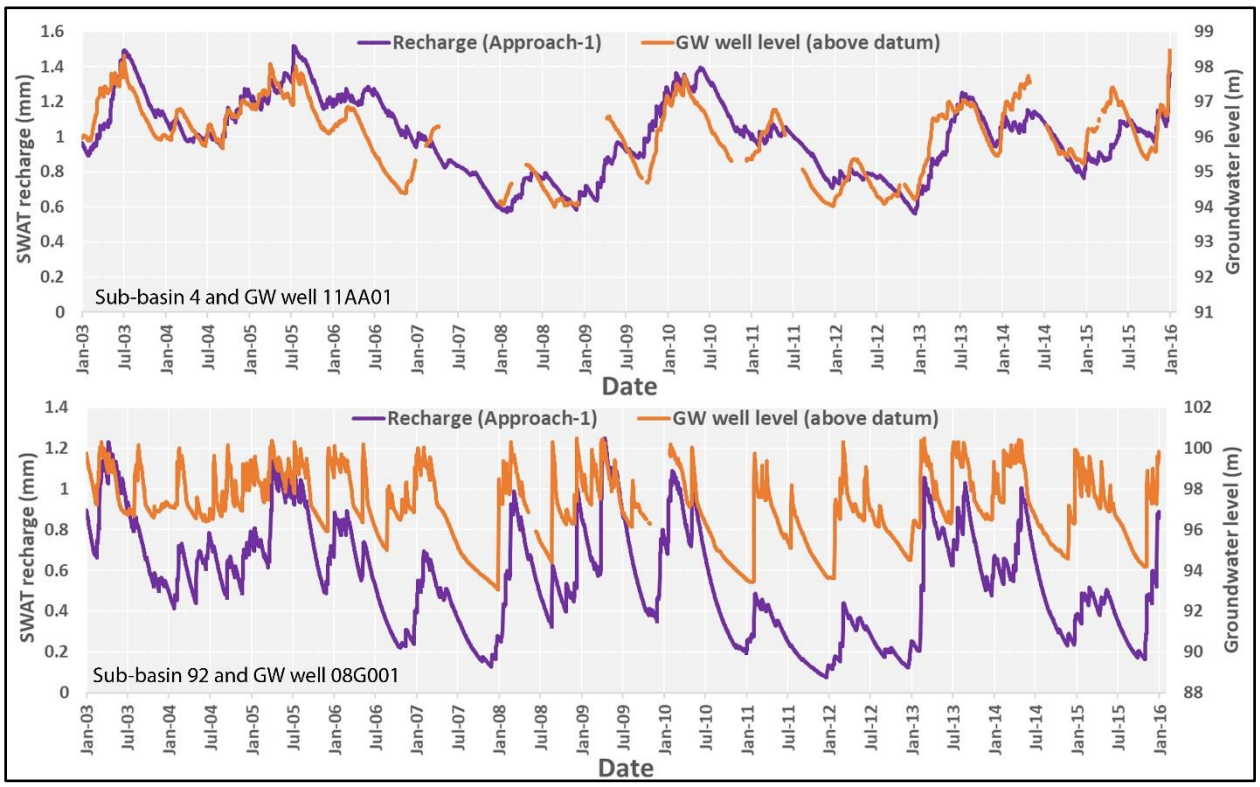

Figure 5.11 Comparison between observed groundwater level and final simulated groundwater recharge after calibration approach-1 for sub-basin 4 (top) and sub-basin 92 (bottom).

5.4.3 Calibration approach-2

Although ET was the first variable calibrated in approach-2 and followed by streamflow calibration, the calibration approach for each variable was the same as described in detail in section

3.2 and used in approach-1. It is also important to note that the evaluation of results for streamflow is presented first, as in section 3.2 for consistency with the discussion of results for approach-1 in section 3.2.

5.4.3.1 Streamflow simulation after calibration approach-2

Evaluation of model streamflow simulation after ET calibration showed that the calibration of ET alone and as the first variable calibrated does not have much influence in streamflow simulation. R^2, NSE, and PBIAS values were poor at all stations for streamflow simulation after ET calibration (Table 5.4). The only measurable difference in performance statistics for streamflow simulation after ET calibration was in the reduction of PBIAS as compared to the default model statistics (Table 5.2) indicating a slight reduction in streamflow volume. This, again, resulted from the increase in ET after calibration of ET, which was underestimated in the default model.

Table 5.4 Model performance for streamflow simulation after sequential calibration of ET and streamflow in calibration approach-2.

	After ET calibration			After streamflow calibration		
USGS streamflow station	**R^2**	**NSE**	**PBIAS (%)**	**R^2**	**NSE**	**PBIAS (%)**
2349605	0.15	-2.06	47.5	0.63	0.62	3.4
2352500	0.16	-2.94	58.9	0.72	0.72	-1.4
2353000	0.14	-4.09	54.9	0.72	0.69	-4.8
2355350	0.09	-18.66	96.5	0.63	0.61	-2.7
2356000	0.13	-5.67	57.1	0.73	0.69	-8.9
2357150	0.04	-30.06	75.4	0.62	0.43	23.4
2358000	0.42	-0.41	21	0.86	0.85	-8.9

Calibration of streamflow after ET calibration, as expected, drastically improved streamflow at all stations with R^2 and NSE above 0.6 and PBIAS less than ±15% for all stations (Table 5.4; Fig. 5.12) except for station 2357150 which had a PBIAS of 23.4% and NSE of 0.43. The model had difficulty simulating streamflow in the complex hydrogeological region that drains to station

2357150 even with calibration approach 2. It is, however, important to note that the final streamflow simulation, after completing all calibration steps in both approaches, was better through approach-2. This shows that if streamflow is the hydrological variable that needs to be simulated most accurately for a study with the model also constrained well for ET simulation, approach-2 works better. Fig. 5.12 shows the graphical comparison between simulated and observed streamflow for all stations using approach-2.

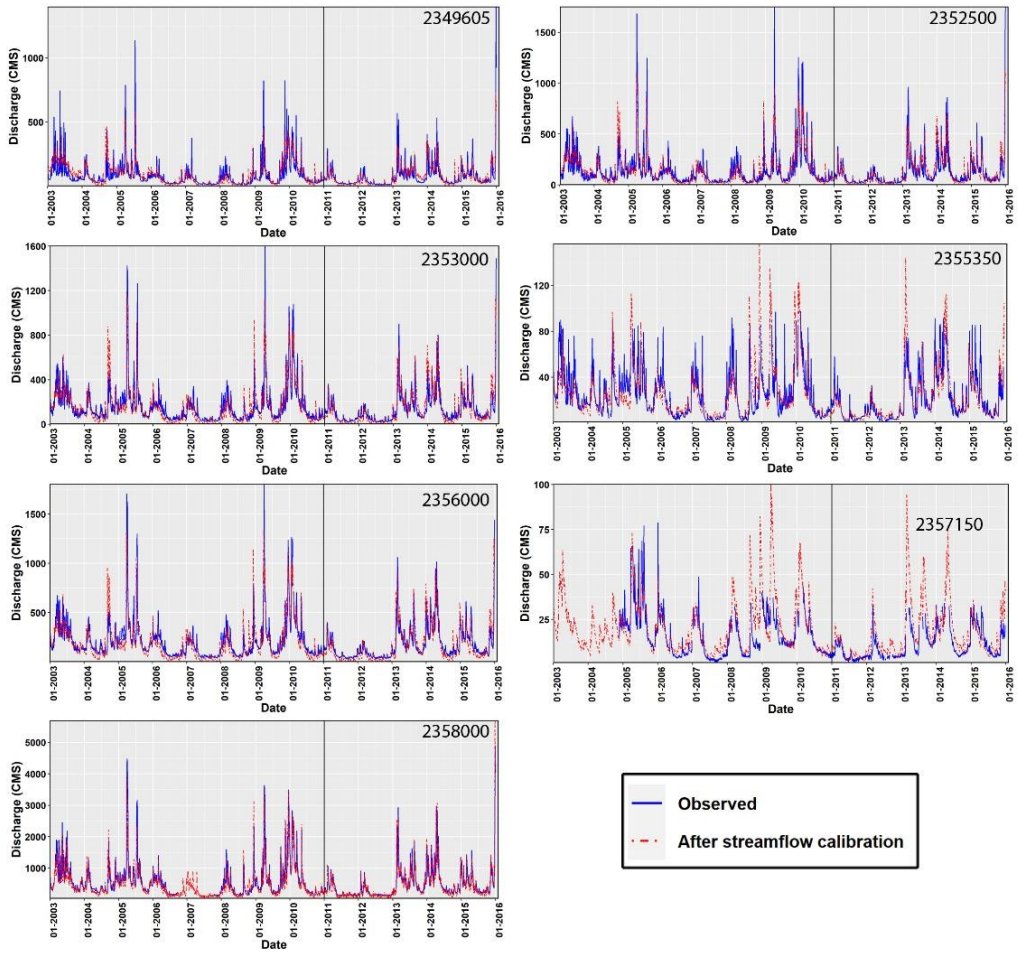

Figure 5.12 Comparison between observed streamflow and SWAT simulated streamflow after ET and subsequent streamflow calibration (approach-2) for all seven stations. The vertical black line indicates the time frame of the observed dataset that was used for streamflow calibration

5.4.3.2 ET simulation after calibration approach-2

ET simulation after calibration showed good improvement with mean R^2, NSE, and PBIAS increasing from 0.5, 0.45, and -17.5% to 0.64, 0.6, and -2.5%, respectively (Fig. 5.13). The model, however, still under simulated ET for most of the study area even after ET calibration, as indicated by the negative PBIAS (Fig. 5.13 – bottom figure – label (b)). Subsequent calibration of streamflow only slightly declined ET simulation with a slight reduction in mean R^2 and NSE values (Fig. 5.13 – top and middle figure). Calibration of streamflow, however, resulted in increased ET over the whole watershed, an effect that was also observed in approach-1. This resulted in the mean PBIAS for ET simulation to be around 0%, but it can be easily observed that the model overestimated ET in the agricultural watersheds and under simulated ET in the forested watersheds even with approach 2. Comparison between the final simulated ET from both approaches shows that either approach does not have a considerable advantage over the other for ET simulation as the performance statistics were similar in both cases (Fig. 5.9 and Fig. 5.13).

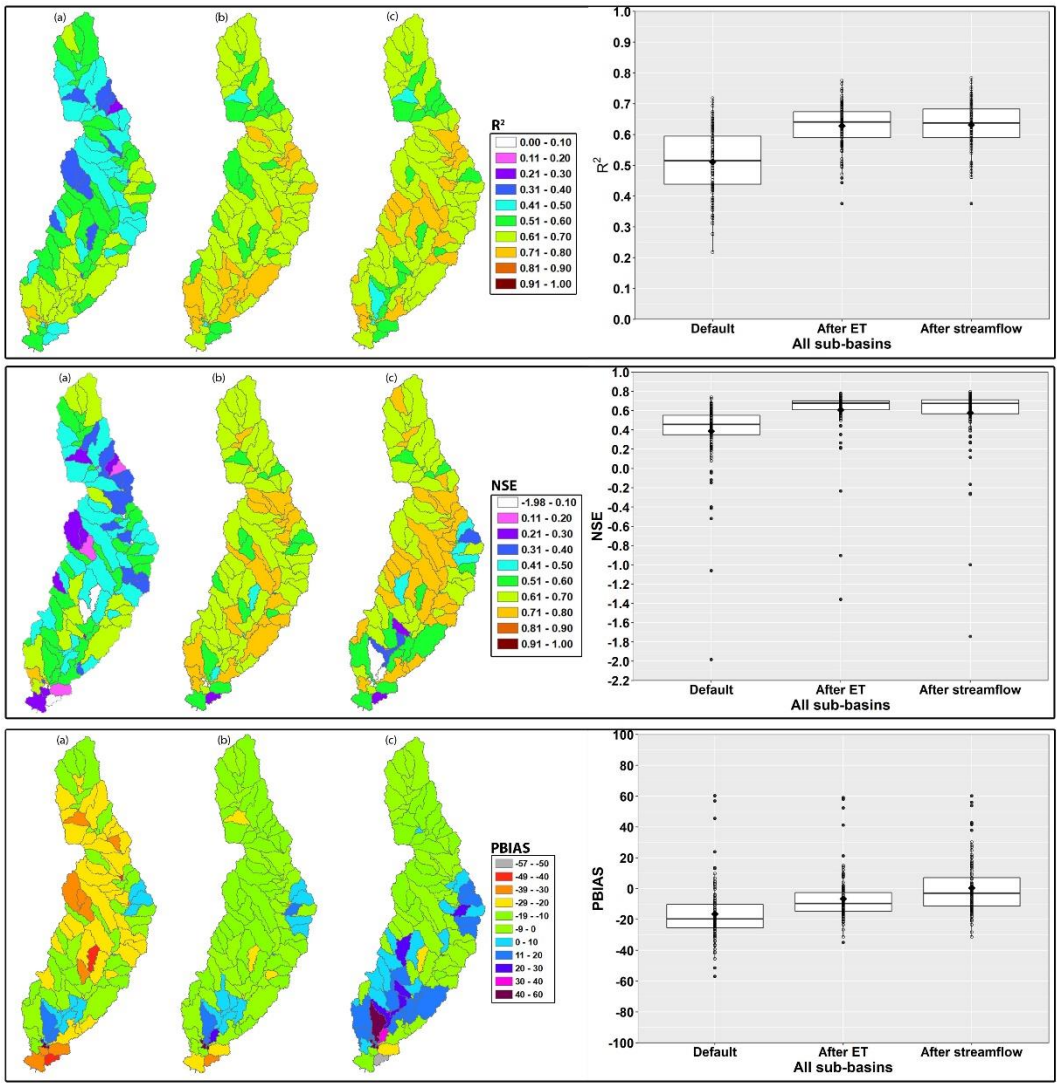

Figure 5.13 Spatial distribution and box plot of R^2 (top), NSE (middle), and PBIAS (bottom) for the (a) default model, (b) ET calibration, and (c) subsequent streamflow calibration (approach-2).

5.4.3.3 Groundwater recharge simulation after calibration approach-2

Groundwater recharge simulation after calibration of only ET was very similar to the recharge simulation in the default model for all three sub-watersheds (Fig. 5.14), indicating that groundwater recharge simulation was not sensitive to the calibration of ET alone. As it was also observed that streamflow simulation is also very poor after only ET simulation (Table 5.4), hydrological simulation in SWAT cannot be adequately constrained by calibrating ET alone, and

the simulated groundwater recharge might not be an accurate representation of the groundwater recharge in a study area.

Subsequent calibration of streamflow resulted in the simulated groundwater recharge to be smoother and have less temporal variation as observed after streamflow calibration in approach-1 (Fig. 5.14). However, it was observed that the simulated groundwater recharge after approach-2 was more episodic with a greater temporal variation for the sub-watersheds contributing to station 2349605 and 2356000 when compared to the groundwater recharge simulation after calibration approach-1. Simulated groundwater recharge for sub-watershed contributing to station 2357150 was also exact opposite in that there was almost no temporal variability in simulated groundwater recharge after approach-2 while it was the most episodic of the three sub-watersheds after approach-1. Simulated groundwater recharge following calibration approach-2 is less representative of the expected groundwater recharge mechanisms, especially when evaluating for sub-watersheds contributing to stations 2349605 and 2357150. Groundwater recharge is expected to be more episodic with a higher temporal variation for station 2357150 as the region is karstic with thin soils and the aquifer very close to the land surface, unlike simulated by approach-2. Similarly, as the region draining to station 2349605 has deep soils, and the aquifer is not close to the land surface, groundwater recharge is expected to have less temporal variation due to the slow movement of water through the deep soil profile.

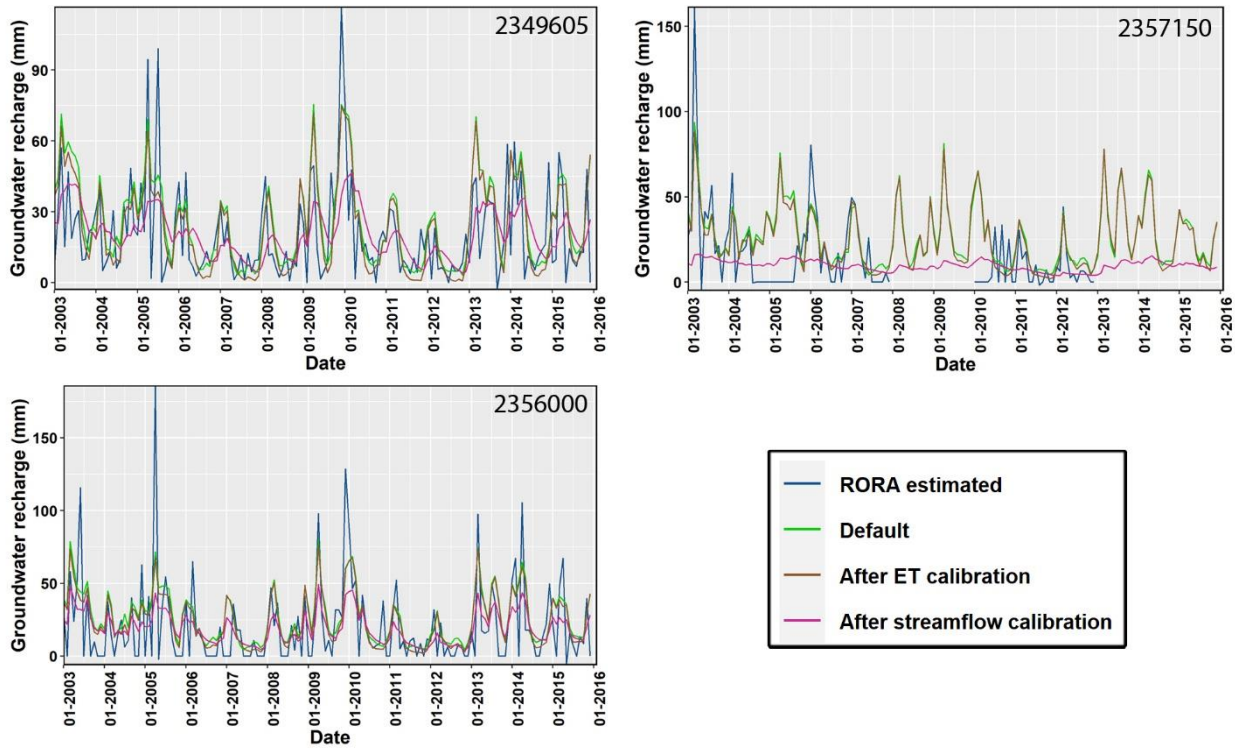

Figure 5.14 Comparison between RORA estimated groundwater recharge and SWAT simulated groundwater recharge for the three sub-watersheds after ET and subsequent streamflow calibration (approach-2).

Comparison between observed groundwater level and simulated groundwater recharge after calibration approach-2 further demonstrated that the simulated groundwater recharge for sub-basin 4 was more episodic than as expected in the region as the change in groundwater recharge was more drastic than the change in groundwater level (Fig. 5.15). On the contrary, simulated groundwater recharge for sub-basin 92 was less episodic than the observed change in groundwater level for that region (Fig. 5.15). This indicated to calibration approach-2 having more difficulty in accurately representing the recharge mechanism when compared to approach-1.

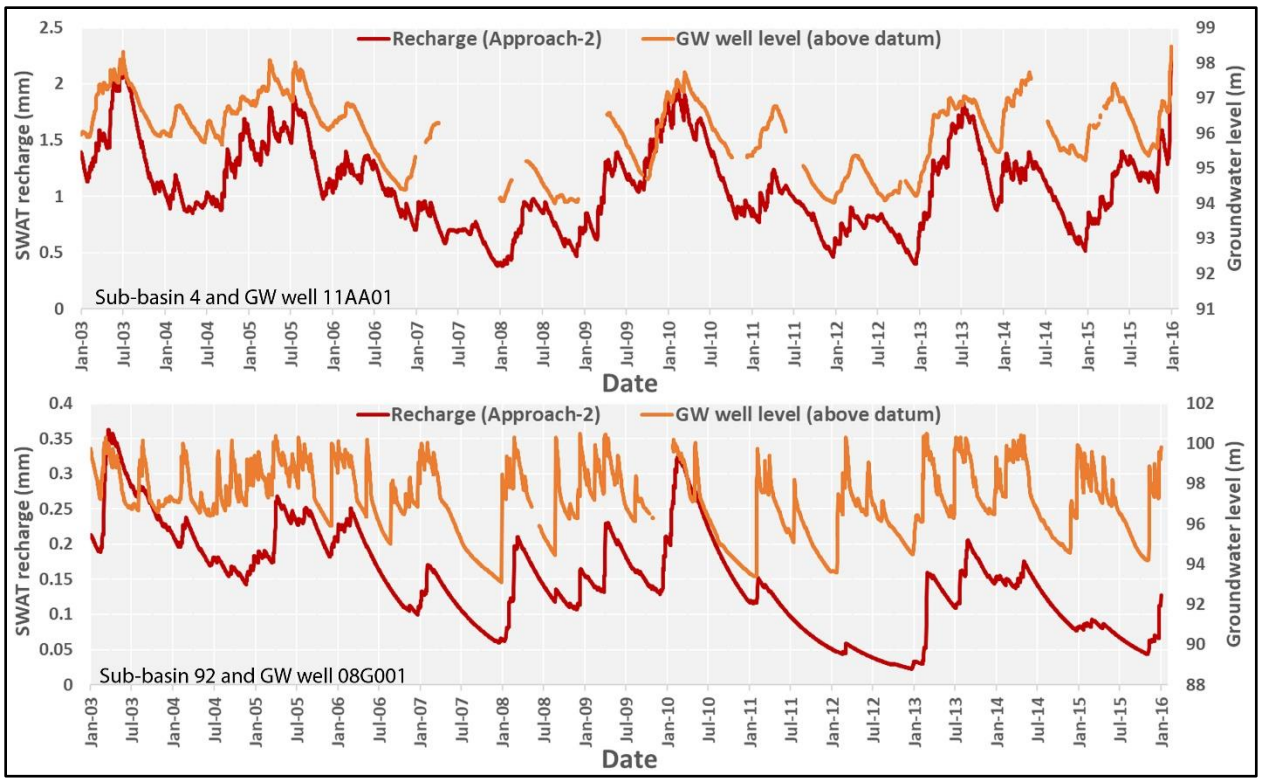

Figure 5.15 Comparison between observed groundwater level and final simulated groundwater recharge after calibration approach-2 for sub-basin 4 (top) and sub-basin 92 (bottom).

5.4.4 Comparison of groundwater parameters and recharge from the two approaches.

The groundwater delay parameter (GW_DELAY in *.gw* file) is one of the most critical parameters for accurate simulation of groundwater recharge in SWAT as it controls the number of days it takes for water to travel from the bottom of the soil profile to the top of the water table and thereby impact the temporal variation in groundwater recharge. Based on the hydrogeological information of the study region (Jones and Torak, 2006; Torak and Painter, 2006), it is clear that the final calibrated values for GW_DELAY through approach-1 is more representative of the region than values derived using approach-2. GW_DELAY values, through approach-1, are the smallest in the region of the study area where the aquifer is close to the land surface (Fig. 5.16a) and water is expected to percolate past the unsaturated soil zone faster while the highest values are located in

the region where the soils are deep. In contrast, GW_DELAY values are highest in the region where the aquifer is close to the land surface and low where the soil zones are thick (Fig. 5.16b), indicating the inability of the model to represent the groundwater dynamics through calibration approach-2 accurately. It is important to note that the starting parameter ranges for all the variables were the same for both approach and the optimized variables for subsequent calibration runs were based on the SWAT-CUP outputs.

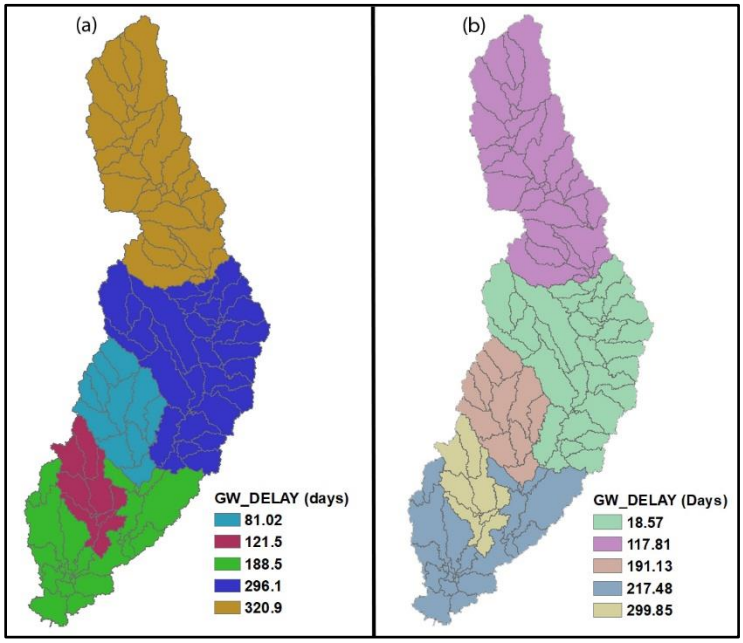

Figure 5.16 Calibrated GW_DELAY parameter for the SWAT model following (a) approach-1 and (b) approach-2.

Evaluation of average annual groundwater recharge for the total simulation period after the two calibration approaches showed some important differences (Fig. 5.17). Estimated groundwater recharge through approach-1 was higher in the lower part of the modeled area when compared to recharge from approach-2. However, the estimated recharge from approach-1 was lower when compared in the upper-middle and upper portion of the modeled area (Fig. 5.17). As the underlying karstic aquifer is close to the land surface and even exposed at the land surface in the lower part

of the study area (Torak and Painter, 2006), recharge in the lower part of the modeled area can be expected to be higher than the upper region of the study area. This spatial variability in recharge was captured better when SWAT was calibrated using approach-1. Lower estimated recharge through calibration approach-2 in the lower part of the study area compounded by the inability of the model to replicate the temporal trends of groundwater recharge observed in groundwater well 08G001 in the same region (Fig. 5.15) also showed that SWAT could have potentially under simulated recharge through calibration approach-2 in the lower part of the modeled area.

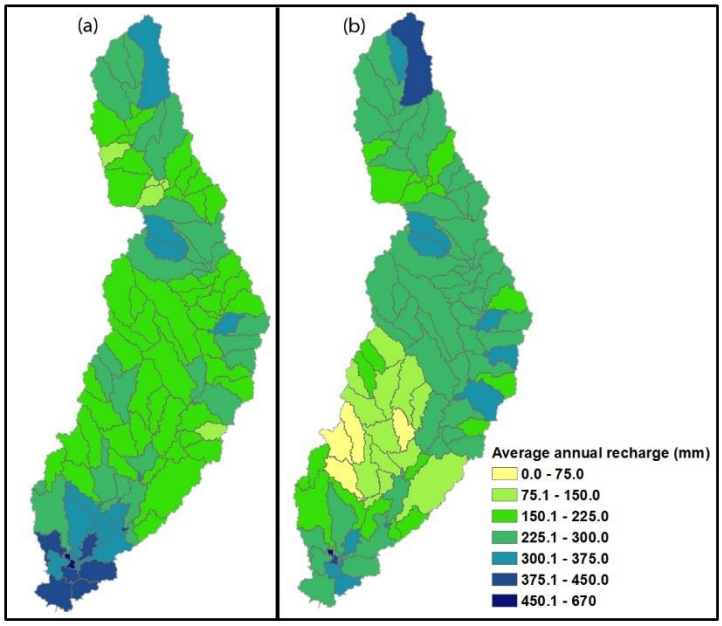

Figure 5.17 SWAT estimated annual average groundwater recharge for the total simulation period after calibrating through (a) approach-1 and (b) approach-2.

5.5 Summary and Conclusions

This study evaluated the impact of separately calibrating streamflow and ET as well as using a multi-variate approach in SWAT on the simulation of groundwater recharge. Evaluation of SWAT simulated groundwater recharge with default parameters for three sub-watersheds in the Flint River Basin by comparing to RORA estimated recharge showed that the model was able to

adequately replicate the groundwater recharge estimated by RORA even with default parameters. However, a comparison of the temporal variability of SWAT simulated groundwater recharge with default parameters to groundwater levels observed in two wells, which are indicative of the temporal distribution of recharge, showed that the SWAT simulated groundwater recharge was more episodic and had greater variability than observed through the groundwater wells.

Calibration of ET alone had a negligible impact in the simulation of groundwater recharge, and there was also minimal improvement in streamflow simulation. Hence, ET calibration alone cannot constrain the hydrological simulation in SWAT enough to accurately simulate the groundwater recharge. It was observed that streamflow is an important and influential variable to be calibrated in SWAT for simulating groundwater recharge accurately as the parameters important for calibrating streamflow in SWAT are more directly related to the simulation of groundwater recharge. Calibration of streamflow tended to make the simulated groundwater recharge smoother and less variable temporally for all three sub-watersheds when compared to the RORA estimated groundwater recharge. However, comparing the simulated recharge after streamflow calibration to groundwater levels observed in the two wells showed that the simulated groundwater recharge replicated the temporal variability of groundwater levels much more accurately after streamflow calibration. The study also pointed out the importance of calibrating streamflow separately for the different sections of the watershed that differ in geology as the parameters that are critical for groundwater recharge simulation can be fine-tuned for the region. This was evident by the difference in calibrated GW_DELAY parameter value for the region with deep soils and where the aquifer was close to the land surface that allowed the model to accurately simulate the temporal variability in groundwater recharge matching the change in groundwater levels observed in wells. Sequential calibration of ET after streamflow calibration slightly reduced groundwater flow in the

forested region and also slightly reduced model performance for streamflow simulation to compensate for the under simulation of ET by the default model. There was, however, no change in temporal variability in groundwater recharge simulation after calibration of ET. Although the sequential calibration of ET followed by streamflow (approach-2) presented better overall simulation results for streamflow simulation, simulated groundwater recharge and the calibrated groundwater variable (GW_DELAY) were not representative for both the region with deep soils and where the aquifer was near the land surface. Hence, the calibration approach in which streamflow was first calibrated followed by ET calibration was identified as the most suitable for multi-variate calibration using a sequential approach for groundwater recharge simulation while streamflow is the single most important hydrological variable to be calibrated for accurate simulation of groundwater recharge in the Flint River Basin.

Evaluation of the calibration approaches in varying hydrogeology within the study area provides confidence in the applicability of the findings from this research over varying land use and soils. Findings from this study can also provide important insight into the calibration of SWAT-MODFLOW in which SWAT simulates the overland hydrologic process and provides recharge estimation into the MODFLOW model (Bailey et al., 2016). It should, however, be noted that the lack of accurate point recharge estimates limited the groundwater recharge evaluation to coarse recharge estimates using the RORA program and observed groundwater level for temporal variability. The study could be further improved and the impacts of streamflow and ET calibration on groundwater simulation in SWAT can be more accurately defined by using more accurate recharge estimates for comparison. It should also be noted that the study area has a humid climate where the surface- and groundwater dynamics can be very different from arid regions and hence further evaluation might be required for different climatic conditions.

5.6 References

Abbaspour, K. C. (2013). SWAT-CUP 2012. *SWAT Calibration and Uncertainty Program—A User Manual*.

Arguez, A., Durre, I., Applequist, S., Vose, R. S., Squires, M. F., Yin, X., … Owen, T. W. (2012). NOAA's 1981--2010 US climate normals: An overview. *Bulletin of the American Meteorological Society*, *93*(11), 1687–1697.

Arnold, J. G., Moriasi, D. N., Gassman, P. W., Abbaspour, K. C., White, M. J., Srinivasan, R., … Van Liew, M. W. (2012). SWAT: Model use, calibration, and validation. *Transactions of the ASABE*, *55*(4), 1491–1508.

Arnold, J. G., Muttiah, R. S., Srinivasan, R., Allen, P. M. (2000). Regional estimation of base flow and groundwater recharge in the Upper Mississippi river basin. *Journal of Hydrology*, *227*(1–4), 21–40. https://doi.org/10.1016/S0022-1694(99)00139-0

Arnold, J. G., Srinivasan, R., Muttiah, R. S., Williams, J. R. (1998). Large area hydrologic modeling and assessment part I: model development 1. *JAWRA Journal of the American Water Resources Association*, *34*(1), 73–89.

Arnold, J. G., Youssef, M. A., Yen, H., White, M. J., Sheshukov, A. Y., Sadeghi, A. M., … others. (2015). Hydrological processes and model representation: Impact of soft data on calibration. *Transactions of the ASABE*, *58*(6), 1637–1660.

Awan, U. K., Ismaeel, A. (2014). A new technique to map groundwater recharge in irrigated areas using a SWAT model under changing climate. *Journal of Hydrology*, *519*, 1368–1382.

Bailey, R. T., Wible, T. C., Arabi, M., Records, R. M., Ditty, J. (2016). Assessing regional-scale spatio-temporal patterns of groundwater–surface water interactions using a coupled SWAT-MODFLOW model. *Hydrological Processes*, *30*(23), 4420–4433. https://doi.org/10.1002/hyp.10933

Baker, T. J., Miller, S. N. (2013). Using the Soil and Water Assessment Tool (SWAT) to assess land use impact on water resources in an East African watershed. *Journal of Hydrology*, *486*, 100–111.

Chen, W.-P., Lee, C.-H. (2003). Estimating ground-water recharge from streamflow records. *Environmental Geology*, *44*(3), 257–265.

Chinnasamy, P., Muthuwatta, L., Eriyagama, N., Pavelic, P., Lagudu, S. (2018). Modeling the potential for floodwater recharge to offset groundwater depletion: a case study from the Ramganga basin, India. *Sustainable Water Resources Management*, *4*(2), 331–344.

Dakhlalla, A. O., Parajuli, P. B., Ouyang, Y., Schmitz, D. W. (2016). Evaluating the impacts of crop rotations on groundwater storage and recharge in an agricultural watershed. *Agricultural Water Management*, *163*, 332–343.

De Vries, J. J., Simmers, I. (2002). Groundwater recharge: an overview of processes and challenges. *Hydrogeology Journal*, *10*(1), 5–17.

Delin, G. N., Healy, R. W., Lorenz, D. L., Nimmo, J. R. (2007). Comparison of local-to regional-scale estimates of ground-water recharge in Minnesota, USA. *Journal of Hydrology*, *334*(1–2), 231–249.

Emam, A. R., Kappas, M., Akhavan, S., Hosseini, S. Z., Abbaspour, K. C. (2015). Estimation of groundwater recharge and its relation to land degradation: case study of a semi-arid river basin in Iran. *Environmental Earth Sciences*, *74*(9), 6791–6803.

Eshtawi, T., Evers, M., Tischbein, B. (2016). Quantifying the impact of urban area expansion on groundwater recharge and surface runoff. *Hydrological Sciences Journal*, *61*(5), 826–843.

Fallatah, O. A., Ahmed, M., Cardace, D., Boving, T., Akanda, A. S. (2019). Assessment of modern recharge to arid region aquifers using an integrated geophysical, geochemical, and remote sensing approach. *Journal of Hydrology*, *569*, 600–611.

Famiglietti, J. S. (2014). The global groundwater crisis. *Nature Climate Change*, *4*(11), 945–948.

Gemitzi, A., Ajami, H., Richnow, H.-H. (2017). Developing empirical monthly groundwater recharge equations based on modeling and remote sensing data--Modeling future groundwater recharge to predict potential climate change impacts. *Journal of Hydrology*, *546*, 1–13.

Gesch, D., Oimoen, M., Greenlee, S., Nelson, C., Steuck, M., Tyler, D. (2002). The national elevation dataset. *Photogrammetric Engineering and Remote Sensing*, *68*(1), 5–32.

Ghaffari, G., Keesstra, S., Ghodousi, J., Ahmadi, H. (2010). SWAT-simulated hydrological impact of land-use change in the Zanjanrood basin, Northwest Iran. *Hydrological Processes: An International Journal*, *24*(7), 892–903.

Githui, F., Selle, B., Thayalakumaran, T. (2012). Recharge estimation using remotely sensed evapotranspiration in an irrigated catchment in southeast Australia. *Hydrological Processes*, *26*(9), 1379–1389.

Gleeson, T., Wada, Y., Bierkens, M. F. P., Van Beek, L. P. H. (2012). Water balance of global aquifers revealed by groundwater footprint. *Nature*, *488*(7410), 197–200.

Gyamfi, C., Ndambuki, J. M., Anornu, G. K., Kifanyi, G. E. (2017). Groundwater recharge modelling in a large scale basin: an example using the SWAT hydrologic model. *Modeling Earth Systems and Environment*, *3*(4), 1361–1369.

Han, W., Yang, Z., Di, L., Mueller, R. (2012). CropScape: A Web service based application for exploring and disseminating US conterminous geospatial cropland data products for decision support. *Computers and Electronics in Agriculture*, *84*, 111–123.

Hass, H. (2020). *Importance of Capturing Forest Dynamics in Hydrological Modeling*. Auburn University.

Healy, R. W. (2010). *Estimating groundwater recharge*. Cambridge University Press.

Izady, A., Davary, K., Alizadeh, A., Ziaei, A. N., Akhavan, S., Alipoor, A., … Brusseau, M. L. (2015). Groundwater conceptualization and modeling using distributed SWAT-based recharge for the semi-arid agricultural Neishaboor plain, Iran. *Hydrogeology Journal*, *23*(1), 47–68.

Jayakody, P., Parajuli, P. B., Sassenrath, G. F., Ouyang, Y. (2014). Relationships between water table and model simulated ET. *Groundwater*, *52*(2), 303–310.

Jones, L. E., Torak, L. J. (2006). *Simulated effects of seasonal ground-water pumpage for irrigation on hydrologic conditions in the Lower Apalachicola-Chattahoochee-Flint River Basin, Southwestern Georgia and parts of Alabama and Florida, 1999-2002*.

Kalin, L., Hantush, M. M. (2009). An auxiliary method to reduce potential adverse impacts of projected land developments: subwatershed prioritization. *Environmental Management*, *43*(2), 311.

Karki, R., Srivastava, P., Bosch, D. D., Kalin, L., Lamba, J., Strickland, T. C. (2020). Multi-Variable Sensitivity Analysis, Calibration, and Validation of a Field-Scale SWAT Model: Building Stakeholder Trust in Hydrologic and Water Quality Modeling. *Transactions of the ASABE*, *63*(2), 523–539.

Kinzelbach, W., others. (2002). *A survey of methods for analysing groundwater recharge in arid and semi-arid regions, Division of Early Warning and Assessment. United Nations Environmental Program*.

Konikow, L. F., Kendy, E. (2005). Groundwater depletion: A global problem. *Hydrogeology Journal*, *13*(1), 317–320.

Lall, U., Josset, L., Russo, T. (2020). A Snapshot of the World's Groundwater Challenges. *Annual Review of Environment and Resources, 45*.

Lee, J. M., Park, Y. S., Kum, D., Jung, Y., Kim, B., Hwang, S. J., … Lim, K. J. (2014). Assessing the effect of watershed slopes on recharge/baseflow and soil erosion. *Paddy and Water Environment, 12*(1), 169–183.

Lin, H.-T., Ke, K.-Y., Tan, Y.-C., Wu, S.-C., Hsu, G., Chen, P.-C., Fang, S.-T. (2013). Estimating pumping rates and identifying potential recharge zones for groundwater management in multi-aquifers system. *Water Resources Management, 27*(9), 3293–3306.

Mechal, A., Wagner, T., Birk, S. (2015). Recharge variability and sensitivity to climate: the example of Gidabo River Basin, Main Ethiopian Rift. *Journal of Hydrology: Regional Studies, 4*, 644–660.

Moriasi, D. N., Gitau, M. W., Pai, N., Daggupati, P. (2015). Hydrologic and water quality models: Performance measures and evaluation criteria. *Transactions of the ASABE, 58*(6), 1763–1785.

Neitsch, S. L., Arnold, J. G., Kiniry, J. R., Williams, J. R. (2011). *Soil and Water Assessment Tool Theoretical Documentation Version 2009*.

Raposo, J. R., Dafonte, J., Molinero, J. (2013). Assessing the impact of future climate change on groundwater recharge in Galicia-Costa, Spain. *Hydrogeology Journal, 21*(2), 459–479.

Risal, A., Parajuli, P. B. (2019). Quantification and simulation of nutrient sources at watershed scale in Mississippi. *Science of the Total Environment, 670*, 633–643.

Ruefenacht, B., Finco, M. V, Nelson, M. D., Czaplewski, R., Helmer, E. H., Blackard, J. A., … others. (2008). Conterminous US and Alaska forest type mapping using forest inventory and analysis data. *Photogrammetric Engineering & Remote Sensing, 74*(11), 1379–1388.

Running, S. W., Mu, Q., Zhao, M., Moreno, A. (2017). MODIS Global Terrestrial Evapotranspiration (ET) Product (NASA MOD16A2/A3) NASA Earth Observing System MODIS Land Algorithm. *NASA: Washington, DC, USA*.

Rushton, K. R., Redshaw, S. C. (1979). *Seepage and groundwater flow: Numerical analysis by analog and digital methods*. John Wiley & Sons.

Rutledge, A. T. (2007). Update on the use of the RORA program for recharge estimation. *Groundwater, 45*(3), 374–382.

Scanlon, B. R., Healy, R. W., Cook, P. G. (2002). Choosing appropriate techniques for quantifying groundwater recharge. *Hydrogeology Journal, 10*(1), 18–39.

Schwarz, G. E., Alexander, R. B. (1995). *State soil geographic (STATSGO) data base for the conterminous United States*.

Seaber, P. R., Kapinos, F. P., Knapp, G. L. (1987). Hydrologic unit maps.

Shiklomanov, I. A., Rodda, J. C. (2003). World water resources at the beginning of the 21st century. International hydrology series. Cambridge University Press, Cambridge.

Siebert, S., Burke, J., Faures, J.-M., Frenken, K., Hoogeveen, J., Döll, P., … others. (2010). Groundwater use for irrigation—a global inventory. *Hydrology and Earth System Sciences*, *14*(10), 1863–1880.

Sun, H., Cornish, P. S. (2005). Estimating shallow groundwater recharge in the headwaters of the Liverpool Plains using SWAT. *Hydrological Processes: An International Journal*, *19*(3), 795–807.

Tadych, D. (2020). *Investigating Soil Parameters Effect on Crop Yields and Hydrology at Field Scale in the Southeast US Using the Soil and Water Assessment Tool*. Auburn University.

Torak, L. J., Painter, J. A. (2006). *Geohydrology of the lower Apalachicola-Chattahoochee-Flint River basin, southwestern Georgia, northwestern Florida, and southeastern Alabama*.

University of Georgia CAES. (2014). *Georgia Farm Gate Value Report*. Retrieved from http://caes2.caes.uga.edu/center/caed/pubs/documents/2014UGACAEDFGVR_FINAL.pdf.

University of Georgia CAES. (2018). *Georgia Farm Gate Value Report 2017*.

USGS. (2019). USGS water data for the Nation: US Geological Survey National Water Information System database.

Wada, Y., Van Beek, L. P. H., Van Kempen, C. M., Reckman, J. W. T. M., Vasak, S., Bierkens, M. F. P. (2010). Global depletion of groundwater resources. *Geophysical Research Letters*, *37*(20).

White, K. L., Chaubey, I. (2005). Sensitivity analysis, calibration, and validations for a multisite and multivariable SWAT model. *JAWRA Journal of the American Water Resources Association*, *41*(5), 1077–1089.

Xia, Y., Mitchell, K., Ek, M., Sheffield, J., Cosgrove, B., Wood, E., … others. (2012). Continental-scale water and energy flux analysis and validation for the North American Land Data Assimilation System project phase 2 (NLDAS-2): 1. Intercomparison and application of model products. *Journal of Geophysical Research: Atmospheres*, *117*(D3).

Zhu, R., Croke, B. F. W., Jakeman, A. J. (2020). Diffuse groundwater recharge estimation confronting hydrological modelling uncertainty. *Journal of Hydrology*, *584*, 124642.

Chapter 6

Application of SWAT-MODFLOW for evaluating the impacts of climate change on the surface- and groundwater resources of the lower Apalachicola Chattahoochee Flint River Basin, USA

6.1 Abstract

The threats of climate change on the surface- and groundwater resources of the lower Apalachicola-Chattahoochee-Flint (ACF) River Basin of southeastern United States (U.S.) is an important concern for the long-term sustainability of agriculture and environment in the region. Evaluation of the potential impacts of climate change requires the development of an integrated modeling system that can adequately simulate the surface- and groundwater resources together due to the intrinsic connection between the resources in the region. Hence, this study developed a coupled SWAT-MODFLOW for the lower ACF River Basin and the underlying Upper Floridan Aquifer (UFA) and evaluated the impacts of climate change predicted under Coupled Model Intercomparison Project 5 (CMIP5) RCP4.5 and RCP8.5 emissions scenario on streamflow, surface- and groundwater (SW-GW) exchange, evapotranspiration (ET), and groundwater recharge. Streamflow evaluation after calibration at six locations showed that the model can adequately replicate streamflow in the region even though it has complex hydrogeology due to its karstic nature. The model also adequately simulated the spatial and temporal variability of groundwater levels in the study region. Comparison of historic monthly averaged daily maximum and minimum temperature to future predicted temperature under the RCP4.5 and RCP8.5 scenarios showed an increase in daily maximum temperature by as much as 2.7℃ with a general increase throughout the year by the middle of the 21st century. A shift in precipitation pattern with higher precipitation in fall months and decrease in precipitation in the early months was also expected. A

general decrease in streamflow was expected under RCP4.5 and RCP8.5 for the late spring and summer months while an increase was expected in the late fall and early months of the year indicating also to a shift in flow pattern in the region under future climate. Evaluation of change in SW-GW exchange showed an increase in flux along the main-stem of the Flint River while there was minimal change in ET in the region ranging from about -4% to 4%.

Introduction

Surface- and groundwater resources in the lower Apalachicola Chattahoochee Flint (ACF) River Basin of southeastern United States (U.S.) play a critical role in the economic and environmental vitality of the region. Agriculture, which serves as the major economic contributor to the region generating more than 2 billion dollars in revenue annually, is heavily dependent on irrigation from the underlying Upper Floridan Aquifer (UFA) (CAES, 2018). The UFA contributes more than 80% of the total irrigation demand in the region and supplied an estimated 1.7 million cubic meters of water for irrigation in 2015 (GA EPD, 2016). The withdrawal, however, can be as high as 3.6 million cubic meters during a drought year (GA EPD, 2016). The aquifer irrigates more than 200,000 hectares of agricultural land through more than 4,000 irrigation wells (GA EPD, 2016) and is also the primary source of water for municipal and industrial use. The UFA, which is made up of karst limestone in the region, is close to the land surface and as a result, is in direct connection with the surficial river and lake systems through incised streambeds, sinkhole ponds, karst sinks, and conduits that exposes the limestone to the surface (Torak and Painter, 2006). The aquifer system contributes tens of million cubic meters of water to many of the surficial rivers daily as baseflow. Hence, the aquifer system serves as a vital component in maintaining streamflow, especially during low flow periods (Torak and Painter, 2006). The river basin also supports a diverse population of flora and fauna. It has the highest density of reptiles and amphibians in North

America (Couch et al., 1996) and is also habitat to multiple federally endangered mussel species as well as striped bass (Couch and McDowell, 2006). However, the surface- and groundwater resources in the region are under increasing stress due to increased irrigation as well as recurring prolonged drought conditions. Multiple studies have indicated to a reduction in baseflow (Golladay et al., 2007; Jones and Torak, 2006; Singh et al., 2016, 2017) as well as short- and long-term decline in groundwater levels (Jones and Torak, 2006; Mitra et al., 2016; Singh et al., 2017; Torak and Painter, 2006) due to increased groundwater withdrawals, especially during drought periods in the region. Flows in the spring-fed streams in the region decreased by 50 to 100% during drought periods (GWC, 2017). Reduced streamflow exacerbated by prolonged drought conditions has also severely impacted the federally endangered mussel species (Gagnon et al., 2004; Golladay et al., 2004; Shea et al., 2013) and bass population (Couch and McDowell, 2006) in the basin.

Along with the impacts of increasing irrigation and climate variability factors, climate change is a growing threat to the environmental and economic sustainability of the region. The temperature in the region has increased by over 1.1℃ since the 1970s (Karl et al., 2009), and an upward trend in precipitation has been identified in more than 70% of the precipitation recording stations in the southeastern United States (U.S.) (Reidmiller et al., 2017). The region has also witnessed an increase in frequency and intensity of extreme precipitation along with more frequent drought conditions and extreme and prolonged heat waves (Reidmiller et al., 2017). Numerous precipitation events that are expected to occur once every 500 years have been observed since 2014 while the decade of 2010s was warmer than any previous decade, and the rise in temperature and increase in extreme precipitation events are expected to increase further in the future (Reidmiller et al., 2017). As a result, climate change is a significant growing threat to environmental and economic sustainability in the region. Globally, the rise in temperature and

subsequent change in climate has already altered the global hydrological cycle and led to change in precipitation patterns and intensity, changes in river discharge patterns, altered the water balance components, affected the frequency and magnitude of fluvial floods, and increased heat waves and droughts (Ahiablame et al., 2017; Leta et al., 2016; Masson-Delmotte et al., 2018; Mohammed et al., 2017; Pachauri et al., 2014; N. K. Shrestha et al., 2017). As the impacts of climate change are already being felt in the region, it is imperative to understand the potential impacts of climate change on the surface- and groundwater resources of the lower ACF River Basin for developing a long-term water resource management plan. Understanding the potential changes in streamflow as well as other vital components of the hydrologic water balance including evapotranspiration (ET), groundwater recharge, and surface- and groundwater (SW-GW) exchange due to climate change in the region can provide important insight to the development of sustainable water resources management plan for environmental and socio-economic sustainability.

Hydrologic models are essential decision support tools that can provide important insight into short- and long-term water resources management plans at the basin-scale as they can simulate watershed hydrology and help evaluate scenarios including potential changes in climate, land use, and management practices. Because of the intricate connection between the surface- and groundwater resources in the study region, an integrated hydrologic modeling system that allows for a detailed simulation of surface- and groundwater systems along with the interactions between the two components is critical to accurately simulate and represent the hydrology of the lower ACF River Basin. It is difficult to understand and quantify the spatio-temporal distribution of SW-GW exchange using only a surface- or groundwater model and the management decisions made based on the scenario results from such results could have little merit.

There are multiple hydrologic models that allow for the simulation of surface- and groundwater resources including HydroGeoSphere (HGS) (Brunner and Simmons, 2012), Parallel Flow (ParFLOW) (Kollet and Maxwell, 2006), MODHMS (HydroGeoLogic, 2000), MIKE SHE (Jaber and Shukla, 2012), Groundwater Surface-Water FLOW model (GSFLOW) (Markstrom et al., 2008), and SWAT-MODFLOW (Bailey et al., 2016). Some of these models allow for the concurrent/simultaneous simulation of surface and groundwater processes (e.g., ParFlow, HGS) while the other models such as SWAT-MODFLOW and GSFLOW couple two or more hydrological modeling codes to develop an integrated modeling system.

SWAT-MODFLOW is an integrated hydrologic model that couples the Soil and Water Assessment Tool (SWAT) model developed by the U.S. Department of Agriculture (USDA) – Agriculture Research Service (ARS) (Neitsch et al., 2011) with a U.S. Geological Survey (USGS) finite-difference three-dimensional modular groundwater flow model (MODFLOW-NWT) (Niswonger et al., 2011). SWAT is a semi-distributed, watershed scale, physically-based, hydrologic model that is robust in simulating flow, sediment, nutrient, and pesticides and has been extensively tested in a range of climatic and geologic conditions and applications, including evaluating impacts of climate change (de Almeida Bressiani et al., 2015; Francesconi et al., 2016; Gassman et al., 2007; Krysanova and Arnold, 2008). The model is, however, limited in the simulation of groundwater flow and storage due to the semi-distributed nature of the model as well as the simplistic representation of the groundwater flow using a linear reservoir approach (Neitsch et al., 2011). This issue and its potential negative impact in streamflow simulation have been highlighted by multiple studies (Gassman et al., 2007; Molina-Navarro et al., 2016; Nguyen and Dietrich, 2018). MODFLOW, on the other hand, has robust groundwater simulation capabilities but is limited in the simulation of surface hydrology and requires distributed groundwater recharge

provided as model input. The coupling of SWAT and MODFLOW allows utilizing the strength of both models to develop an integrated model that is strong in both surface and sub-surface hydrological simulation. Although multiple attempts have been made to couple SWAT and MODFLOW with varying levels of success (Bailey et al., 2016; Gassman et al., 2007), previous versions of SWAT-MODFLOW have been mostly limited to the use by the developers. The SWAT-MODFLOW model developed by Bailey et al. (2016) is publicly available, has a graphical user interface (Bailey et al., 2017), and has added advantages to the previous versions (Bailey et al., 2016), leading to a broader adoption as well as evaluation in different climatic and geologic conditions and for multiple applications including climate change (Aliyari et al., 2019; Chunn et al., 2019; Gao et al., 2019; Guevara-Ochoa et al., 2020; Molina-Navarro et al., 2019; Wei et al., 2019).

Although there have been some large scale studies that evaluated the impacts of climate change on the hydrology of the region (Georgakakos and Yao, 2000; Sun, 2013), there have been limited studies that evaluated the impact of climate change in the lower ACF River Basin (Viger et al., 2011) and none of these studies have utilized an integrated modeling system that simulates the surface- and groundwater resources in detail. Hence, the overall objective of this research is to evaluate the impacts of climate change on the surface- and groundwater resources of the lower ACF River Basin by developing a coupled SWAT-MODFLOW model for the region. Specifically, the impact on streamflow, groundwater recharge, ET, and SW-GW exchange will be evaluated. An important advantage of using this version of SWAT-MODFLOW also includes the capability of the model to simulate the change in irrigation and account for its impact by extracting water from the underlying aquifer based on the plant water demand. Groundwater withdrawal from the underlying aquifers is an important hydrologic component that needs to be accounted for when

evaluating scenarios such as climate scenarios in intensively irrigated watersheds such as the lower ACF River Basin but is often overlooked due to model limitations. As the study region has complex and spatially variable hydrogeology with a karstic aquifer system, the study also provides an opportunity to evaluate the capability of the coupled SWAT-MODFLOW model to simulate surface- and groundwater hydrology and the interaction between them in a karstic watershed, which to the authors' knowledge has not been performed yet. Global climate projections using multiple Global Climate Models (GCMs) from the 5th phase of the Coupled Model Intercomparison Project (CMIP5) under four emissions scenario are freely available to use as inputs into hydrologic models for evaluating the potential impacts of climate change (Taylor et al., 2012). Of the four scenarios, representative concentration pathway (RCP) 8.5 (high emissions scenario) estimates the greenhouse gases to continue increasing with radiative forcing reaching to about 8.5 W m^{-2} by the end of the twenty-first century compared to the pre-industrial conditions. In contrast, RCP4.5 (intermediate scenario) estimates the greenhouse gases to stabilize with the radiative forcing reaching 4.5 W m^{-2} (Taylor et al., 2012). The impacts of projected climate change under these two emissions scenarios was evaluated in this study.

6.2 Methods

6.2.1 Study area

The lower ACF River Basin is located in the southeastern U.S. and includes parts of the lower Flint, middle Flint, Spring, Ichawaynochaway, and Kinchafoonee-Muckalee Hydrologic Unit Codes (HUC-8) watersheds (Seaber et al., 1987) of the Flint River Basin (Fig. 6.1). Agriculture and forestry are the main land use/land cover types, while urban area accounts for only a small portion of the study region. Cotton, corn, and peanuts are the primary crops produced in the region, while loblolly pine (Pinus *taeda*) is the dominant forest type (Homer et al., 2020; Ruefenacht et

al., 2008). The region has a humid subtropical climate characterized by long, hot, and humid summers and mild winters. The average daily temperature ranges from about 17℃ in the winter to about 34℃ in the summer (Arguez et al., 2012). However, temperatures above 37.7℃ (100°F) are not uncommon in the region. Annual precipitation averages from about 1,365 mm in the south to about 1,161 in the north of the study region and is distributed throughout the year (Arguez et al., 2012) with higher precipitation in the winter and summer months. Winter precipitation, however, is more conducive for groundwater recharge due to its frontal, low-intensity, and long duration pattern compared to the convective, high-intensity, and short-duration precipitation of the summer. Flint River is the major river that flows through the study region with Spring creek and Ichawaynochaway creek as important tributaries to the Flint River.

The study area is located in the Coastal Plain physiographic province. It consists mostly of a low-lying karstic region called the Dougherty Plain physiographic district, which is characterized by relatively flat, inner lowland containing sub-surface and internal drainage and heterogeneous stream network (Torak and Painter, 2006). The UFA, which is the primary water-bearing unit in the region, consists of the Ocala Limestone and is overlain by the Upper Semi-Confining Unit (USCU). The USCU is a discontinuous unit of undifferentiated overburden, weathered residuum, and surficial deposits (Torak and Painter, 2006). Major rivers and streams in the region are in direct connection with the underlying UFA through shallow channels incised through the USCU. The thickness of the aquifer ranges from about 9 m in the northwestern parts of the study region where it outcrops to the surface to more than 130 m in the south-eastern end of the study region (Torak and Painter, 2006; Williams and Kuniansky, 2016).

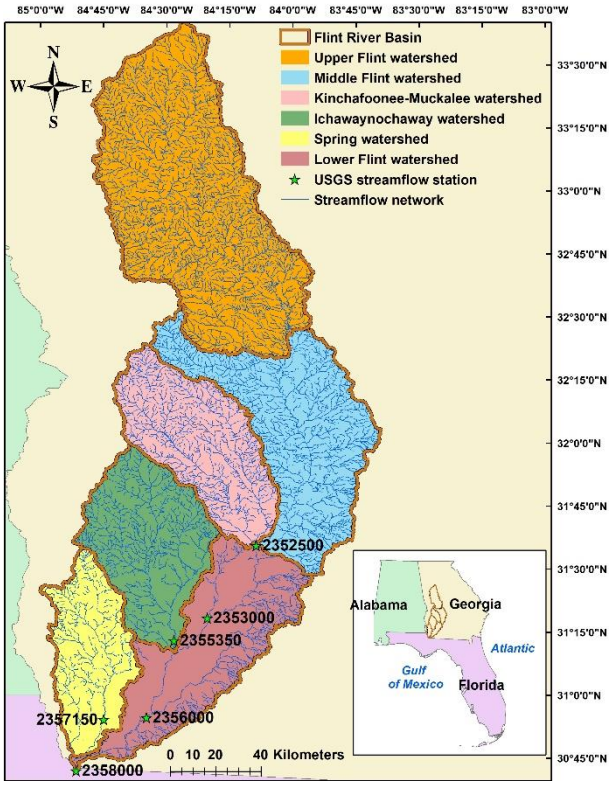

Figure 6.1 The Flint River Basin and the six HUC-8 watersheds associated with the basin.

6.2.2 SWAT-MODFLOW model

This section provides a summary of the SWAT-MODFLOW coupling framework developed by Bailey et al. (2016) and used in this study. Readers are referred to the document as well as Bailey and Park (2019), and Wei and Bailey (2019) for further detail. In the coupled framework, SWAT simulates the land surface processes, crop growth, in-stream processes, and soil zone processes while MODFLOW, which replaces the SWAT groundwater module, simulates three-dimensional groundwater flow along with the sources and sinks associated with the aquifer system. The groundwater delay parameter (GW_DELAY) in the SWAT groundwater module (*.gw* file) is still active to mimic groundwater transport in the vadose zone. Basic steps in the SWAT-MODFLOW coupled simulation includes the simulation of land surface processes by the SWAT model, mapping of the SWAT simulated groundwater recharge and channel depths of streams into the

MODFLOW model, simulation of groundwater level and SW-GW exchange by MODFLOW, passing of SW-GW exchange volumes (groundwater discharge) from MODFLOW into SWAT, and SWAT routing the surface and groundwater discharge volumes through the stream network for each day of the simulation period. SWAT model performs the spatial disaggregation of a watershed into sub-basins, which is further divided into hydrologic response units (HRUs). HRU's are lumped land areas with a unique combination of land use, soil, and slope classes within a sub-basin and the basic units for calculation in SWAT but have no spatial information within a sub-basin. Hence, HRU's are disaggregated (DHRUs), which are then mapped to individual MODFLOW grid cells using mapping files to connect HRUs to DHRUs and DHRUs to MODFLOW grid cells. Similar mapping files are also required to connect MODFLOW river cells to SWAT sub-basins. The coupled model can also map drain cells in MODFLOW to sub-basins in the SWAT model and route water down the SWAT stream network. Similarly, irrigation pumpage from the MODFLOW model can also be mapped to SWAT HRUs.

An important advantage of this SWAT-MODFLOW model over previous versions also includes linking SWAT auto-irrigation routines to water withdrawal from the underlying aquifer. SWAT auto-irrigation function allows for the triggering of irrigation events based on plant water demand or soil water deficit (Neitsch et al., 2011), and the depth of water irrigated each day is converted to water volume through sub-routines in SWAT-MODFLOW which is then extracted from the underlying aquifer using the well package in MODFLOW (Bailey and Park, 2019). This can be important for effectively evaluating scenarios like climate change impacts in intensively irrigated watersheds like the lower ACF River Basin where groundwater withdrawal is an important concern but is hugely dictated by the variability in climate each year as well as during the growing season.

As the SWAT-MODFLOW coupled model development process requires the FullHRU shapefile from the SWAT model to link the two models, users should be careful to develop the SWAT model with 0% threshold when defining HRUs which is important for creating the FullHRU shapefile. It was also realized during the SWAT FullHRU shapefile development process that having a higher number of HRUs that caused the ArcSWAT Access Database to exceed 2 gigabytes caused the process to crash and should be taken into consideration, especially when working with large watersheds.

6.2.3 Model development

6.2.3.1 SWAT model

A SWAT model developed for the region for previous research (detailed in chapter 4) was used in this study for developing the coupled SWAT-MODFLOW model. The model was developed for the entire Flint River Basin, covering an area of about 24,000 km^2. The spatial extent of the SWAT model is presented in Figure 6.2A. Digital Elevation Model (DEM) data of 30m x 30m resolution provided by the USGS was used for the elevation dataset (Gesch et al., 2002) while the soil dataset was provided by State Soil Geographic [STATSGO] (Schwarz and Alexander, 1995). The Cropland Data Layer (CDL) for the year 2015 developed by USDA-National Agricultural Statistics Service (NASS) was used as the land use/land cover dataset for the model (Han et al., 2012). Typical agricultural crop rotations for the study region were identified using multiple years of CDL and performing an overlay analysis which was then incorporated into the model. The model was calibrated for the 2003-2010 period for streamflow and ET. Streamflow was calibrated at seven USGS monitored streamflow stations (USGS, 2019) (Fig. 6.1). ET was calibrated and evaluated for each sub-basin against the MODerate Resolution Imaging Spectroradiometer

(MODIS) global terrestrial ecosystem ET data product (MOD16A2) dataset (Running et al., 2017). The developed SWAT model had 118 sub-basins and 7,068 HRUs.

6.2.3.2 MODFLOW model

Similar to the SWAT model, a MODFLOW-NWT model developed and calibrated for previous research (detailed in chapter 3) was used for developing the coupled SWAT-MODFLOW model. The groundwater model covered an area of about 12,003 km^2 and included parts of south Georgia, southeastern Alabama, and northwestern Florida of the lower ACF River Basin (Fig. 6.2B). The model is two-layered, representing the UFA and the overlying USCU and has a uniform grid size of 750m x 750m. The model has 282 rows and 102 columns with a total of 28,764 grid cells of which 21,394 are active. The model was developed as a transient model from 2007-2013 with monthly stress periods and daily time steps. The regional boundary of the groundwater model was a specified head boundary condition in the northwestern end (CHD) and a general head boundary (GHB) in the remainder of the regional boundary. Ephemeral streams that could go dry were simulated using the drain package (DRN), while the perennial rivers were simulated using the river package (RIV). The two lakes in the model domain (Fig. 6.2B) were also simulated using the GHB package. Groundwater pumpage in the region was simulated using the WEL package, and areal recharge from precipitation into the groundwater model was estimated using the SWAT model. The model was calibrated for groundwater levels using 2,360 observed daily groundwater level data in the groundwater model domain, which was acquired from the USGS National Water Information System [NWIS] (USGS, 2019). The model was also calibrated for the SW-GW exchange at six river reaches in the lower Flint River Basin and the contributing watersheds (chapter 3).

6.2.3.3 SWAT-MODFLOW model

As the spatial extent of the SWAT and MODFLOW models used to develop the coupled model were different, the overlap area where the SWAT and MODFLOW models are coupled is shown in Figure 6.2C. In areas where the SWAT-MODFLOW does not overlap and is not coupled, the SWAT and MODFLOW model runs similar to how the models would run independently i.e. groundwater module for SWAT is activated and MODFLOW receives recharge from the RCH package. The WEL package of the MODFLOW model was modified for developing the coupled SWAT-MODFLOW model so that groundwater withdrawal for each day was initiated by the SWAT auto-irrigation routines (Bailey and Park, 2019). Mapping files required to couple the two models were created by following the detailed steps outlined in Bailey and Park (2019). The coupled SWAT-MODFLOW domain included 69 of the 118 sub-basins in the SWAT model and 20,080 grid cells of the 21,394 active MODFLOW cells. The overlapped domain also included 1,237 drain cells and 669 river cells. Disaggregation of the 7,068 SWAT HRUs resulted in 2,696,425 DHRUs. The model was run from 2003 to 2013 with a 4-year warm-up period. Climate forcing data for model simulation was acquired from the North American Land Data Assimilation Phase-2 (NLDAS-2) climate dataset, which has a spatial resolution of $1/8^{th}$ degree and temporal resolution of 1 hr, covering the continental U.S. (Xia et al., 2012).

Although the SWAT and MODFLOW models used in developing the coupled model were already calibrated, the coupled model required further calibration. SWAT-MODFLOW simulated streamflow was calibrated using six USGS monitored streamflow stations that were within the coupled SWAT-MODFLOW domain (Fig. 6.2C). Streamflow was calibrated from 2007-2010 and validated from 2011-2013. A sequential calibration approach was used in the streamflow calibration process in which flows to streamflow stations that received water from the independent

sub-sections of the watershed as well as the most upstream streamflow station were calibrated first followed by downstream streamflow stations. Calibration of groundwater levels simulated by the model was performed against 2,360 observed daily groundwater levels from 359 wells that tap into the UFA during the simulation period. Model calibration was performed using both automated and manual adjustments to the SWAT and MODFLOW model parameter values. Automated calibration was performed by using a model-independent Parameter Estimation Tool [PEST] (Doherty, 2004) which iteratively adjusts model parameters to reduce the objective function of the weighted square of residuals between observed and simulated values.

Model performance evaluation for streamflow simulation was performed by plotting time series and flow duration curves (FDCs) of simulated vs observed streamflow along with calculating the coefficient of determination (R^2), Nash-Sutcliffe Efficiency (NSE), and percent bias (PBIAS). The three statistical measures have been widely used in evaluating hydrological model performance for streamflow simulation (Moriasi et al., 2015). Assessment of groundwater level simulation was performed by plotting a scatter plot between the simulated and observed groundwater levels as well as calculating the root mean square (RMS), mean, and the absolute mean of the groundwater head residuals.

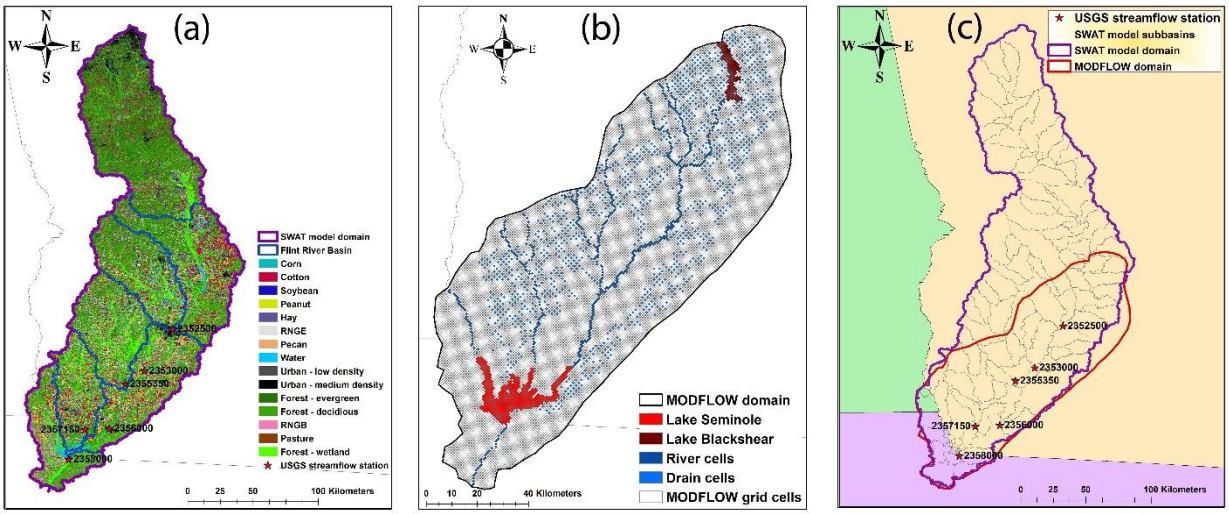

Figure 6.2 Spatial extent of the (a) SWAT model with the land use types and extent of the six HUC-8 watersheds, (b) the MODFLOW domain with the river and drain cells simulating the perennial and ephemeral streams, respectively, and (c) the overlap of the SWAT and MODFLOW domain where the model is coupled to develop the SWAT-MODFLOW model along with the locations of the six USGS streamflow gages used for streamflow evaluation.

6.2.4 Climate scenarios

Climate projection from three GCMs (Table 6.1) under two emission scenarios of RCP4.5 and RCP8.5 for the mid-century time horizon (2041-2060) from the CMIP5 project were used for evaluating the impacts of climate change in the region. Projections from multiple GCMs were used in SWAT as climate forcing to account for the uncertainty associated with different GCMs which can be a significant source of uncertainty for hydrologic modeling (Shrestha et al., 2016). The three GCMs selected were developed by agencies in the U.S. (Table 6.1). As the outputs from GCMs have a coarse resolution as well as biases which if not corrected can lead to errors in impact assessment, GCM outputs need to be downscaled and bias-corrected before using them for regional analysis (Ahmed et al., 2013). Statistically downscaled and bias-corrected precipitation and temperature forcings from the three GCMs using a modification of the Multivariate Adaptive

Constructed Analogs (MACA) (Abatzoglou and Brown, 2012) method with the METDATA (Abatzoglou, 2011) is publicly available (https://climate.northwestknowledge.net/MACA/index.php) and was used for this study. METDATA is a high resolution gridded data that was developed using NLDAS-2 and Parameter-elevation Regressions on Independent Slopes Model (PRISM) data set (Abatzoglou, 2011).

Table 6.1 List of Global Circulation Models (GCMs) of which the climate projections were used from the CMIP5 project.

S.no	Model name	Modeling Center (Group)
1	CCSM4.1	National Center for Atmospheric Research, USA
2	GFDL-ESM2G	NOAA Geophysical Fluid Dynamics Laboratory, USA
3	GFDL-ESM2M	NOAA Geophysical Fluid Dynamics Laboratory, USA

6.3 Results and discussion

6.3.1 Streamflow simulation

As the SWAT and MODFLOW models used in this study were individually calibrated before coupling, initial model evaluation after the coupling showed that the model did an adequate job of simulating groundwater levels but performed poorly in simulating streamflow at all six USGS monitoring stations. Hence, model calibration was more focused on adjusting parameters that were most sensitive to SW-GW exchange and streamflow simulation. As a sequential calibration approach was utilized, streamflow into stations 2355350, 2357150, and 2352500 were calibrated first by running PEST individually for each station so that the parameters could be independently adjusted for the different sub-sections of the watershed. This was followed by simultaneous calibration of stations 2353000, 2356000, and 2358000. Automated calibration was followed by manual parameter refinement for further improving streamflow simulation. Important parameters adjusted during model calibration included river conductance, specific storage, and specific yield

of the MODFLOW model and channel hydraulic conductivity (CN_K2), groundwater delay (GW_DELAY), and bank storage (ALPHA_BNK) of the SWAT model. It is very important to note that both the SWAT and MODFLOW models were already rigorously calibrated in the previous studies and the calibration here can be considered as further model refinement. Readers are referred to chapter 3 and chapter 4 for detailed information of individual calibration of SWAT and MODFLOW.

Model performance evaluation for streamflow simulation after calibration at the six USGS streamflow stations shows that the model does an adequate job of simulating daily streamflow at all stations, except for station 2357150 (Table 6.2). R^2 and NSE for the remaining five stations during calibration were above 0.56 and PBIAS values were less than 15% (Table 6.2) indicating a satisfactory model performance at the five stations according to Moriasi et al., (2015) criteria. Although PBIAS was less than 10%, R^2 and NSE values were only 0.49 and 0.17 respectively for station 2357150 indicating an unsatisfactory model performance for streamflow at this station. It should, however, be noted that a significant portion of observed streamflow data was missing at the station during high flows (Fig. 6.3) which could have attributed to the unsatisfactory model performance for the streamflow station during the calibration period. This can be further corroborated by evaluating the model performance for the station during the validation period which has fewer high flow events, and as a result, show better performance statistics (Table 6.2). It should also be pointed out that the region contributing streamflow to station 2357150 has complex hydrogeology and stream-aquifer interaction. The underlying UFA is thin in the southeastern end of the study domain and the overlying USCU is also thin in the region. This could have also contributed to the model not accurately representing the flow dynamics of the region and hence the reduction in streamflow simulation performance. Streamflow evaluation for the

remaining five stations during the validation period shows that the model performance improved compared to the calibration period (Table 6.2). The time series plot between observed and simulated streamflow for all stations shows that the coupled model is not able to match the high peak flows but matches the low flow periods well, especially in the upstream stations (Fig 6.3). Fewer high flow events during the validation period, as a result, could have resulted in the improved performance. It is, however, noteworthy that the PBIAS increased in all stations during the validation period when compared to the calibration period. The calibration period being much wetter than the validation period could have led to the high PBIAS during the validation period.

Table 6.2 Model performance for streamflow simulation during calibration (2007-2010) and validation (2011-2013).

	Calibration			Validation		
USGS streamflow station	**R^2**	**NSE**	**PBIAS (%)**	**R^2**	**NSE**	**PBIAS (%)**
2352500	0.75	0.71	-6.9	0.8	0.79	14.6
2353000	0.73	0.73	0.2	0.8	0.72	18.5
2355350	0.54	0.49	1	0.71	0.59	9.8
2356000	0.7	0.69	11.4	0.8	0.57	31
2357150	0.46	0.21	-6.5	0.76	0.4	7.8
2358000	0.89	0.88	-2.1	0.91	0.9	7.5

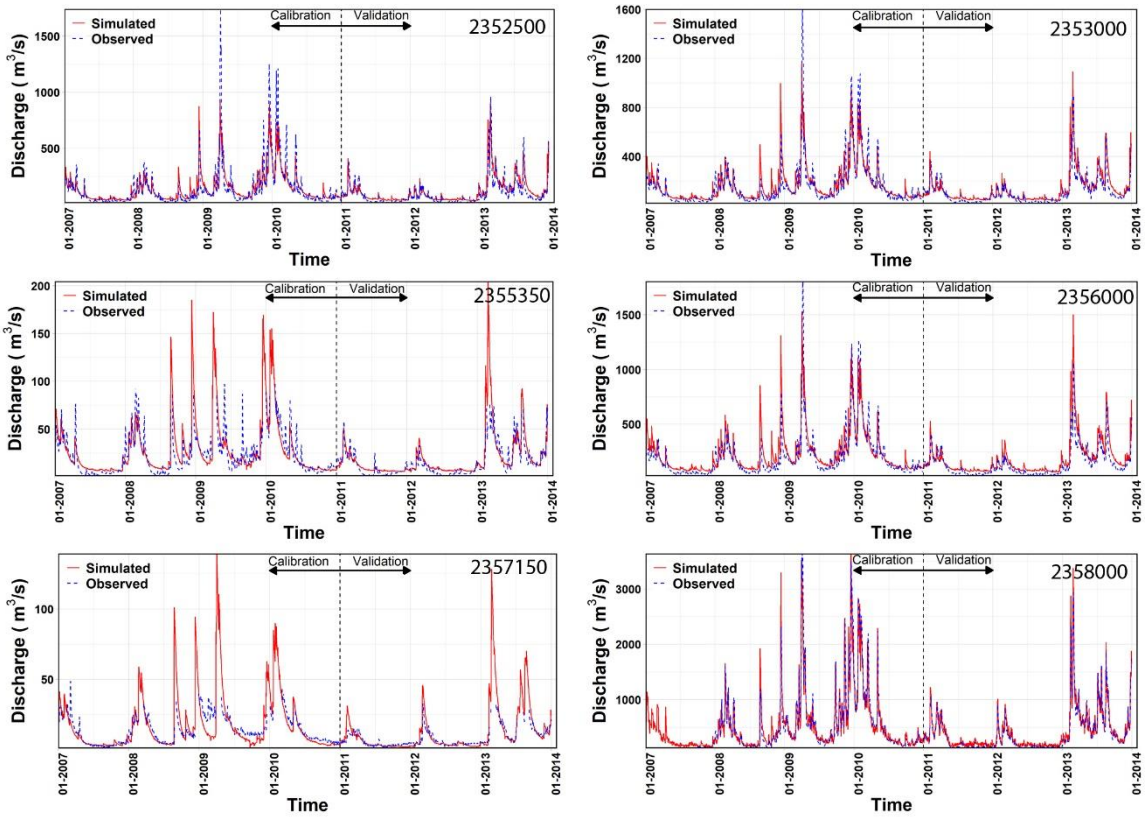

Figure 6.3 Comparison between SWAT-MODFLOW simulated and observed streamflow for the six USGS stations during calibration and validation.

Evaluation of the flow regimes using FDCs between the simulated and observed streamflow for each streamflow station is shown in Figure 6.4. It can be seen from the figure that streamflow stations 2352500, 2353000, and 2356000 have a similar flow pattern with flow rate of less than 500 m^3/s more than 95% of the time and the coupled model does a very good job of replicating these flows. The coupled model, however, is not able to match the very high flow rates which occurred less than 1% of the time. A similar pattern can be observed for the most downstream streamflow station (2358000) in which flows that occurs more than 95% of the time match well between the simulated and observed flow but the model is not able to simulate the high flow conditions that occurred less than 1% of the time (Fig. 6.4). FDC evaluation for station 2355350 and 2357150 shows that the two stream reaches have a much smaller flow rate compared to the

remaining streamflow stations which are located in the mainstem of the Flint River. Streamflow was less than 25 m^3/s and 40 m^3/s more than 80% of the time in station 2357150 and 2355350, respectively (Fig. 6.4). It can also be seen that the model simulated flow matches the observed flow in the two stations that occurs more than 80% of the time but the model slightly over-estimates flow during high flow events (Fig. 6.4).

Overall, it can be stated that the SWAT-MODFLOW model can adequately simulate streamflow in a karstic watershed with complex hydrogeology. The model, however, performed better in the region where the aquifer is thick and the variability in aquifer level did not have a significant impact in streamflow as compared to the region where the aquifer is thin and close to the land surface.

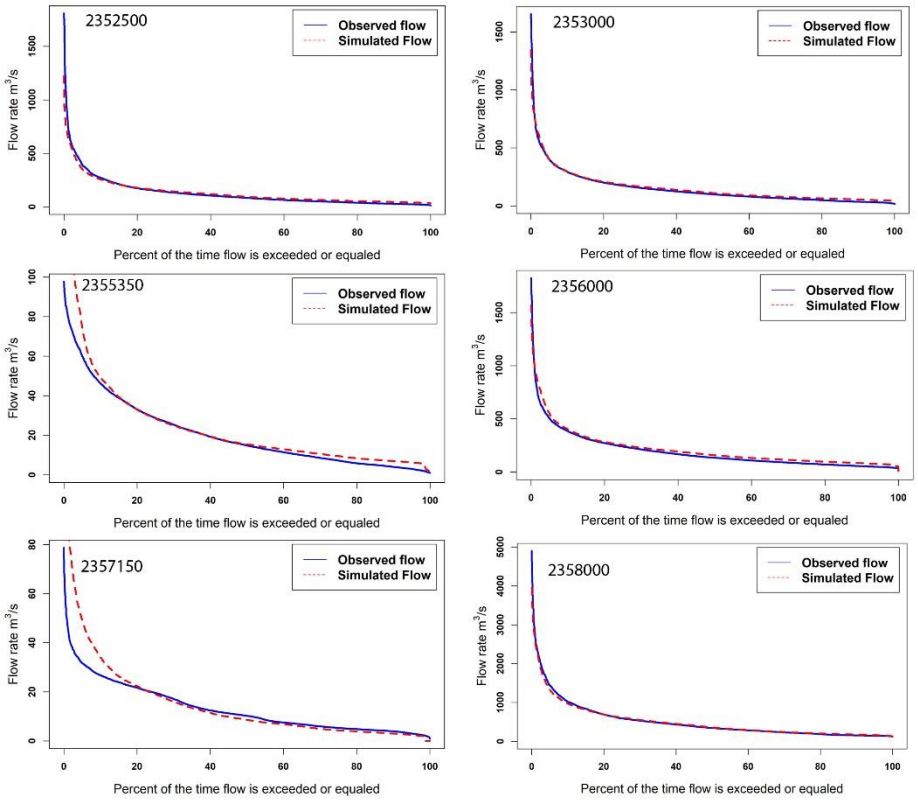

Figure 6.4 Flow duration curves (FDCs) of the SWAT-MODFLOW simulated and observed flow for all six USGS streamflow stations for the total simulation period (2007-2013).

6.3.2 Groundwater level simulation

A scatter plot of the SWAT-MODFLOW simulated vs observed groundwater levels in the UFA shows that the model can adequately simulate the groundwater levels in the aquifer (Fig. 6.5A). The RMS of the residuals between simulated and observed value was 3.04 m while the mean error (ME) was 0.86 m and the mean absolute error (MAE) was 2.12 m. This indicated that the model slightly over simulated groundwater levels in the UFA. A plot of the mean residual for each groundwater well across the model domain shows that the model can adequately simulate the spatial variability in the groundwater level (Fig. 6.5B). As the model was a transient model with both wet and dry periods and the observed groundwater levels were scattered throughout the

simulation period, it can also be inferred that the model can adequately simulate the temporal variability in groundwater levels as well as perform adequately in both wet and dry periods.

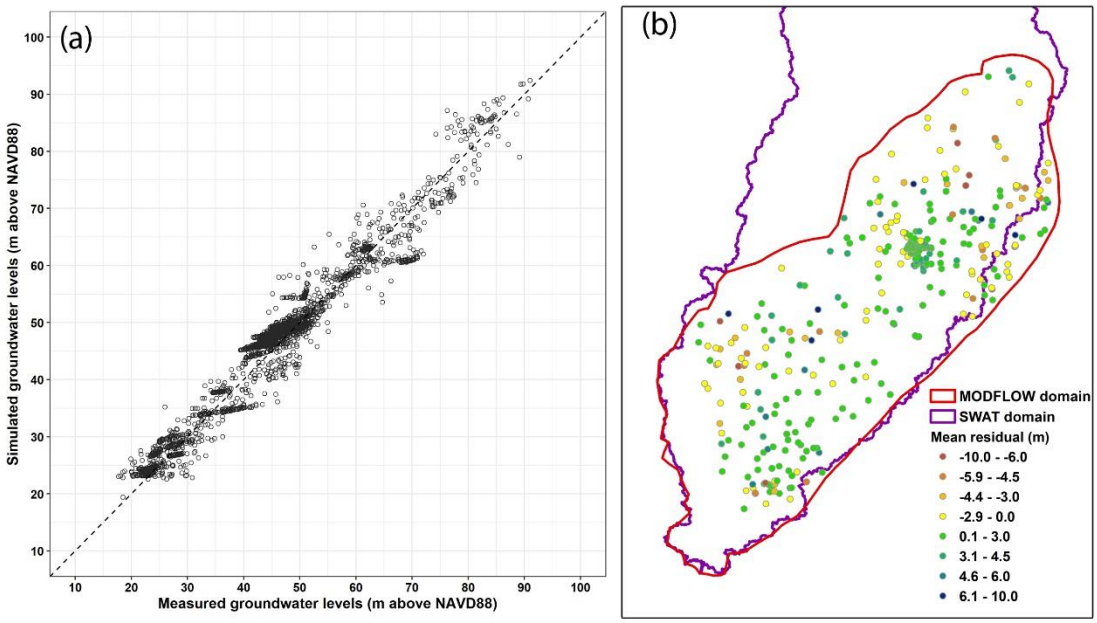

Figure 6.5 (a) scatter plot between model-simulated and observed groundwater levels for the Upper Floridan Aquifer for the whole simulation period (2007-2013) and (b) mean groundwater residual for each groundwater well that was used for collecting the observed groundwater level data.

6.3.3 Evaluation of hydrologic budget components

Evaluation of basin average annual precipitation during the simulation period compared to 30-year normals from 1981-2010 for the region (Arguez et al., 2012) of 1,265 mm showed that the years 2009 and 2013 were very wet while the years 2007, 2010, and 2012 were under drought conditions (Fig. 6.6). Annual average ET for the basin, however, was less variable and close to around 800 mm with slightly higher values in wet years and slightly lower values in dry years. The lack of temporal variability in ET can be attributed to the irrigation management practices incorporated in the model but also demonstrates the importance of the UFA in the region. Annual basin average

groundwater recharge ranged from about 300 mm (about 20% of precipitation; 2013) in a wet year to close to 100 mm (10% of precipitation; 2011) in drought years (Fig. 6.6). On average, about 16% of the precipitation reached as recharge into the underlying aquifer system during the simulation period.

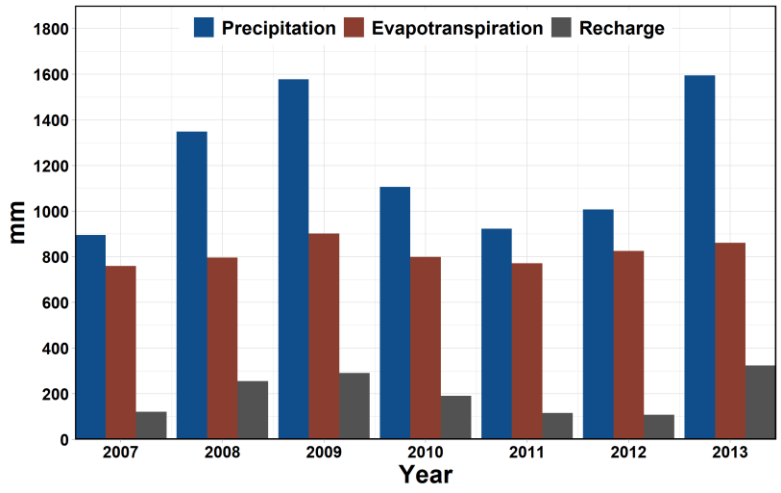

Figure 6.6 SWAT-MODFLOW coupled model domain average annual precipitation, evapotranspiration (ET), and groundwater recharge for the simulation period (2007-2013).

Spatial evaluation of average annual simulated ET for each sub-basin in the model for the simulation period (2007-2013) showed that the Lower Flint watershed had a distinct high ET when compared to the other watersheds. Low ET was observed at the southern end of the model boundary. Simulated ET were similar in the Ichawaynochaway, Kinchafoonee-Muckalee, and Middle Flint watersheds (Fig. 6.7) ranging between 777 mm and 801 mm in much of the area. Average ET ranged from about 661 mm to 1560 mm per year with the highest ET observed in sub-basins that enclosed lake Seminole.

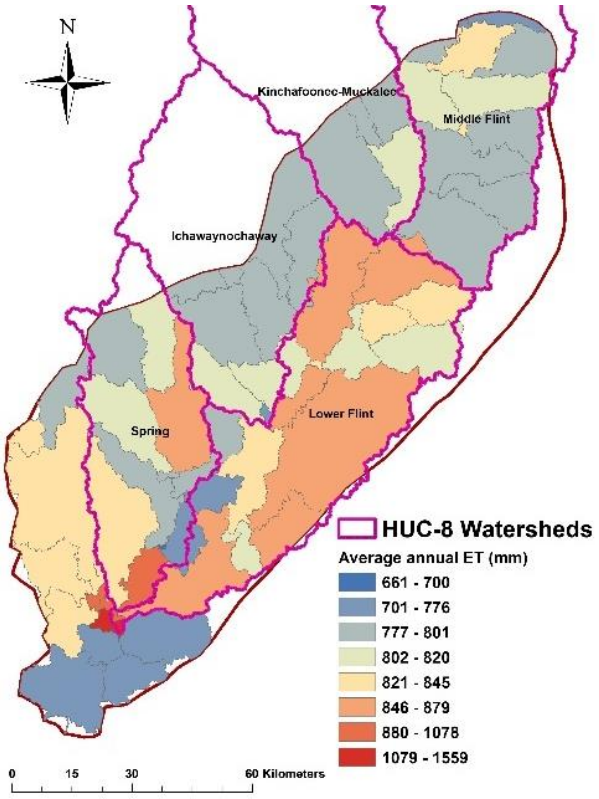

Figure 6.7 Average annual evapotranspiration (ET) for the sub-basins in the SWAT-MODFLOW model domain for the simulation period (2007-2013).

Annual average groundwater recharge ranged from about 100 mm to 628 mm (Fig. 6.8). The highest groundwater recharge, again, were observed in sub-basins that included lake Seminole probably indicating to leakage from lakes, especially after the growing season when the groundwater levels are low but the lakes are maintained at a near-constant level.. Groundwater recharge was high in the southern end of the model domain, the region which had low simulated ET. The southern part of the research area also has higher precipitation than the northern end which can also help explain the high recharge in the area. Groundwater recharge were similar in the sub-basins of the Lower Flint, Ichawaynochaway, and Kinchafoonee-Muckalee watersheds while it was slightly higher in the Middle Flint and Spring watersheds (Fig. 6.8).

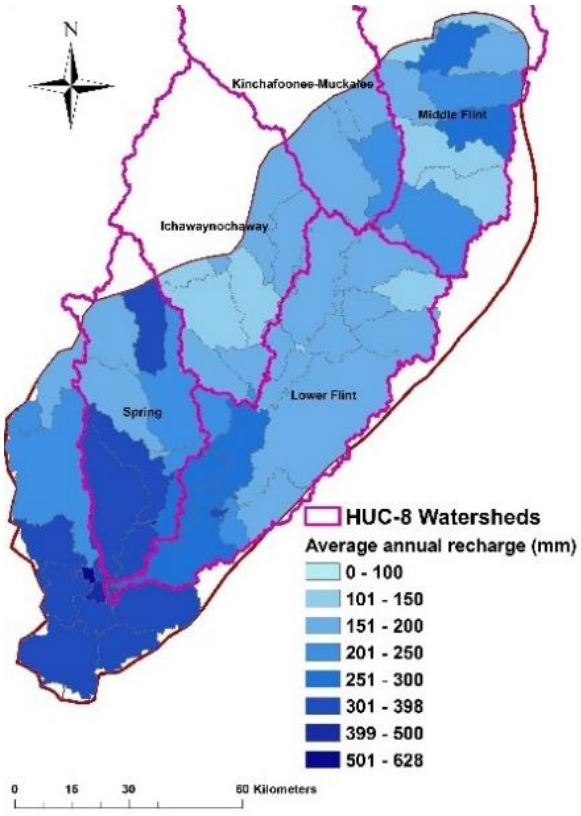

Figure 6.8 Average annual groundwater recharge for the sub-basins in the SWAT-MODFLOW model domain for the simulation period (2007-2013).

The average SW-GW exchange for each sub-basin that had perennial river sections (simulated as RIV cells in the MODFLOW model) for the simulation period (2007-2013) is presented in Figure 6.9. Evaluating the SW-GW exchanges were limited to these sub-basins as the model prints SW-GW exchange output only for the sub-basins that are intersected with the river sections that are simulated as RIV cells in the MODFLOW model. The model does not print SW-GW exchange for DRN cells that were used to simulate the ephemeral streams in the MODFLOW model. A positive value indicates the flow of water from the aquifer to the perennial streams while negative values indicate flow from the river to the aquifer system. It can be seen from the figure that there is positive flux in most of the sub-basins through which the main stem of the Flint River. The highest

positive fluxes of greater than 1 mega cubic meters of water per day was observed in two sub-basins through which the Flint River passes (Fig. 6.9). It is, however, important to note that multiple sub-basins in the Spring and Ichawaynochaway watersheds through which the tributary perennial rivers passed had negative fluxes indicating water loss from the rivers to the aquifer (Fig. 6.9). The underlying aquifer in the Spring and Ichawaynochaway watersheds are not very thick and the occurrence of multiple drought years (2007, 2011, and 2012) could have led to the average flux to be negative in the region. Studies have indicated that flow in the Ichawaynochaway and Spring creeks have reduced by 50 to 100% during drought periods (GWC, 2017). This highlights the vulnerability and impact of drought in streamflow in the region in that multiple-year drought can lead to a reduction in streamflow.

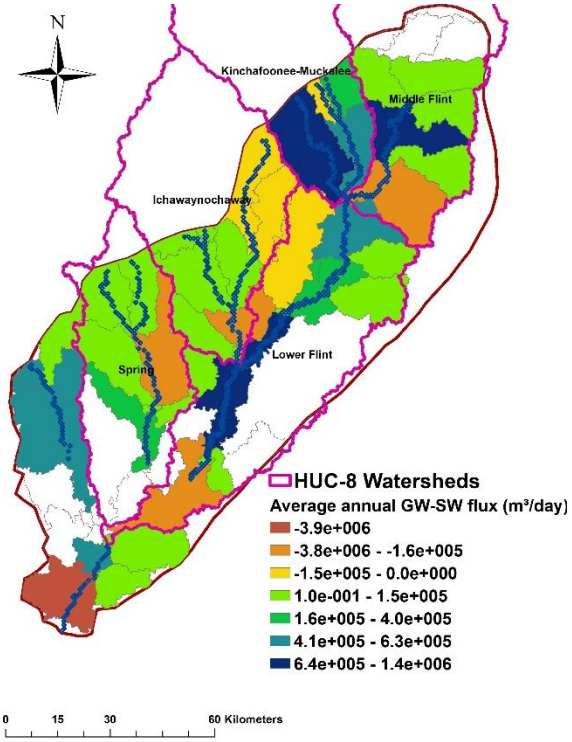

Figure 6.9 Average surface- and groundwater (SW-GW) exchange for the sub-basins in the SWAT-MODFLOW model domain with major rivers for the simulation period (2007-2013).

6.3.4 Impacts of climate change

6.3.4.1 Projected change in precipitation and temperature

Comparison of historical (1979-2005) monthly average precipitation and daily maximum and minimum temperatures obtained through NLDAS-2 to the bias-corrected and downscaled monthly average projections for the three GCMs for RCP4.5 emissions scenario (2041-2060) are presented in Figure 6.10. A discernable trend in the projected precipitation by all three models is the increase in precipitation from July to October. The projected increase in precipitation was highest in August for all three models with ccsm4.1 projecting the precipitation to increase by close to 35 mm when compared to historical averages. Two of the three models also project the precipitation to decrease in winter (Jan-Apr). This indicates a shift in precipitation pattern for the region with increasing precipitation in the fall months and decreasing precipitation in the winter months. Evaluation of the projected change in maximum daily temperature shows that the temperature is projected to increase in all months with the highest projected increase in the summer months. The maximum daily temperature is projected to increase by close to 2℃ in the peak summer months and by about 1℃ in the winter months. Unlike precipitation, all three models follow the same trend in the projected increase in daily maximum temperature. Projected change in daily minimum temperature under the RCP4.5 scenario follows a similar trend to the daily maximum temperature with an increase in temperature in all 12 months (Fig. 6.10). The increase in daily minimum temperature is also expected to be higher in the summer months than in the winter months with the temperature increasing by close to 1.5℃ and 1℃ in the summer and winter months, respectively.

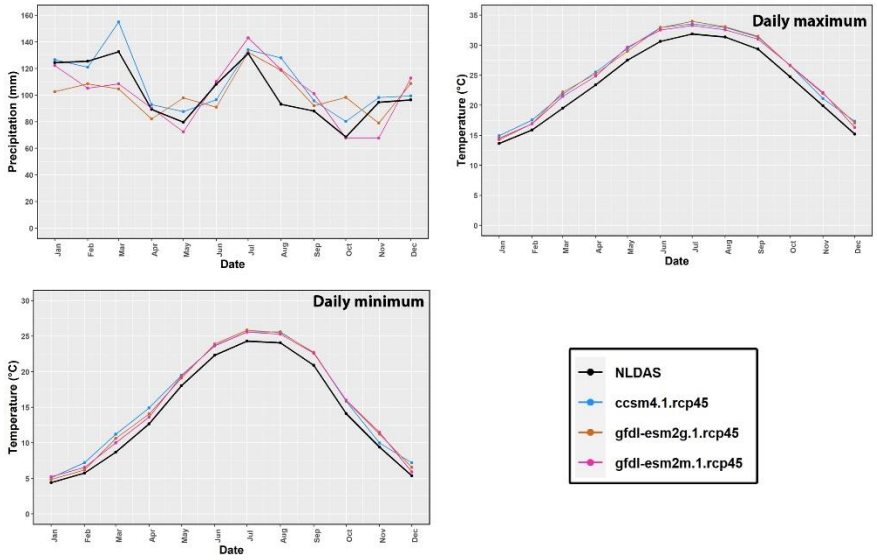

Figure 6.10 Comparison between historical (1979-2005) and bias-corrected and downscaled projected (2041-2060) monthly precipitation (top left), daily maximum temperature (top right), and daily minimum temperature (bottom left) for the three Global Climate Models (GCMs) under RCP4.5 emissions scenario.

Projected precipitation under RCP8.5 follows a similar trend to the RCP4.5 projection with an increase in precipitation from July to October for all three models (Fig. 6.11). The maximum increase in precipitation was again projected for August with gfdl-esm2m projecting an average increase of about 30 mm. There is, however, a slight reduction in precipitation in April and May for all 3 models which was not observed under the RCP4.5 scenario. A shift in precipitation pattern under the RCP8.5 scenario can also be observed with increasing precipitation in the fall months and decreasing precipitation in the early spring months. The daily maximum temperature under the RCP8.5 scenario is projected to further increase when compared to the historical and RCP4.5 scenario throughout the year. The increase in temperature is projected to be higher in the summer months than in winter with an average daily maximum temperature projected to increase by as much as 2.7°C. Winter daily maximum temperature is projected to increase by about 1.5°C. The three climate models also project an increase in daily minimum temperature with the projected

increase, again, being higher than in the RCP4.5 scenario. The minimum daily temperature is expected to increase by more than 1℃ and by close to 2℃ in the summer months in comparison to the historical values.

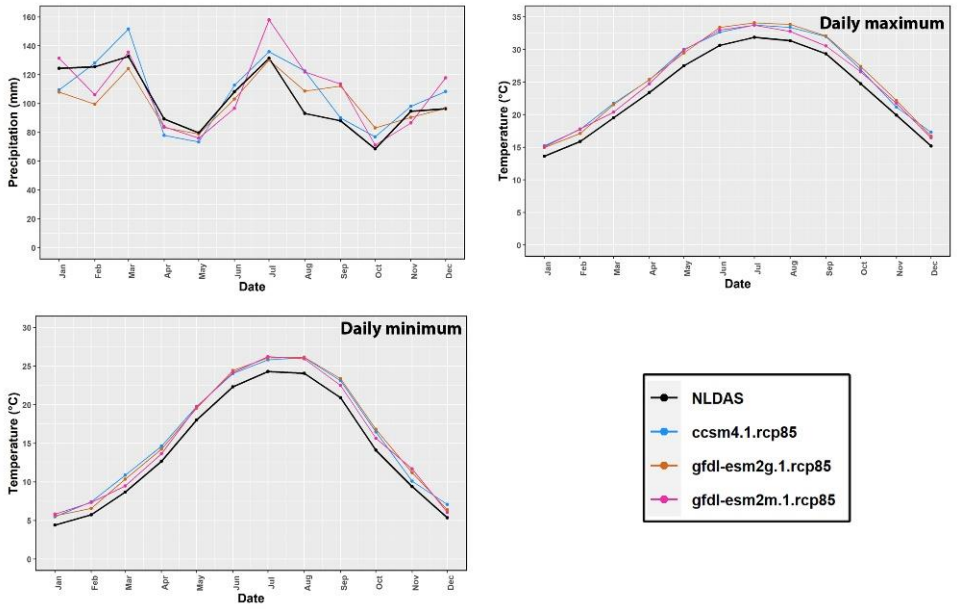

Figure 6.11 Comparison between historical (1979-2005) and bias-corrected and downscaled projected (2041-2060) monthly precipitation (top left), daily maximum temperature (top right), and daily minimum temperature (bottom left) for the three Global Climate Models (GCMs) under RCP8.5 emissions scenario.

6.3.4.2 Projected change in streamflow

The calibrated SWAT-MODFLOW model was run using historical climate data acquired from NLDAS-2 from 1991 to 2015 with a four-year warm-up period to develop a baseline scenario for evaluating the change in hydrological components due to the projected change in the climate.

Change in monthly average flows at the six USGS stations under projected climate data from the three GCMs under the RCP4.5 scenario compared against the baseline flows are presented in Figure 6.12. A reduction in monthly average flow was observed from March to July along the

mainstem of the Flint River at stations 2352500, 2353000, 2356000, and 2358000 under projected climate by at least one of the three GCMs in the RCP4.5 scenario (Fig. 6.12). The highest reduction in flow was observed in April at all four stations with flows at the upstream stations decreasing as much as 25% under the *gfdl_esm2g* GCM. Reduction in flow at the most downstream station (2358000) was close to 15% in April. Flow in the remaining months (September to February) generally increased as compared to the baseline scenario at all four stations except for December during which a distinct reduction in flow was observed by as much as 10% (Fig. 6.12). The increase in monthly flow was as high as 40% at the upstream stations and close to 20% at the most downstream station along the Flint River. The increasing flow in the fall months and decreasing flow in the spring months also indicates a shift in flow pattern in the region under projected climate change in RCP4.5 as the flow is normally low in the fall months and high in the spring months.

Evaluation of change in streamflow at stations 2355350 and 2357150, which are tributaries to the Flint River, showed a slightly different pattern. A reduction in flow was observed for March, April, and May (for at least two GCMs) by as much as 40% similar to the other four stations. However, unlike at other stations, flow at stations 2355350 and 2357150 increased as compared to the baseline for June and July. A reduction in flow was also observed under all three GCMs for December at station 2355350 while a reduction in flow was observed under only one GCM (*gfdl_esm2g*) at station 2357150. The highest increase in flow at the two stations was observed in the fall months of October and November unlike at the remaining four stations which saw the highest increase in January - March.

As the streamflow is normally at its lowest during the summer months due to increased groundwater usage for irrigation as well as a reduction in groundwater recharge, further reduction in streamflow in summer months due to the projected change in climate as shown by this study

can be of concern for the region. Reduction in streamflow can lead to loss of habitat for the endangered mussel species and threatened bass population that depends on continuous streamflow for maintaining their habitat (Shea et al., 2013). This could also lead to increased conflict between the neighboring states due to the reduction in flow downstream of the region which can ultimately threaten the sustainability of agriculture in the region.

Comparison of the FDCs between the baseline and simulated flow under the projected climate forcings from the three GCMs under RCP4.5 shows that there is very little change in flow at all six stations that occurs more than 80% of the time (Fig. 6.13). However, evaluation of the high flows that occurred less than 1% of the time showed a considerable increase at all stations except the most downstream station (2358000) (Fig. 6.13). This indicates the possibility of more flooding events in the majority of the lower ACF River Basin due to the projected change in the climate.

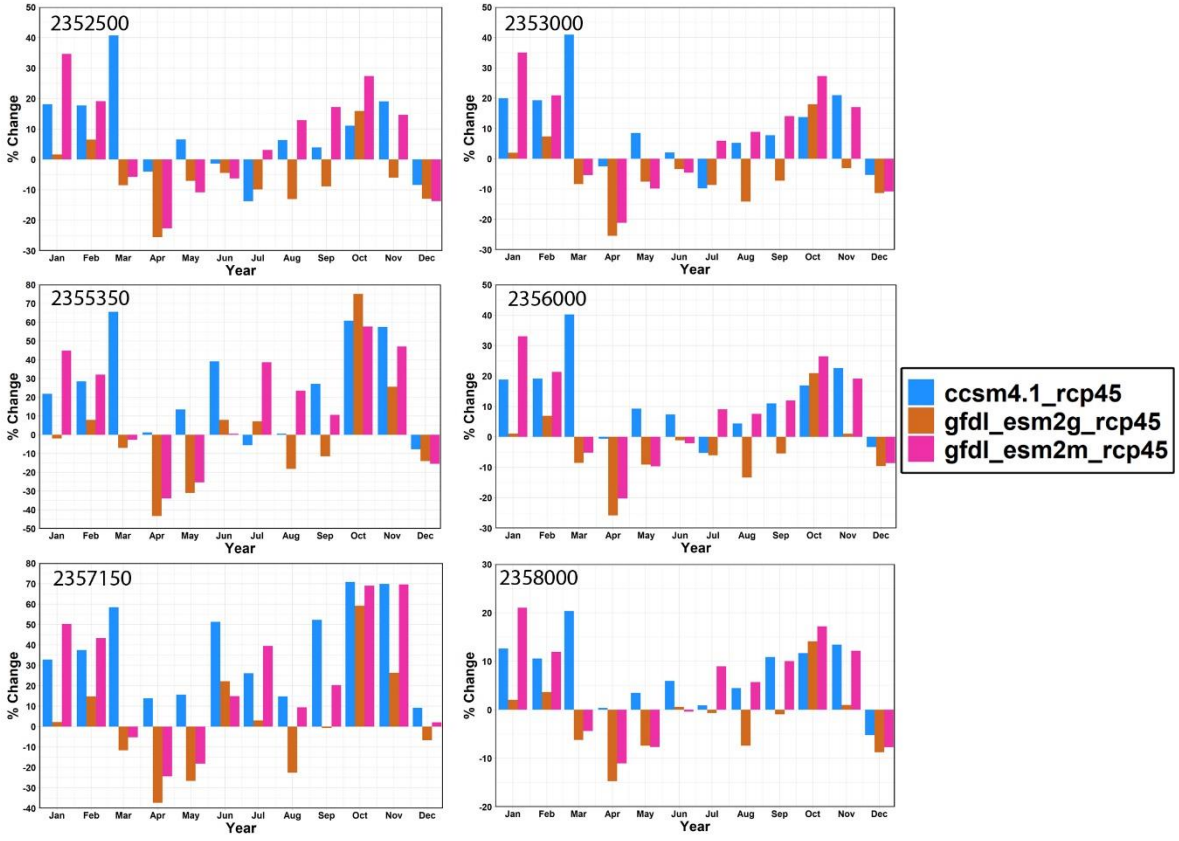

Figure 6.12 Monthly % change in streamflow at each of the six USGS streamflow stations between each Global Climate Model (GCM) and baseline under RCP4.5 emissions scenario.

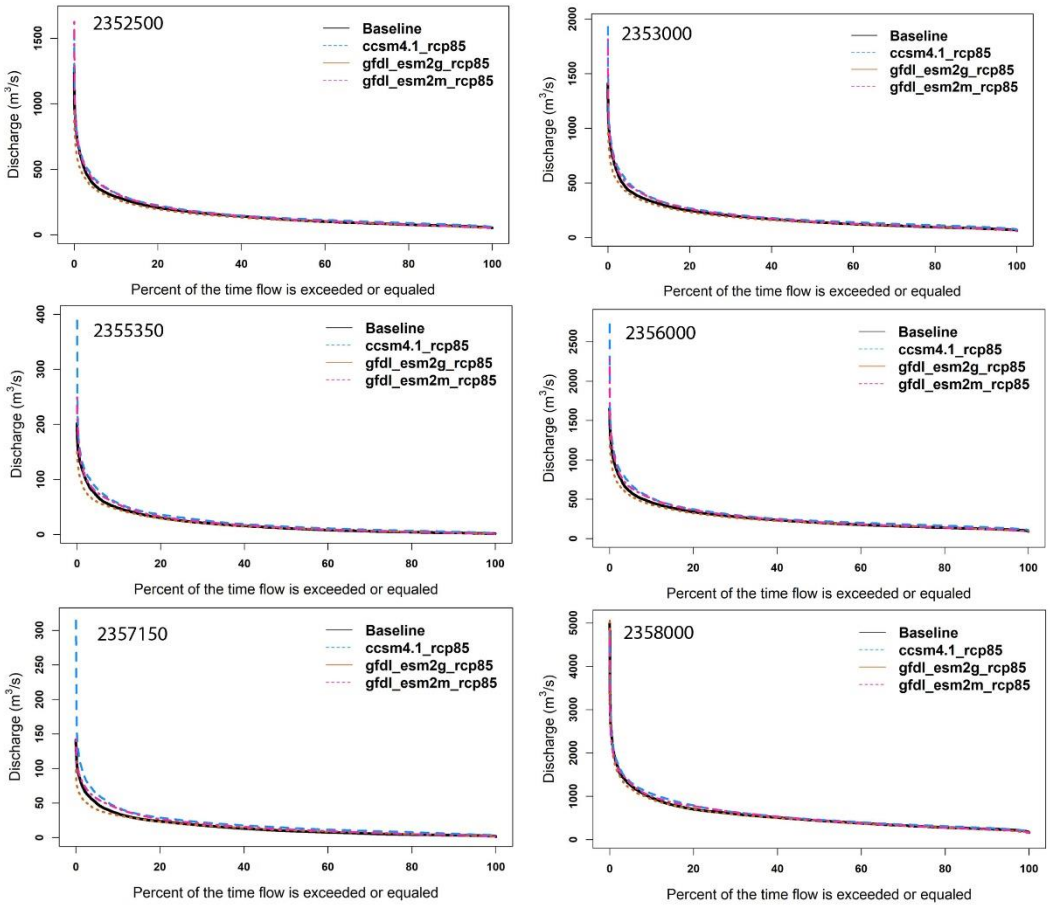

Figure 6.13 Comparison of Flow duration curve (FDCs) between simulated flow under projected climate from each Global Climate Model (GCM) under RCP4.5 emissions scenario and baseline at each USGS streamflow station.

Evaluation of the change in streamflow under projected climate from the RCP8.5 scenario showed similar patterns of change to the RCP4.5 scenario for each station (Fig. 6.14). A reduction in flow was observed from April to June at all stations under projected climate from at least two GCMs. The reduction in flow, however, was lower when compared to the reduction under RCP4.5. A reduction in flow was also observed for December at all stations except station 2357150, which saw an increase in flow. There was a general increase in flow in the remaining months at all stations. The highest increase in flow at all stations was observed in October with flow increasing by more than 100% at stations 2355350 and 2357150. The increase in flow was higher when

compared to the increase in flow under RCP4.5. It is important to note that an increase in flow in the fall months of September and October and reduction in April signals to a change in flow pattern due to the projected change in climate under RCP8.5 as also observed under RCP4.5. Similarly, a reduction in flow in May and June, especially at stations 2357150 and 2355350, where the average flow is low, could indicate the possibility of these streams going dry, especially during drought years.

FDCs analysis between the baseline and simulated flow for the three GCMs under RCP8.5 also showed a similar trend observed under RCP8.5 (Fig. 6.15). There was little change in flow that occurred more than 80% of the time under the projected climate. A considerable increase in flow was also observed in flow that occurred less than 1% of the time at all stations except the most downstream station (2358000), similar to under RCP4.5. The increase in flows were much higher than observed under RCP4.5 for stations 2352500, 2353000, and 2356000 while it was lower at stations 2355350 and 2357150 (Fig. 6.15). In general, the increase in high flows, again, indicates the possibility of an increase in flooding events similar to as observed under RCP4.5.

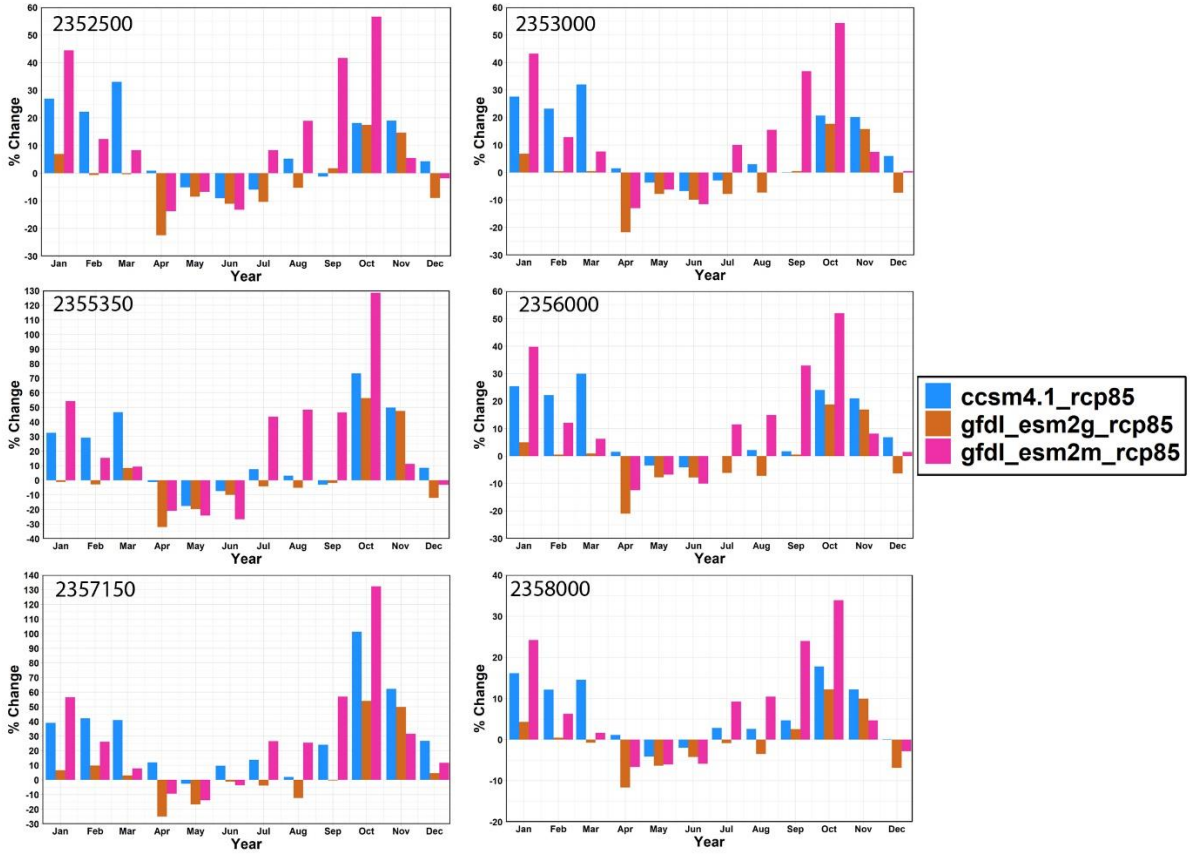

Figure 6.14 Monthly % change in streamflow at each of the six USGS streamflow stations between each Global Climate Model (GCM) and baseline under RCP8.5 emissions scenario.

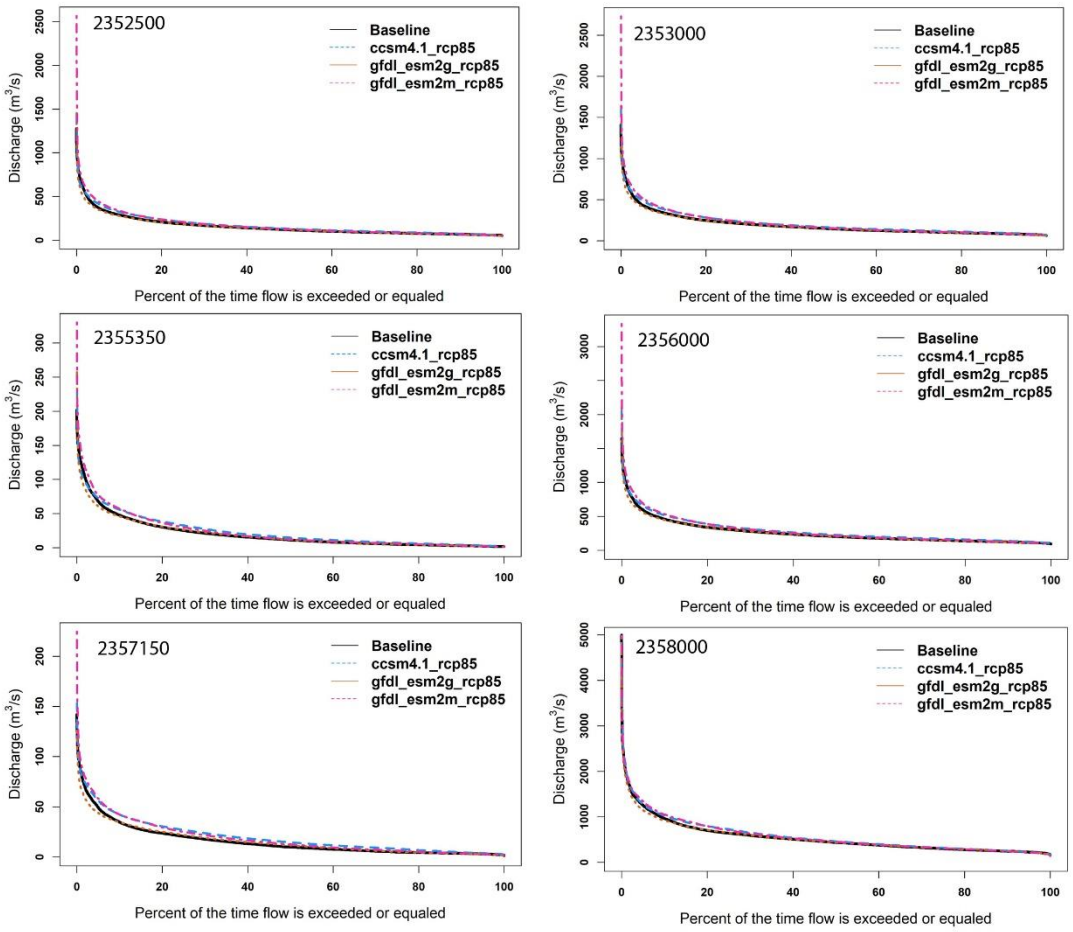

Figure 6.15 Comparison of Flow duration curve (FDCs) between simulated flow under projected climate from each Global Climate Model (GCM) under RCP8.5 emissions scenario and baseline at each USGS streamflow station.

6.3.4.3 Projected change in hydrologic budget components

The % change in ET after comparing the average of ET due to projected climate change from the three GCMs under RCP4.5 and RCP8.5 scenarios to the baseline ET are presented in Figure 6.16A and 6.16B respectively.

Evaluation of the change in ET between the RCP4.5 (Fig. 6.16A) and RCP8.5 (Fig. 6.16 B) scenarios show that there is no considerable difference between the two scenarios possibly because of automated irrigation being simulated by the SWAT model. A decrease in ET was observed in

all of the Middle Flint and Kinchafoonee-Muckalee watersheds while a slight reduction in ET was also observed in the majority of the Ichawaynochaway and parts of Spring watershed. An increase in ET was observed in almost all of the lower Flint River Basin as well as in parts of the Spring watershed. In general, the projected change in climate resulted in a reduction of ET in the northern and north-western part of the model domain, while ET increased in the south and south-eastern part of the model domain. Changes in ET ranged from a reduction of about 4% to an increase of close to 3% under both scenarios (Fig. 6.16A and 6.16B).

Evaluation of the average change in groundwater recharge showed that there was an increase in groundwater recharge in almost all of the coupled model domain under both RCP4.5 and RCP8.5 scenarios (Fig. 6.17A and 6.17B). The average change in recharge under both RCP scenarios was consistent throughout the watershed. The annual average increase in groundwater recharge ranged from less than 1% to as high as 26%. The lowest increase in groundwater recharge was observed in the Middle Flint, Kinchafoonee-Muckalee, and parts of Spring watersheds. Groundwater recharge in the lower Flint watershed varied spatially with the upper region receiving a higher increase in recharge as compared to the lower region under both scenarios (Fig. 6.17A and 6.17B). Although the evaluation of change in groundwater recharge under both scenarios indicated an increase, it is very important to note that the evaluation of change in streamflow (Fig. 6.12 and 6.14) showed reduction throughout the domain in some months (April, May, and June) as well as increase in other months indicating to the temporal variability in groundwater recharge. This also points out to a reduction in groundwater recharge in certain months of the year compared to baseline conditions.

Average annual SW-GW exchange for each sub-basin with the major river sections under projected climate from the three GCMs for RCP4.5 is presented in Figure 6.18A and the % change

in average SW-GW exchange when compared to the baseline values are presented Figure 6.18B. Evaluation of the flux (Fig. 6.18A) shows that majority of the sub-basins through which the Flint River passes have a positive flux while many of the sub-basins in the Ichawaynochaway watershed have a negative average annual flux. This is similar to the SW-GW exchange observed for the model calibration and validation period. In figure 6.18B, an increased % change in SW-GW flux in the sub-basins that had positive SW-GW indicates increasing groundwater discharge from the aquifer while an increased % change in SW-GW flux in sub-basins that had negative SW-GW flux indicates to a reduction in water loss from the streams to the aquifer. Analysis of the % change in average simulated flux under RCP4.5 to baseline indicated an increase in SW-GW flux throughout the model domain which ranged from 1% to 48% (Fig, 18.B). Evaluating the % change in flux (Fig. 6.18B) and average annual flux (Fig. 6.18A) together shows that the highest % changes were observed in sub-basins that had negative average flux indicating to the reduction of water lost from these sub-basins to the aquifer under projected climate. The majority of the sub-basins that had a positive flux saw an increase in flux from 1 – 15% with some sub-basins receiving as high as 23%. It should, however, be noted that although an increase in average annual flux is observed, the observed reduction in streamflow in certain months under projected climate indicates to the reduction in SW-GW exchange in some months of the year.

Evaluation of the average simulated flux and % change, when compared to baseline scenario under RCP8.5, showed a very similar trend to the RCP4.5 scenario (Fig. 6.19A and 6.19B). All sub-basins in the model domain had an increase in SW-GW exchange except for one sub-basin in the southwestern corner of the model domain that had a reduction of less than 1% (Fig. 6.19B). The increase in flux was slightly higher than when compared to the changes in flux observed under RCP4.5.

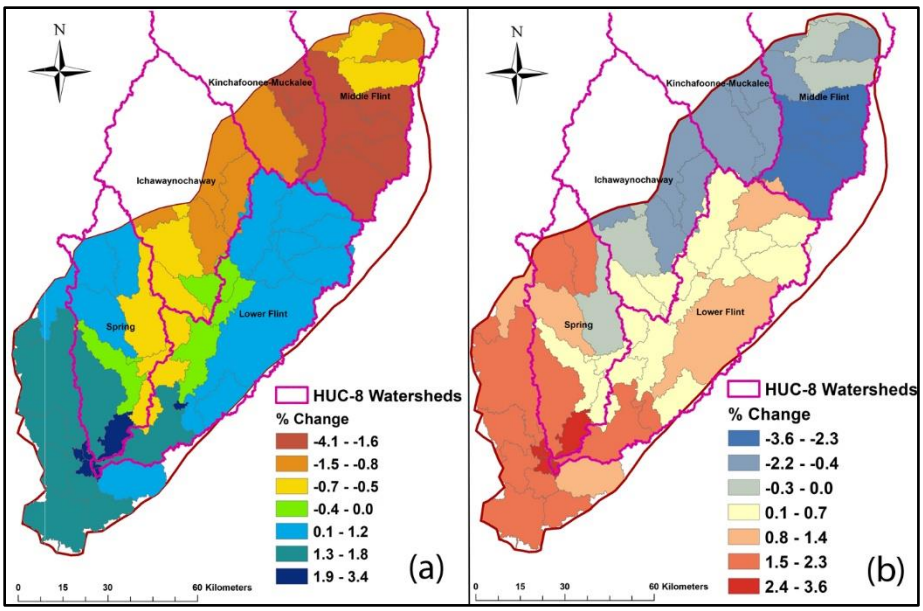

Figure 6.16 Projected change in ET (%) between the average of annual ET under projected climate by all three Global Climate Models (GCMs) and baseline for each sub-basin under emissions scenario (a) RCP4.5 and (b) RCP8.5.

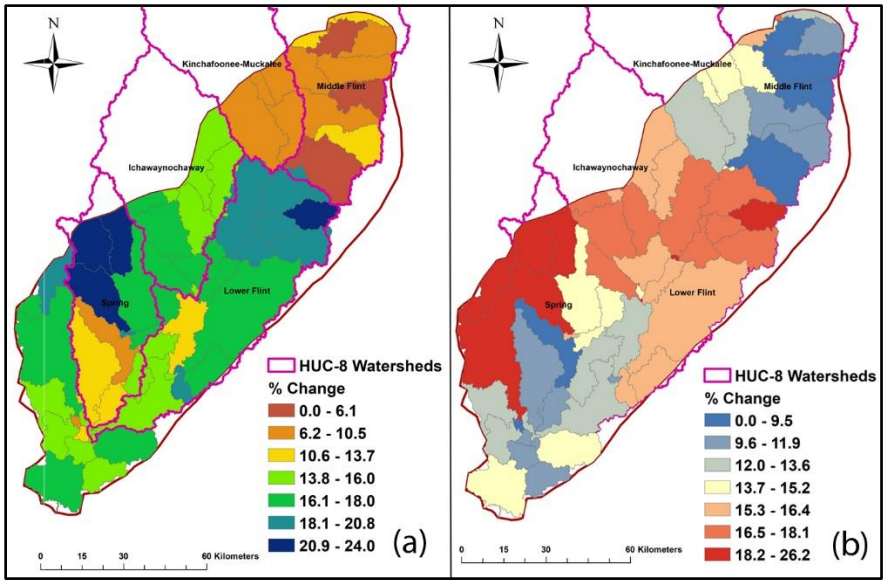

Figure 6.17 Projected change in groundwater recharge (%) between the average of annual groundwater recharge under projected climate by all three Global Climate Models (GCMs) and baseline for each sub-basin under emissions scenario (a) RCP4.5 and (b) RCP8.5.

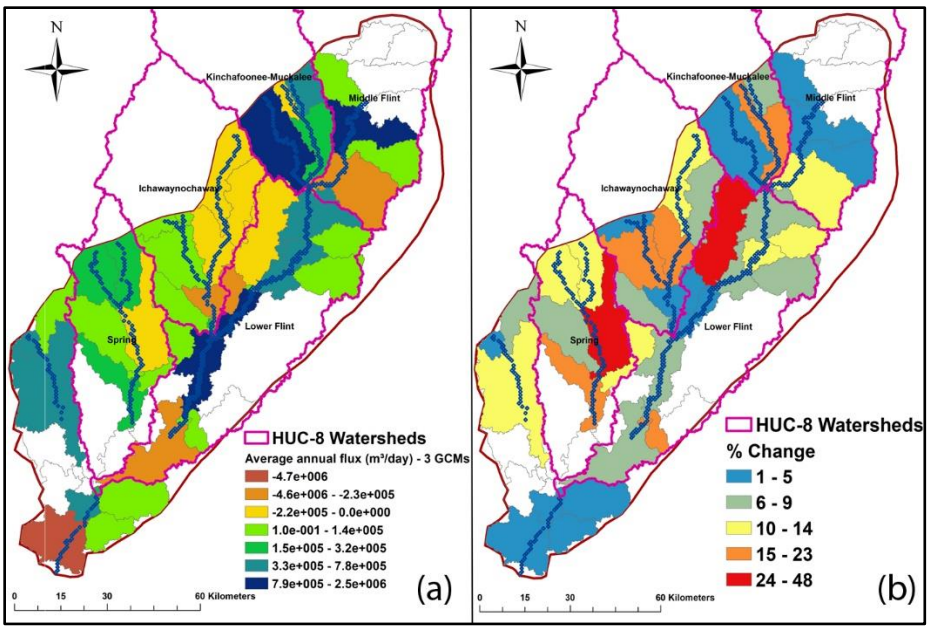

Figure 6.18 (a) Simulated average surface- and groundwater (SW-GW) flux from the three Global Climate Models (GCMs) for the sub-basins with major rivers, and (b) the projected change in SW-GW exchange (%) when compared to baseline fluxes under emissions scenario RCP4.5.

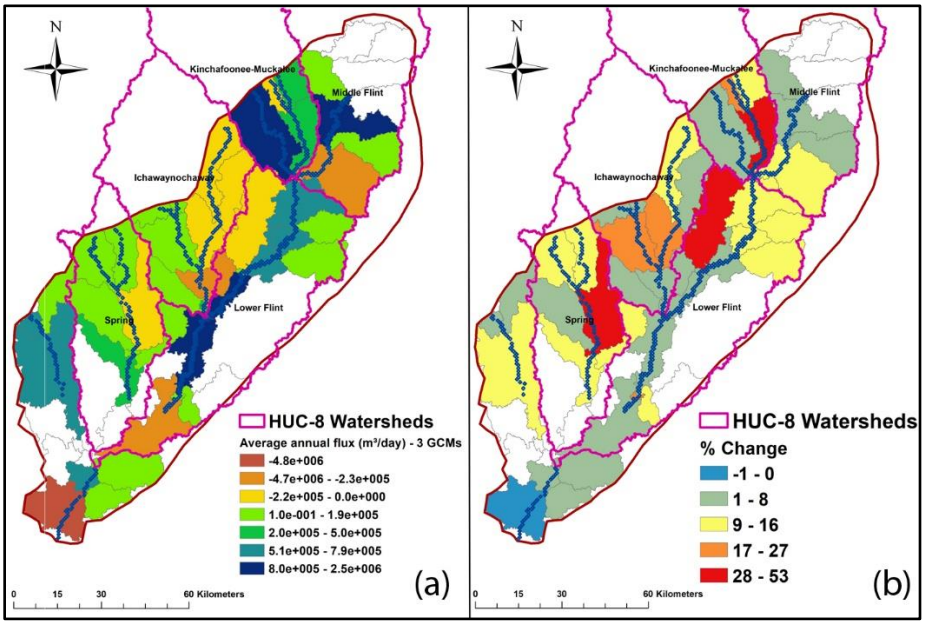

Figure 6.19 (a) Simulated average surface- and groundwater (SW-GW) flux from the three Global Climate Models (GCMs) for the sub-basins with major rivers, and (b) the projected

change in SW-GW exchange (%) when compared to baseline fluxes under emissions scenario RCP8.5.

6.4 Summary and Conclusions

This study developed a coupled SWAT-MODFLOW for the agriculturally intensive region of the lower ACF River Basin to evaluate the potential impacts of climate change on the surface- and groundwater resources of the region. The coupled and calibrated SWAT-MODFLOW model was able to simulate streamflow at most of the model domain satisfactorily. The model, however, had difficulty in replicating the streamflow in the Ichawaynochaway watersheds due to the lack of observed data during high flow events at the USGS station (2357150). The region also has a complex hydrogeology due to its karstic nature and shallow thickness of the underlying UFA compared to the other parts of the model domain. This indicates the possibility that the coupled SWAT-MODFLOW performs better where there is a continuous connection between the surficial rivers and the underlying aquifer which is thick with less variability in groundwater levels. The coupled SWAT-MODFLOW also had difficulty in matching the peak flows observed in the region at all stations but simulated the low flow conditions well. The model adequately matched and simulated the spatial and temporal variability of the groundwater levels in the UFA.

Evaluation of the projected change in temperature and precipitation from the three GCMs under scenarios RCP4.5 and RCP8.5 indicated that the daily minimum and maximum temperature will increase throughout the year with the daily maximum temperature increasing by as much as 2.7°C under the RCP8.5 scenario. A shift in precipitation pattern was observed under both scenarios with increasing precipitation in the fall months and decreasing precipitation in the early months of the year.

Evaluation of the climate change impact on streamflow showed a decrease in streamflow in the late spring and summer months (April – July) and an increase in the streamflow in the late fall (September – October) and early months of the year (January – March) under both RCP4.5 and RCP8.5 scenarios. The increase in streamflow in the late fall and reduction in late spring indicates a change in flow patterns due to the projected change in the climate. The reduction in streamflow, especially in the Ichawaynochaway and Spring watersheds, can be of critical concern as it can severely impact the aquatic habitat for the endangered aquatic species in the region. FDCs showed that there will be very little change in flow that occurs more than 80% of the time in the region. The high flow events that occur less than 1% of the time showed a considerable increase in streamflow at all but one station that was the most downstream indicating the possibility of flooding in the future in the region. Although FDCs did not show change in low flows, reduction in streamflow during the growing season, which can be further exacerbated during drought years, can also be a concern for sustaining aquatic habitat for the endangered species.

Assessment of the change in ET showed that ET will likely decrease in the northern and the northwestern part of the study region but will generally increase in the rest of the study area. The change in ET in the region, however, was not considerable, ranging from about -4% to 4%. Groundwater recharge increased under both RCP climate change scenarios throughout most of the model domain. The increase in recharge was limited in Middle Flint, Kinchfoonee-Muckalee, and parts of Spring watershed while the highest increase in recharge was observed in the lower Flint, Ichawaynochaway, and remaining of the Spring watershed. The coupled model accounted for the change in irrigation and subsequent withdrawal from the underlying aquifer due to climate change by linking automated irrigation with groundwater pumping. This probably helps explain the

minimal change in ET due to climate change as well as the reduction in streamflow in certain months even with increased groundwater recharge.

Evaluation of the change in the SW-GW exchange showed an increase in annual average flux when compared to the baseline for almost all of the sub-basins that had the major river reaches under both RCP scenarios. The highest changes in fluxes (close to 50%) were observed in the sub-basins with negative annual average fluxes indicating the reduction in loss of water from the streams to the aquifer under future climate. An increase in SW-GW exchange in the majority of the sub-basins through which the main-stem of the Flint River flowed ranged from 1 to 15%. The increase in average annual groundwater recharge and the subsequent increase in groundwater levels could be attributed to the increase in SW-GW fluxes. It is, however, very important to note that although an increase in groundwater recharge and SW-GW fluxes is observed under future climate, the reduction in average monthly streamflow of April – June indicates to the possibility of a reduction in groundwater recharge and SW-GW fluxes in certain months of the year under future climate.

It is important to understand that the impacts of climate change in this study were performed under current land use and crops. Impact on streamflow as well as groundwater recharge can worsen with an increase in agricultural land and subsequent increase in irrigation. Similarly, as the study evaluated the changes in streamflow, groundwater recharge, ET, and SW-GW exchange by averaging over the whole baseline (1995 – 2015) and scenario (2041-2060) period, the results could potentially suppress the impacts on years with significant drought or precipitation and hence, the results should be taken with caution.

6.5 References

Abatzoglou, J. T. (2013). Development of gridded surface meteorological data for ecological applications and modelling. *International Journal of Climatology*, *33*(1), 121–131.

Abatzoglou, J. T., Brown, T. J. (2012). A comparison of statistical downscaling methods suited for wildfire applications. *International Journal of Climatology*, *32*(5), 772–780.

Ahiablame, L., Sinha, T., Paul, M., Ji, J.-H., Rajib, A. (2017). Streamflow response to potential land use and climate changes in the James River watershed, Upper Midwest United States. *Journal of Hydrology: Regional Studies*, *14*, 150–166.

Ahmed, K. F., Wang, G., Silander, J., Wilson, A. M., Allen, J. M., Horton, R., Anyah, R. (2013). Statistical downscaling and bias correction of climate model outputs for climate change impact assessment in the US northeast. *Global and Planetary Change*, *100*, 320–332.

Aliyari, F., Bailey, R. T., Tasdighi, A., Dozier, A., Arabi, M., Zeiler, K. (2019). Coupled SWAT-MODFLOW model for large-scale mixed agro-urban river basins. *Environmental Modelling & Software*, *115*, 200–210.

Arguez, A., Durre, I., Applequist, S., Vose, R. S., Squires, M. F., Yin, X., … Owen, T. W. (2012). NOAA's 1981--2010 US climate normals: An overview. *Bulletin of the American Meteorological Society*, *93*(11), 1687–1697.

Bailey, R. T., Park, S. (2019). *SWAT-MODFLOW Tutorial Version 3*.

Bailey, R. T., Rathjens, H., Bieger, K., Chaubey, I., Arnold, J. (2017). SWATMOD-Prep: Graphical user interface for preparing coupled SWAT-MODFLOW simulations. *JAWRA Journal of the American Water Resources Association*, *53*(2), 400–410.

Bailey, R. T., Wible, T. C., Arabi, M., Records, R. M., Ditty, J. (2016). Assessing regional-scale spatio-temporal patterns of groundwater–surface water interactions using a coupled SWAT-MODFLOW model. *Hydrological Processes*, *30*(23), 4420–4433. https://doi.org/10.1002/hyp.10933

Brunner, P., Simmons, C. T. (2012). HydroGeoSphere: a fully integrated, physically based hydrological model. *Ground Water*, *50*(2), 170–176.

CAES. (2018). *Georgia Farm Gate Value Report 2017*.

Chunn, D., Faramarzi, M., Smerdon, B., Alessi, D. S. (2019). Application of an Integrated SWAT--MODFLOW Model to Evaluate Potential Impacts of Climate Change and Water Withdrawals on Groundwater--Surface Water Interactions in West-Central Alberta. *Water*, *11*(1), 110.

Couch, C. A., Hopkins, E. H., Hardy, P. S. (1996). *Influences of environmental settings on aquatic ecosystems in the Apalachicola-Chattahoochee-Flint River Basin* (Vol. 96). US Dept. of the Interior, US Geological Survey.

Couch, C. A., McDowell, R. D. (2006). Flint River Basin Regional Water Development and Conservation Plan.

de Almeida Bressiani, D., Gassman, P. W., Fernandes, J. G., Garbossa, L. H. P., Srinivasan, R., Bonumá, N. B., Mendiondo, E. M. (2015). Review of soil and water assessment tool (SWAT) applications in Brazil: challenges and prospects. *International Journal of Agricultural and Biological Engineering*, *8*(3), 9–35.

Doherty, J. (2004). PEST model-independent parameter estimation user manual. *Watermark Numerical Computing, Brisbane, Australia*, *3338*, 3349.

Francesconi, W., Srinivasan, R., Pérez-Miñana, E., Willcock, S. P., Quintero, M. (2016). Using the Soil and Water Assessment Tool (SWAT) to model ecosystem services: A systematic review. *Journal of Hydrology*, *535*, 625–636.

GA EPD. (2016). *Flint River Basin Regional Water Development and Conservation Plan*.

Gagnon, P. M., Golladay, S. W., Michener, W. K., Freeman, M. C. (2004). Drought responses of freshwater mussels (Unionidae) in coastal plain tributaries of the Flint River basin, Georgia. *Journal of Freshwater Ecology*, *19*(4), 667–679.

Gao, F., Feng, G., Han, M., Dash, P., Jenkins, J., Liu, C. (2019). Assessment of Surface Water Resources in the Big Sunflower River Watershed Using Coupled SWAT--MODFLOW Model. *Water*, *11*(3), 528.

Gassman, P. W., Reyes, M. R., Green, C. H., Arnold, J. G. (2007). The soil and water assessment tool: historical development, applications, and future research directions. *Transactions of the ASABE*, *50*(4), 1211–1250.

Gesch, D., Oimoen, M., Greenlee, S., Nelson, C., Steuck, M., Tyler, D. (2002). The national elevation dataset. *Photogrammetric Engineering and Remote Sensing*, *68*(1), 5–32.

Golladay, S. W., Gagnon, P., Kearns, M., Battle, J. M., Hicks, D. W. (2004). Response of freshwater mussel assemblages (Bivalvia: Unionidae) to a record drought in the Gulf Coastal Plain of southwestern Georgia. *Journal of the North American Benthological Society*, *23*(3), 494–506.

Golladay, S. W., Hicks, D. W., Muenz, T. K. (2007). Stream flow changes associated with water use and climatic variation in the lower Flint River Basin, southwest Georgia.

Guevara-Ochoa, C., Medina-Sierra, A., Vives, L. (2020). Spatio-temporal effect of climate change on water balance and interactions between groundwater and surface water in plains. *Science of the Total Environment, 722,* 137886.

GWC. (2017). *Watering Georgia: The State of Water and Agriculture in Georgia*. Retrieved from https://chattahoochee.org/wp-content/uploads/2018/07/GWC_WateringGeorgia_Report.pdf

Han, W., Yang, Z., Di, L., Mueller, R. (2012). CropScape: A Web service based application for exploring and disseminating US conterminous geospatial cropland data products for decision support. *Computers and Electronics in Agriculture*, *84*, 111–123.

Homer, C., Dewitz, J., Jin, S., Xian, G., Costello, C., Danielson, P., … others. (2020). Conterminous United States land cover change patterns 2001--2016 from the 2016 National Land Cover Database. *ISPRS Journal of Photogrammetry and Remote Sensing*, *162*, 184–199.

HydroGeoLogic. (2000). MODHMS: A comprehensive MODFLOW-based hydrologic modeling system, version 1.1, code documentation and user's guide. HydroGeoLogic Inc. Herndon, Va.

Jaber, F. H., Shukla, S. (2012). MIKE SHE: Model use, calibration, and validation. *Transactions of the ASABE*, *55*(4), 1479–1489.

Jones, L. E., Torak, L. J. (2006). *Simulated effects of seasonal ground-water pumpage for irrigation on hydrologic conditions in the Lower Apalachicola-Chattahoochee-Flint River Basin, Southwestern Georgia and parts of Alabama and Florida, 1999-2002*.

Karl, T. R., Melillo, J. M., Peterson, T. C., Hassol, S. J. (2009). *Global climate change impacts in the United States*. Cambridge University Press.

Kollet, S. J., Maxwell, R. M. (2006). Integrated surface--groundwater flow modeling: A free-surface overland flow boundary condition in a parallel groundwater flow model. *Advances in Water Resources*, *29*(7), 945–958.

Krysanova, V., Arnold, J. G. (2008). Advances in ecohydrological modelling with SWAT—a review. *Hydrological Sciences Journal*, *53*(5), 939–947.

Leta, O. T., El-Kadi, A. I., Dulai, H., Ghazal, K. A. (2016). Assessment of climate change impacts on water balance components of Heeia watershed in Hawaii. *Journal of Hydrology: Regional Studies*, *8*, 182–197.

Markstrom, S. L., Niswonger, R. G., Regan, R. S., Prudic, D. E., Barlow, P. M. (2008). GSFLOW-Coupled Ground-water and Surface-water FLOW model based on the integration of the Precipitation-Runoff Modeling System (PRMS) and the Modular Ground-Water Flow Model (MODFLOW-2005). *US Geological Survey Techniques and Methods*, *6*, 240.

Masson-Delmotte, V., Zhai, P., Pörtner, H.-O., Roberts, D., Skea, J., Shukla, P. R., … others. (2018). *Global Warming of 1.5 OC: An IPCC Special Report on the Impacts of Global Warming of 1.5° C Above Pre-industrial Levels and Related Global Greenhouse Gas Emission Pathways, in the Context of Strengthening the Global Response to the Threat of Climate Chang*. World Meteorological Organization Geneva, Switzerland.

Mitra, S., Srivastava, P., Singh, S. (2016). Effect of irrigation pumpage during drought on karst aquifer systems in highly agricultural watersheds: example of the Apalachicola-Chattahoochee-Flint river basin, southeastern USA. *Hydrogeology Journal*, *24*(6), 1565–1582. https://doi.org/10.1007/s10040-016-1414-y

Mohammed, K., Saiful Islam, A. K. M., Tarekul Islam, G. M., Alfieri, L., Bala, S. K., Uddin Khan, M. J. (2017). Impact of high-end climate change on floods and low flows of the Brahmaputra River. *Journal of Hydrologic Engineering*, *22*(10), 4017041.

Molina-Navarro, E., Bailey, R. T., Andersen, H. E., Thodsen, H., Nielsen, A., Park, S., … Trolle, D. (2019). Comparison of abstraction scenarios simulated by SWAT and SWAT-MODFLOW. *Hydrological Sciences Journal*, *64*(4), 434–454.

Molina-Navarro, E., Hallack-Alegr\'\ia, M., Mart\'\inez-Pérez, S., Ram\'\irez-Hernández, J., Mungaray-Moctezuma, A., Sastre-Merl\'\in, A. (2016). Hydrological modeling and climate change impacts in an agricultural semiarid region. Case study: Guadalupe River basin, Mexico. *Agricultural Water Management*, *175*, 29–42.

Moriasi, D. N., Gitau, M. W., Pai, N., Daggupati, P. (2015). Hydrologic and water quality models: Performance measures and evaluation criteria. *Transactions of the ASABE*, *58*(6), 1763–1785.

Neitsch, S. L., Arnold, J. G., Kiniry, J. R., Williams, J. R. (2011). *Soil and Water Assessment Tool Theoretical Documentation Version 2009*.

Nguyen, V. T., Dietrich, J. (2018). Modification of the SWAT model to simulate regional groundwater flow using a multicell aquifer. *Hydrological Processes*, *32*(7), 939–953.

Niswonger, R. G., Panday, S., Ibaraki, M. (2011). MODFLOW-NWT, a Newton formulation for MODFLOW-2005. *US Geological Survey Techniques and Methods*, *6*(A37), 44.

Pachauri, R. K., Allen, M. R., Barros, V. R., Broome, J., Cramer, W., Christ, R., … others. (2014). Climate change 2014: synthesis report. Contribution of Working Groups I. *II and III to the Fifth Assessment Report of the Intergovernmental Panel on Climate Change*, *151*.

Reidmiller, D. R., Avery, C. W., Easterling, D. R., Kunkel, K. E., Lewis, K. L. M., Maycock, T. K., Stewart, B. C. (2017). Impacts, risks, and adaptation in the United States: Fourth national climate assessment, volume II.

Ruefenacht, B., Finco, M. V, Nelson, M. D., Czaplewski, R., Helmer, E. H., Blackard, J. A., … others. (2008). Conterminous US and Alaska forest type mapping using forest inventory and analysis data. *Photogrammetric Engineering & Remote Sensing*, *74*(11), 1379–1388.

Running, S. W., Mu, Q., Zhao, M., Moreno, A. (2017). MODIS Global Terrestrial Evapotranspiration (ET) Product (NASA MOD16A2/A3) NASA Earth Observing System MODIS Land Algorithm. *NASA: Washington, DC, USA*.

Schwarz, G. E., Alexander, R. B. (1995). *State soil geographic (STATSGO) data base for the conterminous United States*.

Seaber, P. R., Kapinos, F. P., Knapp, G. L. (1987). Hydrologic unit maps.

Shea, C. P., Peterson, J. T., Conroy, M. J., Wisniewski, J. M. (2013). Evaluating the influence of land use, drought and reach isolation on the occurrence of freshwater mussel species in the lower Flint River Basin, Georgia (USA). *Freshwater Biology*, *58*(2), 382–395.

Shrestha, B., Cochrane, T. A., Caruso, B. S., Arias, M. E., Piman, T. (2016). Uncertainty in flow and sediment projections due to future climate scenarios for the 3S Rivers in the Mekong Basin. *Journal of Hydrology*, *540*, 1088–1104.

Shrestha, N. K., Du, X., Wang, J. (2017). Assessing climate change impacts on fresh water resources of the Athabasca River Basin, Canada. *Science of the Total Environment*, *601*, 425–440.

Singh, S., Srivastava, P., Mitra, S., Abebe, A. (2016). Climate variability and irrigation impacts on streamflows in a Karst watershed—A systematic evaluation. *Journal of Hydrology: Regional Studies*, *8*, 274–286.

Singh, S., Srivastava, P., Mitra, S., Abebe, A., Srivastava, P., Abebe, A., Torak, L. (2017). Evaluation of water-use policies for baseflow recovery during droughts in an agricultural intensive karst watershed: Case study of the lower Apalachicola--Chattahoochee--Flint River Basin, southeastern United States. *Hydrological Processes*, *31*(21), 3628–3644.

Taylor, K. E., Stouffer, R. J., Meehl, G. A. (2012). An overview of CMIP5 and the experiment design. *Bulletin of the American Meteorological Society*, *93*(4), 485–498.

Torak, L. J., Painter, J. A. (2006). *Geohydrology of the lower Apalachicola-Chattahoochee-Flint River basin, southwestern Georgia, northwestern Florida, and southeastern Alabama*.

USGS. (2019). USGS water data for the Nation: US Geological Survey National Water Information System database.

Wei, X., Bailey, R. T. (2019). Assessment of system responses in intensively irrigated stream--aquifer systems using SWAT-MODFLOW. *Water*, *11*(8), 1576.

Wei, X., Bailey, R. T., Records, R. M., Wible, T. C., Arabi, M. (2019). Comprehensive simulation of nitrate transport in coupled surface-subsurface hydrologic systems using the linked SWAT-MODFLOW-RT3D model. *Environmental Modelling & Software*, *122*, 104242.

Williams, L. J., Kuniansky, E. L. (2016). *Revised hydrogeologic framework of the Floridan aquifer system in Florida and parts of Georgia, Alabama, and South Carolina*. United States Department of the Interior, United States Geological Survey.

Xia, Y., Mitchell, K., Ek, M., Sheffield, J., Cosgrove, B., Wood, E., … others. (2012). Continental-scale water and energy flux analysis and validation for the North American Land Data Assimilation System project phase 2 (NLDAS-2): 1. Intercomparison and application of model products. *Journal of Geophysical Research: Atmospheres*, *117*(D3).

Chapter 7

Conclusions

7.1 General Conclusions

The impact of intensive groundwater withdrawal from the underlying Upper Floridan Aquifer (UFA) in the surface- and groundwater resources that gets compounded during the frequent drought conditions is an important concern for agricultural and environmental sustainability of the lower Apalachicola-Chattahoochee-Flint (ACF) River Basin. Long-term sustainability concerns in the region include the potential impacts of the projected increase in agricultural water withdrawals from the aquifer along with understanding the potential impacts of climate change in the different hydrologic components of the watershed. As the overall goal of this project was to help improve the short- and long-term agricultural and environmental sustainability of the region, this study performed a detailed field-scale evaluation of the agricultural management practices for the major row crops in the region as well as evaluated the regional impacts of the projected increase in irrigation and climate change. Understanding the impacts of the range of agricultural management practices can help farmers and policymakers make immediate important decisions to reduce the detrimental environmental impacts of agriculture while maintaining high agricultural productivity for profitability. Evaluating the potential regional impacts of an increase in irrigation and climate change, on the other hand, can provide a glimpse into the challenges that lay ahead for the long-term sustainable management of surface- and groundwater resources in the region.

As the Soil and Water Assessment Tool (SWAT) was used as the modeling tool to perform the detailed field-scale evaluation of the range of management practices, it was important to perform a detailed literature review to identify the multiple ways SWAT can be utilized as a field-scale model along with its advantages and disadvantages so that the most appropriate method for setting

up the model for this study could be identified (Dissertation Objective 1). A thorough review identified five basic methods for evaluating the SWAT model output at the field-scale: (1) Simulation of an individual field as a field-scale SWAT model using a single Hydrologic Response Unit (HRU); (2) Modification of SWAT input files such that each field in a watershed is represented by multiple HRUs that reflect the changes in the soil and slope classes within each simulated field; (3) Modification of the SWAT input files such that each HRU corresponds to a unique field located within a simulated watershed; (4) Development of a post-processing tool that uses SWAT output generated with conventional HRU delineation and converts this output to field scale using interpolation and averaging techniques; and (5) Defining a relationship between fields in the simulated watershed and HRUs from the SWAT model set up using a conventional HRU delineation by comparing land use, soil, and slope attributes and evaluating the HRU-level outputs. A modified version of the second method was utilized to set up the field-scale SWAT model by developing a SWAT model for an individual plot but with the plot being represented by multiple HRUs so that the soil and slope heterogeneity within the plot can be preserved and runoff could be simulated.

Evaluation of the range of agricultural management practices for the major row crops (Dissertation Objective 2), cotton and peanut, first required assessing the model's ability to simulate the important hydrological and water quality processes at field-scale, especially as SWAT is often used as a watershed-scale model. Model performance assessment showed that SWAT can adequately simulate surface runoff, soil moisture, cotton, and peanut yields, and nitrate transport at the field scale. It was also observed that a multi-variable calibration for water quality simulation in which nitrate and crop yield were calibrated helped better constrain the model. Assessment of the wide range of agricultural management practices was performed by developing three

management scenarios that covered the range of practices. Comparison of irrigation water use, nitrate loss from the agricultural field, and yield between the three scenarios showed that scenario 1 (Mgt1) with soil moisture sensor-based irrigation, cover crop, and strip tillage had the highest potential for reducing irrigation water use and nutrient loss while maintaining high agricultural productivity. Although scenario 2 (Mgt2), which is the most widely adopted practice in the region, produced a similar yield, it led to higher water use and nutrient loss as compared to Mgt1. Additional costs associated with installing soil moisture sensors and cover crops in Mgt1 are important financial issues that can deter stakeholders and farmers to shift from Mgt1 to Mgt1. This study also demonstrated the ability of SWAT as a tool for evaluating BMPs for crop yield, nutrient transport, and irrigation water use at the field scale.

Regional evaluation of the impacts of an increase in irrigation (Dissertation Objective 3) projected by the Georgia Water Planning and Policy Center (GWPCC) using the MODular groundwater FLOW model (MODFLOW) showed that groundwater levels can decrease by as much as 2.4 meters in the UFA in a drought year when compared to the groundwater levels of the 2011 drought year. The decrease in groundwater level was high in the aquifer regions that are comparatively thinner in the Lower Flint, and the adjoining Kinchafoonee, Ichawaynochaway, and Spring HUC-8 watersheds. Reach sections in the Lower Flint and Kinchafoonee watersheds saw reduction in stream-aquifer flux (groundwater discharge) by as much as 33%. This indicated to the possibility that the aquifer might not be able to sustain the projected increase in groundwater pumpage for irrigation, especially under prolonged drought conditions.

As groundwater recharge from precipitation has a critical influence in the groundwater levels and thereby the SW-GW exchange in the lower ACF River Basin, it was important to make sure groundwater recharge is accurately simulated before evaluating the impacts of climate change in

the surface- and groundwater resources (Dissertation Objective 4). Because confidence in groundwater recharge simulation is often derived by calibrating streamflow and evapotranspiration (ET) in SWAT, it was also important to evaluate the impact of calibrating these variables separately as well as using a multi-variable approach in groundwater recharge simulation in the model to determine if there is a calibration approach that results in better groundwater recharge estimation. The study identified that streamflow was the most influential variable to be calibrated in SWAT for simulating groundwater recharge accurately while calibration of ET alone had a negligible impact in groundwater recharge simulation. Evaluation of multi-variable calibration using a sequential approach showed that streamflow followed by ET provided the best estimates of simulated groundwater recharge. The study also pointed out the importance of calibrating streamflow separately for the different sections of a watershed that differ in geology as the parameters that are critical for groundwater recharge simulation can be fine-tuned for the region. Comparison of SWAT simulated groundwater recharge to recharge estimates derived using RORA the program also showed that the model can accurately simulate groundwater recharge in the lower ACF River Basin.

Assessment of model performance for the integrated SWAT-MODFLOW model after coupling and calibration showed that the model satisfactorily simulated streamflow and groundwater level in most of the model domain. The model performed better in simulating streamflow in regions where the underlying aquifer was thick and there was a continuous connection between the aquifer and the surficial streams. Comparison of the projected temperature to historical observations in the region indicated to the rise in daily maximum and minimum temperature with summer temperatures rising by as much as 2.7°C under the RCP8.5 scenario. A shift in precipitation pattern was also observed with increasing precipitation in the fall months and decreasing precipitation in

the early months of the year. Evaluation of the climate change impact (Dissertation Objective 5) on streamflow showed a decrease in streamflow in the late spring and summer months (April – July) and an increase in streamflow in the late fall (September – October) and early months of the year under both RCP4.5 and RCP8.5 scenarios. The reduction in streamflow, especially in the Ichawaynochaway and Spring watersheds, can be of critical concern as it can severely impact the aquatic habitat for the endangered aquatic system in the region. Comparing the flow duration curves (FDCs) between the projected scenario against the baseline showed that high flow events that occur less than 1% of the time showed a considerable increase in streamflow indicating the possibility of flooding in the future in the region. An increase in groundwater recharge was observed through most of the model domain while there was minimal change in ET with change ranging from -4% to 4%. The SW-GW exchange increased by as much as 15% along the mainstem of the Flint River while a limited increased was observed in the Spring and Ichawaynochaway watersheds.

7.2 Research implications

In general, findings from this study can be important in reducing the stress in the UFA for irrigation, especially during drought periods while helping maintain high agricultural productivity. As the evaluation of management practices was performed at field-scale, the results should, however, be taken with caution. Evaluation of the management practices under a range of soil and climatic conditions would provide an improved understanding of the management practices for better implementation. This study also identified the impacts of the projected increase in irrigation and climate change in the surface- and groundwater resources including the watersheds and stream reaches within the model domain that are most susceptible to these changes. This information can provide vital information about the challenges that lay ahead for the long-term agriculture and

environmental sustainability of the region and help make management and policy decisions to mitigate these challenges.

Along with the importance of these regional findings, this study also contributed to some important research findings. This study demonstrated the importance of multi-variable calibration of SWAT at field-scale, especially, if it is to be used as a tool for BMP evaluation in which crop yield is an important consideration. Understanding the influence of streamflow and ET calibration in the SWAT simulation of groundwater recharge provides important information to researchers for efficiently calibrating the model when using it for groundwater recharge evaluation studies. Although the evaluation of SWAT simulation of groundwater recharge was assessed in different geologic regions within the simulated watershed, the study watershed is characterized by a humid sub-tropical climate. As the dominant hydrologic components of a watershed differ greatly according to climatic conditions, similar evaluation studies under different climatic conditions are required for further understanding the influence of streamflow and ET calibration on groundwater recharge. The study also showed that the integrated SWAT-MODFLOW can adequately simulate streamflow in a karstic watershed but performs better in regions where the aquifer is thick with less variability in groundwater levels than in regions where the aquifer is thin and has greater variability in aquifer levels. The study was, however, limited due to the lack of observed data (missing data) for adequate calibration of streamflow, especially during high flow events, in the study region where the aquifer was thin (Spring and Ichawaynochaway watersheds). Hence, additional investigation using complete observed data over long-term and in different watersheds with similar hydrogeology is needed.

7.3 Future works

Additional/future works that can be performed using this study and its findings as a foundation for further contributing to the science as well as improving the sustainability of agriculture and environment in the lower ACF River Basin are listed below:

1. Evaluate SWAT-MODFLOW for simulating water quality in the complex hydrogeology of the lower ACF River Basin incorporating RT3D.

2. Evaluate the range of agricultural management practices at a regional-scale to evaluate the regional impacts of change in agricultural management practices in the major crops in quantity and quality of surface- and groundwater resources of the lower ACF River Basin.

3. Assess the impacts of change in land use including restoration of long-leaf pines; change agricultural row crop types; and, conversion of agricultural land to pasture in critical areas identified from the above studies, in the quantity and quality of the surface- and groundwater resources of the lower ACF River Basin.

4. Assess the impacts of land use and climate change in the ecological flows of the lower ACF River Basin for developing better sustainability plans for the protection of the endangered and threatened species in the lower ACF River Basin.